



# IMPROVING RISK ASSESSMENT OF CATIONIC SURFACTANTS

Overcoming the Challenges in Analytical  
Determination, Cell-Based Toxicity Assays,  
and Biodegradability Testing

NIELS TIMMER



# **Improving Risk Assessment of Cationic Surfactants**

Overcoming the Challenges in Analytical Determination,  
Cell-Based Toxicity Assays, and Biodegradability Testing

**Niels Timmer**

Improving Risk Assessment of Cationic Surfactants  
Overcoming the Challenges in Analytical Determination, Cell-Based Toxicity Assays, and  
Biodegradability Testing

ISBN/EAN: 978-94-6375-850-5  
Layout and design by: Marilou Maes, [persoonlijkproefschrift.nl](http://persoonlijkproefschrift.nl)  
Printing: Ridderprint | [www.ridderprint.nl](http://www.ridderprint.nl)

Copyright © 2020 Niels Timmer

All rights reserved. No part of this thesis may be reproduced, stored or transmitted in any way or by any means without the prior permission of the author, or when applicable, of the publishers of the scientific papers.

# **Improving Risk Assessment of Cationic Surfactants**

Overcoming the Challenges in Analytical  
Determination, Cell-Based Toxicity Assays, and  
Biodegradability Testing

## **Verbeterde Risicobeoordeling van Kationische Surfactanten**

Omgaan met de Uitdagingen bij Chemische Analyse,  
Toxiciteitsscreening met Cellen, en Biodegradatietesten  
(met een samenvatting in het Nederlands)

### **Proefschrift**

ter verkrijging van de graad van doctor aan de  
Universiteit Utrecht  
op gezag van de  
rector magnificus, prof.dr. H.R.B.M. Kummeling,  
ingevolge het besluit van het college voor promoties  
in het openbaar te verdedigen op

maandag 25 mei 2020 des middags te 2.30 uur

door

### **Niels Timmer**

geboren op 9 juni 1985  
te Leiderdorp

**Promotor:**

Prof. dr. ir. J. Legler

**Copromotoren:**

Dr. S.T.J. Droge

Dr. J.L.M. Hermens

Dit proefschrift werd (mede) mogelijk gemaakt met financiële steun van Unilever, Safety & Environmental Assurance Center (SEAC), Colworth Science Park (United Kingdom).  
[projectnummer CH-2012-0283]

## Table of Contents

<b>Chapter 1</b>	General Introduction	7
<b>Chapter 2</b>	Evaluating Solid Phase (Micro-) Extraction Tools to Analyze Freely Ionizable and Permanently Charged Cationic Surfactants	35
<b>Chapter 3</b>	Sorption of Structurally Different Ionized Pharmaceutical and Illicit Drugs to a Mixed-Mode Coated Microsampler	67
<b>Chapter 4</b>	The Influence of In Vitro Assay Setup on the Apparent Cytotoxic Potency of Benzalkonium Chlorides	97
<b>Chapter 5</b>	Sorption of Cationic Surfactants to Artificial Cell Membranes: Comparing Phospholipid Bilayers with Monolayers Coatings and Molecular Simulations	123
<b>Chapter 6</b>	Toxicity Mitigation and Bioaccessibility of the Cationic Surfactant Cetyltrimethylammonium Bromide in a Sorbent-Modified Biodegradation Study	157
<b>Chapter 7</b>	Sorbent-Modified Biodegradation Studies of the Biocidal Cationic Surfactant Cetylpyridinium Chloride	181
<b>Chapter 8</b>	Application of Seven Different Clay Types in Sorbent-Modified Biodegradation Studies with Cationic Biocides	207
<b>Chapter 9</b>	Summary and General Discussion	235
	References	248
	Nederlandse Samenvatting	276
	Dankwoord	286





# CHAPTER 1

---

## General Introduction

Environmental risk assessment focuses on the potential negative environmental impact of human endeavours. Environmental contaminants from industrial sources or consumer products can be neutral or ionizable chemicals from different categories e.g. food additives, detergents, dyes, and product packaging. Several specific scientific challenges exist to adequately describe, understand, and predict the behaviour of ionizable environmental contaminants. With an estimated annual production volume of 17 million tons – which is roughly equal to 2 kg per capita over the global human population – surfactants are especially relevant within this group of ionizable chemicals [1]. The research described in this thesis focusses specifically on improving risk assessment of positively charged surfactants, more specifically by: 1) developing and testing analytical techniques, 2) studying the effects of bioavailability on toxicity, and 3) determining the effects of bioavailability on biodegradation. Following a general introduction to the concepts of exposure, sorption, bioavailability and degradation, the scope and objectives of this thesis are summarized below.

## 1. Exposure, Sorption, and Bioavailability

### 1.1. The Relevance of Exposure in Environmental Risk Assessment

Any toxicologist will be able to quote the famous sixteenth century Paracelsus: “All things are poison and nothing is without poison, only the dosage makes a thing (not) poison. [2]” This quote can roughly be translated into the concept of exposure in modern toxicology: A chemical can be extremely toxic, but as long as there is no exposure (e.g. the chemical is contained within a glass container), there can be no harmful effects. Exposure is important in different disciplines, both in *in vivo* toxicology with living organisms as well as in *in vitro* toxicology with specific isolated cells or cultivated cellular material. The advent of *in vitro* techniques opened up the possibility to assess toxicity and identify mechanisms of action on a cellular and molecular level, without the excessive use of living organisms in toxicological studies [3]. Nonetheless, acceptance and assimilation of these techniques by regulatory institutes is a lengthy process, perhaps partially due to the difficulties in extrapolating toxic doses in an *in vitro* system to environmentally relevant exposure scenarios [4, 5]. This, in turn, might be caused by poor characterization of the true exposure in *in vitro* systems. Part of this thesis deals with understanding and improving the shortcomings in *in vitro* assays that address toxicity, as well as in microbial biodegradability studies that are used to evaluate environmental persistence of potentially

toxic chemicals. However, it seems appropriate to first illustrate the necessity and relevance of environmental toxicology and risk assessment in general.

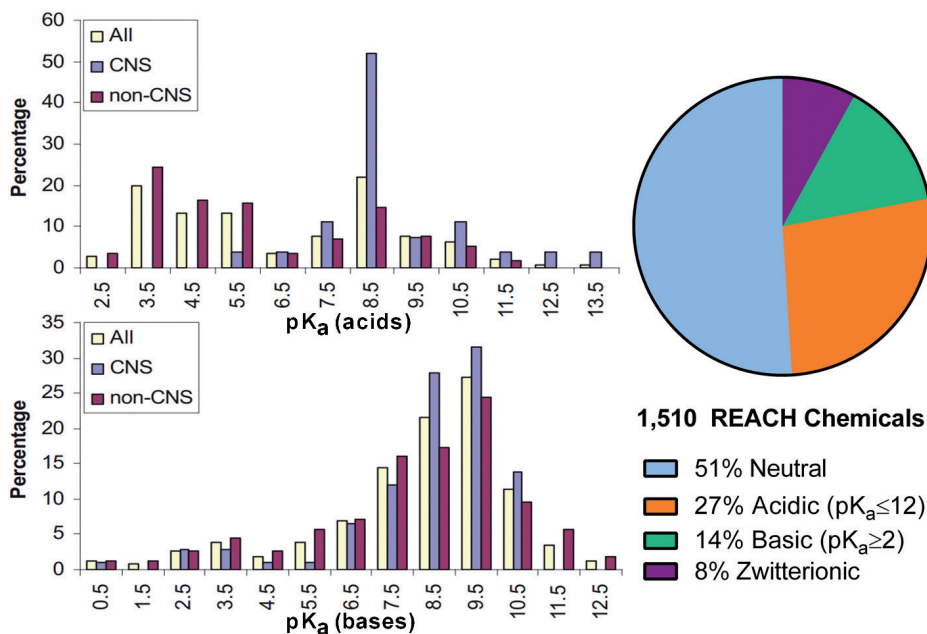
The average human being consumes and uses a plethora of different chemicals on a regular basis – e.g. food additives, colorants, detergents, preservatives, pharmaceuticals, and perfumes – most of these even on a daily basis. This leads to exposure of the general population and exposure of the total environment, as it is inevitable that a significant portion of these chemicals reach the biosphere, which can be illustrated with a very simple mass-balance example. Oversimplified, it could be stated that any xenobiotic that is not fully assimilated or metabolized by an organism is in some way released into the environment. This can be directly, for instance with topically applied products such as cosmetics or personal care products. However, in most cases these chemicals will first be absorbed into the organism and will only reach the environment after excretion in urine, feces, sweat or other routes of secretion. Many of these excreted substances will have undergone some extent of modification through partial metabolism, but the above is an appropriate and convenient example of the considerable chemical strain of modern-day human life. In addition, there are countless industrial and agricultural sources that release chemicals directly into the environment, either by design (e.g. application of pesticides) or due to calamities (e.g. leakage, fires, disaster).

Scientific progress has led to the ongoing discovery and synthesis of new chemicals; as of early 2020 the CAS registry of the American Chemical Society has more than 155 million chemical substances listed, with approximately 15,000 entries added on a daily basis. Because of this vast amount of new chemical entities – and numerous possible metabolites and breakdown products for each of them – it becomes increasingly difficult to predict and prevent possible negative environmental consequences. This creates a universal need for two distinct types of risk assessment: human health-oriented risk assessment to protect the population, and environmental risk assessment (ERA) to identify and decrease unwanted risks for the environment. There are international regulations that make an effort towards adequate risk assessment, of which REACH is probably the most well-known and exhaustive. REACH (Registration, Evaluation, Authorization and Restriction of Chemicals) is a regulation of the European Union [6], addressing the production and usage of virtually any chemical substance, and its potential impact on human and environmental health. Within environmental risk assessment, REACH is strongly aimed at assessment of persistence, bioaccumulative properties, and toxicity (PBT) of chemicals. However, these assessments are almost exclusively focused on the most straightforward piece of the puzzle: neutral

organic chemicals. Obviously, the vast number of chemical stressors that can potentially be released into the environment requires that proper risk assessment should take place, based on comprehensive insight into the most influential processes involved.

## **1.2. Relevance of Ionizable Chemicals**

In general, ionizable organic chemicals are molecules that can acquire a positive or negative charge by gaining or losing  $H^+$  through interaction with basic or acidic functional groups and, in most cases, water. Even though neutral chemicals form the majority of all registered chemicals on the European market, and it would be unwise to ignore or downplay their significance, it could and should be argued that ionizable chemicals are equally important with respect to (environmental) risk assessment. Partitioning behavior, prediction of physicochemical properties, and sampling procedures are all moderately straightforward for neutral chemicals [7-9]. For ionizable chemicals, however, multiple scientific challenges remain to be solved before their behavior can be fully understood and predicted or modeled [10, 11]. Environmental contaminants from consumer products can be neutral or ionizable chemicals and represent very different categories, such as food additives, detergents, fabric softeners, synthetic musks, pharmaceuticals, and various chemicals added to product packaging, such as plasticizers or dyes [12-16]. Detergents and fabric softeners are generally ionizable by nature, as their main active ingredients are surfactants; amphiphiles that usually contain a charged phosphate, sulfonate or quaternary ammonium group that constitutes the hydrophilic head [17].



**Figure 1.1:** Left: Two graphs taken from Manallack [20], showing the extent of ionizable chemicals among pharmaceuticals; CNS = Central Nervous System. Right: Graph taken from Franco et al. [15], showing the proportion of ionizable chemicals in a sample of 1,510 chemicals taken from the REACH database.

The EU regulation for the Registration, Evaluation, Authorization and Restriction of Chemicals (REACH) is an excellent indicator to emphasize the relevance of ionizable chemicals [18]. Reasonable estimates are that 49% of REACH chemicals are ionizable between pH 4 and pH 10; about 14% of REACH chemicals are partially positively charged at environmentally relevant pH levels [19]. Another study that highlights the importance of ionizable chemicals is the work by Manallack, which provides an overview of the  $pK_a$  distribution of pharmaceuticals [20]. From this work, it can be extrapolated that a significant portion of pharmaceuticals will also be ionized at environmentally relevant pH. Two important graphs detailing the findings by Manallack are shown in figure 1.1, in addition to a graph based on the work of Franco et al [15]. Food and beverage aroma chemicals are another group containing a significant portion of ionizable molecules (approximately 13.7%), where the physicochemical properties are totally different for the neutral and the ionized form [21]. While risk assessment models reasonably predict uptake and elimination by humans, environmental distribution, and even toxicity of neutral chemicals, ionizable chemicals still present a challenge, partly because their chemical fate is dependent on additional factors. The toxicity of an ionizable chemical in the environment is determined

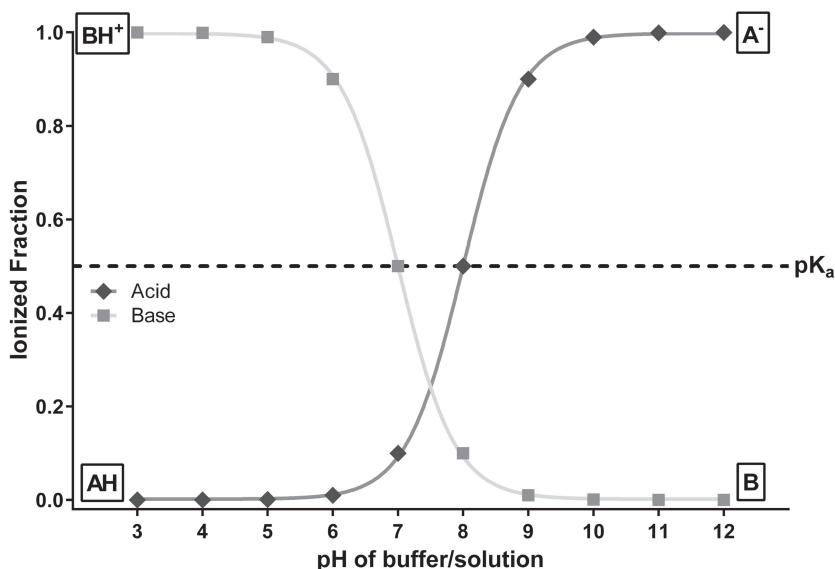
by the complex interplay of pH, soil or sediment composition (organic carbon content and mineralogy), presence of dissolved organic matter, presence of other contaminants, type and concentrations of dissolved ions, and other environmental conditions.

### **1.3. Cationic Chemicals, including cationic surfactants**

The group of positively charged (cationic) organic chemicals is made up of ionizable bases and quaternary ammonium compounds with a permanent positive charge. Basic chemicals are an adequate example to highlight the importance of ionized molecules in risk assessment. The role of pH in the sorption of organic bases to environmentally relevant surfaces is very simple and straightforward. If the pH in the aqueous phase is less than 2 units above the  $pK_a$  of a basic chemical (B), a relevant percentage (>1%) of molecules will associate with  $H^+$  ions in solution, giving rise to  $BH^+$ . The fraction of  $BH^+$  will increase with decreasing pH (see figure 1.2). Chemicals with a basic  $pK_a$  of 7 or higher are most relevant in this perspective, as a significant fraction (i.e.  $\geq 10\%$ ) of any such chemical will bear a positive charge within the environmentally relevant pH range, and will be mostly charged at physiological pH in cells. Although most risk assessment models assume that only the (fraction of) neutral base species determine the binding affinity to all kinds of environmental substrates, partitioning of these charged species can still make a significant contribution to total sorption to e.g. soil at  $pH \geq pK_a + 2$ , where more than 99% of a basic chemical will be in the neutral form [22]. Due to the strong focus of risk assessment modeling on neutral contaminants, it is often overlooked that most environmental substrates (organic carbon, clay minerals) are densely negatively charged.

As noted previously, current environmental risk assessment has a heavy focus on neutral chemicals [14-16], which immediately highlights the need for information on and relevance of ionizable chemicals. More data are available for anionic chemicals (e.g. acidic herbicides and anionic detergents) than for cationic chemicals [23]. This further underscores the importance of gathering more insight and data regarding the behavior of cationic chemicals in the environment. Cationic pollutants can be found in landfills and sewage, which contain cationic chemicals consumed or discharged by typical citizens, such as detergents used in hair conditioner and fabric softener (i.e. cationic surfactants) [24] and various types of pharmaceuticals and illicit drugs [13, 25]. Moreover, organic matter in the environment usually contains carboxylic acids, which after dissociation constitute suitable binding sites for positively charged headgroups of cationic surfactants [26]. This allows for sorption of positively charged molecules to these remnants of organic matter, leading

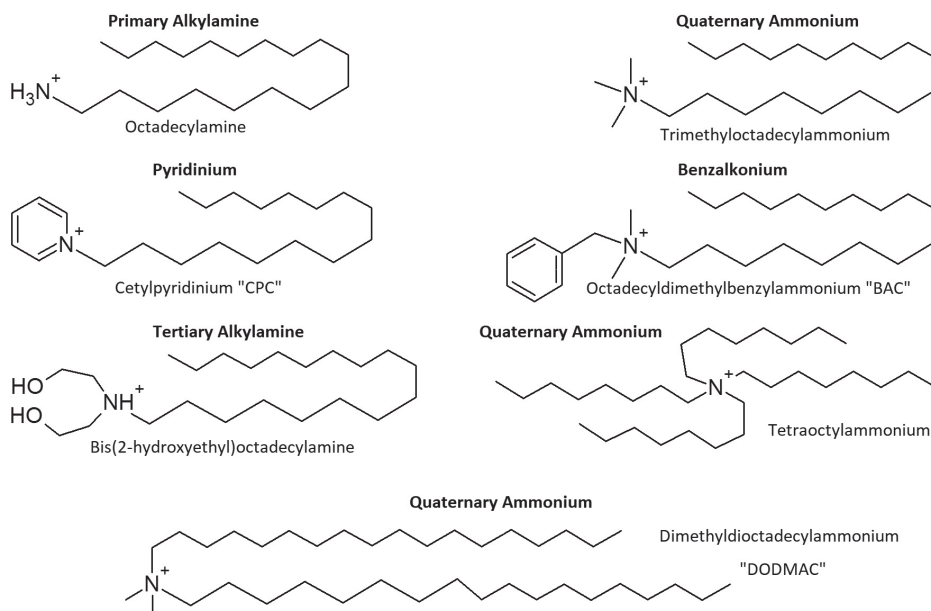
to complex interactions that influence the environmental fate and persistency of these chemicals. The ubiquitous availability of negatively charged surfaces leads to a marked difference in behavior between anionic and cationic chemicals, which further increases the knowledge gap for cationic chemicals.



**Figure 1.2:** Graphical representation of the ionization of acidic (A) and basic (B) molecules as a function of medium pH. Note that these graphs increase in complexity when multiple acidic or basic moieties are present in one molecule.

Surfactants are the most widely discharged synthetic chemicals [27]. Surfactants, by definition, contain lipophilic and hydrophilic moieties. The most common form is a hydrophilic (highly polar or ionized) headgroup attached to a lipophilic linear hydrocarbon (alkyl) chain of variable length [28]. Important anthropogenic sources of cationic surfactants are fabric softeners, biocides and drilling mud [29-31], although surfactants also have significant natural sources for release into the environment [32]. These toxicologically relevant substances can enter the environment through different routes, such as wastewater discharge [33], pesticide formulation additives to improve efficiency, remediation efforts to clean polluted ground water or soil [34, 35], additives in industrial resource extraction [29], or secretion from aquatic plants [32].

Cationic surfactants contain ionizable amine or permanently charged ammonium moieties in their headgroup. Due to their positive charge they can interact specifically with negatively charged surfaces such as hairs or cotton; the ionic bond with the cationic surfactants covers these negatively charged surfaces with an oily film of surfactants that create a soft and shiny layer. Commercially, quaternary ammonium compounds comprise the most important group while ionizable alkylamines find limited application. Quaternary ammonium compounds are permanently charged, which complicates their environmental risk assessment as there is no neutral homologue for which a hydrophobicity indicator such as the commonly used octanol-water partition coefficient  $K_{OW}$  can be determined or estimated in order to perform modelling calculations. Therefore, in the scope of this project, several series of analogous ionizable alkylamines form an interesting group, since it is possible to determine the  $K_{OW}$  for their neutral form. In addition,  $K_{OW}$  for the neutral form of ionizable amines might provide some understanding on how lipophilicity is influenced by degree of N-methylation and changes in alkyl chain length. In this respect, testing series of analogous ionizable amines might provide insight into the expected lipophilicity of quaternary ammonium compounds with comparable alkyl chain lengths.



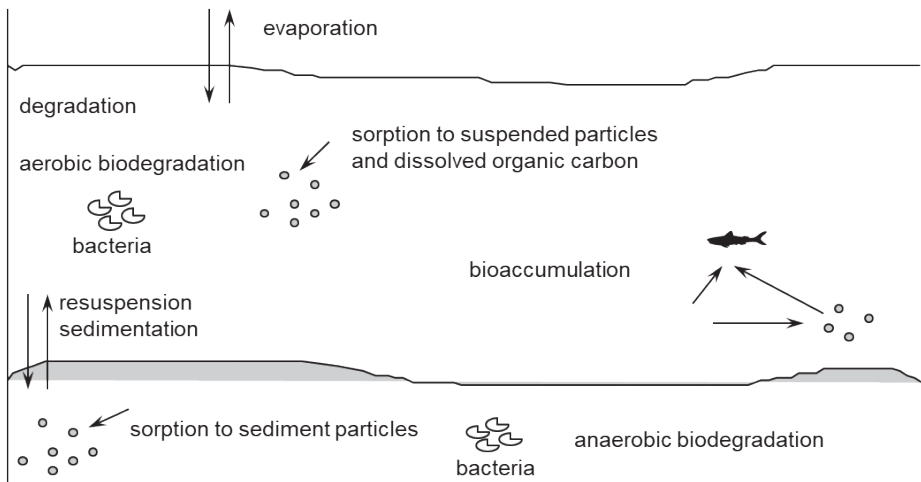
**Figure 1.3:** Examples of ionizable amines and permanently charged ammonium compounds.



Notable examples of permanently charged cationic surfactants are alkyltrimethylammonium compounds (ATMAC), benzalkonium compounds (BAC), cetylpyridinium compounds (CPB or CPC), and ammonium compounds with more than one alkyl chain (e.g. DODMAC) [17, 36, 37]. Figure 1.3 shows the chemical structure for some of these cationic surfactants. Detectable levels of surfactants can remain in sewage sludge or effluent after wastewater treatment [38, 39]. For cationic surfactants with longer alkyl chain lengths concentrations are 3-300 mg/kg in sewage sludge [40], 1-50 µg/L in river water [41], 10-100 µg/L in industrial effluent [42], and 1-10 mg/kg in sediments [42, 43].

#### 1.4. Sorption and Bioavailability in the Environment

Sorption is an important process governing environmental risk assessment, as it can have tremendous effects on the distribution of a chemical among different compartments in the environment, including the aqueous phase, soil, sediment and biota. An overview of these processes – which include evaporation, chemical degradation, microbial degradation, sorption and accumulation – is given in figure 1.4.



**Figure 1.4:** Overview of processes in the environment which are relevant for environmental fate, bioavailability, and exposure.

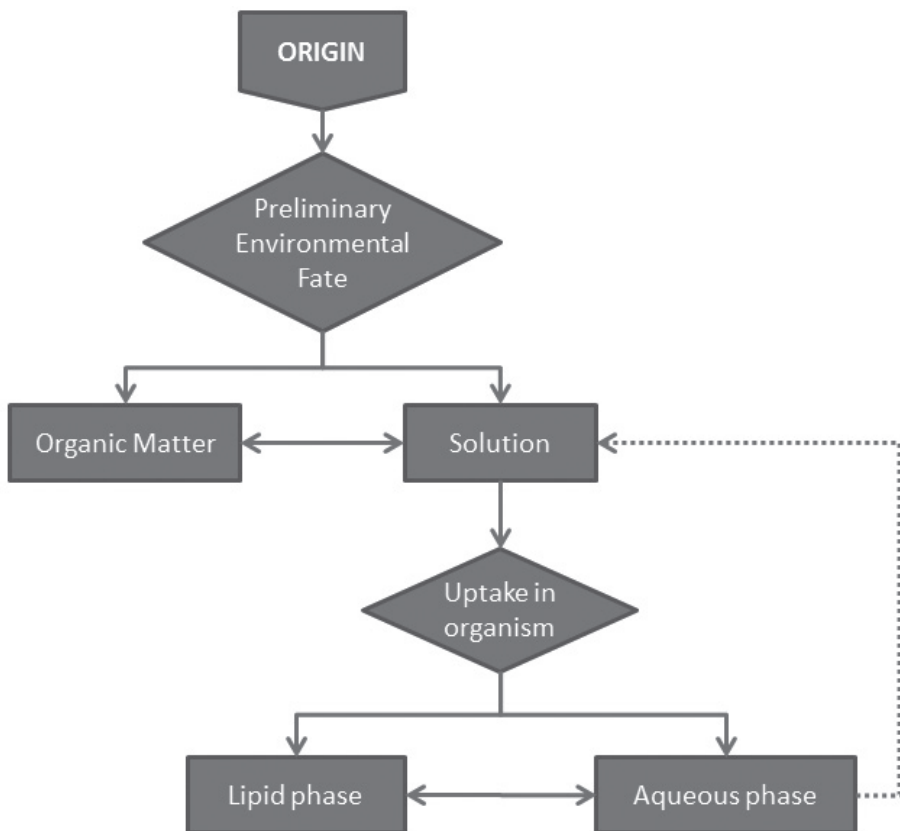
Information about dissolved organic matter in lake or river water, and the fraction of organic carbon in sediment or soil is sufficient to calculate the sorption and bioavailability of neutral chemicals [44]. Other sorption processes have to be taken into account to predict

the bioavailability of organic cations. Cations sorb to organic matter mainly because it is rich in negatively charged carboxylates that are part of a hydrophobic backbone [45, 46]. Other natural sorbents such as clay minerals are also – in essence – negatively charged structures, which can attract organic cations and thereby influence bioavailability.

Clay consists of phyllosilicates; thin sheets of aluminosilicate crystals, stacked together to form a dense and firm, semi-solid material. Mostly due to imperfections in the crystal composition (e.g.  $Mg^{2+}$  on the position of  $Al^{3+}$  or  $Al^{3+}$  on the position of  $Si^{4+}$ ) the ideally neutral layers of clay can have a relatively weak or strong negative charge. In addition, specific acidic groups on the surface of the clay sheets can dissociate when in contact with water at a certain pH, e.g. R-SiOH groups can dissociate into R-SiO<sup>-</sup>. The negative surface charge on the clay mineral surface is normally neutralized by  $K^+$  or  $Na^+$  ions, but these inorganic cations can be displaced by multivalent metal cations [47], or organic cations [48]. A convenient example of this are the industrially produced organoclays; clays treated with cationic surfactants to coat the sheets with lipophilic alkyl chains, which are then used to remediate soils or to remove organic contaminants from polluted water [49, 50]. Also in natural soil, where clay and organic matter are packed together, organic cations can have relatively strong interactions with negatively charged clay surfaces.

The interchange of inorganic and organic cations is a form of competition for a limited number of binding sites. Negatively charged sites on clay particles are commonly filled with ubiquitous ions like  $K^+$ ,  $Na^+$ ,  $Ca^{2+}$  or  $Mg^{2+}$ . Divalent metal ions usually have stronger interactions with negatively charged binding sites than, for instance,  $Na^+$  [26]. Some organic cations have stronger sorption affinities than  $Ca^{2+}$ , and competition for adsorption sites is thus a balance between sorbate concentration and relative sorption affinities, since freely dissolved concentrations of inorganic metal cations are usually orders of magnitudes higher than those of organic cations. In practice, this means that effective sorption affinity of  $BH^+$  to a sorbent is dependent on multiple factors, including the composition of the sorbent (% organic matter; clay type; particle size) as well as the aqueous phase (ionic strength, pH). Due to the negatively charged surface of naturally occurring sorbents the sorption affinity of  $BH^+$  can even be higher than that of B, even in soils and sediments with a high content of organic matter. Literature provides numerous examples of basic substances whose affinity significantly increases with decreasing pH [51-53]. With this in mind it is easy to realize that cationic surfactants, having both a positively charged headgroup and a hydrophobic alkyl chain, preferentially sorb to all kinds of environmental substrates, easily displacing inorganic cations.

Within the aqueous phase itself, sorption to dissolved organic matter and suspended particulate matter may affect bioavailability, bioaccessibility, bioaccumulation and biotic effects [54, 55], as already highlighted in figure 1.4. The sorption processes that more directly impact bioavailability of neutral chemicals are presented schematically (somewhat simplified) in figure 1.5. Particularly for strongly sorbing cationic surfactants, bioavailability is an important feature in risk assessment [56, 57]. Bioaccessibility can impact both toxicity (enhancing or decreasing exposure) as well as persistency (optimum bioaccessibility might make chemicals more susceptible to degradation by microorganisms).



**Figure 1.5:** Schematic and simplified representation of how sorption processes can impact bioavailability and exposure concentrations in the environment as well as within an organism.

After release into the environment, there is partitioning between organic matter and the aqueous phase (see figure 1.5). Ongoing exchange between these phases means that organic matter with sorbed pollutants can function as a long term reservoir, releasing additional pollutant in the aqueous phase if the dissolved concentration decreases [58]. This release of sorbed molecules back into solution is also called bioaccessibility, to distinguish this fraction from the very strongly sorbed molecules that cannot be readily released back into solution. Bioaccessibility is governed by the organic carbon-water partition coefficient  $K_{OC}$ , where the bioaccessible fraction is released to reinforce the equilibrium between sorbed fraction and freely dissolved fraction if the latter decreases, e.g. due to biodegradation, or uptake in organisms. The combination of direct exposure through pore water and semi-direct exposure of sediment dwelling organisms through ingestion of sediment particles complicates risk assessment for aquatic ecosystems [59].

The fraction of a substance that simply remains in solution is more straightforward to incorporate into risk assessment. This freely dissolved fraction will disperse through the available aqueous phase by diffusion, until a uniform concentration is reached. It is a generally accepted notion that only freely dissolved molecules are available for uptake into an organism, which makes the dissolved fraction the most important one from a risk assessment perspective; this fraction is usually called the bioavailable fraction, although a distinction should be made with pharmacological bioavailability which is a different concept. The aqueous phase is also the major phase for degradation, as dissolved molecules are available for uptake by microorganisms.

### **1.5. Prediction of Sorption, Bioavailability and Toxicity**

Predictions for (preliminary) environmental fate (see figure 1.5) are based almost entirely upon octanol-water partitioning and the resulting  $K_{OW}$  partition coefficient [60]. Since scientific evidence supports the notion that the affinity for organic matter in soil is related to the affinity for octanol, models used in risk assessment usually calculate  $K_{OC}$  – the organic carbon normalized partition coefficient – from  $K_{OW}$  [61]. This means that, for neutral chemicals, sorption and bioavailability are generally estimated based on the  $K_{OW}$ .

The next link between exposure and toxic effects on an individual level is uptake into an organism. Uptake is divided between fat and fluids, defined in figure 1.5 as *lipid phase* and *aqueous phase*, respectively. Cell membranes are also composed of lipids (phospholipids), and form a critical target for nonspecific toxicity of any organic chemical.

Since risk assessment is dedicated to neutral molecules, partitioning between bulk water and the organism's lipid compartment – and also toxicological effects – are modeled using the established relationship between  $K_{OW}$  and bioconcentration factor (BCF), and toxic effect concentrations ( $IC_{50}/LC_{50}$ , i.e. the (nominal) concentration at which inhibitory or, respectively, lethal effects are observed in 50% of the exposed population). These types of models are available for well-known model organisms such as the water flea and fathead minnow [62]. As expected, these  $K_{OW}$ -based models are poorly capable of dealing with cationic surfactants and ionizable molecules in general. Furthermore, risk assessment based on exposure is complicated by the fact that it can be extremely difficult to accurately determine actual exposure in controlled experimental studies, especially when dealing with ionizable chemicals that are prone to sorb to all kinds of surfaces, including lab equipment (e.g. cationic surfactants).

To overcome the issues with  $K_{OW}$ -based approaches, some models to estimate or predict uptake of organic chemicals into organisms have been developed explicitly for ionizable or cationic chemicals, such as the octanol-water distribution coefficient-based (log D) bioconcentration model postulated by Fu et al. [63], a model based on estimated membrane distribution coefficients by Armitage et al. [64], and a quantum chemical based model for monovalent organic ions in fish [55]. However, the concept of log D is prone to some of the same erroneous assumptions that decrease the applicability of  $K_{OW}$ -based models [64]. Therefore, models have also been constructed based on liposome partitioning coefficients ( $K_{PLIPW}$ ), using artificially constructed vesicles made up of phospholipids that are also the main building block for actual cellular membranes [65]. Neuwoehner et al. developed an elegant model combining  $K_{PLIPW}$ -based partitioning prediction that includes an ion-trapping hypothesis, where differences between intracellular and extracellular pH lead to intracellular accumulation of ionizable amines [66]. This ion-trapping is yet another aspect of toxicity that is exclusively applicable to ionizable chemicals, and can have great influence on legitimate toxic effects while it is completely absent from  $K_{OW}$ -based risk assessment regimes.

In addition to the complex sorption behavior of organic ions in organic matter and sediments, also the partitioning of ionic chemicals into organisms is much more complex than for neutral chemicals. Firstly, the ionized species can have different partitioning behavior than the neutral molecule, which means that there is a fixed partitioning coefficient for the neutral fraction and a pH-dependent partitioning coefficient for the ionized fraction. Although it is generally considered that ionized molecules are not able to

cross biological membranes [67], there is ample evidence to support the opposite [66, 68, 69], and even minute neutral fractions may facilitate passive transport across membranes. In addition, for toxic effects to become apparent it is technically not even necessary for a chemical to be taken up into intracellular compartments; uptake into the phospholipid membrane can be sufficient to cause toxicity [70-72], both for unicellular organisms as well as directly exposed organs like eyes, gills, and the gut. This is especially relevant for cationic surfactants, as the majority of these chemicals have a structure resembling the phospholipids that make up cellular membranes, and are therefore able to be taken up into the cell membrane, thereby disrupting or even destroying these vital membranes [73, 74]. This is highlighted by publications describing toxic effects to bacteria and mammalian cell lines [75], rabbit corneal epithelial cells [76], and isolated human lymphocytes [77].

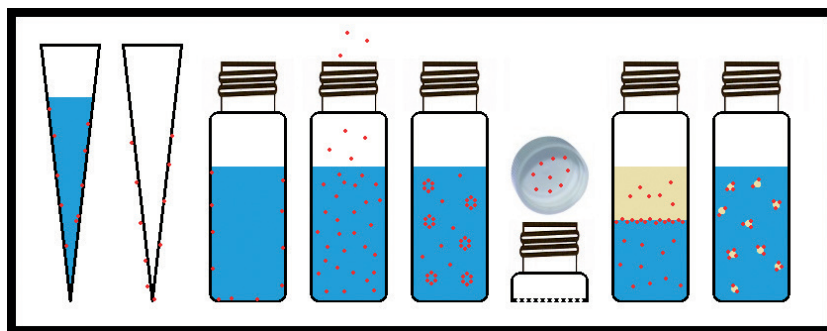
## **2. Sorption and Analytics**

### **2.1. Sorption to Labware**

Surfactants in general and cationic surfactants in particular are prone to have strong sorption affinities to a multitude of environmental and artificial surfaces, including labware and even components of analytical equipment e.g. autosamplers [57, 78-80]. It is also well known that surfactants can accumulate on gas-liquid, liquid-liquid, and liquid-solid interfaces. Negatively charged surfaces such as laboratory glassware, well-plate plastic, soil particles, dissolved organic matter, and biomolecules such as proteins provide additional sorption sites for cationic surfactants [54, 78], and most of these surfaces cannot be avoided in experimental work. Figure 1.6 provides an overview of the most relevant potential losses when working with cationic surfactants and illustrates the difficulties of working accurately with these difficult chemicals; most processes in this figure are related to sorption. Cationic surfactants are even known to sorb to polytetrafluoroethylene (PTFE) lined septa and PTFE containers [81, 82], as well as negatively impacting efficiency of electrospray ionization as used in MS/MS equipment [83].

Most of the aforementioned examples of sorption are expected to increase with hydrophobicity e.g. length of the alkyl chain surfactant tail [84], making the long chain cationic surfactants extremely challenging to work with. Binding to relatively simple surfaces such as laboratory glassware is hypothesized to be dependent on salinity and presence of multivalent cations, with an increase in salinity or concentration of multivalent cations resulting in lower glass binding due to electrostatic screening and competition

effects [24, 78, 85-87]. However, for environmental risk assessment it is rarely possible to adjust concentration and valence of electrolytes, and care should be taken to evaluate and, if necessary, quantify the (potential) impact on experimental outcome by losses through sorption. Lastly, it should also be considered that cationic surfactants could sorb to pipette tips, and might quickly desorb if the pipette tip comes into contact with solvents. Even the quantification steps to measure experimental losses may thus be influenced by sorption processes.



**Figure 1.6:** Overview of major sources of potential losses when working with cationic surfactants. From left to right: sorption to inside of pipette tip; sorption to outside of pipette tip; sorption to glass wall; evaporation; micelle formation; sorption to septa; phase separation and sorption to interface; sorption to dissolved matter.

## 2.2. Introduction SPME and mixed-mode SPME

Solid-phase microextraction (SPME) is an analytical sampling technique, developed by Arthur and Pawliszyn in 1990 as a faster and cleaner alternative for then-existing sampling and extraction techniques [88]. SPME, as the name implies, typically works with samplers in the 100  $\mu\text{L}$  range, where the goal is not exhaustive sampling but sampling at equilibrium and then using a fiber-water partitioning coefficient to calculate the corresponding concentration in the aqueous phase. Therefore, under favorable conditions, sampling with SPME will not influence the system being sampled, allowing – for instance – repeated sampling from the same replicate [67], or immersion of SPME samplers in an ongoing experiment. The concept of sampling so little solute that the system remains unaffected is known as negligible depletion SPME (nd-SPME) [89, 90]; since the work presented in this thesis only focuses on nd-SPME the shortened abbreviation SPME will be used to refer to nd-SPME.

SPME is typically carried out using thin fibers, usually consisting of an inert core (glass or metal), coated with a polymer that is the actual solid extraction phase. This SPME-fiber is then introduced into the matrix containing the analyte. Although this matrix might include binding molecules such as proteins or humic substances, only the freely dissolved fraction of the analyte is sampled. In general, sampling is deemed complete once equilibrium between the SPME-fiber and the matrix is reached. At equilibrium, the fiber concentration ( $C_{\text{fiber}}$ ) correlates to the freely dissolved concentration in the sampled matrix ( $C_{\text{free}}$ ) [91]. This relationship between  $C_{\text{fiber}}$  and  $C_{\text{free}}$  is called the fiber-water partitioning coefficient ( $K_{\text{FW}}$ ), and is compound as well as matrix specific, while also depending on coating type and fiber dimensions [92].

SPME is currently broadly used to measure polar and non-polar analytes in a range of different matrices [93-96]. More recently, polyacrylate (PA) SPME has also been applied to sample quaternary ammonium based cationic surfactants [78, 97]. PA-coated SPME fibers have sufficient cation-exchange capacity (CEC) to effectively adsorb several nitrogen-based cationic surfactants to the fiber surface, while providing non-depletive extraction in most samples [54, 78]. PA-SPME has specific benefits when dealing with environmental samples: (i) the SPME coating is in direct equilibrium with  $C_{\text{free}}$ , (ii) the small fiber volume (extraction phase) leads to selective isolation of analytes, resulting in relatively clean samples which can be analyzed without matrix effects, (iii) pH-modification of samples to neutralize bases is not required for quantitative purposes since PA-SPME has sufficient affinity for positively charged species and can be calibrated at the required sample pH, (iv) the fiber structure eliminates problems related to typical sample clean-up steps using SPE or filter cartridges, such as solid phase clogging with suspensions and breakthrough volume with voluminous samples [98].

### **3. Bioavailability, Membrane Partitioning, and *in vitro* Toxicity**

In environmental sciences, a molecule is deemed bioavailable if it can readily be taken up into an organism, i.e. as a freely dissolved molecule passing skin, gill, gut, or even only a single cell membrane. This is to separate the fraction or concentration available for uptake from the fraction not directly accessible by an organism [99], e.g. the molecules sorbed to soil and sediment, or to particulate matter in the aqueous phase. Bioavailability is an important concept, as it is an essential link between the hazard – intrinsic quality of a given toxicant – and the associated risk (the chance the hazard will express itself) [100].



Unsurprisingly, there is a relation between CEC of soil and sediment, and observed toxicity thresholds in soil and sediment dwelling organisms [56].

### 3.1. Bioavailability and *in vitro* Toxicity of Ionized Molecules

The prevalent consensus in environmental risk assessment legislation is that only neutral molecules are available for uptake into an organism i.e. bioavailability is determined by the neutral fraction [61, 101]. For organic bases, uptake rates start decreasing when pH approaches the pKa, but this decrease levels off as pH gets lower [102], although the neutral fraction can drop by two orders of magnitude over two pH units [103]. Bioavailability of ionized species is further established by uptake rates under experimental conditions, where total uptake is larger than what could be attained by uptake of solely the neutral fraction [104]. For adequate risk assessment it is important to realize which factors influence bioavailability, and how these factors vary between neutral molecules and ionized species [55].

Accurately determining bioavailability in *in vitro* test systems can be more complicated than in traditional *in vivo* test setups, especially for cationic organic molecules and strongly sorbing chemicals such as surfactants. The cell culture medium is essentially the liquid phase (e.g. blood) that is usually sampled in traditional test setups to determine bioavailability. However, due to the small test volumes (usually <1 mL and <200  $\mu$ L in most setups) and low concentrations it is difficult to sample the volumes required for proper chemical analysis. Additional complications arise from the fact that cell culture medium generally contains high concentrations of buffer salts and proteins, which interfere with virtually all types of column chromatography. Sample preparation with traditional extraction techniques is hindered by the low sample volumes, which makes SPME an excellent candidate to determine bioavailability in *in vitro* assays.

### 3.2. Using $K_{OW}$ and $K_{MW}/K_{PLIPW}$

Current models rely heavily on the octanol-water partition coefficient  $K_{OW}$  as a determinant for both environmental fate and baseline toxicity.  $K_{OW}$  is a sensible choice to predict the behavior of neutral molecules [7], but the octanol-water system is unable to support specific interactions possible with ionized chemicals, for instance their interactions with biological membranes and negatively charged surfaces [105]. Although octanol is a fair proxy for storage lipid, actual organisms are also made up of membrane lipids and proteins.

Even though the triglyceride composition of storage lipids has no significant influence on partitioning [106], partition coefficients for neutral organic chemicals can be up to two log units higher for membrane lipids than for storage lipids [7]. This is a well-known notion in forensic toxicology, where lipophilic and cationic chemicals are known to accumulate in tissues rich in phospholipids, such as the liver [107]. In addition,  $K_{OW}$  values obtained for ionizable molecules are dependent on test system pH and ionic strength, as well as the method used [108]. Therefore, it would be wise to explore other avenues – such as partitioning into biolipids – when dealing with ionizable chemicals, especially since  $K_{OW}$  is difficult to determine for ionized molecules and surfactants in particular [109].

Even though diffusion of charged molecules through lipid membranes is not predicted based on octanol-water partitioning, it is clear that charged species partition more strongly into biomembranes than anticipated from octanol-based predictions [110-113]. Although octanol can be a useful model system for neutral chemicals, it is not possible to predict ionic interactions in biological membranes based on  $K_{OW}$  [113]. In addition, also neutral hydrophilic pharmaceuticals like atenolol and morphine can partition more easily into membranes than suggested by  $K_{OW}$  predictions [110]. The amphiphilic nature of surfactants not only makes it very challenging to determine or predict their  $K_{OW}$  [109], it also means they resemble the phospholipids that make up biological membranes, which also have amphiphilic properties. This resemblance may further increase their membrane affinity beyond what might be expected based on  $K_{OW}$ , because they can effectively align parallel to the structured phospholipids in cell membrane bilayers [114]. An important realization in this aspect is the fact that the most abundant phospholipids are zwitterionic phosphatidylcholines, with a positively charged choline group near the aqueous phase and a negatively charged phosphate slightly closer to the core of the membrane [115]. Neutral chemicals will tend to sorb near the core region of the membrane, while cationic chemicals will have their charged moiety positioned in the direction of the phosphate head group, an effect known as the pH piston hypothesis [115].

Several different experimental techniques and simulations have been devised over the last two decades to provide estimated or predicted sorption coefficients to membrane lipids. Terminology to describe the obtained partitioning coefficient can vary; notable examples are  $K_{MW}$  (membrane-water),  $K_{LIPW}$  (liposome-water) and  $K_{PLIPW}$  (phospholipid-water). Experimental techniques include micellar liquid chromatography [116], equilibrium dialysis using artificially prepared liposomes [117], potentiometric titration [111], chromatographic methods using specifically created stationary phases (immobilized artificial membrane or

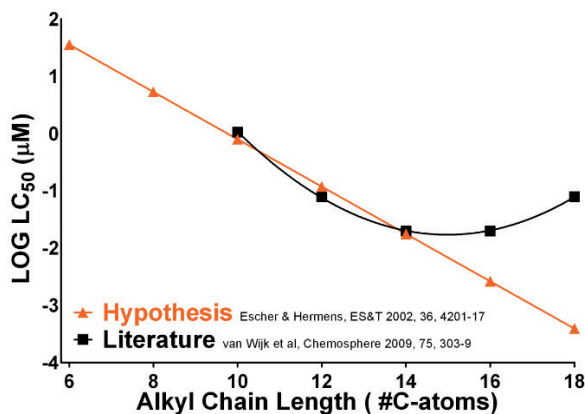
IAM-HPLC) [111, 118-122], and a coating of artificial liposomes applied to a solid support e.g. glass beads (solid-supported lipid membrane or SSLM) [111, 118]. Interestingly, a fundamental publication by Escher et al. indicated questionable suitability of IAM-HPLC for ionic chemicals [111], while later studies rated the IAM-HPLC as quite robust [121], although some refinement could be mandatory in order to obtain trustworthy results [120]. In recent years there has also been an increasing number of models to predict sorption coefficients to membrane lipids, such as molecular dynamics modelling [116], poly-parameter linear free energy relationship (pp-LFER) descriptors [123], and quantum-chemistry based calculations such as those performed by COSMOmic [116-119, 123].

### 3.3. Using $K_{MW}/K_{PLIPW}$ to Improve Predictive Models for In Vitro Toxicity Data

Narcosis – a reversible and nonspecific destabilization of biomembranes – is considered to be a common cause of environmental toxicity for chemicals that lack a specific mode of action [124]. Due to their resemblance to phospholipids, which are the major building blocks of such biomembranes, and the virtual absence of functional groups, it can be assumed that surfactants will exert their toxic effects largely through narcosis. This assumption would be especially relevant for *in vitro* test systems, which lack interconnected organ systems and most of the complexity of actual organisms and, therefore, are less susceptible to complex toxic effects. Historically, narcosis has been evaluated extensively in fish acute toxicity assays [125-128]. It therefore makes sense to evaluate *in vitro* toxicity of surfactants in a primary fish cell line, such as the rainbow trout gill cell line RTgill-W1 [129].

Using the affinity for phospholipids or biomembranes ( $K_{PLIPW}/K_{MW}$ ), it should be straightforward to predict the threshold of toxic effects for chemicals that act through narcosis, since the lethal membrane burden is calculated to be between 40-160 mmol/kg lipid [70]. In this respect, it is interesting to compare hypothesized decreases in  $LC_{50}$ , based on a QSAR presented for polar chemicals by Escher and Hermens [130], with experimentally determined algal toxicity of cationic surfactants by van Wijk et al. [57] (see figure 1.7). While theory predicts incrementally lower  $LC_{50}$ , experimentally observed toxicity levels off and even start to decrease at progressively longer alkyl chain lengths. Such effects have been observed more often [131-135], and a mechanistic explanation has been postulated by Balgavý and Devínský [132]. Should a similar plateau be observed for experimentally derived or predicted  $K_{MW}/K_{PLIPW}$  values, this would provide evidence the results observed are not an artefact. However, if such a plateau is not observed with  $K_{MW}/K_{PLIPW}$  data this

would be an indication that experimental techniques and actual exposure concentrations should be evaluated critically. This statement is especially relevant for cationic surfactants, as it can be expected that these chemicals are progressively more difficult to sample and analyze with increasing alkyl chain lengths, while the potential of losses to the exposure system are likely to increase as well.



**Figure 1.7:** Illustration how modeled  $LC_{50}$  data based on a QSAR for polar chemicals deviate from actual  $LC_{50}$  data for cationic surfactants from literature. Based on data from Escher and Hermens [130], and van Wijk et al. [57].

## 4. Bioavailability and Biodegradation

### 4.1. Linking Sorption and Exposure

Strong sorption can decrease exposure through decreasing bioavailable concentrations, while at the same time increasing exposure duration and persistency for strongly but reversibly sorbing chemicals. Chemicals that are highly persistent as well as strongly sorbing are detected in the environment and in sewage sludge, up to the mg/kg range [40]. Numerous cationic surfactants falling in this category have been banned or have had their production decreased by industry voluntarily [40]. The di-alkyl-based surfactant DODMAC/DTDMAC has been largely replaced by the di-ester analogue DEEDMAC in rinse conditioner products [136]. The ester moieties connecting the two alkyl chains to the central ammonium moiety can be hydrolyzed, resulting in fast removal by biodegradation. DEEDMAC is therefore considered non-persistent [137, 138].

Pollutants from sewage can reach the environment through a number of pathways, with most of these pathways linked to sorption processes as far as cationic surfactants are concerned. The most direct pathway is residual contamination of effluent, when after sewage treatment fractions remain of substances that are – at present – technically or financially impossible to be fully removed. Numerous studies dealing with trace level detection have been performed, as reviewed by Lapworth et al. in 2012 [13]. Sewage sludge forms a second source of environmental contamination that can be traced back to waste water treatment processes. Sewage sludge is the semi-solid microbial biomass material remaining after modern industrial wastewater treatment processing. Due to its high nutritious value, sewage sludge is widely used in numerous countries as a fertilizer, a practice where liquid or dried sludge is applied to agricultural soil. However, this procedure is virtually a direct injection of sorbed contaminants into soil, since there is ample evidence that significant concentrations of many hydrophobic contaminants, including cationic surfactants, remain in sewage sludge [13, 40].

## **4.2. Introduction Biodegradation Testing**

Chemical persistence, especially of potentially toxic chemicals, is an important property in environmental risk assessment, as persistent chemicals can accumulate and be transported over great lengths in the environment. Therefore, numerous tests exist to determine the extent of biodegradation under standardized conditions [139-144], operating under the assumption that any chemical that is rapidly degraded in such tests will not be persistent in the environment. Reliable information on persistence –and thus biodegradability – is pivotal in environmental risk assessment, as even a relatively toxic chemical will carry a smaller risk if it is rapidly degraded or, alternatively, a chemical of low toxicity that is very persistent might eventually reach unsafe levels. In addition, it is logical to assume that chemicals that are easily biodegraded will not be bioaccumulative. Biodegradation testing can therefore be considered as a cornerstone of environmental risk assessment. However, the use of recommended and relatively high-test concentrations (10 mg/L range) makes it difficult to properly assess chemicals with toxic or inhibitory effects to the microorganisms used in these tests.

## **4.3. Using Sorption to Our Advantage: Toxicity Mitigation**

The preceding sections have emphasized the difficulties arising from the physicochemical behavior of cationic surfactants and surfactants in general. Conversely, if surfactants or

chemicals with surfactant-like properties are known or anticipated to have inhibitory effects to micro-organisms used in biodegradation testing, these physicochemical properties can be used advantageously. Several studies exist in which inorganic and sometimes organic sorbents are introduced to biodegradation tests, in order to lower the bioavailable concentration to below the inhibitory threshold [145-147]. This effect is called toxicity mitigation, as the inhibitory or toxic effects of the test chemical are mitigated or negated through the addition of a sorbent. Toxicity mitigation can be considered as a refinement of biodegradation testing, and – due to the importance of biodegradability and associated persistency classification in environmental risk assessment – as an enhancement of overall environmental risk assessment with respect to persistency rating. However, up to now toxicity mitigation has received relatively little attention in literature, and therefore ample opportunity remains to elucidate the most efficient method to apply toxicity mitigation.

#### **4.4. Existing Biodegradability Studies to Explore**

As important ingredients of personal care products, paints, industrial cleaning agents, drilling mud, and antiseptics, surfactants have a relatively high environmental discharge, especially due to their use in a large range of down-the-drain products [27, 29-31]. Quaternary ammonium based surfactants are the most relevant group of cationic surfactants. Biodegradability of these ammonium surfactants is known to depend on the alkyl chain length and number of alkyl chains attached to the nitrogen, with an increase in alkyl chain length or number of alkyl chains leading to a decrease in biodegradability [148]. Attempts have been made to reduce inhibitory effects and increase bioavailability through the use of organic and inorganic sorbents [145-147], and by optimizing the amount of competent microorganisms in the sludge used to inoculate the test vessels [149], although the use of such 'optimized' sludge is not allowed in most biodegradability testing guidelines. A different optimization, introduced by the industry that produces these surfactants, was to include ester bonds in previously very persistent gemini surfactants, significantly improving their biodegradability [150, 151].

More specialized test designs have also been used specifically to assess biodegradability of cationic surfactants, such as a specifically designed flow through system utilizing columns packed with silica gel and preconditioned inoculum [152], which was used to test quaternary ammonium surfactants and gemini surfactants of differing alkyl chain lengths. In another attempt to improve biodegradability testing of cationic surfactants and toxic organic chemicals in general, van Ginkel and Stroo proposed a method to prolong

the standard closed bottle test (OECD 301 D) up to 200 days [139, 153]. More recently, biodegradability of a range of nitrogen-containing surfactants (including one quaternary ammonium surfactant) was evaluated and found to be very efficient in a continuously fed activated sludge reactor (OECD 303 A), which is essentially a simulated waste water treatment plant [141, 154]. However, these setups are highly specialized, costly to maintain, and a positive result in such customized designs is not always admissible to officially classify the test chemical as readily biodegradable.

Unfortunately, a comparison of different standardized test methods showed a high degree of false negatives and limitations by the slow onset of biodegradation with test chemicals that are otherwise degraded efficiently [155]. In addition, specific studies suggest combinations of different strains of microorganisms are required for efficient breakdown of cationic surfactants and surfactants in general [156, 157], and specific strains that are capable to efficiently degrade cationic surfactants usually depend on distinct other strains in order to maximize their potential [158]. These factors make it understandable that preadapted or preconditioned inocula lead to much higher and, arguably, more environmentally relevant biodegradation rates. In this thesis it was hypothesized that addition of clay sorbents might constitute a viable alternative, as sorption of test chemical will mitigate inhibitory effects and give the microorganisms more time to flourish, while simultaneously acting as a support for the formation of a biofilm in which coexisting strains can work together optimally to degrade the test chemical [159, 160].

## 5. Scope and Objectives of this Thesis

The scope of my project was to improve environmental risk assessment for ionizable chemicals, specifically looking at cationic chemicals and surfactants in particular. The overall goals of the work in this thesis were to 1) advance understanding of the behavior of cationic surfactants, more specifically the mechanisms that underlie sorption to environmentally relevant sorbent materials e.g. sediments, and 2) determine how sorption impacts bioavailability and toxicity in biodegradation and aquatic toxicity tests. Within this context, the primary focus was on monoalkyl quaternary ammonium surfactants. In order to achieve these goals, the following objectives were identified:

1. Obtain a large and diverse set of amine-based cationic surfactants, encompassing multiple structurally diverse classes, preferably with multiple alkyl chain lengths per class.

2. Develop analytical methods to accurately and quantitatively sample and measure the surfactants obtained under 1.
3. Develop SPME tools to measure a selection of the surfactants obtained under 1, and establish the applicability domain of these SPME tools.
4. Apply the SPME tools developed under 3, to determine sorption affinity to environmentally relevant sorbent materials for a selection of the surfactants obtained under 1.
5. Apply the SPME tools developed under 3, to determine the freely dissolved concentration in toxicity assays using a selection of the surfactants obtained under 1.
6. Use the knowledge gained under 4 and 5 in innovative biodegradation and/or toxicity studies, e.g. by mitigating inhibitory effects or as a means of passive dosing.
7. Refine models linking physico-chemical properties of the surfactants obtained under 1 to the sorptive and/or toxic properties established under 4, 5 and 6.
8. Apply the data and insights resulting from this thesis to improve environmental risk assessment of cationic surfactants.

To evaluate the analytical difficulties and develop a suitable method to accurately quantify cationic surfactants from aqueous samples, we first studied extraction of a selection of 32 amine-based cationic surfactants (**Chapter 2**). The main goal was to identify where analytical challenges could be expected, both in the chemical space of cationic surfactants as well as the typical laboratory equipment used. Sorption to 120 mL flasks, 40 mL vials, and 1.5 mL autosampler vials was determined in 15 mM NaCl. Aqueous concentrations and extraction recoveries were quantified using weak cation exchange SPE cartridges, followed by analysis on LC-MS/MS. Sorption to outside of standard pipette tips was expected and was therefore also quantified for a selection of cationic surfactants. We then used the methods developed to determine sorption of several cationic surfactants to PA-SPME fibers with a coating thickness of 7  $\mu\text{m}$  or 35  $\mu\text{m}$ . The impact of pH and ionic strength of medium on partitioning to the fiber was also investigated. We used the data obtained to assess differences in sorption mechanism between charged cationic surfactants and ionizable cationic surfactants in their neutral form. Lastly, we tried to determine an applicability domain for all methods developed, looking primarily at alkyl chain length.

Based on the results obtained with the PA-SPME fibers, we then decided to investigate the suitability of mixed-mode (MM) SPME fibers to sample cationic and neutral chemicals (mainly pharmaceutical compounds) (**Chapter 3**). We used fibers consisting of a nitinol wire coated with a mixed sorbent containing  $\text{C}_{18}$  material as well as strong cation exchange



(SCX) groups. In total, 30 chemicals were tested, covering a broad  $pK_a$  range and with varying hydrogen bonding capability. The main aim of this work was to define the structural limitations of the MM-SPME fibers for this category of analytes. In order to do so, linearity of sorption isotherms and a cut-off point below which all tested chemicals showed linear sorption were determined. In addition, the impact of alkyl chain length on sorption affinity of chemicals with limited hydrogen bonding capacity was investigated and related to octanol-water partition coefficients. Implications for the applicability of MM-SPME to sample relatively small or large molecules could then be determined, which was helpful to assess suitability of MM-SPME for further studies within the scope of this thesis. Lastly, the data gathered for the 30 chemicals tested were used to conclude on the suitability of MM-SPME to sample freely dissolved concentrations of ionizable chemicals.

The original scope of this thesis was to then apply SPME to determine the freely dissolved concentration in *in vitro* toxicity assays with a set of benzalkonium compounds with increasing alkyl chain lengths (**Chapter 4**). However, due to the limitations identified in the chapter 2 and 3, it was decided to perform these studies without using SPME. The main aim of this chapter was to elucidate how sorption of benzalkonium compounds to different components of *in vitro* test systems would impact their apparent toxicity, and how alkyl chain length influences this impact. Seven benzalkonium compounds, with alkyl chain lengths ranging from 6 to 18 carbon atoms, were tested using the rainbow trout gill cell line. Toxicity readings after a 48 hour exposure in medium with 0.6  $\mu\text{M}$  bovine serum albumin, 10% fetal bovine serum, or without any additions were compared. Benzalkonium concentrations were determined analytically and compared with nominal concentrations. Median effect concentrations ( $EC_{50}$ ) calculated with measured and nominal concentrations could then be compared to elucidate the effect of sorption on apparent toxicity rating. Differences between nominal and measured  $EC_{50}$  were also related to alkyl chain length, to allow evaluation of our findings in perspective of alkyl chain length dependent processes discovered in the first two chapters.

Amine-based cationic surfactants based on a singly alkyl chain are unlikely to have a specific toxic mode of action, and probably exert toxic effects due to membrane destabilization. In order to put the findings of the *in vitro* toxicity study in perspective, we therefore decided to determine the cell membrane binding affinity for a series of 19 cationic surfactants, including several benzalkonium compounds (**Chapter 5**). We used a solid-supported lipid membrane (SSLM) system, with fused silica beads coated with a bilayer phospholipid membrane. We tried to optimize the existing SSLM protocol by

transferring the coated beads from 96-well plates to 1.5 mL autosampler vials, in order to correct for several confounding effects due to phospholipid leaching and the specific difficulties encountered with cationic surfactants in the first few chapters. We determined membrane/water distribution coefficients ( $D_{MW}$ ) at different pH to assess the contribution of ionized and neutral species. SSLM measurements were compared with immobilized artificial membrane (IAM) HPLC and quantum chemistry-based calculations performed using COSMOmic. By testing several series of chemicals with increasing alkyl chain lengths, we tried to establish the applicability domain for SSLM when determining  $D_{MW}$  of cationic surfactants.

Finally, the knowledge gained in chapters 2 through 5 was applied in biodegradation studies with two biocidal  $C_{16}$ -based cationic surfactants: cetyltrimethylammonium bromide (CTAB) and cetylpyridinium chloride (CPC). CTAB has been demonstrated to cause toxicity to inoculum during biodegradation testing, while no peer reviewed biodegradation studies have been published for the commonly used antiseptic CPC. The aim of these studies was to develop and evaluate a systematic testing approach to incrementally optimize bioavailability or bioaccessibility for biodegradation studies with cationic surfactants. This directly incorporated the insights gained on sorptive potential and expected toxicity of cationic surfactants, and recent developments of automated continuous digital manometric detectors. Potentially more efficient biodegradation test designs could be defined compared to the standard test designs with *a priori* uncertain outcomes. In the first stage, the use of silicon dioxide ( $SiO_2$ ) and commercial illite clay (illite) to mitigate inhibitory effects was investigated (**Chapter 6 and 7**). It was observed in the analytical and *in vitro* studies that cationic surfactants with relatively long alkyl chain lengths sorb relatively strong to available substrates, decreasing freely dissolved concentrations. We hypothesized that this mechanism could be employed beneficially in biodegradation studies. Our goal was to investigate if it was possible, with data on inhibitory effect levels and sorption affinity to the used sorbent, to match a certain concentration of sorbent with a given concentration of test chemical and end up with a freely dissolved concentration that would no longer exert inhibitory effects. Several experiments were performed to further perfect this stepwise approach. Finally, to test the general applicability of this approach seven different clay types were tested extensively with CTAB and CPC (**Chapter 8**). Ultimately, my findings were evaluated, discussed, and integrated in the context of environmental risk assessment in **Chapter 9**, with primary focus on the order-of-magnitude miscalculations that can arise if not properly taking into account the specific challenges when dealing with cationic surfactants.





# CHAPTER 2

---

## Evaluating Solid Phase (Micro-) Extraction Tools to Analyze Freely Ionizable and Permanently Charged Cationic Surfactants

Niels Timmer<sup>1</sup>, Peter Scherpenisse<sup>1</sup>,  
Joop L.M. Hermens<sup>1</sup> and Steven T.J. Droge<sup>1,2</sup>

<sup>1</sup>Institute for Risk Assessment Sciences, Utrecht University, P.O. Box 80177, 3508 TD Utrecht, the Netherlands.

<sup>2</sup>Institute for Biodiversity and Ecosystem Dynamics, Department Freshwater and Marine Ecology, P.O. Box 94248, 1090 GE Amsterdam, The Netherlands

**Keywords:** WCX-SPE, cationic surfactants, quaternary ammonium compounds, glass binding, PA-SPME, LC-MS/MS, pH-dependent sorption, passive sampling, sample preparation.

**Analytica Chimica Acta, 1002, 26-38 (2018)**

## Abstract

For a selection of 32 amine based cationic surfactants (including C8 to C18 alkylamines, C14 dialkyldimethylammonium, C8-tetraalkylammonium, benzalkonium and pyridinium compounds), the extraction from aqueous samples was studied in detail. Aqueous concentrations were determined using solid phase extraction (SPE; 3 mL/60 mg Oasis WCX-SPE cartridges) with recoveries of  $\geq 80\%$  for 30 compounds, and  $\geq 90\%$  for 16 compounds. Sorption to glassware was evaluated in 120 mL flasks, 40 mL vials and 1.5 mL autosampler vials, using 15 mM NaCl, where the glass binding of simple primary amines and quaternary ammonium compounds increased with alkyl chain length. Sorption to the outside of pipette tips ( $\leq 20\%$  of total amount in solution) when sampling aqueous solutions may interfere with accurate measurements. Polyacrylate solid phase microextraction (PA-SPME) fibers with two coating thicknesses (7 and 35  $\mu\text{m}$ ) were tested as potential extraction devices. The uptake kinetics, pH-dependence and influence of ionic strength on sorption to PA fibers were studied. Changing medium from 100 mM  $\text{Na}^+$  to 10 mM  $\text{Ca}^{2+}$  decreases  $K_{\text{f,w}}$  with one order of magnitude. Results indicate that for PA-SPME neutral amines are absorbed rather than adsorbed, although the exact sorption mechanism remains to be elucidated. Further research remains necessary to establish a definitive applicability domain for PA-SPME. However, results indicate that alkyl chain lengths  $\geq 14$  carbon atoms and multiple alkyl chains become problematic. A calibration curve should always be measured together with the samples. In conclusion, it seems that for amine based surfactants PA-SPME does not provide the reliability and reproducibility necessary for precise sorption experiments, specifically for alkyl chain lengths beyond 12 carbon atoms.

## Introduction

Cationic surfactants are commercially important compounds with diverse applications in industrial and household preparations such as detergents, preservatives, antiseptics, fabric softeners, and personal care products [161, 162]. The combination of a positively charged head group and one or more hydrophobic alkyl chains gives cationic surfactants their amphiphilic properties. It is well known that these cationic surfactants have a strong sorption affinity to different kinds of surfaces [163], and they are acknowledged as emerging contaminants in sewage sludge and sediments [164]. In environmental risk assessment, sorption is an important parameter that has an effect on the distribution of a compound among different compartments in the environment, including the aqueous phase, soil, sediment and biota. Within the aqueous phase itself, sorption to dissolved organic matter may affect the bioavailability, bioaccumulation and effects on biota [54]. Particularly for strongly sorbing cationic surfactants, bioavailability is an important feature in risk assessment [56, 163]

Within the context of bioavailability, the concept is that only freely dissolved molecules can cross biomembranes, and only the freely dissolved external concentration ( $C_{free}$ ) will equilibrate with the internal tissue concentrations to exert (adverse) effects [165-167]. Solid-phase microextraction (SPME) is broadly used to measure the  $C_{free}$  of polar and non-polar analytes in a range of different matrices [93-96]. More recently, polyacrylate (PA) SPME has also been applied to sample quaternary ammonium based cationic surfactants [78, 97]. PA-coated SPME fibers have sufficient cation exchange capacity (CEC) to effectively adsorb several nitrogen-based cationic surfactants to the fiber surface, whereas the CEC is low enough to prevent depletive extraction in most samples [54, 78]. PA-SPME has specific benefits when dealing with environmental samples: (i) the SPME coating is in direct equilibrium with  $C_{free}$ , (ii) the small fiber volume (extraction phase) leads to selective isolation of analytes, resulting in relatively clean samples which can be analyzed without matrix effects, (iii) pH-modification of samples is not required for quantitative purposes since PA-SPME has sufficient affinity for positively charged species and can be calibrated at the required sample pH, (iv) the fiber structure eliminates problems related to typical sample clean-up steps using SPE or filter cartridges, such as solid phase clogging with suspensions and breakthrough volume with voluminous samples [98]. Thin film SPME (TFME) is a relatively new technique that has also been applied to sample cationic surfactants [168]. A detailed optimization of the TFME procedure was presented, including the evaluation of matrix effects [168]. TFME is mostly a depletive extraction technique,

while for some situations non-depletive sampling might be preferable. Liquid-phase microextraction (LPME) has also been suggested for analysis of cationic surfactants, but preparation of LPME is more time consuming and the applicability is less versatile [169]. PA-SPME opens the possibility of non-depletive sampling and can also be applied offline, for instance during toxicity testing or when sampling multiple phases in a closed system (anaerobic sediment, aerobic sediment, supernatant). However, the sorption coefficient to the PA-SPME fiber has to be carefully calibrated for each cationic surfactant in every medium of interest.

The main aim of this chapter was to elucidate the challenges and limitations when using PA-SPME to sample the  $C_{\text{free}}$  of a wide range of cationic surfactants, thereby determining the boundaries of the applicability domain. Cationic surfactants were selected based on structural diversity and environmental relevance. Whereas previous studies with PA-SPME were limited to permanently charged quaternary ammonium compounds (QACs), the current study also included primary, secondary and tertiary amines, as well as several other types of QACs. Ionizable amines were included specifically as they exist partly as ionized and neutral species, depending on the pH, which may affect their affinity for PA-SPME [97, 170].

It is well known that working with – and analysis of – cationic surfactants can be problematic, in the sense that aqueous concentrations are difficult to control. Losses can be expected from accumulation on gas-liquid or liquid-solid interfaces, and adsorption to negatively charged surfaces such as glassware, dissolved organic matter, clay particles, and biomolecules [54, 78]. Significant binding to glassware and other laboratory equipment can be expected [54], as well as sorption to PTFE lined septa and surfaces [81, 82]. Furthermore, the efficiency of electrospray ionization frequently employed with MS/MS analyses can be influenced by surfactants in a concentration-dependent matter [83].

In order to more easily determine and confirm aqueous concentrations in SPME calibration studies and adsorptive studies with laboratory equipment, this study tested the performance of a weak cation exchange solid phase extraction (WCX-SPE) cartridge for a wide range of cationic surfactants. In addition, sorption losses to glass vials and pipette tips was studied to assess flaws in experimental procedures and to design special methods to sample cationic surfactants most adequately. Sorption to glass was measured with five primary alkylamines (chain length range  $C_{10-18}$ ) and five quaternary alkyltrimethylammonium compounds (chain length range  $C_{10-18}$ ). Sorption was expected



to increase with increasing chain length [84], which makes working with the longest chain cationics extremely challenging. Therefore, one of the objectives was to identify the boundaries for application of SPE and PA-SPME with respect to longer alkyl chain isomers.

Combining findings regarding glass binding and SPE, the recovery of WCX-SPE was measured for all test chemicals. WCX-SPE was then used to measure aqueous concentrations when calibrating PA-SPME fibers in different matrices. Calibration under different conditions opens the possibility to determine fiber-water sorption affinity ( $K_{fw}$ ) as a function of exposure time, analyte concentration, pH or ionic composition, and reproducibility of the PA-SPME batch applied. Measuring  $K_{fw}$  of structural homologues could also lead to better understanding of the contribution of molecular structure to  $K_{fw}$  for PA-SPME fibers. The conclusions presented could guide future studies on the use of PA-SPME in environmental and toxicological studies for (hydrophobic) cationic surfactants.

## Materials and Methods

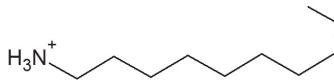
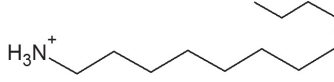
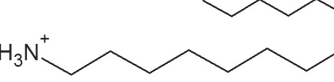
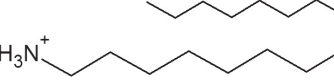
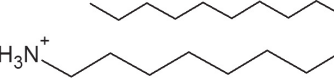
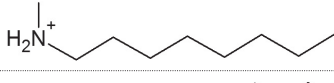
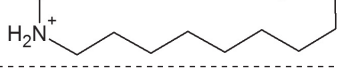
### Selection of chemicals

An overview of the 32 selected compounds is given in Table 2.1. In their simplest form, these amines contain one alkyl chain (primary amines "P10, P12, P14, P16, P18"), and in addition one (secondary amines "S10, S12, S18"), two (tertiary amines "T10, T16") or three (quaternary ammonium "Q10, Q12, Q14, Q16, Q18") methyl groups. Tertiary diethanolamines ("2EtOH-T8,-T12,-T18"), benzalkonium ("BAQ-12,-14,-16,-18") and pyridinium ("PYR12,-16") compounds were added because of their environmental significance, and to evaluate the influence of more complex functional groups on sorption behavior. Amines with multiple alkyl chains were also included; secondary dialkylamine "S2-C10", tertiary trialkylamines ("T3-C8, T3-C12"), quaternary dialkyldimethylammonium ("Q2-C10, Q2-C12, Q2-C14") and tetraalkylammonium ("Q4-C8"). These amines with multiple alkyl chains are more hydrophobic than most single chain surfactants and constitute a challenge from an experimental and analytical perspective, because of their relatively stronger adsorptive properties. Amines with two long alkyl chains are widely used in various applications [36, 171], and it is of specific interest to determine how the second alkyl chain influences sorption in comparison to single chain surfactants.

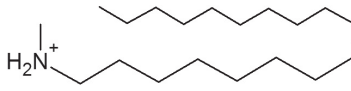
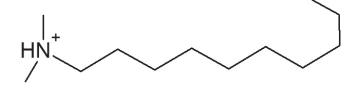
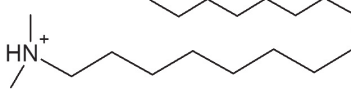
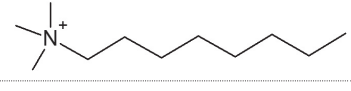
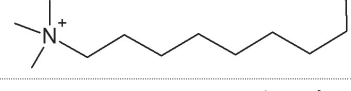
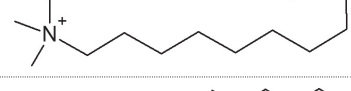
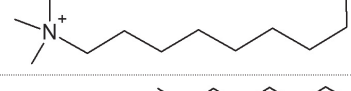
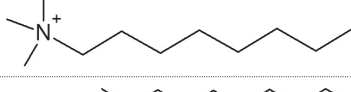
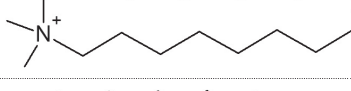
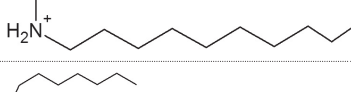
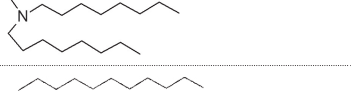
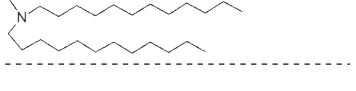
## Chemicals and other materials

The molecular structures, suppliers, purities and physico-chemical properties of the 32 amine based cationic surfactants are listed in the supporting information (table S1). Buffer salts and other salts were of analytical grade and were obtained from Merck (Darmstadt, Germany), except for  $\text{CaCl}_2$  which was obtained from Sigma-Aldrich (Zwijndrecht, The Netherlands). Trifluoroacetic acid (TFA) and formic acid (FA) were also obtained from Sigma-Aldrich. All aqueous solutions were prepared using MilliQ ultrapure water ( $>18.2 \text{ M}\Omega\text{-cm}^{-1}$ , Millipore, Amsterdam, The Netherlands). Methanol (analytical grade) was obtained from BioSolve (Valkenswaard, The Netherlands). Aqueous concentrations of surfactants were determined using solid phase extraction (SPE), utilizing 3 mL/60 mg OASIS weak cation-exchange cartridges (WCX-SPE), obtained from Waters (Etten-Leur, The Netherlands). The 7  $\mu\text{m}$  and 35  $\mu\text{m}$  coated solid phase micro-extraction (SPME) fibers were obtained from Polymicro Technologies (Phoenix, AZ, USA), from a different batch than those applied in studies by Wang et al. and Chen et al. [78, 97, 172]

**Table 2.1.** Overview of test chemicals.

Chemical name	Code	Molecular structure
Decylamine	P10	
Dodecylamine	P12	
Tetradecylamine	P14	
Hexadecylamine	P16	
Octadecylamine	P18	
N-methyl-1-octanamine	S8	
N-methyl-1-dodecanamine	S12	

**Table 2.1.** (Continued)

Chemical name	Code	Molecular structure
N-methyl-1-octadecanamine	S18	
N,N-dimethyl-1-decanamine	T10	
N,N-dimethyl-1-hexadecanamine	T16	
N,N,N-trimethyl-1-octanaminium bromide	Q8	
N,N,N-trimethyl-1-decanaminium bromide	Q10	
N,N,N-trimethyl-1-dodecanaminium chloride	Q12	
N,N,N-trimethyl-1-tetradecanaminium chloride	Q14	
N,N,N-trimethyl-1-hexadecanaminium chloride	Q16	
N,N,N-trimethyl-1-octadecanaminium chloride	Q18	
N-decyl-1-decanamine	S2-C10	
N,N-dioctyl-1-octan-1-amine	T3-C8	
N,N-didodecyl-1-dodecan-1-amine	T3-C12	

**Table 2.1.** (Continued)

Chemical name	Code	Molecular structure
N,N-didecyl-N,N-dimethylammonium bromide	<b>Q2-C10</b>	
N,N-didodecyl-N,N-dimethylammonium bromide	<b>Q2-C12</b>	
N,N-ditetradecyl-N,N-dimethylammonium bromide	<b>Q2-C14</b>	
N,N,N-trioctyl-1-octanaminium bromide	<b>Q4-C8</b>	
N,N-dimethyl-N-dodecylbenzylaminium chloride	<b>BAQ12</b>	
N,N-dimethyl-N-tetradecylbenzylaminium chloride	<b>BAQ14</b>	
N,N-dimethyl-N-hexadecylbenzylaminium chloride	<b>BAQ16</b>	
N,N-dimethyl-N-octadecylbenzylaminium chloride	<b>BAQ18</b>	
1-N-dodecylpyridinium chloride monohydrate	<b>PYR12</b>	
1-N-hexadecylpyridinium chloride monohydrate	<b>PYR16</b>	
N,N-bis(2-hydroxyethyl)octylamine	<b>2EtOH-T8</b>	
N,N-bis(2-hydroxyethyl)dodecylamine	<b>2EtOH-T12</b>	
N,N-bis(2-hydroxyethyl)octadecylamine	<b>2EtOH-T18</b>	

## Overview of experiments

SPE recovery was determined using two different aqueous media compositions: unbuffered 10 mM  $\text{CaCl}_2$  solution and Dutch Standard Water (DSW). DSW has a pH of 8.2-8.4 and contains 1.36 mM  $\text{Ca}^{2+}$  and 0.73 mM  $\text{Mg}^{2+}$  as most important cations [173]. The 10 mM  $\text{CaCl}_2$  solution is the OECD-guideline recommended medium for sorption experiments [87], while DSW approximates the general ionic composition of hard (Dutch) freshwater and has been applied as such in ecotoxicological experiments [173]. If SPE recovery would not be negatively impacted by 10 mM of divalent  $\text{Ca}^{2+}$  cations, we expected WCX-SPE to be effective for most common testing media. Sorption to glassware was initially evaluated in 15 mM NaCl, following up on previous glass binding experiments [78]. Because of the lower suppression of the glass surface potential in medium of 15 mM NaCl compared to 10 mM  $\text{CaCl}_2$  [87], DSW, and phosphate buffered saline (PBS), 15 mM NaCl was regarded as a medium where glass binding is most prominent. In these other media, higher ionic strength and/or divalent cations are expected to reduce glass binding of cationic surfactants. If glass binding has negligible impact on PA-SPME calibration in 15 mM NaCl medium, we pose that glass binding will not be an issue in other commonly applied test media. Sorption to pipette tips was studied only in 10 mM  $\text{CaCl}_2$ . Sorption studies with 7  $\mu\text{m}$  and 35  $\mu\text{m}$  PA fibers always applied 10 mM  $\text{CaCl}_2$ , as one of the future applications of PA-SPME could be in standardized soil sorption studies with cationic surfactants. In PA-SPME calibration experiments with ionizable amines the medium was always buffered with BES (N,N-Bis(2-hydroxyethyl)-2-aminoethanesulfonic acid, Sigma-Aldrich, Zwijndrecht, The Netherlands) at pH 6.5, to ensure that >99.95% of the surfactant molecules (with  $\text{pK}_a > 10$ ) were in the charged form. The pH-dependent affinity for PA-SPME fibers was studied for P12 and Q12 using phosphate and carbonate buffers, with an ionic strength of 100 mM  $\text{Na}^+$ .

## Determination of SPE recovery for cationic surfactants

Recovery upon elution from WCX-SPE cartridges (Waters, Etten-Leur, The Netherlands) was determined for the full set of test compounds. The method for this was adapted from Chen et al. [78]. The 3 cc 60 mg Cartridges were conditioned with 1 mL of MeOH, pre-equilibrated with 1 mL of MilliQ and equilibrated with 2 mL of DSW or 10 mM  $\text{CaCl}_2$ . The test medium used in the equilibration phase was spiked while still retained on top of the SPE layer in the cartridge, using 50  $\mu\text{L}$  of a MeOH stock solution. This was followed immediately by transfer of an additional 2 mL of medium into the cartridge, dispersing the methanol stock solution throughout the sample. Spiking was done on an analytical

scale to quantify the amount of stock solution added precisely. This spiking method was chosen to avoid binding of test compound to glassware and pipette tips. Through the addition of 4 mL medium in total, test concentrations of 6 and 120 nM were simulated. Following sample loading, each cartridge was washed two times with 3 mL of MilliQ and one time with 3 mL of MilliQ acidified with 0.5% TFA, bringing the WCX material into a neutral form. Finally, cationic analytes were eluted using 3 mL of acidic eluent mixture (90% MeOH, 10% MilliQ, 0.1% TFA v/v), with the final volume being weighed. This procedure was carried out in triplicate for each concentration and matrix. Controls were prepared in quadruplicate by spiking 3 mL acidic eluent mixture directly with 50  $\mu$ L of stock solution, again on an analytical scale.

### **Sorption of cationic surfactants to glassware and pipette tips**

Glass binding was measured by adding, in triplicate, 200  $\mu$ L of stock solution (in MeOH) to either a clear glass 40 mL vial (Supelco 27181, supplied by Sigma-Aldrich, Zwijndrecht, The Netherlands) or an amber glass 120 mL flask (Supelco 23234, supplied by Sigma-Aldrich, Zwijndrecht, The Netherlands). In addition, 1.5 mL short thread autosampler vials (Grace, Discovery Sciences) were tested. Vials were then filled to the top (in order to minimize headspace) with 15 mM NaCl solution. Control vials were instead filled to the top with MeOH; glass binding was not expected in 100% organic solvent. The final nominal concentration in all vials was approximately 4  $\mu$ M. All vials were then placed on roller mixers for 24 hours in a darkened, climate controlled room ( $20\pm 1^\circ\text{C}$ ). Roller mixers (Stuart Roller Mixer SRT9, set at 33 rpm) were used, as horizontal and orbital shakers may cause foaming, decreasing the freely dissolved concentration. After this a 3 mL aliquot of the samples in 15 mM NaCl was extracted from 40 and 120 mL flasks using the SPE method that was validated previously. The pipette tip used to sample a 3 mL aliquot in a single draw from the 40 mL vial or 120 mL flask was flushed with the acidic 90/10 eluent used for the SPE step, in order to extract any compound that might have adsorbed to the inside of the pipette tip. HPLC vials were transferred directly to the LC-MS/MS autosampler. Control vials were sampled without SPE and served as a 100% control where no glass binding was expected, which was verified by mass balance calculation. Subsequently, glass vials containing 15 mM NaCl solution were emptied using a Pasteur pipette, with less than 40  $\mu$ L of the original solution (< 0.1%) remaining in all cases. In order to extract any remaining compound from the glassware, 3 mL of the acidic 90/10 eluent was added to the emptied vials prior to placing them back on the roller mixer for several minutes. Glass binding was then evaluated by (i) direct comparison of aqueous samples with MeOH samples, and (ii)

evaluation of the amount of compound extracted from glassware. In addition, sorption to the outside of pipette tips was assessed in a separate experiment. Without drawing up the aqueous solution, pipette tips were submerged by approximately 1 cm for 10 seconds in 1.5 mL vials containing a surfactant solution. After wiping off any drops of aqueous solution on the outside of the pipette tip, the tip was emerged in acidic eluent solution to extract cationic surfactant bound to the outside of the pipette tip.

### **Measuring of SPME uptake profiles and sorption isotherms with 7 $\mu\text{m}$ and 35 $\mu\text{m}$ PA fiber**

Sorption measurements to the PA-SPME fibers for a broad variety of surfactants were primarily executed using 10 mM  $\text{CaCl}_2$  medium, buffered at pH 6.5 with 100  $\mu\text{M}$  BES. Experiments focusing on pH dependency of sorption isotherms were performed by using different phosphate and carbonate buffers to produce media with the desired pH, all with buffer strength of 10 mM and no additional salts added. Kinetic uptake profiles into the PA-SPME fibers were determined for P12 and Q12, based on 10 mM  $\text{CaCl}_2$  medium where possible and using alternative media for higher pH levels. Fibers were exposed in clear glass 40 mL vials with aluminum lined septa, placed on a roller mixer in a dark and climate controlled ( $20 \pm 1^\circ\text{C}$ ) room. The 7  $\mu\text{m}$  PA-SPME fibers were cut to  $50 \pm 0.2$  mm and 35  $\mu\text{m}$  PA-coated SPME fibers to  $40 \pm 0.2$  mm, using a bundle of SPME fibers packed in a stretch of folded aluminum foil and a laser guided paper cutter. Exposure duration was 4 days unless noted otherwise. Following exposure, fibers were blotted dry, gently wiped along a wet tissue and subsequently cut into  $\sim 1$  cm pieces that were collected in a single autosampler vial. Fibers were desorbed in a weighed volume of the acidic eluent mixture for at least 60 minutes, vortexed for 10 seconds, and stored at  $4^\circ\text{C}$  until analysis. The volume of eluent added was based on the expected  $C_{\text{fiber}}$  upper and lower detection limits, and practical limitations. If necessary, eluent was further diluted before analysis. The aqueous concentration at the time of SPME sampling was determined following SPE clearance of inorganic medium salts, or direct injection of the salt medium to the LC-column. Direct injection of medium was done by pipetting a 200  $\mu\text{L}$  aliquot from the test vial into an autosampler vial already containing 600  $\mu\text{L}$  of eluent, rinsing the pipette tip five times with the eluent inside the autosampler vial to wash out any compound stuck to the inside of the pipette tip. These direct aqueous samples were analyzed using a solvent switch, in order to divert poorly-retaining inorganic salts to the waste outlet, before switching to a steep gradient that introduced the surfactant into the MS (see below). SPE eluted aqueous samples were analyzed using an isocratic HPLC method with shorter run time.

## Chemical analysis

Two Kinetex XB-C18 columns (Phenomenex, Torrance, USA) were used, which were end-capped with trimethylsilyl and additional isobutyl groups at the base of the C18 chain. Core-shell columns were used because of their relatively low operating pressure and reduced band broadening when analyzing surfactants [174]. The specific placement of isobutyl sidechains helped to diminish peak tailing, which is otherwise expected when analyzing cationic surfactants using a silica-based stationary phase. A Kinetex 2.6  $\mu\text{m}$ , 100  $\text{\AA}$  50 mm  $\times$  2.1 mm column was used with a flow rate of 200  $\mu\text{L}/\text{min}$  for clean samples; i.e. SPE samples or fiber extracts. A similar column with larger particles (5  $\mu\text{m}$ ) was used for gradient analysis, as the increased particle size allowed for a higher flow rate (350  $\mu\text{L}/\text{min}$ ) with decreased backpressure. Mobile phase was a mixture of A (MilliQ water with 0.1 % formic acid) and B (MeOH with 0.1 % formic acid). Clean samples were analyzed using an isocratic flow of A and B; information on percentages of A and B for each compound is listed in table S3. Aqueous samples of P12 and Q12 were analyzed using a gradient of A and B, starting with 95% A for 2.5 minute which was then increased to 95% B over 1 minute using a convex gradient, after which the flow was kept at 95% B for 2.2 minutes to be instantly changed back to 95% A to equilibrate the column for the next injection. During the first 2.5 minutes of the run analytes were effectively trapped on the column, allowing for dissolved salts to be washed off the column and be diverted to waste by using a solvent switch. LC-MS/MS settings are listed in table S2.

## Data analysis

All data was analyzed using GraphPad Prism 6 for Windows (version 6.07).



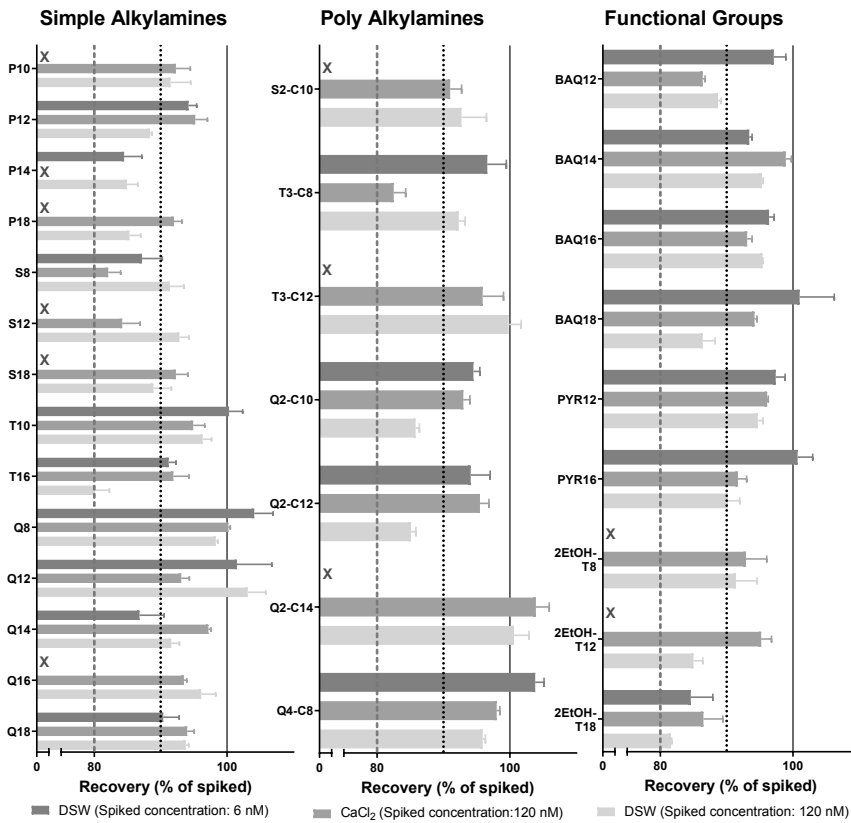
## Results and Discussion

### Performance of analytical equipment

Replicate sampling was used in all experiments, preferably with triplicate samples and duplicate or triplicate fibers. For PA-SPME samples, deviations between replicates of  $\leq 20\%$  were regarded as acceptable for surfactants [78, 175]. For aqueous samples and standards, deviations between replicates of  $\leq 10\%$  were regarded as acceptable. Calibration standards were also subject to replicate injections. Quality of calibration data was assessed by back-calculation, where a deviation of  $\leq 10\%$  was deemed acceptable. For most compounds the LC-MS/MS performed best between concentrations of 5 nM and 20  $\mu\text{M}$ , roughly four orders of magnitude. Since aqueous samples were always diluted four times with the acidic eluent mixture, the effective LOQ for aqueous samples was approximately 20 nM.

### SPE recovery for cationic surfactants

As shown in Figure 1.1, Oasis WCX-SPE columns displayed a recovery  $\geq 80\%$  in all cases, and  $\geq 90\%$  for 16 of the 30 compounds tested. We thereby show that this SPE protocol can be confidently used to extract, retain, and elute all cationic surfactants tested from aqueous samples (see Figure 2.1), ranging from C8 to C18 alkylamines, including, C14-dialkyldimethylammonium, C8-tetraalkylammonium, and benzalkonium and pyridinium compounds. The mixed-mode retention mechanism ensures favorable interaction between cationic surfactant and Oasis WCX sorbent when flushing the cartridge with water or even solvent at alkaline pH, because both ionic and hydrophobic interactions retain the surfactants, as well as when flushing with acidified water because then hydrophobic interactions with the neutralized WCX material still retain the surfactants. Elution is easily achieved for even the more hydrophobic cationic surfactants when using acidified solvent, which diminishes both ionic and hydrophobic interactions. Strong retention of analyte when flushing with acidified water is important, as (inorganic) cations that might be retained on the cartridge could cause artefacts if they are injected into the MS/MS. This WCX material should also be effective for complex technical cationic surfactant mixtures and environmental samples, as long as the ion-exchange capacity of the WCX material is not exceeded.

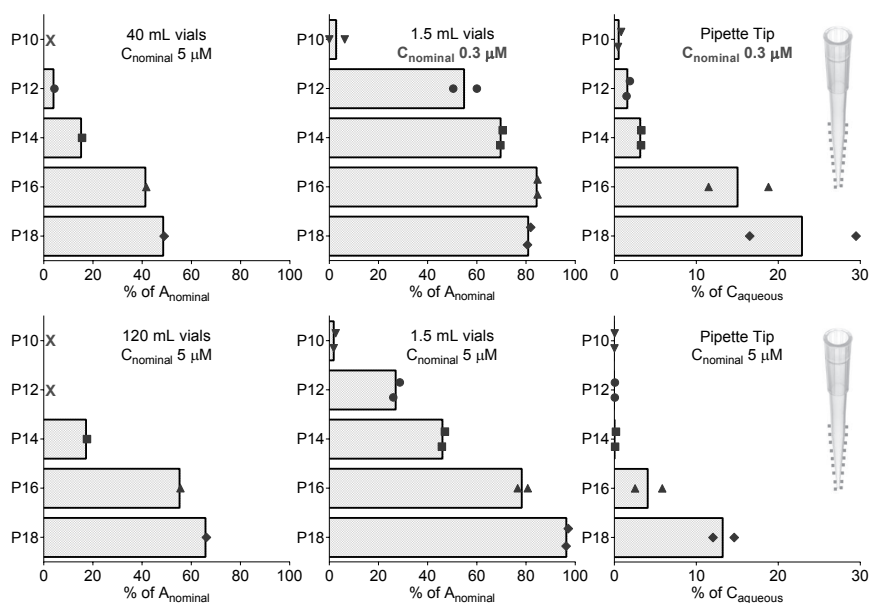


**Figure 2.1.** SPE recovery for a broad series of cationic surfactants. Determined in DSW and 10 mM CaCl<sub>2</sub>.

### Sorption of cationic surfactants to glassware and pipette tips

The extent of glass binding of simple primary amines increased considerably with alkyl chain length above a certain minimum length, as shown in Figure 2.2. Using the data obtained with glassware extractions, for example, for pH 6 buffered solutions with 15 mM NaCl as electrolyte for P10 less than 10% loss to the glass of 1.5 mL autosampler vials was determined, while more than 50% of the total spiked amount was sorbed to glass for P12 amines (in the ~0.3 μM spiked group), which increased up to >80% for primary amines with longer alkyl chains. Direct comparison of aqueous samples with MeOH samples were generally in good agreement and lead to comparable estimates of extent of glass binding. This warrants against testing or storing such hydrophobic cationic surfactants in aqueous

solution in such small glass vials without careful measurement, as the actually dissolved concentrations may be several factors lower than nominal(ly intended) concentrations. Overall losses from the dissolved phase to glass surface in 40 and 120 mL flasks is markedly lower than in autosampler vials due to the lower area/volume ratio, but fractions lost to the glass surface were still >40% for P16 and P18. Results for the 1.5 mL autosampler vials also indicate a minor concentration dependency, with lower relative losses at higher spiked concentrations. The results for P18 seem somewhat counterintuitive, because at 0.3  $\mu\text{M}$  the relative losses for P16 are higher than for P18 (Figure 2.2).

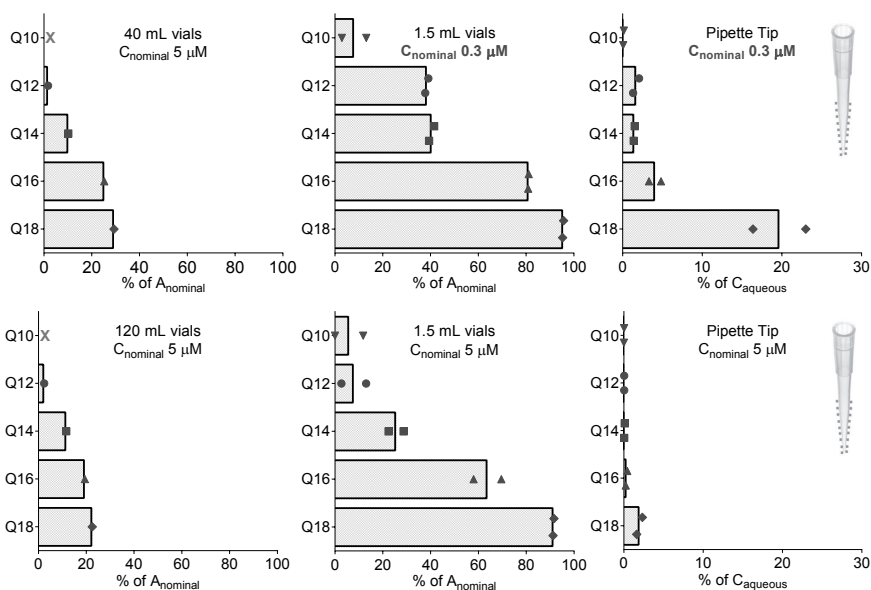


**Figure 2.2.** Glass binding and pipette tip binding for a series of primary amines. Determined in 10 mM  $\text{CaCl}_2$ .

Significant binding of surfactant to the outside of 200  $\mu\text{L}$  polypropylene (PP) pipette tips, which were dipped into aqueous solution, may lead to overestimation of the actually dissolved concentration when this amount is co-extracted upon releasing the pipetted sample into a vial filled with solvent. As shown in Figure 2.2, compared to glass surface binding, PP tip binding was significant only at higher alkyl chain lengths, and showed a more pronounced concentration dependency; considerably stronger at lower concentrations. For primary amines P10, P12 and P14, PP tip binding does not seem to be a significant artefact when sampling, but for P16 and P18 in 1.5 mL vials more than 20% of the total amount in aqueous solution (thus, excluding the glass sorbed fraction) can be sorbed

to the outside of the tip, which may cause a strongly confounding increase in sampled surfactant. P10 is the only compound with insignificant sorption in all instances. For P12 and P14 sorption to glassware is increased, but sorption to pipette tips is still negligible. P16 and P18 have significant sorption losses to both PP tips and glass in all experiments. At pH 6.5, it is unlikely that sorption to glassware is influenced by the neutral form (<0.1%).

Sorption to glassware was generally lower for quaternary amines (see Figure 2.3), when compared with primary amines with equal alkyl chain length. Differences are especially obvious for 120 mL and 40 mL glass vials, where quaternary amines have approximately two times smaller adsorbed fractions. This does contradict sorption trends for several aluminosilicate clays, where quaternary ammonium displayed higher affinities than analogue primary amines [176, 177]. Sorption to 1.5 mL vials is roughly comparable with primary amines, with some slight differences for the shorter alkyl chain lengths. Binding to PP tips is much lower for quaternary amines than analogue primary amines. There is virtually no significant sorption to PP tips at 5  $\mu\text{M}$ , except for Q18. Sorption is stronger at 0.3  $\mu\text{M}$ , though, but is still only significant for the longer alkyl chain lengths of  $\geq\text{Q16}$ .



**Figure 2.3.** Glass binding and pipette tip binding for a series of quaternary amines. Determined in 10 mM  $\text{CaCl}_2$ .

Previous studies indicated that sorption of cationic surfactants to kaolinite increases with alkyl chain length [84]. Moreover, decreases in  $C_{\text{free}}$  due to sorption to a surface (e.g. glass) is often more substantial at lower concentrations because the surface sorption sites may become saturated at relatively high concentrations. This can significantly decrease  $C_{\text{free}}$  in aqueous samples, hampering mass balance based calculations. In studies with an additional sorbent phase such as sediment or humic substances, glass binding might pose less of a challenge, if other sorption phase(s) are dominant by volume or affinity. Glass binding is hypothesized to be highest in solutions containing monovalent electrolytes with low salinity, whereas increases in salinity and presence of divalent cations lead to lower glass binding [24, 85, 86]. In addition, with glass adsorption being nonlinear this leads to concentration-dependent losses that are enhanced as analyte concentrations decrease.

### Sorption of cationic surfactants to PA fiber

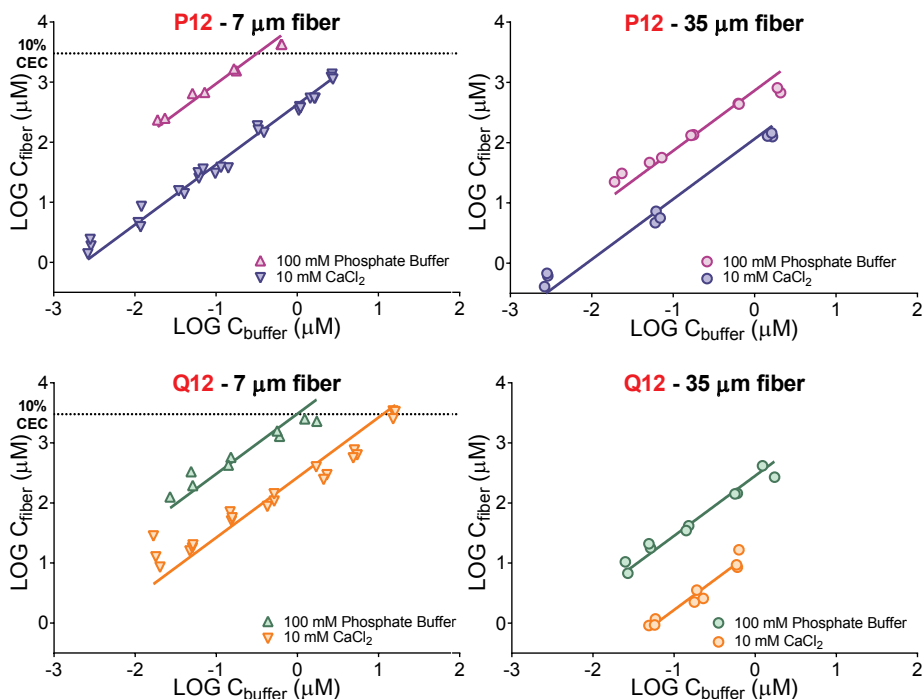
Initial sorption experiments were carried out on a large set of simple cationic surfactants of varying alkyl chain lengths. In contrast to previous publications from our lab on PA-SPME with quaternary ammonium compounds, however, for most compounds relatively large variability (>1 order of magnitude) within and between experiments was found (see figure S1 to S5). These effects seemed to increase with number of alkyl chains as well as alkyl chain length. Together, these results indicate that reproducibility of the PA-SPME taken from this batch of fiber material becomes too low, and uncertainty becomes too high, for accurate determination of  $C_{\text{free}}$  by passive sampling for compounds with more than one alkyl chain or an alkyl chain length of  $\geq 14$  carbon atoms. Similar findings of unfavorable sorption behavior of the current batch of 7  $\mu\text{m}$  PA-SPME for anionic surfactants, compared to an older 7  $\mu\text{m}$  PA-SPME batch [178, 179], were reported in one of our labs other recent studies [180]. As a partial solution, it is strongly advisable to perform a calibration and the full experiment with SPME fibers cut from one length of fiber, to rule out effects of variability in coating thickness along the length of a batch of fiber. Results of these more controlled experiments are presented in figures 2.4, 2.5, and 2.6. Combining these findings with previous research [78, 172, 181], it is difficult to establish a definitive applicability domain for PA-SPME, while the exact sorption mechanism of PA-SPME remains to be elucidated [78, 170, 180]. Nor did it seem feasible anymore to systematically determine structural trends in  $K_{\text{fw}}$  for cationic surfactants on 7  $\mu\text{m}$  PA-SPME, and define a  $K_{\text{fw}}$  QSAR, as was one of our key intentions with the current study. It was decided that detailed PA-SPME experiments in this chapter were limited to one ionizable and one permanently charged  $C_{12}$ -chain cationic surfactant.

## **Uptake kinetics with 7 and 35 $\mu\text{m}$ PA-SPME fibers, for the ionizable P12 and permanently charged Q12**

Combining  $K_{\text{fw}}$  calibration samples with each experiment, uptake kinetics of two relatively short chain length surfactants onto PA-SPME fibers of two different polymer thicknesses, 7 and 35  $\mu\text{m}$ , were measured: an ionizable primary amine (P12) and quaternary ammonium compound (Q12). Kinetics for Q12 were determined only at pH 6.5; results are presented in figure S6. Both fiber coatings reach >90% of equilibrium in less than 6 hours. Overnight exposure is therefore sufficient for sampling of Q12. Kinetics for P12 were determined at pH 6.5 and pH 11.1 (Figure S7 and S8), to assess kinetics of both the ionic and the neutral form ( $\text{pK}_{\text{a}}$  P12  $\sim 10.5$ ). Both PA-coatings reach equilibrium at pH 6.5 fast enough to render overnight exposure is suitable to measure P12 under standard conditions. The neutral form of P12 needs more time to reach equilibrium, an effect that is correlated with coating thickness, which is a strong indication that the neutral form is absorbed into the PA polymer rather than adsorbed to the (charged) PA-surface (groups). At pH 11.1, >90% of equilibrium is reached in approximately 10 hours for the 7  $\mu\text{m}$  fiber, while the 35  $\mu\text{m}$  fiber needs 23 hours. Also of note is the more than one order of magnitude increase in  $K_{\text{fw}}$  of P12 between pH 6.5 and 11.1, for both PA-coatings. In theory, both fiber types are suitable to sample P12 at alkaline pH, although implementation of the PA coating at alkaline pH should be subject to additional testing.

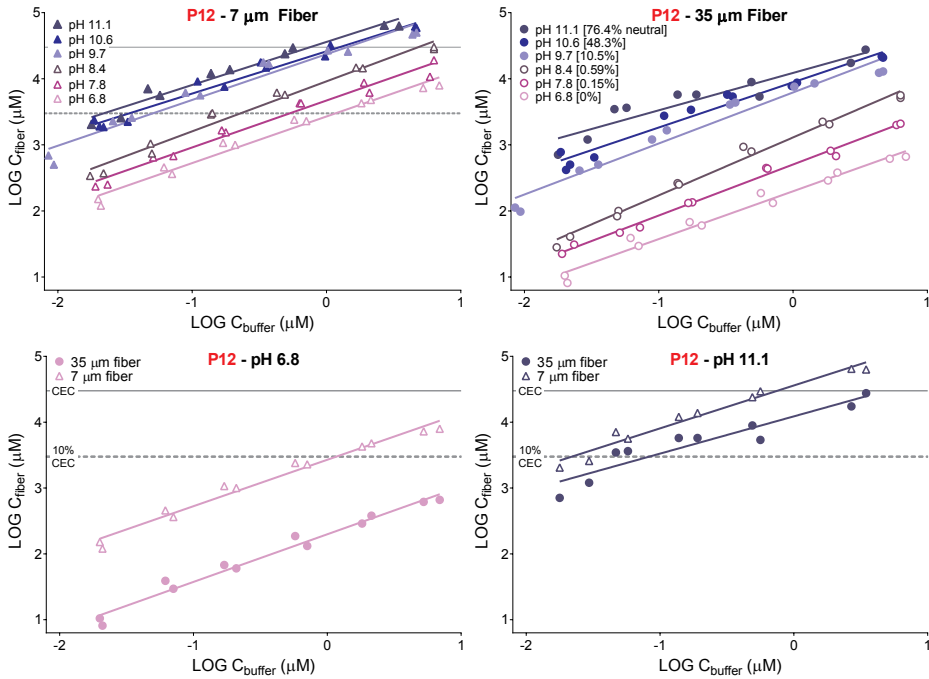
### **Effect of ionic composition and pH on PA-SPME calibration curves**

The effect of ionic composition of exposure medium on fiber uptake was measured for P12 and Q12 in two exposure media: 100 mM phosphate buffer (pH  $7.8 \pm 0.1$ ) and 10 mM  $\text{CaCl}_2$  buffered with 1 mM BES (pH  $7.5 \pm 0.1$ ). Results are presented in Figure 2.4. Switching medium from 100 mM  $\text{Na}^+$  to 10 mM  $\text{Ca}^{2+}$  leads to an order of magnitude decrease in  $K_{\text{fw}}$ . This effect seems to be similar for P12 and Q12 and between fiber types, leading to the hypothesis that the higher competition of  $\text{Ca}^{2+}$  with cationic surfactants (in comparison with  $\text{Na}^+$ ) for cation exchange sites, and in more detail, the much stronger reduction of the surface potential by divalent cations that attracts the organic cations near the charged surface, are the principal causes [78].



**Figure 2.4.** Influence of medium composition on fiber affinity. Higher fiber affinity is seen for 100 mM Na<sup>+</sup> in all cases.

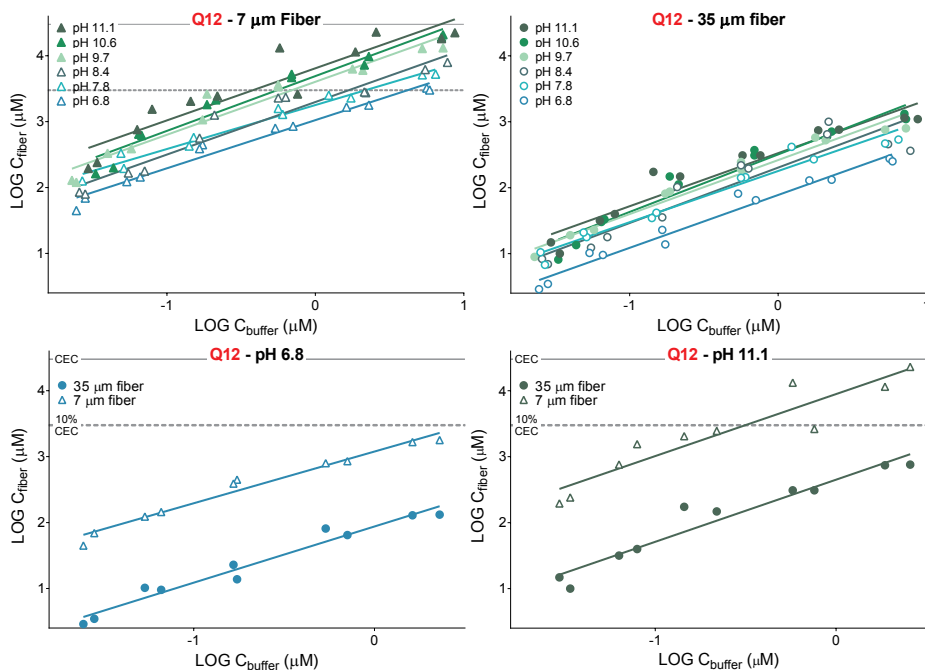
Effects of pH on PA-SPME calibration isotherms are presented in Figure 2.5 and 2.6 for P12 and Q12, respectively. The associated Freundlich coefficients and  $K_{fw}$  are presented in table S4 and S5, respectively. As expected based on the results of kinetic experiments, partitioning of the ionizable amine P12 to both PA-fiber coatings is highly pH-dependent (Figure 2.5), with a higher affinity of the neutral amine species compared to the protonated form. This effect is more pronounced in 35 μm coating, likely due to the lower cation-exchange capacity of the 35 μm PA coating (Haftka et al. [170]) compared to the 7 μm PA coating, as suggested by Chen et al. [78]. When results for 7 and 35 μm PA-coatings are plotted together in Figure 2.5, it becomes obvious that  $K_{fw}$  is much more similar at pH 11.1. This further supports the hypothesis that the neutral amine fraction is absorbed into the fiber coating, a process that is unlikely to be impacted by differences in cation exchange capacity, and which can be corrected for by using concentration units per volume of coating. Assuming that the cationic amine has a maximum affinity at pH 6.8, the increase in affinity to the fiber with higher pH can be assumed to be due to the neutral fraction, and a  $pK_a$  may be fitted to the data.



**Figure 2.5.** Influence of medium pH on fiber sorption for P12, determined in 100 mM Na<sup>+</sup>.

The sorption affinity of the permanent cation Q12 to PA fibers, however, showed a minor but distinct influence of medium pH above pH 6.8 (Figure 2.6), with about 0.8 log units for 7  $\mu\text{m}$  fiber and 0.5 log units for the 35  $\mu\text{m}$  fiber. This suggests that the number of ion-exchange groups on the PA material surface may not be constant, and not only have a fixed  $\text{pK}_a$  of approximately 5, as assumed by Chen et al [78], but surface acid groups with  $\text{pK}_a$  values between pH 6-10 likely exist. As a result, it is not possible to accurately derive the  $\text{pK}_a$  value of P12 from the PA fiber isotherm data. Also, this stresses the need to always perform a calibration study in the exact same media as applied in test samples.





**Figure 2.6.** Influence of medium pH on fiber sorption for Q12, determined in 100 mM Na+.

These ionic composition tests and pH series implicate that quaternary ammonium surfactants, as well as the cationic form of ionizable surfactants, have at least an order of magnitude higher affinity for the 7  $\mu\text{m}$  PA fiber compared to the 35  $\mu\text{m}$  PA fiber, as shown for the Q12 sorption isotherm differences at both pH 6.5 and pH 11. This corresponds to measured differences between these two PA-coatings reported previously for other cationic organic compounds [182], using different PA-fiber batches. This was assumed to be the result of a higher density of cation exchange sites on the surface of the 7  $\mu\text{m}$  PA fiber. Cation exchange capacity (CEC) for the 7  $\mu\text{m}$  fiber was determined in earlier work using  $\text{Ba}^{2+}/\text{Ca}^{2+}$  substitution [78]. The CEC of  $\sim 20$  mmol/L corresponds with the maximum  $C_{\text{fiber}}$  of quaternary ammonium surfactants below their respective CMC. The ion exchange groups are presumably unpolymerized carboxylic acids originating from the polyacrylate or polymethacrylate used to produce the fiber coating. In earlier work by Chen et al. the sorption affinity of quaternary ammonium surfactants was shown to increase in the pH range of 2-6, but did not differ between pH 6 and 8 [78]. These results led to the hypothesis that ion exchange sites dominate the sorption process of cationic surfactants to the PA fiber, i.e. sole interaction of hydrophobic alkyl chains with the PA surface is not a significant contributor. The decreasing affinity between pH 6 and 8 corresponds with the expected

$pK_a$  of carboxylic acids (4-6), which are also important cation exchange sites in humic acids and the Oasis WCX-SPE cartridge. Based on this hypothesis, it was expected that the CEC of the 7  $\mu\text{m}$  PA fiber would remain constant at  $\text{pH} \geq 6.0$ , and that cationic surfactants would therefore have a constant affinity throughout the alkaline pH range. However, experimental results in this work have shown that this was not entirely the case.

## Conclusions

The data presented in this publication on significant sorption to the outside of polypropylene pipette tip and various glassware, as well as irreproducible or highly scattered SPME sorption isotherms, show that analytically justified experiments with hydrophobic cationic surfactants are challenging. Sorption to glass becomes significant for surfactants with a carbon chain length above 10 carbon atoms. Sorption to glass surface may be as high as 90 % of the total added amount of C18 cationic surfactants, rendering ten times lower dissolved concentration than intended. Using pipette tips to sample hydrophobic cationic surfactants from aqueous solution, on the other hand, may substantially overestimate the amount of surfactant sampled from the medium when flushing the pipette tip in solvent (to make sure that the amount sorbed to the inside of the tip is included). Unwanted effects due to sorption are lower but can still be significant for quaternary ammonium surfactants. However, cationic surfactants with a diversity of structures, including multiple alkyl chains and functional groups and ionizable as well as permanently charged compounds, can be efficiently extracted from an aqueous phase with a weak cation exchange solid phase extraction (WCX-SPE) column. Extraction efficiencies were above 90 for almost all chemicals.

SPME is not a universal solution to measure cationic surfactants. There are certain specific issues beyond what was expected beforehand. The ultimate goal of this work was to lay down an applicability domain for PA-SPME in the context of sampling cationic surfactants. Although it proved to be difficult to establish detailed boundaries for such an applicability domain, the results indicate that alkyl chain lengths longer than 14 carbon atoms and the presence of multiple alkyl chains are highly likely to give irreproducible measurements. If PA-SPME is employed a calibration curve should always be measured together with the samples, using the same medium and batch of fiber. Although the PA-SPME calibration isotherms are confirmed to be near linear for low, environmentally relevant concentrations (Figure 2.4), the PA-SPME calibration curves become more non-linear at high concentrations, which approach the CEC of the polymer (Figure 2.5-2.6)

[78]. Toxic effects of cationic surfactants in sediments have been observed at sorbed concentrations approximating 15% of the CEC of the sorbent [56], and the proportionally high freely dissolved concentrations in such systems are likely to be in the non-linear SPME calibration range. Unfortunately, this further hampers accurate use of PA-SPME for toxicity testing in the presence of mitigating sorbent [54]. At present, it seems that the PA-SPME material of the currently available batch does not provide enough reliability and reproducibility to warrant use for precise experiments on the environmental fate of cationic surfactants, especially with alkyl chain lengths beyond 12 carbon atoms.

### **Acknowledgements**

This study was funded by Unilever, Safety & Environmental Assurance Centre (SEAC), Colworth Science Park, U.K. under project CH-2012-0283. Todd Gouin, Geoff Hodges and Theo Sinnige provided many useful comments and fruitful discussions on this work.

## Supporting Information

Evaluating Solid Phase (Micro-) Extraction Tools to Analyze Freely Ionizable and Permanently Charged Cationic Surfactants

### Contents:

**Table S1:** Properties of test compounds

**Table S2:** LC-MS settings

**Table S3:** HPLC settings

**Figure S1:** Fiber isotherm for P12

**Figure S2:** Fiber isotherm for S12

**Figure S3:** Fiber isotherm for Q12

**Figure S4:** Fiber isotherm for PYR12

**Figure S5:** Fiber isotherm for Q2-C10

**Figure S6:** Fiber uptake kinetics for Q12 in 7  $\mu\text{m}$  and 35  $\mu\text{m}$  fibers at pH 6.5

**Figure S7:** Fiber uptake kinetics for P12 in 7  $\mu\text{m}$  fibers, at pH 6.5 and pH 11.1

**Figure S8:** Fiber uptake kinetics for P12 in 35  $\mu\text{m}$  fibers, at pH 6.5 and pH 11.1

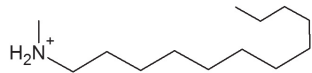
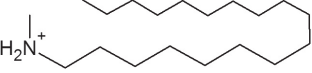
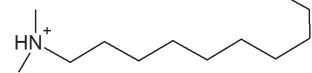
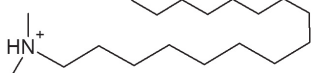
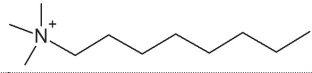
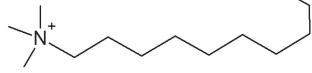
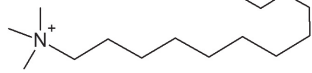
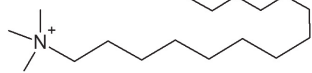
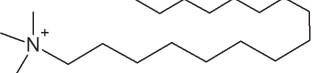
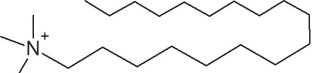
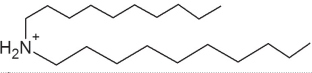
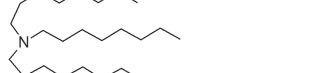
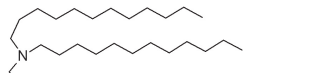
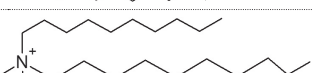
**Table S4:** Freundlich coefficients (7  $\mu\text{m}$  fiber, 100 mM Na<sup>+</sup>)

**Table S5:** Freundlich coefficients (35  $\mu\text{m}$  fiber, 100 mM Na<sup>+</sup>)

**Table S1:** Properties of test compounds.

Chemical name	Code	pK <sub>a</sub> <sup>1</sup>	CMC (mM)	Purity (%)	Molecular structure
Decylamine	P10	10.6	48 <sup>a</sup>	99.2	
Dodecylamine	P12	10.6	20 <sup>b</sup>	>99.5	
Tetradecylamine	P14	10.6	4.2 <sup>c</sup>	>98.5	
Hexadecylamine	P16	10.6	2.4 <sup>a</sup>	98	
Octadecylamine	P18	10.6	0.78 <sup>d</sup>	98	
N-methyl-1-octanamine	S8	10.9	–	98	

**Table S1:** (Continued)

Chemical name	Code	pK <sub>a</sub> <sup>1</sup>	CMC (mM)	Purity (%)	Molecular structure
N-methyl-1-dodecanamine	S12	10.5	–	97	
N-methyl-1-octadecanamine	S18	10.5	–	98	
N,N-dimethyl-1-decanamine	T10	9.8	–	>93	
N,N-dimethyl-1-hexadecanamine	T16	9.8	–	>95	
N,N,N-trimethyl-1-octanaminium bromide	Q8	N/A	260 <sup>e</sup>	>98	
N,N,N-trimethyl-1-decanaminium bromide	Q10	N/A	95 <sup>f</sup>	>98	
N,N,N-trimethyl-1-dodecanaminium chloride	Q12	N/A	23 <sup>g</sup>	>99	
N,N,N-trimethyl-1-tetradecanaminium chloride	Q14	N/A	3-6 <sup>f,h</sup>	>98	
N,N,N-trimethyl-1-hexadecanaminium chloride	Q16	N/A	0.94 <sup>i,j</sup>	96	
N,N,N-trimethyl-1-octadecanaminium chloride	Q18	N/A	0.1-0.3 <sup>k,h</sup>	98	
N-decyl-1-decanamine	S2-C10	11.0	–	97	
N,N-dioctyloctan-1-amine	T3-C8	10.7	–	98	
N,N-didodecyldodecan-1-amine	T3-C12	11	–	95	
N,N-didecyl-N,N-dimethylammonium bromide	Q2-C10	N/A	0.97 <sup>l,l</sup>	98	

**Table S1:** (Continued)

Chemical name	Code	pK <sub>a</sub> <sup>1</sup>	CMC (mM)	Purity (%)	Molecular structure
<b>N,N-didodecyl-N,N-dimethylammonium bromide</b>	<b>Q2-C12</b>	N/A	0.09 <sup>l,m</sup>	98	
<b>N,N-ditetradecyl-N,N-dimethylammonium bromide</b>	<b>Q2-C14</b>	N/A	–	>97	
<b>N,N,N-trioctyl-1-octanaminium bromide</b>	<b>Q4-C8</b>	N/A	–	>98	
<b>N,N-dimethyl-N-dodecylbenzylammonium chloride</b>	<b>BAQ12</b>	N/A	6-9 <sup>n,o</sup>	>99	
<b>N,N-dimethyl-N-tetradecylbenzylammonium chloride</b>	<b>BAQ14</b>	N/A	2.1 <sup>n,o</sup>	>99	
<b>N,N-dimethyl-N-hexadecylbenzylammonium chloride</b>	<b>BAQ16</b>	N/A	0.48 <sup>l,n</sup>	–	
<b>N,N-dimethyl-N-octadecylbenzylammonium chloride</b>	<b>BAQ18</b>	N/A	–	90	
<b>1-N-dodecylpyridinium chloride monohydrate</b>	<b>PYR12</b>	N/A	–	98	
<b>1-N-hexadecylpyridinium chloride monohydrate</b>	<b>PYR16</b>	N/A	1.1 <sup>p</sup>	98	
<b>N,N-bis(2-hydroxyethyl) octylamine</b>	<b>2EtOH-T8</b>	9.2	–	–	
<b>N,N-bis(2-hydroxyethyl) dodecylamine</b>	<b>2EtOH-T12</b>	8.5 <sup>2</sup>	1.0 <sup>q</sup>	>98	
<b>N,N-bis(2-hydroxyethyl) octadecylamine</b>	<b>2EtOH-T18</b>	9.2	–	–	

<sup>1</sup> calculated values; <sup>2</sup> [181]; <sup>a</sup> [183]; <sup>b</sup> [184]; <sup>c</sup> [185]; <sup>d</sup> [186]; <sup>e</sup> [187]; <sup>f</sup> [188]; <sup>g</sup> [189]; <sup>h</sup> [190]; <sup>i</sup> [191]; <sup>j</sup> [192]; <sup>k</sup> [193]; <sup>l</sup> [194]; <sup>m</sup> [195]; <sup>n</sup> [196]; <sup>o</sup> [197]; <sup>p</sup> [198]; <sup>q</sup> [199]; N/A = not applicable; – = data not available

**Table S2:** LC-MS settings.

The interface for the MS-MS was a Turbo Ion spray in positive ionization mode operated at 400°C. The following settings were used for all compounds: nebulizer gas (NEB) = 8; collision cell gas (CAD) = 3; collision cell entrance potential (EP) = 10 V; collision cell exit potential (CXP) = 12 V. Compound-specific settings can be found in the table. (CUR = curtain gas; IS = ion spray voltage; DP = declustering potential; FP = focusing potential; CE = collision energy)

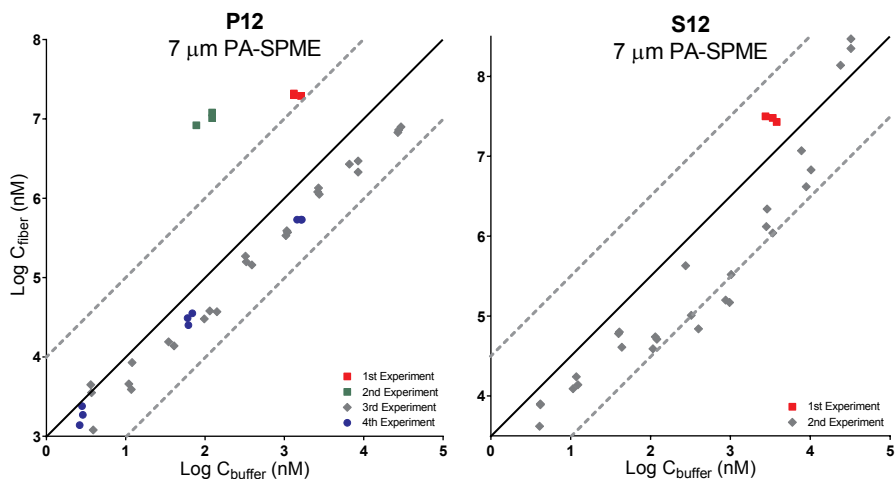
Compound	M1 m/z	M3 m/z	CUR	IS (V)	DP (V)	FP (V)	CE (V)
<b>P10</b>	158.3	57.1	6	4900	70	320	23
<b>P12</b>	186.4	70.9	7	4500	33	186	20
<b>P14</b>	214.4	57.1	6	4250	80	370	30
<b>P16</b>	242.5	57.2	8	4500	44	240	33
<b>P18</b>	270.3	57.2	7	4500	36	215	41
<b>S8</b>	144.1	71	7	4500	60	250	19
<b>S12</b>	200.2	70.9	7	4500	75	220	24
<b>S18</b>	284.3	57.2	8	5500	40	240	45
<b>T10</b>	185.9	57.1	7	4500	70	350	33
<b>T16</b>	270.5	57.1	6	5300	46	230	48
<b>Q8</b>	172.3	60	7	4500	43	292	34
<b>Q10</b>	200.3	60	8	3200	51	300	27
<b>Q12</b>	228.3	60	7	4500	58	292	39
<b>Q14</b>	256.5	60	7	4500	58	292	44
<b>Q16</b>	284.5	60	7	2050	54	325	52
<b>Q18</b>	313.5	60	7	5500	50	345	55
<b>S2-C10</b>	298.5	158.1	7	4500	113	212	30
<b>T3-C8</b>	354.5	57.1	7	3000	125	320	58
<b>T3-C12</b>	522.2	354.6	6	4000	65	290	54
<b>Q2-C10</b>	326.4	186.4	6	1800	64	236	40
<b>Q2-C12</b>	382.4	214.5	6	1750	45	245	44
<b>Q2-C14</b>	438.4	242.4	9	4500	74	240	51
<b>Q4-C8</b>	466.4	156.2	7	3000	90	300	58
<b>BAQ12</b>	304.4	90.9	9	5500	68	292	47
<b>BAQ14</b>	332.4	240.4	9	5000	58	345	32
<b>BAQ16</b>	360.4	268.4	7	4500	56	330	34
<b>BAQ18</b>	388.3	91	7	3000	100	175	57
<b>PYR12</b>	248.4	80.1	7	4500	45	270	33
<b>PYR16</b>	304.2	80.1	7	1750	45	290	45

**Table S3:** HPLC settings.

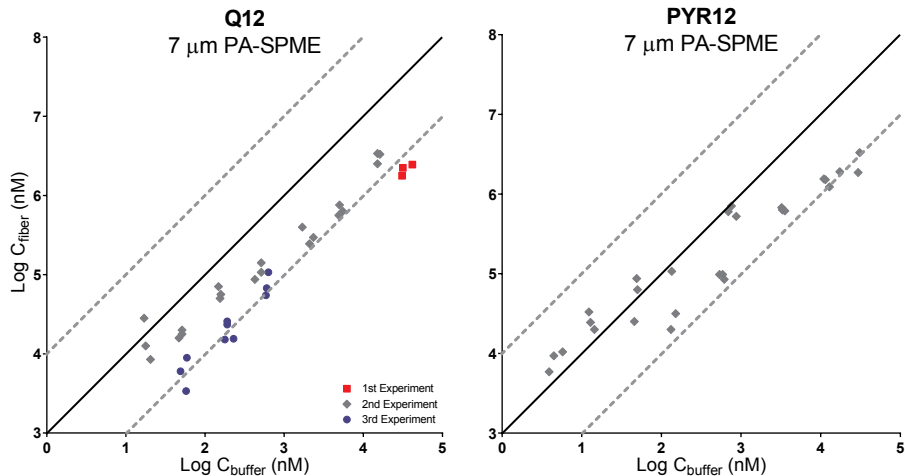
HPLC settings and resulting retention times when operating with isocratic mobile phase. A = MilliQ with 0.1% formic acid, B = analytical grade methanol with 0.1% formic acid.

<b>Compound</b>	<b>% A</b>	<b>% B</b>	<b>Runtime</b>	<b>Retention time</b>
<b>P10</b>	47	53	5.5	3.7
<b>P12</b>	39.5	60.5	6.6	4.6
<b>P14</b>	31.5	68.5	5.3	3.5
<b>P16</b>	33	67	6.4	4.3
<b>P18</b>	17	83	4.8	3.1
<b>S8</b>	63	37	6.4	4.4
<b>S12</b>	39	61	4.4	3.0
<b>S18</b>	21.5	78.5	6.4	4.3
<b>T10</b>	48	52	6	4.1
<b>T16</b>	25	75	5.4	3.7
<b>Q8</b>	65	35	5.4	3.6
<b>Q10</b>	51	49	5	3.1
<b>Q12</b>	39.5	60.5	4.6	3.0
<b>Q14</b>	32.5	67.5	5.4	3.7
<b>Q16</b>	26	74	4.8	3.3
<b>Q18</b>	20.5	79.5	5.6	3.8
<b>S2-C10</b>	26	74	5.2	3.3
<b>T3-C8</b>	24	76	5.2	3.5
<b>T3-C12</b>	11	89	5.2	3.4
<b>Q2-C10</b>	27	73	5.8	3.8
<b>Q2-C12</b>	19	81	5.6	3.7
<b>Q2-C14</b>	14	86	5.6	3.5
<b>Q4-C8</b>	17	83	5.7	3.6
<b>BAQ12</b>	32.5	67.5	5.8	3.8
<b>BAQ14</b>	29.5	70.5	5.8	4.1
<b>BAQ16</b>	24	76	6.4	4.5
<b>BAQ18</b>	19	81	6.4	4.3
<b>PYR12</b>	38	62	6	4.1
<b>PYR16</b>	26	74	5.6	3.8

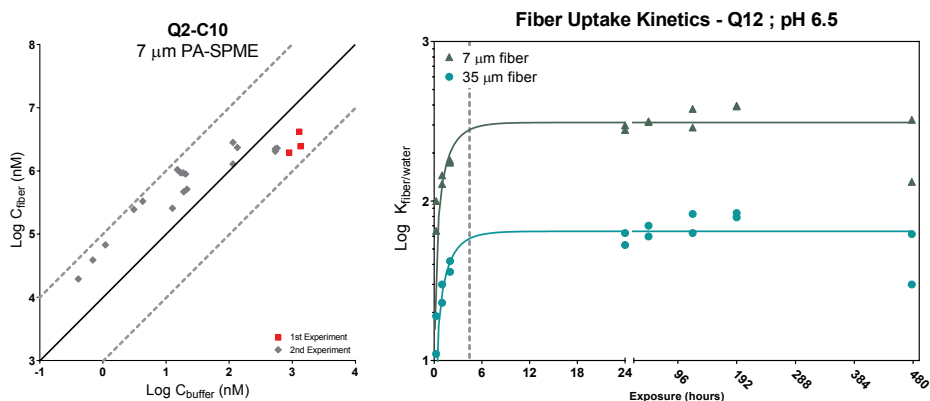




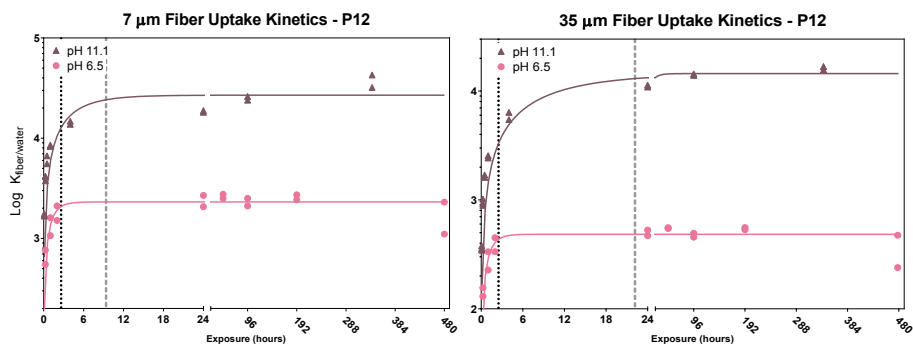
**Figure S1 (left):** Fiber isotherm for P12. While the 3<sup>rd</sup> and 4<sup>th</sup> experiment both show relatively linear isotherms and good overlap, results for the 1<sup>st</sup> and 2<sup>nd</sup> experiment are significantly different. **Figure S2 (right):** Fiber isotherm for S12. Results are relatively erratic along the whole measurement range, with poor consistency between the 1<sup>st</sup> and 2<sup>nd</sup> experiment.



**Figure S3 (left):** Fiber isotherm for Q12. Difference in slope between 2<sup>nd</sup> and 3<sup>rd</sup> experiment leads to approximately 1 order of magnitude lower sorption coefficient at a concentration of 10 nM. **Figure S4 (right):** Fiber isotherm for PYR12. Results show poor consistency with deviations >1 order of magnitude along the whole measurement range.



**Figure S5 (left):** Fiber isotherm for Q2-C10. Results become more erratic above a buffer concentration of 10 nM; fiber uptake seems to level off above a fiber concentration of 1 mM. **Figure S6 (right):** Fiber uptake kinetics for Q12 in 7 μm and 35 μm fibers at pH 6.5. Dotted line indicates 90% of fiber  $C_{\max}$  which is identical for both coating thicknesses.



**Figure S7 (left):** Fiber uptake kinetics for P12 in 7 μm fibers, at pH 6.5 and pH 11.1. Dotted line indicates 90% of fiber  $C_{\max}$  at pH 6.5; broken line indicates 90% of fiber  $C_{\max}$  at pH 11.1. Reaching  $C_{\max}$  takes considerably longer at pH 11.1, supporting our hypothesis of absorption of the neutral fraction. **Figure S8 (right):** Fiber uptake kinetics for P12 in 35 μm fibers, at pH 6.5 and pH 11.1. Dotted line indicates 90% of fiber  $C_{\max}$  at pH 6.5; broken line indicates 90% of fiber  $C_{\max}$  at pH 11.1. Reaching  $C_{\max}$  takes considerably longer at pH 11.1, supporting our hypothesis of absorption of the neutral fraction. It is also evident that this difference is much larger than observed for the 7 μm fiber, which further supports our hypothesis as molecules that are observed need more time to diffuse through the thicker coating.

**Table S4:** Freundlich coefficients (7  $\mu\text{m}$  fiber, 100 mM Na<sup>+</sup>).

Compound	pH	Freundlich coefficient	Log K	Number of datapoints
P12	6.8	0.71 $\pm$ 10.8%	3.43 $\pm$ 0.07	12
P12	7.8	0.71 $\pm$ 11.1%	3.67 $\pm$ 0.08	12
P12	8.4	0.76 $\pm$ 11.0%	3.96 $\pm$ 0.08	12
P12	9.7	0.69 $\pm$ 15.1%	4.37 $\pm$ 0.12	12
P12	10.6	0.64 $\pm$ 11.9%	4.42 $\pm$ 0.08	12
P12	11.1	0.65 $\pm$ 15.1%	4.56 $\pm$ 0.10	10
Q12	6.8	0.73 $\pm$ 11.6%	3.02 $\pm$ 0.08	12
Q12	7.8	0.67 $\pm$ 11.8%	3.25 $\pm$ 0.07	11
Q12	8.4	0.80 $\pm$ 18.2%	3.30 $\pm$ 0.14	12
Q12	9.7	0.80 $\pm$ 17.1%	3.61 $\pm$ 0.13	12
Q12	10.6	0.83 $\pm$ 16.2%	3.69 $\pm$ 0.12	12
Q12	11.1	0.79 $\pm$ 26.6%	3.81 $\pm$ 0.19	12

**Table S5:** Freundlich coefficients (35  $\mu\text{m}$  fiber, 100 mM Na<sup>+</sup>).

Compound	pH	Freundlich coefficient	Log K	Number of datapoints
P12	6.8	0.72 $\pm$ 10.8%	2.30 $\pm$ 0.07	12
P12	7.8	0.77 $\pm$ 6.3%	2.70 $\pm$ 0.05	12
P12	8.4	0.88 $\pm$ 7.5%	3.11 $\pm$ 0.07	12
P12	9.7	0.77 $\pm$ 14.6%	3.79 $\pm$ 0.13	12
P12	10.6	0.68 $\pm$ 13.7%	3.95 $\pm$ 0.10	12
P12	11.1	0.57 $\pm$ 28.9%	4.07 $\pm$ 0.17	10
Q12	6.8	0.80 $\pm$ 12.3%	1.89 $\pm$ 0.09	12
Q12	7.8	0.78 $\pm$ 14.2%	2.25 $\pm$ 0.11	12
Q12	8.4	0.84 $\pm$ 25.4%	2.31 $\pm$ 0.20	12
Q12	9.7	0.82 $\pm$ 12.6%	2.42 $\pm$ 0.10	12
Q12	10.6	0.87 $\pm$ 17.2%	2.50 $\pm$ 0.13	12
Q12	11.1	0.81 $\pm$ 20.2%	2.52 $\pm$ 0.15	12



# CHAPTER 3

---

## Sorption of Structurally Different Ionized Pharmaceutical and Illicit Drugs to a Mixed-Mode Coated Microsampler

Hester Peltenburg<sup>1,#</sup>, Niels Timmer<sup>1,#</sup>, Ingrid J. Bosman<sup>2</sup>,  
Joop L.M. Hermens<sup>1</sup>, Steven T.J. Droge<sup>1</sup>

<sup>1</sup> Institute for Risk Assessment Sciences, Utrecht University, P.O. Box 80177, 3508 TD Utrecht, The Netherlands.

<sup>2</sup> Netherlands Forensic Institute, P.O. Box 24044, 2490 AA The Hague, The Netherlands.

<sup>#</sup>These authors contributed equally to this work.

**Journal of Chromatography A, 1447, 1-8 (2016)**

## Abstract

The mixed-mode (C18/strong cation exchange-SCX) solid-phase microextraction (SPME) fiber has recently been shown to have increased sensitivity for ionic compounds compared to more conventional sampler coatings such as polyacrylate and polydimethylsiloxane (PDMS). However, data for structurally diverse compounds to this (prototype) sampler coating are too limited to define its structural limitations. We determined C18/SCX fiber partitioning coefficients of seventeen cationic structures without hydrogen bonding capacity besides the charged group, stretching over a wide hydrophobicity range (including amphetamine, amitriptyline, promazine, chlorpromazine, triflupromazine, difenzoquat), and eight basic pharmaceutical and illicit drugs ( $pK_a > 8.86$ ) with additional hydrogen bonding moieties (MDMA, atenolol, alprenolol, metoprolol, morphine, nicotine, tramadol, verapamil). In addition, sorption data for three neutral benzodiazepines (diazepam, temazepam, and oxazepam) and the anionic NSAID diclofenac were collected to determine the efficiency to sample non-basic drugs. All tested compounds showed nonlinear isotherms above 1 mmol/L coating, and linear isotherms below 1 mmol/L. The affinity for C18/SCX-SPME for tested organic cations without H-bond capacities increased with longer alkyl chains, ranging from logarithmic fiber-water distribution coefficients ( $\log D_{fw}$ ) of 1.8 (benzylamine) to 5.8 (triflupromazine). Amines smaller than benzylamine may thus have limited detection levels, while cationic surfactants with alkyl chain lengths  $>12$  carbon atoms may sorb too strong to the C18/SCX sampler which hampers calibration of the fiber-water relationship in the linear range. The  $\log D_{fw}$  for these simple cation structures closely correlates with the octanol-water partition coefficient of the neutral form ( $K_{ow,N}$ ), and decreases with increased branching and presence of multiple aromatic rings. Oxygen moieties in organic cations decreased the affinity for C18/SCX-SPME.  $\log D_{fw}$  values of neutral benzodiazepines were an order of magnitude higher than their  $\log K_{ow,N}$ . Results for anionic diclofenac species ( $\log K_{ow,N}$  4.5,  $pK_a$  4.0,  $\log D_{fw}$  2.9) indicate that the C18-SCX fiber might also be useful for sampling of organic anions. This data supports our theory that C18-based coatings are able to sorb ionized compounds through adsorption and demonstrates the applicability of C18-based SPME in the measurement of freely dissolved concentrations of a wide range of ionizable compounds.

## Introduction

Solid-phase microextraction (SPME) is a simple, passive sampling technique [200]. This technique has been evolving rapidly in the last decade, with innovations in coatings or extraction phases used [201-203], changes in experimental set-ups to allow for high-throughput sampling [204], and expanding to other fields of application including forensics [205], biomedical analysis [206], and *in vivo* sampling [207].

One of the recent advances in SPME is the use of so-called “mixed-mode” coatings. These coatings employ a mixture of two extraction mechanisms, thereby increasing analyte coverage. The C18/SCX fiber, consisting of a hydrophobic phase (C18) and strong cation exchange sites (SCX), is one of these “mixed-mode” coatings. The first publication on this fiber showed increased metabolite coverage ( $\log K_{ow}$  ranging between -3 to 7) compared to other SPME coatings in an untargeted metabolomics profiling study in human plasma [208]. The authors later showed that this SPME coating could also be used *in vivo*, when it was applied in mice [208], pigs [209, 210] and rats [211]. The major benefit of the C18/SCX fiber is the relative high sorption affinity for hydrophilic compounds, such as amino acid analogues [212], neurotransmitters [213] and glucuronide drug conjugates [214]. These studies show the high sensitivity of C18/SCX SPME in metabolomics.

Additionally, steps have been made to elucidate the sorption mechanism of the C18/SCX fiber. Using cationic amphetamine [182, 215] and cationic amitriptyline [215], a large number of variables have been identified that can influence sorption to the C18/SCX fiber. In general, the C18/SCX fiber shows increased sorption affinity for ionizable compounds compared to more conventional coatings, and over a wide pH range [181, 182]. Although C18/SCX fibers are not yet commercially available, these coatings could provide useful sampling tools in clinical application, where ionized or ionizable compounds are numerous, and for *in vivo* sampling, where matrix-modifying steps to ensure a large neutral fraction are impossible or undesirable.

Although the C18/SCX coating apparently has high sensitivity for cationic drugs, current data is limited to a few compounds. The chemical applicability domain of the mixed-mode SPME as a passive sampler depends to a large extent on the range of sorption affinities; not too high to (i) deplete systems, (ii) readily saturate the sampler, and/or (iii) hamper calibration of the fiber in the linear range, and not too low to meet adequate detection limits at relevant concentration ranges. Here, we present data on the sorption of

various structurally different compounds to the C18/SCX fiber. We studied the sorption of a number of ionized amines and ammonium compounds with different alkyl chain lengths, to assess the influence of amine class and hydrophobicity. Additionally, we studied a large set of basic pharmaceuticals and illicit drugs with a  $pK_a > 8$  containing additional polar moieties besides the charged group, as well as 3 neutral benzodiazepines and the acidic non-steroidal anti-inflammatory drug (NSAID) diclofenac ( $pK_a$  4.0).

## Materials and methods

### Chemicals and materials

SPME fibers with mixed-mode coating (C18/propylsulfonic acid; C18/SCX) are prototype fibers provided by Supelco, Sigma Aldrich (Bellefonte, PA, USA). They are produced in a nearly identical way as commercially available biocompatible C18-SPME fibers. The C18/SCX fibers consisted of a 3 cm piece of nitinol wire with a diameter of 202  $\mu\text{m}$  of which 1.5 cm contains the SPME coating, with an average thickness of 45  $\mu\text{m}$  (fiber volume 524 nL), delivered without the hypodermic needle used in the biocompatible C18-SPME fiber. Both C18 and propylsulfonic acid (2-2.5% sulfur loading) are bonded on porous HPLC column grade silica material (3  $\mu\text{m}$  particles, mean pore size 100 Å, total surface area  $\sim 450 \text{ m}^2\text{g}^{-1}$ ), which is then bound to the wire with a biocompatible polymeric binder (Supelco, personal communication). Phosphate buffered saline (PBS; pH 7.4) consisted of 138 mM NaCl, 8 mM  $\text{Na}_2\text{HPO}_4$ , 1.5 mM  $\text{KH}_2\text{PO}_4$  and 2.7 mM KCl (all Merck, Darmstadt, Germany) dissolved in Milli-Q water (18.2  $\text{M}\Omega\cdot\text{cm}$ , Millipore, Amsterdam, The Netherlands). Some compounds were tested at pH 6.3 to ensure that  $>99\%$  was present as the charged species. Tests at pH 6.3 were carried out using a 10 mM phosphate buffer with 50 mg/L  $\text{NaN}_3$  and NaCl, to a total ionic strength of 150 mM  $\text{Na}^+$ . Ammonia solution (25%) was obtained from Merck, trifluoroacetic acid was obtained from Sigma Aldrich (Zwijndrecht, The Netherlands). Methanol and acetonitrile were HPLC-grade (BioSolve, Valkenswaard, The Netherlands). A list of all test compounds including molecular structures is given in table S1.

### SPME procedure

Test solutions with different concentrations of analyte were made by spiking buffer using stock solutions in methanol, ensuring methanol fractions of  $<1\%$ . During SPME fiber exposure, samples were placed on a roller mixer (40 rpm). After equilibrium was reached, fibers were transferred to vials containing 120  $\mu\text{L}$  desorption fluid. Equilibrium times were



either determined empirically or fibers were exposed for at least 18 hours. Fibers were wiped gently using a paper tissue to remove any buffer droplets before placing them in desorption fluid. Desorption fluid for all compounds consisted of 90% acetonitrile and 10% Milli-Q water with 0.1%  $\text{NH}_3$  (of end volume), with a resulting pH of 11. After desorption and removal of the fiber, desorption solution was acidified to pH 2-3 using 60  $\mu\text{L}$  0.1 M HCl, to approximate the pH of the mobile phase [182]. To re-use the fibers, they were pooled after use, kept in desorption fluid overnight and subsequently stored in 50/50 methanol/Milli-Q at room temperature. C18/SCX SPME fibers show excellent repeatability and reproducibility, as previously described [215]. Fiber blanks (in triplicate) were incorporated in every experiment, using buffer solutions that had not been spiked to confirm the absence of carry-over between experiments. Since these fibers are intended for single use, they were checked regularly to monitor changes in sorption capacity after repeated use. If sorption capacity was decreased, new fibers were used for the next experiment.

For the linear alkyl amines, which were analyzed using LC-MS, fibers were desorbed using 90% acetonitrile and 10% Milli-Q water with 0.1% trifluoroacetic acid (of end volume) with a pH around 2 [78], as linear alkyl amines are volatile in their neutral form ( $\text{pH} > 8.5$ ). Aqueous samples for analysis were prepared by transferring 200  $\mu\text{L}$  of the aqueous phase to 600  $\mu\text{L}$  of this acidic desorption fluid. The resulting sample was mixed by repeated pipetting using the same pipette tip, to minimize loss of analyte to the tip. The acidic desorption fluid contained the tertiary amine N,N-dimethyldecylamine (T10) as internal standard to account for deviations in ionization efficiency.

The data in this paper has not been published previously, with exception of amphetamine [182], amitriptyline [215], diazepam [216], tramadol [216] and C12-DEA [181].

### **HPLC and LC-MS/MS parameters**

All pharmaceuticals were analyzed using HPLC with either UV or fluorescence detection. Only the linear alkyl amines were analyzed using LC-MS/MS. For all equipment and parameters used, see Supporting Information section S2 and S3.

## Quantification and data analysis

Fiber concentrations as well as aqueous concentrations were always measured. Sorption coefficients were calculated using the aqueous concentration after exposing the fiber instead of the initial concentration. A calibration curve made from aqueous concentrations before exposure was used to calculate the remaining aqueous concentration after exposure and calculate depletion using a mass balance approach. A calibration curve in acidified desorption fluid was used to calculate the concentration in fiber desorption samples and to confirm the mass balance. Calibration curves for the linear alkyl amines were made in the previously described acidic desorption fluid, again with T10 added as internal standard. For the lowest aqueous concentrations of amitriptyline, promazine, chlorpromazine and triflupromazine, quantification was not possible as these aqueous concentrations were below the LOQ of the current HPLC method. To still establish a sorption isotherm at these concentrations, the mass balance approach was used to calculate the aqueous concentration after exposure, assuming negligible sorption to the vial surfaces (as was shown by complete mass balances obtained at all other tested concentrations).

Data was plotted and analyzed using GraphPad Prism 6 for Windows. All samples were prepared in triplicate, unless specified otherwise. Data are plotted as mean  $\pm$  standard deviation in both x- (measured aqueous concentrations after fiber exposure) and y-direction (measured fiber concentrations). Fiber-water sorption coefficients ( $\log D_{f,w}$ ) are obtained by extrapolation of log linear curve to a sorbed concentration of 1 mmol/L fiber coating (at  $\log Y=0$ ). Although the porous coating material on the C18/SCX fibers represents a specific surface area rather than a bulk sorbent volume, a fiber coating volume of 524 nL was used as calculated according the average thickness of the fiber coating and the diameter of the nitinol wire, following refs [181, 182, 215].

## Results

### Normalizing the sorption affinity to C18/SCX at an equal chemical activity of 1 mmol/L coating

Before comparing sorption affinities between chemicals, we had to normalize the sorption affinity to a similar sorbed concentration, a similar “activity” in the sorbed state because all currently tested compounds display nonlinear sorption isotherms over wide concentration ranges, as previously reported by us [182] and others [217-219]. For all of the tested cationic and neutral compounds, C18/SCX-SPME sorption isotherm data span at least two orders of magnitude of aqueous concentrations. The anionic diclofenac was only tested at three concentrations in order to get comparable C18/SCX sorption data to measurements on the C18 fiber reported in [215]. All tested cationic and neutral compounds showed nonlinear isotherms above sorbed fiber concentrations of 10 mmol/L coating (Figure 3.1).

As we have discussed before [215], the C18-based SPME coatings are produced using highly porous silica particles for which adsorption is the main sorptive process. Apparently at loadings around 10 mmol/L, sorption sites reach critical levels where competition effects reduce the partition coefficients of both neutral and ionic compounds. Sorption eventually reaches a maximum loading (readily visualized for the dataset on the tricyclic antidepressant chlorpromazine, Figure 3.1). Below fiber concentrations of 1 mmol/L coating, however, the slopes of the isotherms for all compounds are all close to a value of 1 on logarithmic scale plots, suggesting that sorption is a linear process at these sorbent loadings. Since nearly all compounds were measured at, or close to, sorbed fiber concentrations of 1 mmol/L coating, we could fit the logarithmic fiber-water distribution coefficient ( $\log D_{fw}$ ) at 1 mmol/L coating (Tables 3.1 and 3.2), with exception of compound #12 (N-C-Phen-C8).  $\log D_{fw}$  was estimated using a Freundlich fit of the data below 10 mmol/L coating, thus only incorporating data in the linear concentration range.

**Table 3.1.** Fiber-water distribution coefficients ( $D_{fw}$ ) and octanol-water partition coefficients of organic cations: simple structures containing only C, H and N.

Compound #	Amine type	Name <sup>a)</sup>	Abbreviation <sup>b)</sup>	Log $D_{fw}$ <sup>c)</sup>	Log $K_{ow,N}$ selected <sup>d)</sup>
Same carbon chain length, different amine type					
1	NH <sub>3</sub> <sup>+</sup> (1°)	1-octanamine	N - C8	3.39	3.06
2	NH <sub>2</sub> <sup>+</sup> (2°)	N-methyl-1-octanamine	N (C) - C8	3.83	3.29
3	NH <sup>+</sup> (3°)	N,N-dimethyl-1-octanamine	N (C) (C) - C8	3.78	3.78
4	N <sup>+</sup> (4°)	N,N,N-trimethyl-1-octaminium	N (C) (C) (C) - C8	3.52	-
Primary amines, different carbon chains					
5	NH <sub>3</sub> <sup>+</sup>	1-decanamine	N - C10	4.27	4.12
6	NH <sub>3</sub> <sup>+</sup>	4-phenyl-1-butanamine	N - C4 - Phen	2.79	2.36
7	NH <sub>3</sub> <sup>+</sup>	amphetamine <sup>e)</sup>	N - C3 - Phen	2.64	1.81
8	NH <sub>3</sub> <sup>+</sup>	2-phenylethanamine	N - C2 - Phen	2.26	1.46
9	NH <sub>3</sub> <sup>+</sup>	1-phenylmethanamine	N - C - Phen	1.76	1.09
10	NH <sub>3</sub> <sup>+</sup>	1-(4-methylphenyl) methanamine	N - C - Phen - C1	2.25	1.55
11	NH <sub>3</sub> <sup>+</sup>	1-(4-butylphenyl) methanamine	N - C - Phen - C4	3.97	3.14
12	NH <sub>3</sub> <sup>+</sup>	1-(4-octylphenyl) methanamine	N - C - Phen - C8	-	5.27
Quaternary amines					
13	N <sup>+</sup>	N-benzyl-N,N-dibutyl-1-butanaminium chloride	N (C4) (C4) (C4) - C - Phen	4.28	-

a) Structures of the test chemicals are presented in Table S1 of the Supporting Information.

b) Abbreviation is based on the structure.

c) Sorption coefficients including 95% confidence interval are presented in Table S4 of the SI file.

d)  $K_{ow}$  values are taken from different sources (see Table S5 of the SI file).

e) Amphetamine is a drug, but because of its simple structure it is included in this data set. The C3 moiety contains a branched methyl group.

**Table 3.2.** Fiber-water distribution coefficients ( $D_{fw}$ ) and octanol-water partition coefficients of pharmaceutical and drugs. These organic cations containing C, H, N and in most cases H-bond donor and acceptor groups. Also, one anionic and three neutral compounds are included.

Compound #	Amine type	Name <sup>a)</sup>	No. Of H-bond donor (D) and acceptor (A) <sup>b)</sup>	Log $D_{fw}$ <sup>c)</sup>	Log $K_{ow,N}$ <sup>d)</sup> selected
Tertiary amines, tricyclic compounds					
14	NH <sup>+</sup>	Amitriptyline	-	4.51	4.92
15	NH <sup>+</sup>	Promazine	1 A	4.56	4.55
16	NH <sup>+</sup>	Chlorpromazine	1 A	4.84	5.41
17	NH <sup>+</sup>	Triflupromazine	1 A	5.37	5.54
Diverse compounds					
18	NH <sub>2</sub> <sup>+</sup>	MDMA	2 A	3.19	2.15
19	NH <sup>+</sup>	Tramadol	1 D, 2 A	3.31	2.51
20	NH <sup>+</sup>	Morphine	2 D, 3 A	2.38	0.89
21	NH <sup>+</sup>	Nicotine	1 A	2.43	1.17
22	NH <sup>+</sup>	Verapamil	5 A	4.94	3.79
23	NH <sup>+</sup>	C12-DEA <sup>e)</sup>	2 D, 2 A	4.55	4.69
24	N <sup>+</sup>	Difenzoquat <sup>e)</sup>	-	4.29	-
Secondary amines, beta blockers					
25	NH <sub>2</sub> <sup>+</sup>	Atenolol	2 D, 3 A	2.34	0.16
26	NH <sub>2</sub> <sup>+</sup>	Metoprolol	1 D, 3 A	4.03	1.88
27	NH <sub>2</sub> <sup>+</sup>	Alprenolol	1 D, 2 A	4.07	3.10
Neutral compounds, benzodiazepines					
28	Neutr.	Diazepam	2 A	4.15	2.82
29	Neutr.	Temazepam	1 D, 2 A	4.02	2.19
30	Neutr.	Oxazepam	2 D, 3 A	3.67	2.24
Anionic compound					
31	COO <sup>-</sup>	Diclofenac	1 D, 2 A	2.76	4.51

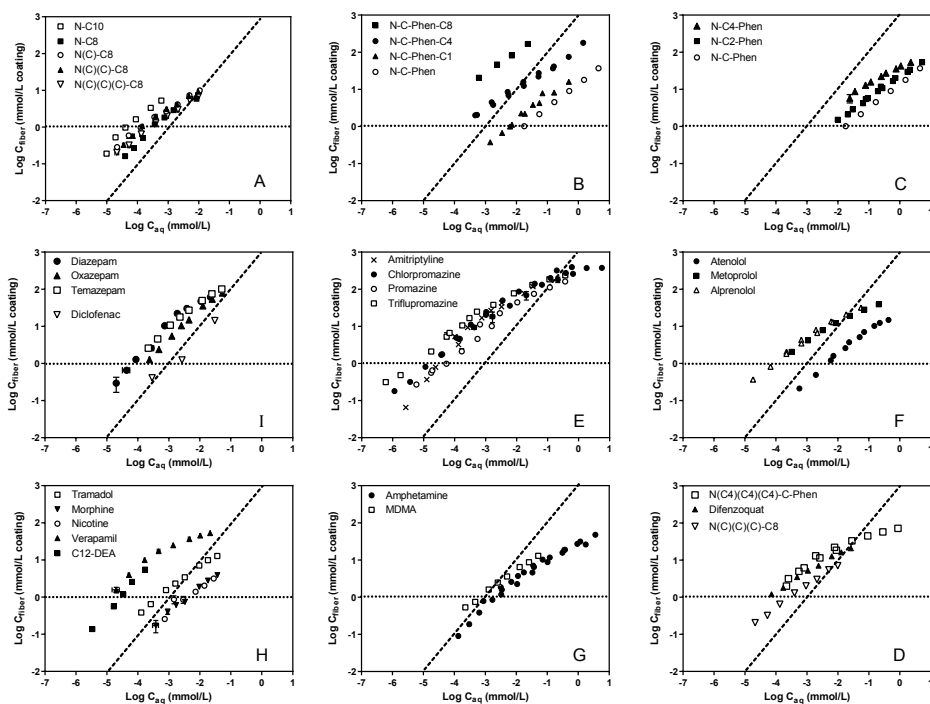
a) Structures of the test chemicals are presented in Table S1 of the Supporting Information.

b) H-bond donor and acceptor moieties were taken from [220].

c) Sorption coefficients including 95% confidence interval is presented in Table S4 of the SI file.

d)  $K_{ow}$  values are taken from different sources (see Table S5 of the SI file).

e) C12-DEA is a surfactant, difenzoquat is a pesticide.



**Figure 3.1.** Sorption isotherms to the C18/SCX fiber exposed in PBS medium for 48-96h. Broken lines indicate a linear relationship between concentrations on C18/SCX fibers and dissolved concentrations with a  $D_{fw}$  of 1000 ( $\log D_{fw}$  of 3). Horizontal dotted lines indicate sorbed concentrations of 1 mmol/L C18/SCX which are used to calculate  $\log D_{fw}$  values. Graphs (A-D) represent organic cations without oxygen containing H-bonding functional groups. Graph (E) are tricyclic antidepressant bases (also organic cations without oxygen containing H-bonding functional groups). Graph (F) are beta-blocker bases, graph (G) amphetamine bases, graph (H) analgesic bases, the basic calcium channel blocker (verapamil), and the cationic surfactant lauryl diethanolamine (C12-DEA), graph (I) benzodiazepines and the acidic NSAID diclofenac. Data for amphetamine is taken from ref. [182], data for amitriptyline from ref. [215], data for diazepam and tramadol are from [216], data for C12-DEA is from ref. [181], all with publisher permission. X- and Y-axes were kept identical to enable easy comparison.

### C18/SCX sorption affinity of organic cations with only C and H atoms

Sorption affinities to the C18/SCX fiber were determined for several series of cationic  $C_xH_yN$  structures that lack hydrogen bonding moieties besides the amine or ammonium. Compared to series of more complex pharmaceutical test compounds, these simple cationic structures allow for a more straightforward evaluation of the influence on the C18/SCX sorption affinity of (i) amine type (comparing 1<sup>o</sup>, 2<sup>o</sup>, 3<sup>o</sup> octylamines and 4<sup>o</sup> octyltrimethylammonium), (ii) different alkyl chain lengths (alkylbenzylamines), (iii)

presence of an aromatic ring, (iv) alkyl chain branching. This set of simple cations further allowed us to study the relationship between sorption affinities and simple molecular descriptors, as a framework to compare and predict the affinities of more complex organic cation structures.

Table 3.1 lists compounds with relatively simple structures with only C, H and N atoms. Using this small data set allows for a tentative estimation of fragment values for the contribution of simple molecular fragments, such as aliphatic carbon units, aromatic carbon units, and charged nitrogen moieties to the fiber-water sorption coefficient. Based on multiple linear regression of data for the eleven amines, fragment values were estimated (see Table 3.3 and Table S6). Fragment values for the different nitrogen head groups were not significant because each fragment for the head group occurs only once in the data set. Still – using the octylamines – there is a clear trend in the influence of amine type on sorption affinities, in the order  $2^\circ \approx 3^\circ > 4^\circ > 1^\circ$ , with a difference of 0.4 log units between  $2^\circ$  and  $1^\circ$  octylamines (Table 3.1). Interestingly,  $4^\circ$  octyltrimethylammonium has three methyl groups attached to the nitrogen atom, but does not have the highest sorption affinity of the linear alkyl amines as would be expected based on the contribution of an additional methyl group. Quaternary ammonium compounds may show lower sorption than expected, as the charge delocalization around the nitrogen atom can be unfavorable in sorption processes. Since these simple amines were tested as >99.9% ionic species, it is unlikely that the fraction of neutral species contributed to sorption to the C18/SCX coating.

The trend in fragment values for  $D_{fw}$  follows the trend in  $K_{ow,N}$  based fragments for neutral nitrogen head groups (see Table 3.3). Clearly, the values for the N entities for sorption to the C18/SCX are much higher than values of the same fragments for the octanol-water system because of the lack of electrostatic interactions in octanol [221].

Fragment values for aliphatic carbon and for aromatic carbon in a phenyl group were significant:  $0.48 \pm 0.06$  for aliphatic carbon and  $0.29 \pm 0.07$  for an aromatic carbon (Table 3.3). These values of 0.48 and 0.29 are very similar to fragment values for partitioning between water and octanol for neutral compounds: 0.49 for an aliphatic  $\text{CH}_2$  fragment and 0.23 for an aromatic carbon atom (Table 3.3). The difference in these fragment values for aliphatic and aromatic carbon atoms is related to differences in molecular volume or surface area of an aliphatic hydrocarbon chain versus an aromatic hydrocarbon. The van der Waals surface area (SA) of hexane (aliphatic C6) and benzene (aromatic C6) are 178 and  $110 \text{ \AA}^2$ , respectively [222]. The ratio in SA of benzene versus hexane of 0.62 is similar as the

ratio in fragment values ( $C_{\text{aliphatic}} / C_{\text{aromatic}}$ ) for  $D_{\text{fw}}$  of 0.60. In addition to the influence of surface area, the hydrogen bond accepting character of an aromatic ring may also have a slight influence on sorption of aromatic compounds.

The  $D_{\text{fw}}$  of tributylbenzylammonium (compound #13) is lower than predicted via these fragments. The reason is likely the extensive charge delocalization on all branches on the amine (by one phenyl and three C4 chains) and the more bulky structure of this molecule. It also shows considerably lower affinity to C18/SCX as the simple aromatic amines. Amphetamine only has 1 branched methyl unit, and fits closely to the relationship observed for all simple aromatic amines.

**Table 3.3.** Fragment values for fiber–water partitioning ( $K_{\text{fw}}$ ) and octanol–water partition coefficient (see details in Table S6 of the SI).

Fragment	Fragment value for sorption to C18/SCX fiber	Fragment	Fragment value for partitioning to octanol (neutral compound) <sup>d</sup>
- NH <sub>3</sub> <sup>+</sup>	-0.51 ± 0.59 <sup>a)</sup>	- NH <sub>2</sub>	-1.41
- NH <sub>2</sub> <sup>+</sup> (C)	-0.03 ± 0.55 <sup>a)</sup>	- NH (C)	-0.95
- NH <sup>+</sup> (C)(C)	-0.08 ± 0.55 <sup>a)</sup>	- N (C)(C)	-0.72
- N <sup>+</sup> (C)(C)(C)	-0.34 ± 0.55 <sup>a)</sup>		n.a. <sup>d)</sup>
CH <sub>2</sub> (aliphatic)	0.48 ± 0.07 <sup>b)</sup>	CH <sub>2</sub> (aliphatic)	0.49
CH (aromatic)	0.29 ± 0.09 <sup>b)</sup>	CH (aromatic)	0.23

a) Fragment value is not significant (see text for explanation).

b) Fragment value is significant ( $p < 0.01$ ).

c) Derived from EpiSuite [223].

d) Fragment value for quaternary nitrogen not available.

### C18/SCX sorption affinity of pharmaceuticals and drugs with additional hydrogen bonding moieties

To study the sorption of more polar cations to the C18/SCX fiber, we used a set of 14 different pharmaceutical and illicit drugs. Most of them are >98% cationic at test pH, with the exception of diazepam, oxazepam, temazepam (all neutral), and diclofenac (>99% anionic). Table 3.2 lists all log  $D_{\text{fw}}$  values (at a  $C_{\text{fiber}}$  of 1 mmol/L coating) for these more polar compounds. We found relatively high sorption affinities for all compounds tested. For the  $C_xH_yN^+$  amine amphetamine, the C18/SCX fiber was shown to have increased sorption affinity compared to polyacrylate fibers [182], and this was also shown for a more hydrophobic cationic surfactant lauryl diethanolamine (C12-DEA) [181]. Haftka et al. measured sorption affinity of chlorpromazine to polyacrylate fibers at pH 7 and found log



$D_{fw}$  values of 3.12 [170], while the C18/SCX fiber displays a 50-fold higher sorption affinity for chlorpromazine ( $\log D_{fw} = 4.84$  at pH 6.3, see table 3.2).

The following discussion of the sorption data to the C18/SCX fiber and the effects of chemical structure on sorption is based on a comparison with octanol-water partition coefficients of the neutral form of the compounds ( $\log K_{ow,N}$ ). Of course  $\log K_{ow,N}$  is typically used to describe the hydrophobicity driven sorption behavior of neutral compounds, and typically  $\log K_{ow,N}$  accounts for differences due to the presence of aliphatic carbon chains and aromatic rings and many polar functional groups. Experimentally derived  $\log K_{ow,N}$  values are available for the neutral form of several of our compounds (Tables 1 and 2), and can be predicted with limited accuracy for the remaining set of compounds, e.g. using the EpiSuite algorithm or the ACD Labs software (see Table S5). Using  $\log K_{ow,N}$  however, precludes the analysis of quaternary ammonium compounds, since there is no neutral form for these organic salts. Since experimental  $\log K_{ow,N}$  values are not available for several simple  $C_xH_yN^+$  amines, ACD labs estimates are used. For the set of organic cations,  $\log K_{ow,N}$  is a useful descriptor of the organic cations without an oxygen containing H-bond donor/acceptor group, as shown in Figure 3.2. The tricyclic compounds agree well with the other simple amines based on their  $\log K_{ow,N}$ . Apparently the additional sulfur atom and chlorine or fluorine atoms do not lead to a significant increase in the sorption to the C18/SCX fiber.

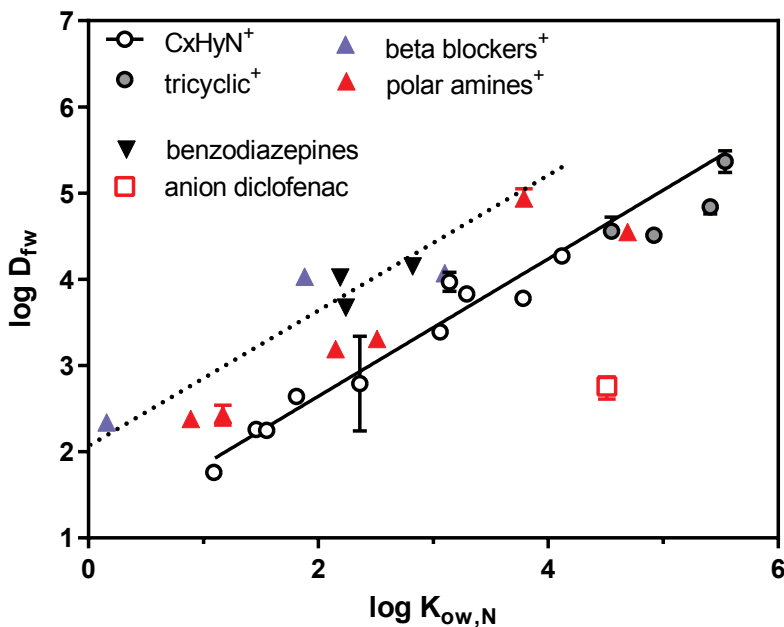
When these groups of organic cations are combined they give a strong simple regression for all amines, only disregarding amines with oxygen containing H-bonding functionality:

$$\log D_{fw,cation} \text{ (at } <1 \text{ mmol/L C18/SCX)} = 0.80 (\pm 0.07) \cdot \log K_{ow,N} + 1.05 (\pm 0.19), \quad (\text{eq. 1})$$

$$n=10, R^2=0.946, \text{ sy.x (standard deviation of the residuals, as } (SS/df)^{0.5}) = 0.213$$

For three neutral benzodiazepine compounds, sorption affinity to the C18/SCX fiber does not appear to be readily predictable based on (experimentally derived)  $\log K_{ow,N}$  values alone. Diazepam, oxazepam and temazepam are structurally very similar but do show significant differences in sorption affinity. Compared to diazepam, temazepam has an extra OH group, which causes a decrease in sorption affinity of approximately 0.1 log units (though not significant), while experimental  $\log K_{ow,N}$  values differ by 0.6 log units. Oxazepam contains the same OH group but is also demethylated, further decreasing the C18/SCX sorption affinity by 0.3 log units, while experimental  $\log K_{ow,N}$  values do not differ between oxazepam and temazepam (Table 3.2).

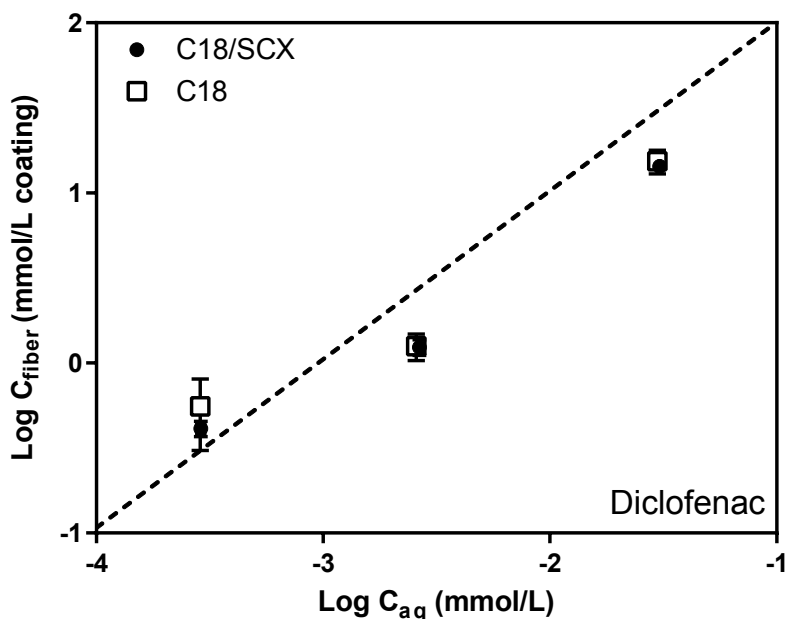
The relationship in equation 1 illustrates again that cationic species sorb stronger than expected to the porous C18/SCX material on the mixed mode SPME fibers, taking into account that these ionized compounds also display a very high aqueous solubility. Similar conclusion can be drawn from the fragment values in Table 3.3. It is also interesting to note that six polar compounds are well predicted with the  $\log K_{ow,N}$  relationship, while three are substantial outliers that sorb much stronger to the C18/SCX fiber than predicted by the  $\log K_{ow,N}$  of the neutral form. The three cationic beta-blockers have a similar backbone, containing multiple polar groups, but with different substitutions on the aromatic ring: atenolol ( $\log K_{ow,N}$  0.16, methylamide in para-position) and metoprolol ( $\log K_{ow,N}$  1.88, methoxyethyl in para-position) sorb a factor 15 and 30, respectively, stronger to the C18/SCX material than predicted by eq. 1, while the more hydrophobic beta-blocker alprenolol ( $\log K_{ow,N}$  3.10, vinyl group in ortho-position) differs only by a factor of 3. The only other polar organic cation that differs more than a factor of 5 is the large calcium channel blocker verapamil ( $\log K_{ow,N}$  3.79, two aromatic rings, 4 ethers). The other polar organic cations nicotine (heterocyclic nitrogen), MDMA (methylenedioxy), tramadol (hydroxy and methoxy units), morphine (complex polycyclic diol) all sorb up to a factor 3 stronger when compared to the regression based on simple  $C_xH_yN^+$  amines. The cationic surfactant C12-DEA appears to follow the sorption as predicted based on  $\log K_{ow,N'}$  while containing 2 ethanol groups.



**Figure 3.2.** Relationship between octanol-water partitioning of neutral species (ACD Labs estimates for  $C_xH_yN^+$  amines, experimental values for all others) and linear sorption affinity to the C18/SCX coating of the corresponding cationic species.  $C_xH_yN^+$  compounds are from table 3.1, with exception of the quaternary amines (compounds 4 and 13, as these have no  $\log K_{ow,N}$ ) and compound 11 (as  $\log D_{fw}$  could not be extrapolated accurately). The polar amines are listed in table 3.2, compounds 18-23. The dotted line indicates a 10x higher sorption affinity to the C18/SCX fiber compared to the  $\log K_{ow,N}$  relationship (line =  $0.80 \cdot \log K_{ow,N} + 2.05$ ).

Other physicochemical descriptors than  $\log K_{ow,N}$  may be sought to derive an overall polyparameter relationship for organic cations, which includes the sorption values of atenolol, verapamil and metoprolol, to predict the linear sorption affinity to C18/SCX. For instance, Difilippo and Eganhouse [224] combined sorption affinities of hydrophobic organic compounds to polydimethylsiloxane (PDMS) coated fibers and were able to predict sorption through a polyparameter linear solvation energy relationship (LSER), using parameters related to the refractive index, polarizability and hydrogen bonding capacities in addition to the molecular volume. A similar compilation was made by Endo et al. [92] for a diverse set of neutral organic compounds, where sorption to polyacrylate coated SPME fibers could be predicted through polyparameter linear free energy relationship (PP-LFER) models. Limitation of these polyparameter predictions is that they only seem to be applicable to sorption of neutral compounds to neutral SPME coatings, and the

required experimental molecular descriptors are (i) not equally relevant, and likely even different for charged chemicals, and (ii) none are available for the neutral form of the tested chemicals in our study.



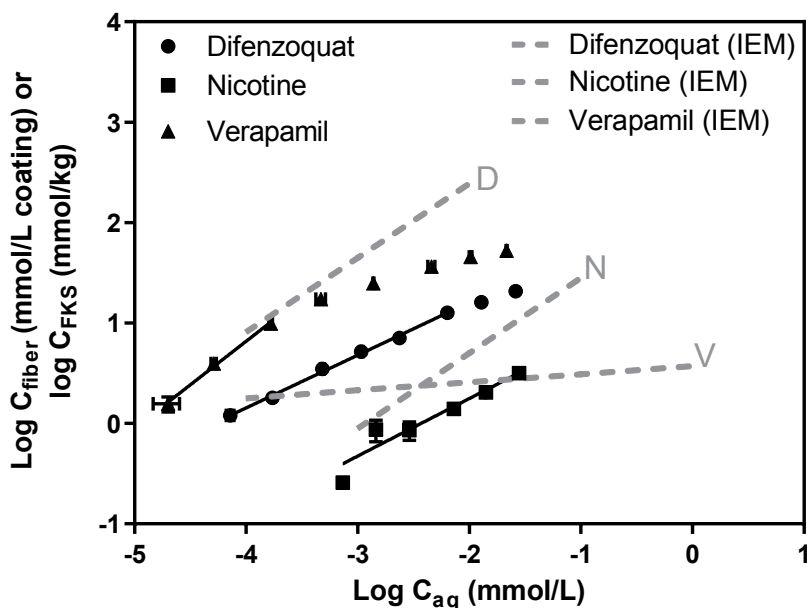
**Figure 3.3.** Comparison of sorption of diclofenac to the C18/SCX and C18 fiber. Exposure time was 72 hours. Dotted line indicates linearity.

The predominantly anionic compounds diclofenac shows substantial sorption to the C18/SCX fiber, which is surprising as it was expected that the anionic species are repulsed from the (presumably) negatively charged C18/SCX surface. Based on its  $\log K_{\text{ow},N'}$  diclofenac indeed sorbs a factor 64 lower than predicted by the organic cation regression of equation 1. At pH 7.4, only 0.04% of diclofenac is present in the neutral form. Comparison of the C18/SCX fiber and C18 fiber (without strong cation exchange sites) shows equal sorption of diclofenac to both fiber types (figure 3.3). The strong cation exchange groups in the C18/SCX coating do not appear to inhibit sorption of anionic diclofenac. However, as sorption of diclofenac is lower than the predicted sorption based on  $\log K_{\text{ow},N'}$  which could indicate that both the C18 and the C18/SCX coating contain sorbent material that repulses anions. We have previously hypothesized that deprotonated free silanol groups might contribute to the sorption of cations, and counteract the sorption of anions [182, 215]. However, to be

able to predict sorption behavior of anionic compounds, the data set on these compounds should be extended.

### Comparison of C18/SCX fibers with cation-exchange membranes

Recently, ion-exchange membranes were applied to study freely dissolved concentration of ionized compounds [219]. A cation exchange membrane (IEM) was used to study the sampler affinity in HBSS buffer (pH 7.4) for the cationic compounds nicotine, difenzoquat and verapamil. Here, we studied the sorption affinity of these compounds to the C18/SCX fiber and compared sorption affinities and Freundlich slopes ( $n_F$ ) of both passive sampling devices (figure 3.4).



**Figure 3.4.** Comparison of sorption isotherms for difenzoquat, nicotine and verapamil to the C18/SCX fiber and ion-exchange membranes [219].

Using the IEM, good results were obtained for difenzoquat and nicotine. However, sorption of verapamil resulted in a nearly constant concentration in the IEM at any water concentration tested, reflected by the Freundlich slope of 0.08 [219]. According to the authors, the IEM was already saturated at the lowest water concentration tested. However, this is inconsistent with the total ion-exchange capacity of these membranes, which is

reported at 1200 mmol/kg. Using the C18/SCX fiber, good results were obtained for all three compounds. Freundlich slopes are somewhat more nonlinear than those obtained with the IEM, with exception of verapamil (table 3.4). As the cation-exchange capacity of the C18/SCX fibers (~400 mmol/L coating) is a factor three lower than that of the IEM, sorption of cationic compounds to the C18/SCX fiber starts to level off at a lower fiber loading compared to the IEM.

For both passive sampling materials, molecular size and structural geometry could influence the accessibility of the ion-exchange sites. It is likely that sorption of verapamil to the IEM is limited by its large molecular size, thereby limiting the occupation of all cation-exchange sites. This compound has more predictable sorption to the C18/SCX fiber, as highlighted by the higher Freundlich coefficient. This could be the result of the highly porous nature of the C18/SCX coating, making it more accessible for larger compounds. This porosity can also have disadvantages, such as fouling of the device in protein-containing samples. A good example is fouling with bovine serum albumin (BSA). This fouling effect is larger for the IEM at low BSA concentrations, but larger for the C18/SCX fiber at high BSA concentrations [216].

**Table 3.4.** Comparison of sorption isotherm parameters for difenzoquat, nicotine and verapamil using ion-exchange membranes [219] or C18/SCX fibers.

Compound	This study			Oemisch et al.		
	$K_F$ (10 $\mu\text{M}$ )	$n_F$ (0.01-1 mmol/L)	$\log D_{fw}$ at 1 mmol/L	$K_F$ (10 $\mu\text{M}$ )	$n_F$ (1-100 $\mu\text{M}$ )	$\log K_{IEM/water}$ at 1 mmol/kg
difenzoquat	3.21	0.53	4.29	4.40	0.74	5.23
nicotine	2.25	0.57	2.43	2.70	0.75	2.93
verapamil	4.55	0.87	4.94	2.32	0.08	7.12

Distribution coefficients ( $\log K_{IEM/water}$  for the ion-exchange membranes and  $\log D_{fw}$  for the C18/SCX fibers) are calculated at  $C_{aq}$  of 10  $\mu\text{M}$  using the Freundlich equation with exponent  $n_F$  over the tested dissolved concentration range, and at a constant sorbed "activity" of 1 mmol/kg.

## Conclusion

The C18/SCX fiber has previously shown to be capable of extracting cationic compounds. Here, the data set for sorption of cationic compounds is expanded. In addition, sorption of three neutral compounds and one anionic compound is incorporated. As all compounds show sorption to the C18/SCX fiber, this strongly supports our hypothesis that ionized compounds sorb to C18-based SPME coatings through adsorptive processes. The strong cation exchange groups in the C18/SCX fiber increase sensitivity of this fiber for cationic compounds, but could also make the C18/SCX fiber more prone to competitive effects of salts, especially for polar cations with relatively low sorption affinities (e.g.  $\log D_{fw} < 2$ ). This makes modeling sorption of ionizable compounds to the C18/SCX fiber difficult. However, there is a clear linear relationship between molecular weight and sorption affinity for alkyl amines and aromatic amines without oxygen-containing H-bonding groups. Moreover, this relationship also exists for all  $C_xH_yN^+$  cations based on  $\log K_{ow,N^+}$  facilitating the expectations for the calibration feasibility of the C18/SCX fiber for related organic cation structures, e.g. cationic surfactants. More polar compounds, i.e. cations with oxygen-containing H-bonds, sorb as strong as or stronger to the C18/SCX fiber than predicted based on this  $\log K_{ow,N}$  relationship.

## Supporting Information

Sorption of Structurally Different Ionized Pharmaceutical and Illicit Drugs to a Mixed-Mode Coated Microsampler

### Contents:

**Table S1:** *Properties of test compounds*

**Table S1:** *Molecular structures of all test compounds*

**Section S2:** *HPLC analysis parameters*

**Section S3:** *LC-MS parameters*

**Table S4:** *Sorption coefficients for all test compounds including confidence interval*

**Table S5:** *Octanol-water partition coefficients*

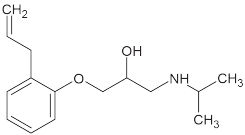
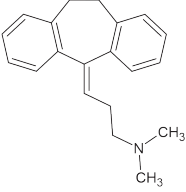
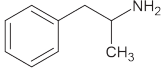
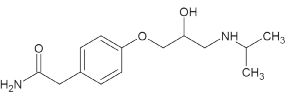
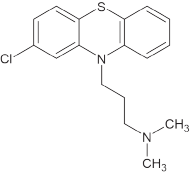
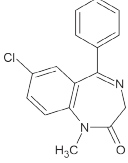
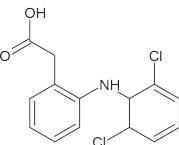
**Table S6:** *Fragment value calculations*



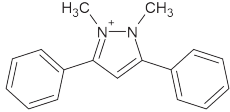
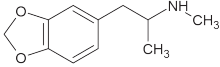
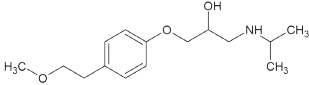
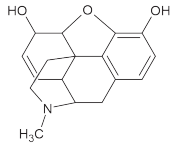
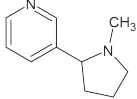
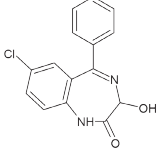
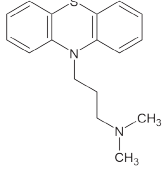
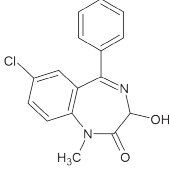
**Table S1:** Test compounds $C_xH_yN$  compounds

Compound	Supplier	CAS number	Molecular structure
<b>N-C-Phen</b> 1-phenylmethanamine	Sigma-Aldrich	100-46-9	
<b>N-C-Phen-C1</b> 1-(4-methylphenyl)methanamine	Sigma-Aldrich	104-84-7	
<b>N-C-Phen-C4</b> 1-(4-butylphenyl)methanamine	Chemos	57802-79-6	
<b>N-C2-Phen</b> 2-phenylethanamine	Sigma-Aldrich	64-04-0	
<b>N-C4-Phen</b> 4-phenyl-1-butanamine	Sigma-Aldrich	13214-66-9	
<b>N-C-Phen-C8</b> 1-(4-octylphenyl)methanamine	Chemos	176956-02-8	
<b>N (C4) (C4) (C4) - C-Phen</b> N-benzyl-N,N-dibutyl-1-butanaminium chloride	Acros	54225-72-8	
<b>N-C8</b> 1-octanamine	Alfa Aesar	111-86-4	
<b>N-C10</b> 1-decanamine	Sigma-Aldrich	2016-57-1	
<b>N (C) -C8</b> N-methyl-1-octanamine	Alfa Aesar	2439-54-5	
<b>N (C) (C) -C8</b> N,N-dimethyl-1-octanamine	Sigma-Aldrich	7378-99-6	
<b>N (C) (C) (C) -C8</b> N,N,N-trimethyl-1-octaninium bromide	Sigma-Aldrich	2083-68-3	
<b>C12-DEA</b> N-dodecyl-N,N-diethanol amine	Akzo Nobel	1541-67-9	

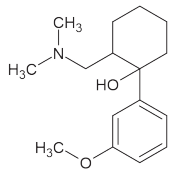
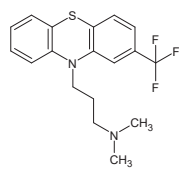
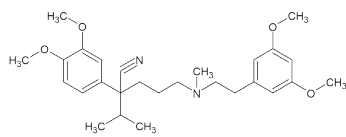
## Pharmaceuticals and illicit drugs

Compound	Supplier	CAS number	Molecular structure
Alprenolol	Sigma-Aldrich	13655-52-2	
Amitriptyline	Sigma-Aldrich	50-48-6	
Amphetamine	Spruyt Hillen	300-62-9	
Atenolol	Dr. Ehrenstorfer	29122-68-7	
Chlorpromazine	Sigma-Aldrich	50-53-3	
Diazepam	Spruyt Hillen	439-14-5	
Diclofenac	Sigma-Aldrich	15307-86-5	

## Pharmaceuticals and illicit drugs (Continued)

Compound	Supplier	CAS number	Molecular structure
Difenzoquat	Sigma-Aldrich	49866-87-7	
MDMA (methylene dioxy methamphetamine)	Duchefa	42542-10-9	
Metoprolol	Dr. Ehrenstorfer	51384-51-1	
Morphine	Spruyt Hillen	57-27-2	
Nicotine	Sigma-Aldrich	54-11-5	
Oxazepam	Spruyt Hillen	604-75-1	
Promazine	Sigma-Aldrich	58-40-2	
Temazepam	Spruyt Hillen	846-50-4	

## Pharmaceuticals and illicit drugs (Continued)

Compound	Supplier	CAS number	Molecular structure
Tramadol	Sigma-Aldrich	27203-92-5	
Triflupromazine	Sigma-Aldrich	146-54-3	
Verapamil	Sigma-Aldrich	52-53-9	

**Table S2:** HPLC analysis parameters

The LC system used was a Prominence HPLC, consisting of two pumps, an autosampler, a column oven, a UV-detector and fluorescence detector, all from Shimadzu ('s-Hertogenbosch, The Netherlands), and a C18 column (GraceSmart RP18, ID 150 x 2.1 mm, 5  $\mu$ m particle size, Grace, Breda, The Netherlands). Column oven was set at 40°C, mobile phase flow rate was 0.4 mL/min (with exception of nicotine, which was 0.2 mL/min). For all drugs, isocratic elution was achieved by using a ratio of 10 mM phosphate buffer at pH 3 and organic phase. Some linear alkyl amines were separated using a gradient. Detection was either with UV or fluorescence. For any compound that could be detected using fluorescence, UV detection was usually also employed, but the fluorescence signal was used for quantification. Used ratios of buffer and organic phase, UV wavelength and/or fluorescence excitation and emission wavelengths for each compound are summarized in the table below.

*C<sub>x</sub>H<sub>y</sub>N* compounds

<b>Compound</b>	<b>Ratio buffer : organic</b>	<b>UV wavelength</b>	<b>Fluorescence (<math>\lambda_{ex}/\lambda_{em}</math>)</b>	<b>LOQ (nM)</b>
N-C-Phen	97 : 3 (A)	208 nm	-	1050
N-C-Phen-C1	98 : 2 à 40 : 60 (A)	211 nm	-	400
N-C-Phen-C4	100 : 0 à 40 : 60 (A)	217 nm	-	175
N-C-Phen-C8	80 : 20 à 25 : 75 (A)	208 nm	-	1350
N-C2-Phen	96 : 4 (A)	208 nm	-	375
N-C4-Phen	91.5 : 8.5 (A)	208 nm	-	385
N(C4)(C4)(C4)-C-Phen	100 : 0 à 25 : 75 (A)	208 nm	-	200

*Pharmaceutical and illicit drugs*

<b>Compound</b>	<b>Ratio buffer : organic</b>	<b>UV wavelength</b>	<b>Fluorescence (<math>\lambda_{ex}/\lambda_{em}</math>)</b>	<b>LOQ (nM)</b>
Alprenolol	70 : 30 (A)	220 nm	230/302 nm	10
Amitriptyline	65 : 35 (A)	239 nm	-	420
Amphetamine	95 : 5 (A)	208 nm	204/280 nm	45
Atenolol	94 : 6 (A)	220 nm	230/302 nm	15
Chlorpromazine	48 : 52 (M)	255 nm	-	60
Diazepam	55 : 45 (A)	240 nm	-	175
Diclofenac	55 : 45 (A)	276 nm	-	965
Difenzoquat	70 : 30 (A)	254 nm	-	215
MDMA	90 : 10 (A)	205 nm	285/320 nm	175
Metoprolol	85 : 15 (A)	220 nm	230/302 nm	10
Morphine	95 : 5 (A)	NA	235/345 nm	1085
Nicotine	95 : 5 (A)	260 nm	-	120
Oxazepam	55 : 45 (A)	240 nm	-	65
Promazine	48 : 52 (M)	251 nm	-	50
Temazepam	55 : 45 (A)	240 nm	-	260
Tramadol	85 : 15 (A)	205 nm	200/300 nm	100
Triflupromazine	43 : 57 (M)	256 nm	-	50
Verapamil	70 : 30 (A)	210 nm	280/315 nm	10

Mobile phase composition and detection wavelengths for all study compounds. Organic phase is acetonitrile (A) or methanol (M).

**Table S3:** LC-MS parameters

The compounds without UV absorption, i.e. the linear alkyl amines, were analyzed using LC-MS/MS. A Perkin-Elmer liquid chromatography system (Norwalk, CT, USA) was coupled to a triple quadrupole/linear ion trap mass spectrometer (MDS Sciex API3000 LC-MS/MS System, Applied Biosystems, Foster City, CA, USA). The interface was a Turbo Ion spray source set in positive ionization mode at 4500V and operated at 400°C. Separation occurred through a Kinetex 2.6 µm XB-C18 column (50 × 2.1 mm, 100Å) with a UPLC C18 guard column. Mobile phase consisted of Milli-Q water and methanol both containing 0.1% formic acid, and each compound was run using a gradient. Run started at 5% methanol for 3.5 minutes, then increasing to 95% methanol in 1 minute. 95% methanol was maintained until 5.8 minutes, then immediately returned to 5% methanol until the end of the run (6.8 minutes). N(C)(C)-C10 is the internal standard used in the LC-MS analysis for each of the linear alkyl amines. A solvent switch was set to waste from 0 to 3.9 minutes, to MS from 4.0 until 6.4 minutes, and then to waste until end of the run. Acquisition was achieved using Analyst 1.4.2 (MDS Sciex Applied Biosystems) in selected reaction monitoring mode with fragmentation at specific m/z values.

<b>Compound</b>	<b>DP (V)</b>	<b>FP (V)</b>	<b>CV (V)</b>	<b>M1 m/z</b>	<b>M3 m/z</b>	<b>LOQ (nM)</b>
N-C8	70	200	16	130.1	70.9	<5
N-C10	35	200	18	158.2	71.1	<1
N(C)-C8	60	250	19	144.1	71.0	<1
N(C)(C)-C8	80	200	30	158.4	46.0	<5
N(C)(C)(C)-C8	43	292	34	172.3	60.0	<1
N(C)(C)-C10 (IS)	70	350	33	185.9	57.1	-

DP: declustering potential

FP: focusing potential

CV: collision voltage

Analysis details of C12-DEA are provided in: Wang F, Chen Y, Hermens JLM, Droge STJ, *Evaluation of passive samplers with neutral or ion-exchange polymer coatings to determine freely dissolved concentrations of the basic surfactant lauryl diethanolamine: Measurements of acid dissociation constant and organic carbon–water sorption coefficient*. *Journal of Chromatography A* (2013): 1315; 8-15.

**Table S4:** Sorption coefficients of all test compounds including confidence interval

<b>Compound</b>	<b>Log D<sub>fw</sub> (95% CI)</b>	<b>N</b>
1-octanamine	3.39 (3.33-3.45)	21
N-methyl-1-octanamine	3.83 (3.79-3.87)	24
N,N-dimethyl-1-octanamine	3.78 (3.73-3.84)	24
N,N,N-trimethyl-1-octaminium bromide	3.52 (3.49-3.55)	24
1-decanamine	4.27 (4.21-4.33)	17
4-phenyl-1-butanamine	2.79 (2.24-3.34)	8
Amphetamine	2.64 (2.59-2.69)	43
2-phenylethanamine	2.26 (2.20-2.31)	19
1-phenylmethanamine	1.76 (1.74-1.78)	12
1-(4-methylphenyl)methanamine	2.25 (2.20-2.30)	26
1-(4-butylphenyl)methanamine	3.97 (3.86-4.08)	18
1-(4-octylphenyl)methanamine	-	-
Amitriptyline	4.51 (4.45-4.56)	18
Promazine	4.56 (4.51-4.72)	17
Chlorpromazine	4.84 (4.76-4.91)	11
Triflupromazine	5.37 (5.24-5.49)	10
N-benzyl-N,N-dibutyl-1-butanaminium chloride	4.28 (4.11-4.45)	15
Difenzoquat	4.29 (4.25-4.34)	18
MDMA	3.19 (3.16-3.23)	21
Atenolol	2.34 (2.30-2.38)	18
Metoprolol	4.03 (3.94-4.13)	6
Alprenolol	4.07 (4.02-4.13)	16
Tramadol	3.31 (3.28-3.34)	21
Morphine	2.38 (2.32-2.43)	21
Nicotine	2.43 (2.31-2.54)	18
Verapamil	4.94 (4.84-5.05)	9
N-dodecyl-N,N-diethanol amine	4.55 (4.45-4.62)	6
Diazepam	4.15 (4.11-4.20)	27
Temazepam	4.02 (3.98-4.05)	24
Oxazepam	3.67 (3.65-3.70)	24
Diclofenac	2.76 (2.61-2.87)	6

**Table S5:** Octanol-water partition coefficients

Compound	Log $K_{ow}$		
	Exp.	EpiSuite	ACD
1-octanamine	2.90	2.80	3.06
N-methyl-1-octanamine	-	3.27	3.29
N,N-dimethyl-1-octanamine	-	3.48	3.78
N,N,N-trimethyl-1-octaminium bromide	-	-	-
1-decanamine	-	3.78	4.12
4-phenyl-1-butanamine	2.40	2.54	2.36
Amphetamine	1.76	1.76	1.81
2-phenylethanamine	1.41	1.34	1.46
1-phenylmethanamine	1.09	1.07	1.09
1-(4-methylphenyl)methanamine	1.46	1.62	1.55
1-(4-butylphenyl)methanamine	-	3.09	3.14
1-(4-octylphenyl)methanamine	-	5.05	5.27
Amitriptyline	4.92	4.95	4.92
Promazine	4.55	4.56	4.63
Chlorpromazine	5.41	4.32	5.20
Triflupromazine	5.54	5.52	5.70
N-benzyl-N,N-dibutyl-1-butanaminium chloride	-	-	-
Difenzoquat	-	-	-
MDMA	2.15	2.28	1.81
Atenolol	0.16	-0.03	0.10
Metoprolol	1.88	1.69	1.79
Alprenolol	3.10	2.81	2.88
Tramadol	2.51	3.01	2.51
Morphine	0.89	0.72	0.43
Nicotine	1.17	1.00	0.72
Verapamil	3.79	4.80	3.90
N-dodecyl-N,N-diethanol amine	-	4.11	4.69
Diazepam	2.82	2.70	2.91
Temazepam	2.19	2.15	2.15
Oxazepam	2.24	2.32	2.31
Diclofenac	4.51	4.02	4.06

All  $K_{ow}$  values were obtained from Chemspider ([www.chemspider.com](http://www.chemspider.com)). For all pharmaceuticals, experimental values were used. In general, predicted values from ACD labs were closer to experimental values than predicted values from EpiSuite. Therefore, predicted values from ACD labs were used for all other compounds.



**Table S6:** Fragment value calculations

	X1	X2	X3	X4	X5	X6
Y	N	NC	NCC	NCCC	C	phenyl
3,39	1	0	0	0	8	0
3,83	0	1	0	0	8	0
3,78	0	0	1	0	8	0
3,52	0	0	0	1	8	0
4,27	1	0	0	0	10	0
2,25	1	0	0	0	2	1
3,97	1	0	0	0	5	1
2,79	1	0	0	0	4	1
2,26	1	0	0	0	2	1
1,76	1	0	0	0	1	1
2,64	1	0	0	0	3	1

*Regression Statistics*

Multiple R	0,998879
R Square	0,997759
Adjusted R Square	0,795518
Standard Error	0,226894
Observations	11

## ANOVA

	<i>df</i>	<i>SS</i>	<i>MS</i>	<i>F</i>	<i>Significance F</i>
Regression	6	114,5976	19,0996	371,0026	1,93E-05
Residual	5	0,257405	0,051481		
Total	11	114,855			

	<i>Coefficients</i>	<i>Standard Error</i>	<i>t Stat</i>	<i>P-value</i>	<i>Lower 95%</i>	<i>Upper 95%</i>	<i>Lower 95,0%</i>	<i>Upper 95,0%</i>
Intercept	0	#N/A	#N/A	#N/A	#N/A	#N/A	#N/A	#N/A
N	-0,51221	0,592176	-0,86496	0,426604	-2,03445	1,01003	-2,03445	1,01003
NC	-0,02974	0,555174	-0,05357	0,959353	-1,45686	1,397379	-1,45686	1,397379
NCC	-0,07974	0,555174	-0,14363	0,891401	-1,50686	1,347379	-1,50686	1,347379
NCCC	-0,33974	0,555174	-0,61195	0,567323	-1,76686	1,087379	-1,76686	1,087379
C	0,482468	0,063336	7,61753	0,00062	0,319656	0,645279	0,319656	0,645279
phenyl	1,756883	0,432284	4,064187	0,009689	0,645662	2,868105	0,645662	2,868105



# CHAPTER 4

---

## The Influence of In Vitro Assay Setup on the Apparent Cytotoxic Potency of Benzalkonium Chlorides

Floris A. Groothuis<sup>†</sup>, Niels Timmer<sup>†</sup>, Eystein Opsahl<sup>†</sup>, Beate Nicol<sup>‡</sup>,  
Steven T.J. Droge<sup>†</sup>, Bas J. Blauboer<sup>†</sup>, Nynke I. Kramer<sup>†</sup>

<sup>†</sup> Institute for Risk Assessment Sciences, Utrecht University, PO Box 80177, 3508 TD Utrecht, The Netherlands

<sup>‡</sup> Unilever U.K., Safety & Environmental Assurance Centre, Colworth Science Park, Sharnbrook, Bedford  
MK44 1LQ, United Kingdom

**Keywords:** Free concentration, cytotoxicity, quantitative *in vitro in vivo* extrapolation (QIVIVE), dose metrics, benzalkonium chlorides

**Chemical Research in Toxicology, 32(6), 1103-1114 (2019)**

## Abstract

The nominal concentration is generally used to express concentration-effect relationships in *in vitro* toxicity assays. However, the nominal concentration does not necessarily represent the exposure concentration responsible for the observed effect. Surfactants accumulate at interphases and likely sorb to *in vitro* system components such as serum protein and well plate plastic. The extent of sorption and the consequences of this sorption on *in vitro* readouts are largely unknown for these chemicals. The aim of this study was to demonstrate the effect of sorption to *in vitro* components on the observed cytotoxic potency of benzalkonium chlorides (BAC) varying in alkyl chain length (6-18 carbon atoms, C<sub>6-18</sub>) in a basal cytotoxicity assay with the rainbow trout gill cell line (RTgill-W1). Cells were exposed for 48h in 96-well plates to increasing concentration of BACs in exposure medium containing 0, 60  $\mu$ M Bovine Serum Albumin (BSA) or 10% fetal bovine serum (FBS). Before and after exposure, BAC concentrations in exposure medium were analytically determined. Based on freely dissolved concentrations at the end of the exposure, median effect concentrations (EC<sub>50</sub>) decreased with increasing alkyl chain length up to 14 carbons. For BAC with alkyl chains of twelve or more carbons, EC<sub>50</sub>s based on measured concentrations after exposure in supplement-free medium were up to 25-times lower than EC<sub>50</sub> calculated using nominal concentrations. When BSA or FBS was added to the medium, a decrease in cytotoxic potency of up to 22 times was observed for BAC with alkyl chains of eight or more carbons. The results of this study emphasize the importance of expressing the *in vitro* readouts as a function of a dose metric that is least influenced by assay setup to compare assay sensitivities and chemical potencies.

## Introduction

*In vitro* assays play a central role in toxicity testing in the twenty-first century [225, 226]. Traditionally, research in *in vitro* toxicology focused on developing assays for hazard identification. Nowadays, *in vitro* assays are increasingly used to define toxic doses for hazard characterization [227]. *In vitro* concentration-effect relationships are frequently based on nominal concentrations, *i.e.* the amount of chemical added to the system divided by the volume of the exposure medium. However, the nominal concentration is not necessarily the concentration reaching cells or target sites where toxic events are initiated. For example, serum in *in vitro* exposure medium increases the observed effect concentrations of chemicals with high binding affinity to serum constituents [228-231]. The increased observed effect concentration has been attributed to a reduction of the free, unbound concentration of the test chemical, which is considered to be available for uptake into cells. The free concentration related more directly to the biologically effective dose (BED, the concentration at the target in cells) than the nominal concentration [232, 233]. Additionally, evaporation, degradation, metabolism and sorption to laboratory equipment may further reduce the free and therefore effective concentration *in vitro* [234-237].

In recent years, progress has been made with regards to understanding and characterizing the distribution of test chemicals in *in vitro* assays [54, 227, 237-246]. A number of distribution models have been developed relating the octanol-water partition coefficient ( $\log K_{ow}$  or  $\log D$ ) to the sorption affinity of these chemicals to assay components [230, 238, 241, 242, 247-249]. However, most of these models have not been validated with analytically measured concentrations of test chemicals in plastic, cells and exposure medium. Furthermore, chemicals like ionic surfactants fall outside the chemical applicability domain of these models since they do not have a meaningful  $\log K_{ow}$  [250]. The distribution of ionic surfactants is likely to differ significantly from more simple ions because they are amphiphilic, *i.e.* they have a hydrophobic alkyl chain and hydrophilic headgroups. Knowledge of the *in vitro* distribution of charged chemicals, particularly ionic surfactants, is limited. This can be considered worrisome as most drugs and many industrial chemicals, including many surfactants, are charged at physiological pH [251, 252].

Quaternary ammonium surfactants are a group of permanently positively charged surfactants. They are widely used as biocides and anti-electrostatic agents in, amongst others, fabric softeners, personal care products and antiseptics [253, 254]. They are expected to accumulate at interfaces in an *in vitro* system [54]. A schematic representation

of the distribution of surfactants is depicted in figure 4.3.1. It shows the processes that may reduce the free concentration of surfactants in *in vitro* assays.

The aim of this study was to investigate the effect of assay setup and the dose metric on the observed basal cytotoxic potency of seven benzalkonium chlorides (BACs) with varying alkyl chain length (6-18 carbon atoms, figure 4.3.2) in the rainbow trout gill cell line (RTgill-W1). The RTgill-W1 cell line was chosen in this study as the cells can be exposed to test chemicals in closed chambers, at room temperature and in serum-free medium. This cell line has been used regularly in the past to study chemical kinetics *in vitro*, but also as a gill disease model, for the detection of toxicant responses, ranking of chemical potencies and *in vitro in vivo* extrapolation [243, 246, 255, 256]. Cytotoxicity was assessed using alamarBlue and CFDA-AM assays. Median effect concentrations of individual BACs were determined in assays varying in exposure time (24h versus 48h), presence of serum proteins, chemical delivery (*i.e.* direct versus indirect dosing), well plate type (48- versus 96-well plates) and the degree of shaking. This study highlights that cytotoxic potencies strongly depend on *in vitro* assay conditions, especially for cationic surfactants with long alkyl chain lengths. As a result, this dependency can influence the potency ranking of surfactants, which subsequently hampers the use of *in vitro* data for quantitative *in vitro in vivo* extrapolation (QIVIVE).

## Experimental Procedures

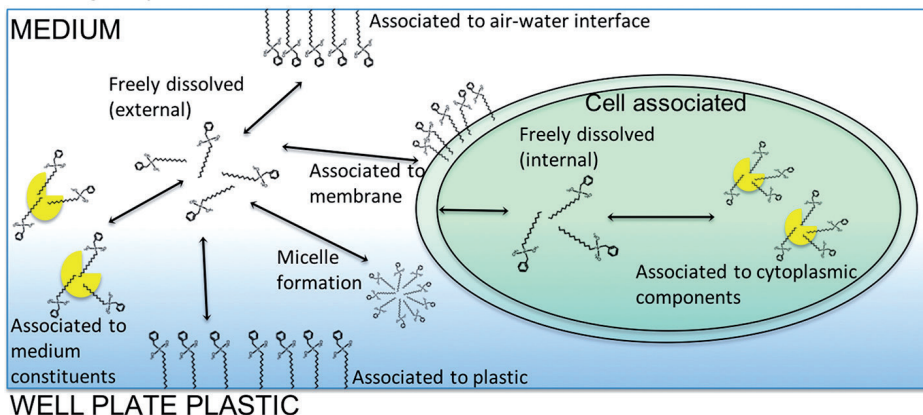
The Experimental Procedures section of this study is described in more detail than is customary. This is because the replicability of the study being highly dependent on the labware, pipetting technique, exposure conditions and extraction methods used [257].

### Chemicals, media and solvents

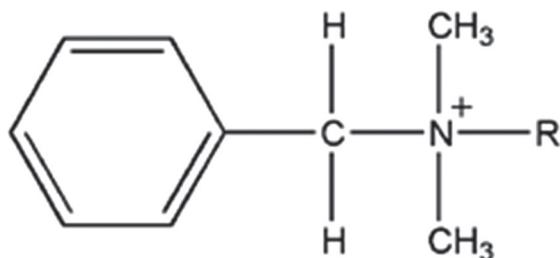
Benzalkonium chlorides, essentially fatty-acid and  $\gamma$ - globulin free Bovine Serum Albumin (BSA), Dulbecco's phosphate buffered saline (PBS), formic acid and reference chemicals used for the plasma protein binding (PPB) measurements were purchased from Sigma Aldrich (Zwijndrecht, The Netherlands, table 4.1). Benzyltrimethylstearylammmonium chloride (BAC18) had a purity of >90%; Benzyltrimethylhexylammmonium chloride (BAC6), Benzyltrimethyloctylammmonium chloride (BAC8), Benzyltridecyltrimethylammmonium chloride (BAC10), Benzyltrimethyloctylammmonium chloride (BAC12), Benzyltrimethyltetradecylammmonium chloride (BAC14), Benzyltrimethyl-

hexadecylammonium chloride (BAC16), and 1-dodecylpyridinium chloride monohydrate (C12-Pyr), were at least 96% pure. Solvents (acetonitrile, methanol, isopropanol and ultrapure water (ULC/MS grade) were provided by Biosolve (Valkenswaard, The Netherlands). Dulbecco vials and caps were supplied by Grace Discovery Sciences (Breda, The Netherlands): 10 mL precision thread headspace vials with 18mm Butyl Red/PTFE screw caps and clear 1.5 mL autosampler vials with silicone white/PTFE caps.

## HEADSPACE



**Figure 4.1.** A schematic representation of the distribution of chemicals in *in vitro* assays. Chemicals that enter the solution may sorb to serum proteins, well-plate plastic and cells. In case of surfactants, they may also associate with the air-medium interface or form micelles at high concentrations. Similar illustrations are found in [227], [230] and [228].



**Figure 4.2.** Structure of benzalkonium chlorides (R is the alkyl chain, containing 6-18 carbons)

The following cell culture media and equipment were supplied by Life Technologies (Breda, The Netherlands): Leibovitz's L15 medium, versene, trypsin-EDTA, FBS, 10000 U/L penicillin and 10 mg/L streptomycin, culture flasks (75 cm<sup>2</sup>), Greiner bio-one's CELLSTAR<sup>®</sup> transparent

flat bottom 96 multi-well plates (96WP), 48 multi-well plates (48WP), alamarBlue and CFDA-AM (5-carboxyfluorescein diacetate, acetoxymethyl ester) assays. The RTgill-W1 cell line was purchased from American Type Culture Collection (CCL-163, Manassas, VA) and used from passage 5 to passage 10. Exposure medium (L15/ex) was prepared as described by [258] using cell culture grade components purchased from Sigma Aldrich (Zwijndrecht, The Netherlands): 8 g/L sodium chloride, 0.4 g/L potassium chloride, 0.09767 g/L magnesium sulfate, 0.0937 g/L magnesium chloride, 0.19 g/L sodium phosphate dibasic, 0.06 g/L potassium phosphate, 0.14 g/L calcium chloride, 0.55 g/L sodium pyruvate and 0.9 g/L galactose dissolved in ultrapure Millipore water (MP).

**Table 4.1.** BSA binding constants of test and reference chemicals.

Name	Literature $K_{BSA}$	unit	%bound to 60 $\mu$ M BSA	logtR	logK	estimated log K with BSA column	estimated % bound to 60 $\mu$ M BSA	Reference
Isoniazid	0.00		0.00	0.00	0.00	0.00	0.00	[259]
Amphetamine	0.002	L/ $\mu$ mol	9.64	-0.31	-1.05	-1.44	9.35	[216]#
Amitriptyline	0.03	L/ $\mu$ mol	66.00	0.56	0.17	0.68	78.14	[216]#
Diazepam	0.02	L/ $\mu$ mol	59.00	0.47	-0.03	0.44	66.26	[216]#
Tramadol	0.003	L/ $\mu$ mol	12.72	-0.16	-1.24	-1.08	16.55	[216]#
b-estradiol	0.09	L/ $\mu$ mol	84.23	0.56	0.63	0.68	78.09	[260]
Testosterone	0.03	L/ $\mu$ mol	64.76	0.45	0.00	0.41	54.88	[261]
Phenanthrene	1.10	L/ $\mu$ mol	98.51	0.77	1.36	1.19	96.34	[230]
Bisphenol A	758.58	L/kg	75.21	0.57	0.40	0.70	79.26	[262] (37 °C)
Pyrene	8.58	L/ $\mu$ mol	99.81	0.90	1.93	1.50	98.90	[263]
BAC6	n/a	n/a	n/a	-0.13	0.00	-1.02	17.29	This study
BAC8	n/a	n/a	n/a	0.30	0.00	0.05	48.77	This study
BAC10	n/a	n/a	n/a	0.50	0.00	0.53	65.61	This study
BAC12	0.02	L/ $\mu$ mol	59.23	0.61	0.08	0.80	80.04	[54]
BAC14	n/a	n/a	n/a	0.63	0.00	0.84	85.83	This study
BAC16				0.72	0.00	1.05	91.36	
BAC18				0.79	0.00	1.23	94.86	

# Values obtained from samples with the lowest tested analyte and highest tested BSA concentration.

## Cell culture and cytotoxicity assay

To study the effects of serum constituents on the apparent cytotoxic potency of BACs, L15/ex was used as stand-alone exposure medium or supplemented with either 60  $\mu$ M (4 g/L) BSA or 10% FBS. The amount of BSA or FBS added to the medium contributed a similar level



of proteins (0.8 mg/well), which was confirmed using a fluorescamin assay according to the method described by Kramer et al. [264]. Assuming BSA is representative of other dissolved proteins in serum with regards to binding affinities, sorption to the protein fractions in medium supplemented with 60  $\mu\text{M}$  BSA or 10% FBS should be comparable. Stock solutions of BACs were prepared in methanol. To obtain the desired test concentrations of BACs in medium (0.01-1000  $\mu\text{M}$ ), stock solution in methanol were diluted 200 times in sterilized glass 10 mL vials with exposure medium.. The methanol concentration in medium was 0.5% (v/v) across all assays. The vials were left overnight on a roller mixer (Stuart SRT9, VWR, Amsterdam, The Netherlands) at 40 RPM, 20 °C in the dark, to ensure proper mixing before adding the spiked medium to the cells. This is referred to as “indirect dosing” since the chemical is first added to the medium and then added to the cells [265].

RTgill-W1 cells were grown in culture medium consisting of Leibovitz's L15 medium supplemented with 10% (v/v) fetal bovine calf serum (FBS) and 100  $\mu\text{g}/\text{mL}$  streptomycin and 100 U/mL penicillin. Cells were left to grow in the dark at 20 °C in closed culture flasks. Unless stated otherwise, cells were seeded in 96WP with a density of  $30 \times 10^3$  cells/well in 150  $\mu\text{L}$  culture medium. After 48h, the culture medium was replaced by 200  $\mu\text{L}/\text{well}$  exposure medium containing either BAC, vehicle control (0.5% methanol in medium) or just exposure medium (blanks). There was no difference in viability readouts between blanks and vehicle controls, suggesting the vehicle did not influence viability. Replacement of the culture medium with spiked medium was performed using a multidispenser pipette (Sartorius Biohit, Fischer Scientific, Landsmeer, The Netherlands) with a volume of 1 mL. Pipette tips were flushed once with spiked exposure medium to saturate binding sites on the inside of the tip. Thereafter, 200  $\mu\text{L}$  aliquots were dispensed into triplicate wells and 2x 200  $\mu\text{L}$  was dispensed into two autosampler vials prefilled with 800  $\mu\text{L}$  acetonitrile containing 0.1% formic acid (exposure reference standard), using a single pipette tip and single draw of medium into the tip. By dosing the cells in this way, the variability of the concentrations at the start of the exposure to cells ( $C_{t=0h}$ ) of the chemicals in medium between replicates was reduced. Another 200  $\mu\text{L}$  aliquot of each concentration was added to a single well without cells in the top and bottom rows (A and H) of the well plate. These wells were used to estimate the sorption to the plastic of the wells of 96WPs, since no further loss because of other processes such as evaporation was expected. All assays were made have been done at least thrice. This includes both three technical replicates and three biological replicates for the cytotoxicity assays described in this study.

After 48 hours of exposure, the medium from the wells was transferred to autosampler vials with acidified acetonitrile for LC-MS/MS analysis. Wells were then washed with bare L15/ex and viability of the cells was determined using the alamarBlue and CFDA-AM assays. Assay procedures are described in [264]. Briefly, cells were incubated for 45 minutes in the dark at 20 °C, with 50 µL/well working solutions of 5% v/v alamarBlue and 4 µM CFDA-AM in L15/ex. Fluorescence of alamarBlue and CFDA-AM was determined at 540/590 nm (excitation/emission) and 493/541 nm, respectively, using a Tecan infinite M200 plate reader (Tecan Group, Ltd., Männedorf, Switzerland).

The cell protein concentration in each well was measured to confirm that cell densities between plates were constant. The cell protein content was measured using a fluorescamin assay as described by Kramer et al. [264]. The alamarBlue and CFDA-AM solutions were discarded and wells were washed with 200 µL fixative (containing 59 g/L CaCl<sub>2</sub> and 0,25% formaldehyde) and 200 µL PBS. Wells were subsequently filled with 50 µL Millipore water and frozen at -80°C for >1h. Well plates were thawed and 100 µL/well PBS with 50 µL/well acetonitrile containing 48 mg/L fluorescamin was added. No cells were grown in the outer rows of the 96WP, and the initial 50 µL Millipore water in these wells was discarded and replaced by known BSA (protein) concentrations (0.018 - 2.25 mg/mL) to calibrate the fluorescamin assay. Well plates were wrapped in aluminum foil and gently shaken (20 RPM, 5 °C) for 5 min on a plate shaker. Fluorescence was determined on the Tecan infinite M200 spectrophotometer at 360/460 nm. .

Additional assay setup conditions were varied in the RTgill-W1 assay to investigate the impact of assay setup on the apparent cytotoxic potency of benzalkonium chlorides. The impact of assay setup on potency measurements were studied using BAC10, BAC14 and BAC18. Exposure times were reduced to 24h. Slow shaking of the plates at 10 RPM and 5° height was applied. Seeding densities were reduced to 100,000/mL. Forty-eight well plates (48WP with 1mL/well exposure medium were used. In addition, cells were “directly dosed” by adding 5 µL 200x concentrated BAC in methanol to the 200 µL medium/well. The effect of repeated dosing on median effect concentrations was also tested by replacing the exposure medium with freshly spiked exposure medium every 12 hours. Finally, DMSO was used as a vehicle instead of methanol and the medium volumes in wells were halved. The experiments were performed using three technical replicates and two biological replicates.

## Chemical analysis

After the exposure period, the complete volume of medium of each well was transferred from the 96WP to glass autosampler vials containing 600  $\mu\text{L}$  cold (5  $^{\circ}\text{C}$ ) acetonitrile with 0.1% formic acid and an internal standard (C12-Pyr). In case of the 48 well plates (48WP), 200  $\mu\text{L}$  aliquots were sampled from the (1 mL) medium in the wells. Pipette tips used for medium transfer were flushed three times in the autosampler vial with acetonitrile before discarding. This method was used to prevent surfactant loss to pipette tip plastic, allowing accurate measurement of the total amount of dissolved BACs. Samples were kept at 5  $^{\circ}\text{C}$  for at least 30 minutes before being centrifuged at 4  $^{\circ}\text{C}$  at 1500 rcf (2539 RPM) using a Beckman Coulter Allegra X12-R centrifuge (Beckman Coulter, Woerden, The Netherlands). Clean supernatant (450  $\mu\text{L}$ ) was transferred to another autosampler vial and stored at 4  $^{\circ}\text{C}$  until LC-MS/MS analysis. Samples stored for longer than 7 days were kept at -20  $^{\circ}\text{C}$ . Loss of test chemicals to sorption to *in vitro* system components was calculated by taking the ratio of the measured concentration of the chemical in exposure medium after exposure over the nominal concentration or measured concentration of test chemical in exposure medium at the start of the exposure. The LC-MS/MS consisted of a Perkin Elmer (Norwalk, CT) liquid chromatography system equipped with a Kinetex 5  $\mu\text{m}$  XB-C18 column (50  $\times$  2.1 mm; 100  $\text{\AA}$ ) with a C18 guard column, coupled to a triple quadrupole/linear ion trap mass spectrometer (MDS Sciex API 3000 LC-MS/MS System, Applied Biosystems, Foster City, CA). The turbo ion spray source was set in the positive ion mode at 400  $^{\circ}\text{C}$ . The injection volume was 2  $\mu\text{L}$  and the mobile phase consisted of a gradient flow (0.4 mL/min), starting at 95:5 Millipore:methanol (MP:MeOH) both containing 0.1% (v/v) formic acid. Between 3.2 and 6.2 min, the gradient was changed non-linearly (S curve) to 5:95 MP:MeOH. This was further increased to 2:98 MP:MeOH at 7.5 min, after which the mobile phase was reset to 95:5 MP:MeOH. The column was allowed to equilibrate for 1.5 min before the next run. A solvent switch was used to direct the initial eluent (containing salts) to the waste; at 4.6 min the eluent flow was redirected towards the MS/MS. Analyte retention time was typically between 5-8 minutes with LOQ between 1.9-6 nM although BAC18 had an LOQ of 17nM. The M/Z of the parent and daughter ions were 220.2/91.0, 248.2/91.0, 276.4/91.0, 304.3/91.0, 332.4/90.4, 360.4/90.9 and 388.1/91.0 for BAC6 - BAC18 respectively. The recoveries after 48h of exposure as percentage of the measured dosed amounts ( $t = 0\text{h}$ ) were calculated and lost analyte was assumed to be bound to cells and plastic.

Binding affinities to BSA were measured using a Shimadzu Prominence HPLC system ('s-Hertogenbosch, the Netherlands), equipped with a LC-20AD pump, SIL-20A autosampler, CTO-20A oven, SPD-20AV UV detector, RF-20A xs fluorescence detector, CBM-20A controller and a Resolvisil BSA-7 column (Machery Nagel). The HPLC and data analysis method was similar to the one developed by Valko et al. [266] for a human serum albumin (HSA) column. Details of the method and performance are discussed elsewhere [267]. The mobile phase consisted of PBS and isopropanol with a gradient flow (0.7 mL/min) starting with 100% PBS that was increased linearly to 30% isopropanol over 7 min. Between 7 and 25 min, the isopropanol concentration was kept constant, after which the mobile phase was reset to 100% PBS in 1 minute. The column was allowed 4 min of equilibration time before the next run.

## Data analysis

Concentration-effect curves were constructed using nonlinear regression: log inhibitor versus response function in GraphPad Prism 7.0 (GraphPad Software Inc., San Diego, CA), requiring log concentrations and the percentage of absorbance compared to the controls (viability). Quantification of the responses was based on the nominal concentration, the measured concentration in medium at the start of exposure (time,  $t = 0$ h) and the measured concentration after exposure ( $t = 48$ h). Median effect concentrations ( $EC_{50}$ ) were considered as different from one another when the 95% confidence intervals of the  $EC_{50}$  did not overlap.

Sorption of BAC to well plate plastic was calculated by comparing measured medium concentrations before and after exposure for 48h to wells without cells. The sorption coefficient to plastic ( $K_{\text{Plastic}}$ ) is expressed as the amount associated to plastic (nmol) per area of plastic ( $\text{cm}^2$ ), divided by the concentration in the medium (nM or  $\text{nmol}/\text{cm}^3$ ) resulting in a single unit (cm or m). The surface area of the exposed plastic was calculated to be  $1.56 \text{ cm}^2$  for 200  $\mu\text{L}$  volume of medium in a 96WP well. BSA binding constants of the BACs were calculated by comparing the relative retention time (tR) to the relative retention of reference chemicals with known association to BSA (see table 4.1). Further details on these calculations can be found in the paper by Valko et al. [266] and Groothuis et al. [267]. BSA binding constants were used to estimate the freely dissolved concentration in medium with 4 g/L BSA. New concentration-effect relationships were constructed using these free concentrations, which were compared to the concentration-effect relationships quantified based on the nominal and measured total concentrations.

## Results and Discussion

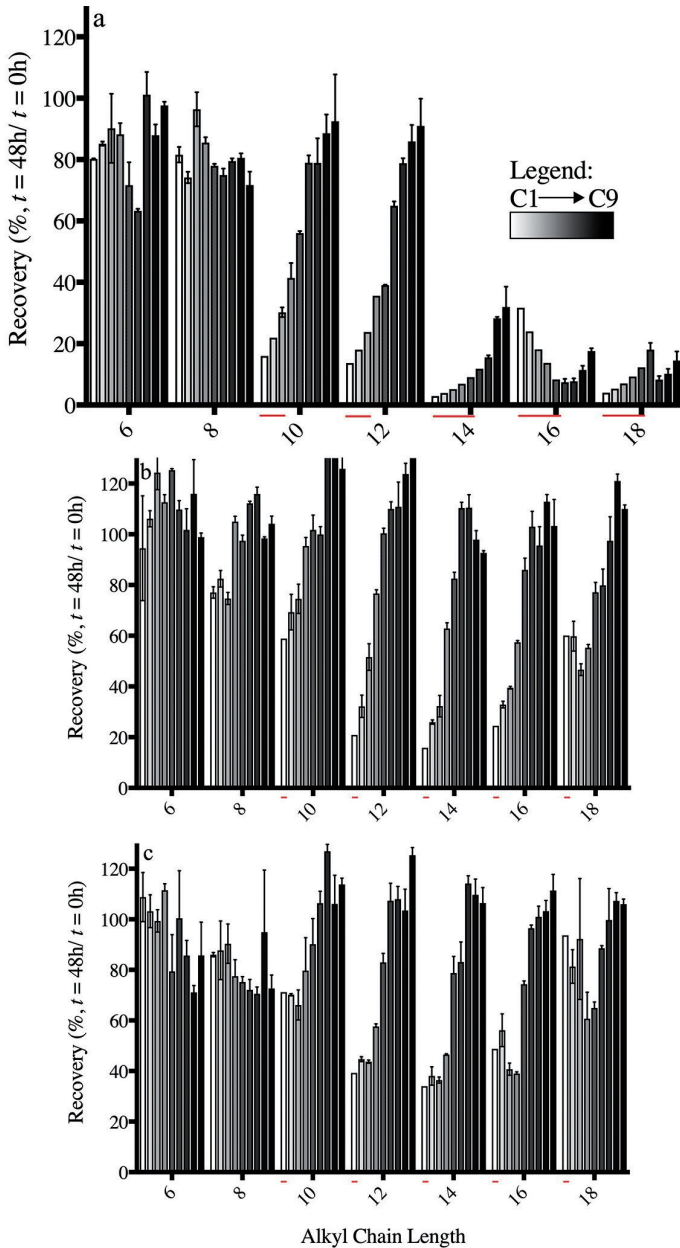
Unless otherwise stated, results are derived from cytotoxicity assays with RTgill-W1 in 96WPs exposed for 48h to BACs. The “indirect dosing” procedure was used to spike exposure medium with and without 4 g/L BSA or 10% FBS.

### Investigation of Plastic Binding based on Recoveries

When comparing the analytically determined concentrations ( $C_{t=0h}$ ) of BACs in exposure medium containing either BSA or FBS to the nominal concentration ( $C_{t=0h}/C_{\text{nominal}}$ ), recovered fractions of BACs were high (82% - 125%). In exposure medium without serum constituents, the recoveries for BACs with alkyl chains longer than 10 carbons were concentration dependent and ranged from 7% to 117%. The low and variable recoveries indicate losses due to sorption to the glass vials and pipette tips used for transferring medium to the microtiter plates. These results confirm previous findings on adsorptive losses to glass and pipette tips with cationic surfactants [257]. To circumvent the issues associated with sorption to pipette tips and glass, replicate aliquots of exposure medium with BACs were added, using a single multidispenser pipette tip, to designated wells in the microtiter plates and autosampler vials containing acetonitrile. BAC concentrations in the autosampler vials with medium and acetonitrile were subsequently analytically determined to discern the concentration of BAC to which cells were exposed at the start of the exposure ( $C_{t=0h}$ ). A complete extraction of BAC from exposure medium after exposure to the cells was ensured by transferring all medium per well to autosampler vials with acetonitrile and the pipette tip flushed in the resulting acetonitrile/medium solution.

Losses by sorption to plastic microtiter plates are observed when the analytically determined medium concentration at the end of the exposure is compared to the concentration at the start of the exposure ( $C_{t=48h}/C_{t=0h}$ , figure 4.3). Table 4.2 lists the recovered fraction at a measured dosed concentration between 1 and 2  $\mu\text{M}$  (depicted between brackets). After 48h of exposure, the analytically determined total concentration in the exposure medium containing serum constituents for chemicals with an alkyl chain length of  $\geq 12$  carbons, was reduced to at most 30%, suggesting up to 70% of BACs was associated with the well-plate plastic and cells. In addition, the concentration in medium without medium constituents was reduced further to 3% when comparing  $C_{t=48h}$  to  $C_{t=0h}$  (figure 4.3). Recoveries from medium after exposure increase with higher dosing concentrations (figure 4.3), indicating that sorption to the microtiter plastic is saturable. These findings indicate that more BAC

is retained in solution in the presence of BSA or FBS, likely because of sorption to the proteins in these serum constituents, resulting in a reduction of the fraction lost to plastic or glass. Similarly, greater losses to plastic with decreasing serum concentrations have been reported with polycyclic aromatic hydrocarbons (PAHs) in *in vitro* bioassays by Schirmer et al. [258] and Kramer et al. [230, 238].



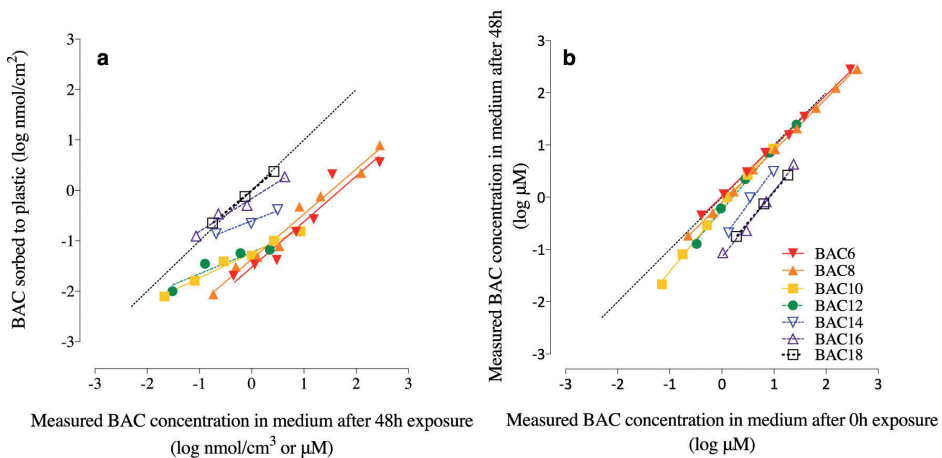
**Figure 4.3 (left page).** Percentage ( $\pm$  SD, n=3) of BAC recovered from exposure medium after 48 hours of exposure to RTgill-W1 in 96 well plates. Panels a, b and c respectively depict the percentages recovered from L15/ex, L15/ex with 4 g/L BSA, and L15/ex with 10% FBS. The recovered percentages are sorted by the concentration at the start of the exposure (from low (C1) to high (C9), white to black bars). The concentrations are 0.01-25  $\mu$ M in L15/ex for BAC10-BAC18, 0.04-50  $\mu$ M for BAC10-BAC18 in L15/ex with medium constituents, 0.2-250  $\mu$ M for BAC8, and 0.5-500  $\mu$ M for BAC6 in L15/ex or 0.5-1000  $\mu$ M for BAC8 and 1.5-1000  $\mu$ M for BAC6 in L15/ex with medium constituents. The percentage of chemical not recovered from medium after exposure is assumed to have sorbed to plastic and cells. Note that stripes (—) below bars refer to recoveries calculated using estimated concentrations after exposure. Actual concentrations could not be established because they were below the limit of quantification. Estimations were based on dilution factors.

Isotherms of concentrations of BAC sorbed to plastic versus concentrations in medium after exposure are plotted in figure 4.4. Freundlich exponents (n) and concentration dependent plastic association constants ( $\log K_{\text{Plastic}}$ ) can be found in table 4.2. Values for  $K_{\text{Plastic}}$  were calculated at a measured concentration after 48h close to 0.2  $\mu$ M because saturation of plastic at higher concentrations complicates the comparison of the  $\log K_{\text{Plastic}}$  values between chemicals. The concentration of 0.2  $\mu$ M was the lowest concentration measured for BAC6 at the end of exposure. BACs with longer alkyl chain lengths have higher plastic binding association constants and smaller Freundlich exponents. When assuming no saturation,  $\log K_{\text{Plastic}}$  may be used to estimate (worst case) the fraction bound to well plate plastic in *in vitro* assays with varying microtiter plate dimensions and exposure medium volumes.

**Table 4.2.** Freundlich exponents and concentration dependent plastic association constants ( $\log K_{\text{Plastic}}$ ) obtained from sorption isotherms of benzalkonium chlorides to well plate plastic.  $\log K_{\text{Plastic}}$  is calculated using test concentrations in medium nearest to 0.2  $\mu$ M. At higher medium concentrations, saturation of the plastic surfaces of wells in well plates was observed.

Chemical name	$\log K_{\text{Plastic}}$ (cm) at $C_{t=48h} = \pm 0.2 \mu\text{M}$	n of $K_{\text{Plastic}} \pm$ SE (Freundlich exponent)	$K_{\text{BSA}}$ ( $\mu\text{M}^{-1}$ )	% bound in medium with 60 $\mu\text{M}$ BSA	% recovered at 48h (at $C_{t=0h}$ in $\mu\text{M}$ )	% recovered at 48h (at $C_{t=0h}$ in $\mu\text{M}$ ) with 60 $\mu\text{M}$ BSA
BAC6	-1.30	0.90 $\pm$ 0.11	0.02	20.05	85.2 (1.3)	94.5 (1.5)
BAC8	-1.26	0.89 $\pm$ 0.05	0.04	53.31	96.4 (1.3)	82.5 (1.8)
BAC10	-0.74	0.49 $\pm$ 0.03	0.06	69.62	78.9 (1.3)	101.7 (1.3)
BAC12	-0.21	0.43 $\pm$ 0.12	0.10	80.04	63.7 (1.0)	100.4 (1.3)
BAC14	-0.29	0.40 $\pm$ 0.06	0.16	87.58	28.2 (1.0)	82.5 (1.4)
BAC16	0.06	0.65 $\pm$ 0.08	0.26	92.37	7.8 (1.0)	85.9 (1.4)
BAC18	0.18	0.85	0.43	95.41	8.3 (1.9)	77.2 (1.5)

Another way to characterize partitioning to plastic is to compare concentrations in medium at the end of exposure directly to the concentrations at the start of exposure (figure 4.4b). The trend lines, especially for BACs with longer alkyl chain lengths, approaches the 1:1 line where no plastic binding occurs. Therefore, the fraction of BAC sorbed to plastic decreases (and the free fraction increases) with increasing medium concentrations of the tested chemicals (saturation), which was also observed from the recoveries (table 4.2, figure 4.3). This is illustrated further by table 4.2, where the listed Freundlich exponents (calculated from figure 4.4a) decrease far below 1 for BACs with alkyl chain lengths >10 carbons.



**Figure 4.4.** Sorption isotherms of benzalkonium chlorides to well plate plastic. Isotherms were fitted using the Freundlich equation ( $R^2$  of all fits > 0.95). In panel (a), estimated concentrations sorbed to the plastic in 96 well plate wells without cells are correlated with concentration in medium without medium constituents. In panel (b), measured concentrations in medium after exposure are correlated with concentrations in medium without medium constituents before exposure. No sorption to plastic occurs on the 1:1 line.

Sorption affinity of BACs to plastic increases with increasing alkyl chain length. Few plastic association constants have been published in literature, making it difficult to place the constants measured in this study into context. Kramer et al. [238] reported association constants to well plate plastic ( $\log K_{\text{Plastic}}$ ) for polycyclic aromatic hydrocarbons (PAHs) ranging from -2.64 m for fluorene to -0.86 m for benzo(a)-pyrene. Timmer et al. [250] proposed to use the distribution coefficient to (artificial) phospholipid membranes ( $\log D_{\text{MW}}$ ) as a more suitable parameter compared to the  $\log K_{\text{OW}}$  to predict the affinity to cells and estimate critical (target) membrane burdens of surfactants. The  $\log D_{\text{MW}}$  of the PAHs tested in ranges from 1.6 to 3.9 [238]. The  $\log K_{\text{Plastic}}$  at the lowest measured



medium concentration ranged from -0.0021 to 0.018 m for BACs with a log  $D_{MW}$  range of 4 to 8 [250]. The difference in affinity to plastic between PAHs and BACs according to their log  $D_{MW}$  may be explained by the lower hydrophobicity of BACs compared to PAHs. Nevertheless, increasing alkyl chain length of the BACs is associated with higher membrane partitioning and stronger lipophilicity [250], which correlates with increasing plastic association constants similar to chemicals within other chemical subgroups such as PAHs, where higher lipophilicity is associated with higher losses to plastic.

### **Determination of binding affinity of Benzalkonium chlorides to BSA**

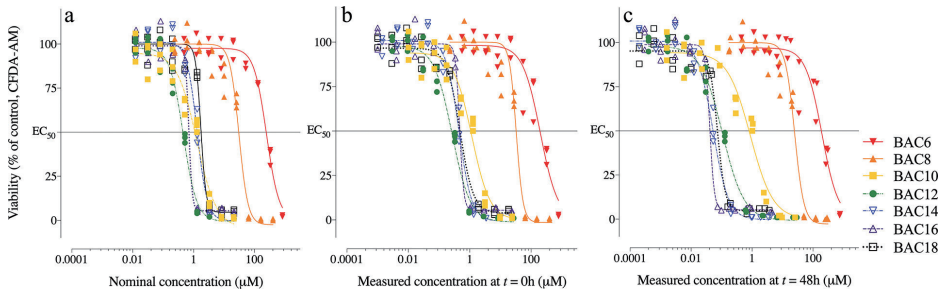
Binding affinities of BACs to BSA were determined using High Performance Affinity Chromatography (HPAC) in a separate study [267]. The binding affinities enable the calculation of free medium concentrations and its relationship with the observed cytotoxic potency. The relative retention times on the HPLC column (log tR) were plotted against the log K (linearized %bound to 60  $\mu$ M BSA) of reference chemicals with known affinity to BSA (table 4.1) and fit using a linear regression model. LogK values for the test chemicals were derived from this regression and used to estimate the percentage bound in medium containing 60  $\mu$ M (4 g/L) BSA (table 4.2). Similar to plastic binding, the percentage BSA bound BAC increases with increasing alkyl chain length. BAC18 is calculated to be 95% bound to protein in medium with 60  $\mu$ M BSA, while BAC6 is 20% bound. This suggests the bioavailable concentration of BACs with long alkyl chain lengths is expected to be significantly lowered in a cytotoxicity assay with BSA or FBS in the medium compared to bare exposure medium.

### **Cytotoxic potency, effect concentrations calculated with different dose metrics**

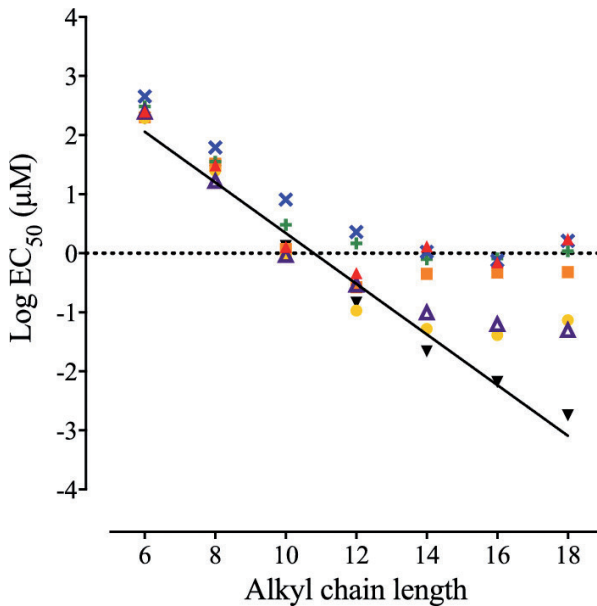
To study the effect of sorption to serum constituents and well plate plastic on the apparent cytotoxic potency of BACs, RTgill-W1 cells were exposed for 48h to the BACs in protein free L15/ex medium or L15/ex containing either BSA or FBS. Concentration-effect relationships (figure 4.5) were constructed with different dose metrics (nominal concentrations and analytically determined medium concentrations at  $C_{t=0h}$  and  $C_{t=48h}$ ).  $EC_{50}$  values from the CFDA-AM assay for all tested BACs and exposure conditions are summarized in table 4.3. CFDA-AM assay-based  $EC_{50}$  values are on average 2.8 (1.7-4.0 depending on the dose metric and serum protein levels) times higher than alamarBlue assay-based  $EC_{50}$  values [268, 269]. AlamarBlue is therefore a more sensitive biomarker of cytotoxicity of BACs than

CFDA-AM is. However, both markers show similar trends in potency between chemicals and exposure conditions.

Free median effect concentrations were predicted (figure 4.6, solid black line) based on a critical cell burden (CCB) for baseline toxicity of 50 mmol/kg lipid in fish [270] and membrane association constants as determined by Droge et al. [271] and Timmer et al. [250]. Note that the membrane affinity of BACs with a long alkyl chain (BAC16 and BAC18) were extrapolated from the affinity of the BACs with smaller alkyl chain lengths as they could not be measured directly by Droge et al. [271]. Predicted baseline median effect concentrations were compared to measured median effect concentrations ( $EC_{50}$ ). The correlation between predicted and measured  $EC_{50}$  was dependent on the dose metric. Cytotoxic potency increases significantly with alkyl chain lengths up to BAC12 (figure 4.5, table 4.3). When effect concentrations are calculated using  $C_{nominal}$ , the toxic potency decreases for BACs with longer alkyl chain lengths. The toxic potency of BACs with long alkyl chain lengths therefore do not overlap with the predicted free median effect concentrations. However, when quantified using analytically determined (free) concentrations after 48h of exposure, the toxic potency continues to increase to BAC14 and thus better correlates with predicted free median effect concentrations (figure 4.4c, table 4.3). The  $EC_{50}$  values of BAC14-BAC18 do not differ from one another as the confidence intervals overlap. In addition, for BAC14-18, up to 25-fold smaller  $EC_{50}$  values are found when based on  $C_{t=48h}$  compared to the  $EC_{50}$  values based on  $C_{nominal}$ . The  $EC_{50}$  values calculated with  $C_{t=0h}$  instead of  $C_{nominal}$  are significantly higher (11-fold) in comparison to the  $EC_{50}$  values calculated with  $C_{t=48h}$ . Therefore, sorption to plastic of BACs with alkyl chain lengths above 12 carbons significantly impacts the observed cytotoxic potency in these assays.



**Figure 4.5.** Concentration-effect relationships of benzalkonium chlorides constructed using different dose metrics (a-c). RTgill-W1 were exposed to BAC6-18 for 48h in supplement-free exposure medium and the CFDA-AM assay was used to assess cell viability. The different dose metrics used to calculate the concentration-effect relationships were: a) the nominal concentration, b) the analytically determined dosed concentrations ( $C_{t=0h}$ ) and c) the analytically determined concentration at the end of exposure ( $C_{t=48h}$ ). Corresponding  $EC_{50}$  values are listed in table 4.3.



**Figure 4.6.** Plot showing the relationship between cytotoxic potency (depicted as  $\log EC_{50}$  in a CFDA-AM assay with RTgill-W1) and alkyl chain length of benzalkonium chlorides (BACs).  $EC_{50}$  is calculated using different dose metrics:  $EC_{50}$ s depicted as a downward black triangle (▼) are calculated by multiplying the lethal membrane concentration in fish (narcosis mode of action) by the affinity for the membrane, as reported by Droge et al. [271]. The  $EC_{50}$  values were quantified using the nominal concentration (▲), measured concentration at the start of exposure (■), measured concentration in the wells after exposure (●), Measured total concentration in the presence of BSA after exposure (+), measured concentration in the presence of FBS after exposure (×) and the estimated free concentration in the presence of BSA after exposure (△).

**Table 4.3.** Median cytotoxic concentrations ( $EC_{50}$ ) of benzalkonium chlorides (BAC) differing in alkyl chain length<sup>a</sup>

BAC (alkyl chain length)	$EC_{50} \pm SE$ ( $\mu M$ , nominal)	$EC_{50} \pm SE$ ( $\mu M$ , measured t = 0 h). Medium without supplements.	$EC_{50} \pm SE$ ( $\mu M$ , measured t = 48 h). Medium without supplements.	$EC_{50} \pm SE$ ( $\mu M$ , measured t = 48 h). Medium with 60 $\mu M$ BSA.	$EC_{50} \pm SE$ ( $\mu M$ , measured t = 48 h). Medium with 10% serum.
6	24790 $\pm$ 2.94	19910 $\pm$ 4.36	19510 $\pm$ 4.36	30530 $\pm$ 2.32	45200 $\pm$ 5.39
8	30886 $\pm$ 0.73	32.86 $\pm$ 0.70	25.01 $\pm$ 0.63	35.59 $\pm$ 0.78	61.83 $\pm$ 1.24
10	1.27 $\pm$ 0.74	1.18 $\pm$ 0.76	0.89 $\pm$ 1.02	3.03 $\pm$ 0.29	8.09 $\pm$ 0.21
12	0.46 $\pm$ 0.04	0.27 $\pm$ 0.02	0.11 $\pm$ 0.01	1.47 $\pm$ 0.56	2.28 $\pm$ 0.20
14	1.30 $\pm$ 0.28	0.45 $\pm$ 0.04	0.05 $\pm$ 0.00	0.79 $\pm$ 0.33	1.05 $\pm$ 1.39
16	0.70 $\pm$ 0.40	0.47 $\pm$ 0.17	0.04 $\pm$ 0.00	0.82 $\pm$ 0.37	0.75 $\pm$ 0.26
18	1.73 $\pm$ 0.32	0.48 $\pm$ 0.12	0.07 $\pm$ 0.01	1.08 $\pm$ 1.61	1.62 $\pm$ 0.57

<sup>a</sup>  $EC_{50}$  values were calculated using three different dose metrics. Cytotoxicity to RTGill-W1 for each BAC was determined using in three replicate CFDA-AM assays. BACs were exposed to cells in medium containing no supplements ( $EC_{50}$  in  $\mu M$  measured at t=48h), containing 60  $\mu M$  (4 g/L) BSA ( $EC_{50}$  in  $\mu M$  measured in medium with 60  $\mu M$  BSA).

Although it is difficult to compare different types of surfactants, the toxic potency of the quaternary ammonium surfactants with 12-16 carbons in the alkyl chain used by Sandbacka et al. [272] were lower than our values for BACs in a primary culture of rainbow trout gill cells. This can be explained by the absence of the benzyl group in the chemicals used by Sandbacka et al. [272] since the presence of this group is assumed to increase the toxic potency by increasing the membrane affinity compared to quaternary trimethyl ammonium chlorides [250]. Additionally, the results may differ because a primary cell culture was used instead of the cell line in our study and their assay had a shorter exposure time and contained more cells, which likely decreased the observed cytotoxicity.

Similarly to our results, Sandbacka et al. [272] observed that the toxic potency of their test chemicals calculated based on nominal concentrations, reached a plateau after a “cut-off point” at longer alkyl chain lengths. This phenomenon has been quite often observed with surfactants in particular with regards to hemolytic effects [131-133]. One of the most prominent mechanistic explanations of the cut-off point is the free volume theory [132]. According to this theory, amphiphilic chemicals can create free volumes in the bilayer membrane. Smaller amphiphilic chemicals will create larger free volumes, destabilizing the membrane to a greater extent compared to the surfactants with longer alkyl chains. On the other hand, surfactants with shorter alkyl chain lengths will have a lower affinity for the membrane. As a result, there might be a maximum level of toxic potency via narcosis as a result of these counteracting effects.

In an earlier study, Isomaa et al. [134] investigated the interaction of amphiphilic agents, including cationic surfactants, with *in vitro* erythrocyte membranes. They observed a similar cut-off point (at an alkyl chain length of 14 carbons) with alkyltrimethylammonium bromides that they tested to protect erythrocytes against hemolysis. The authors suggested that the apparent cut-off point might be caused by an effect of unknown kinetic interactions of the studied chemicals. Interestingly, the cut-off point found in this study does shift from 12 to 14 carbon atoms in the alkyl chain when  $C_{t=48h}$  is used instead of  $C_{\text{nominal}}$  or  $C_{t=0h}$ . In addition, the toxic potency of the BACs with longer alkyl chain lengths levels off, instead of decreasing after the cut-off point, which was observed for  $C_{\text{nominal}}$ . One explanation could be that the medium contains a small fraction of dissolved organic carbon (DOC) to which the surfactants with long alkyl chain length bind significantly, making them less bioavailable. Chen et al. [254] calculated that a DOC content of 0.1 mg/L can reduce the bioavailability of BAC12 with about 50%, while this is often the limit of water purification systems. Since the  $\text{LogD}_{\text{MW}}$  of BAC12 is 6, while that of BAC16

and BAC18 are approximately 7.3 and 8 respectively, only a very small fraction of DOC is likely able to reduce the bioavailability of BAC16 and BAC18 to significant extent. Another consideration is that the measured concentration might not represent an amount of chemical evenly distributed in the wells, especially for surfactants with longer alkyl chain lengths. Surfactants are known to accumulate at the interfaces. Therefore, the measured (average) concentration may not directly relate to the amount affecting cells. It is thus not certain whether any of the dose metrics used are appropriate to accurately quantify the observed cytotoxic potency. However, the phenomenon described above may be less prominent in the presence of proteins (e.g. BSA or FBS). Proteins in the medium might facilitate diffusion and enhance homogenization by providing an additional protein-water interface, which is distributed relatively evenly throughout the medium. Concentration-effect relationships determined in media containing proteins may therefore diminish the effect of a non-homogenous distribution.

When estimated free concentrations in L15/ex medium with BSA are used to calculate  $EC_{50}$  values, the trend and cut-off point is similar to those based on  $C_{t=48h}$  in protein free medium. (figure 4.5, clear purple upward triangles). Interestingly no additional shift in cut-off point is observed even though this could have been expected due to a possible homogenization of surfactant in the presence of BSA. There is a small difference when using alamarBlue data as the cut-off point is shifted from BAC14 to BAC16. The assumption that BSA homogenizes the surfactant distribution is partly supported by the data based on alamarBlue, but not CFDA-AM. The data gathered in this study is therefore partially able to explain the cut-off point based on BAC kinetics of the chemicals by using different dose metrics to quantify toxic potency. Possibly there is indeed a mechanistic explanation for the cut-off point, in addition to a kinetic one. The predicted  $EC_{50}$  values of BACs with longer alkyl chain lengths (BAC16 - BAC18) were extrapolated from the BACs with shorter alkyl chain lengths assuming a linear relationship, therefore the predictions could overestimate their toxicity. In addition, the median effect concentration of BAC16 and BAC18 based on any dose metric are higher compared to the predicted baseline toxicity, which may be a result of better integration in the phospholipid membranes without disturbing the integrity in line with the free volume theory. Considering that fish lipid does not solely consist of membranes and the overall negative charge of cell membranes should attract cationic chemicals more than general lipid tissue, estimated free effect concentrations may be lower (an overestimation) than actual values. The free median effect concentrations of the BACs should then fall below the line in figure 4.6, which suggests that BACs may not act solely through a narcotic mode of action. The narcotic mode of action might become

more significant for BACs with longer alkyl chain lengths compared to a specific mode of action relative to BACs with shorter alkyl chain lengths. Regardless, these considerations may only be conclusively elucidated by analytically measuring membrane concentrations, which is a challenging task and beyond the scope of the work presented in this chapter.

In summary, this section illustrates that the toxic potency of surfactants increases with alkyl chain length. This is, however, more conclusively observed using analytically determined concentrations to quantify the toxic potency. Additionally, sorption to plastic increases the apparent  $EC_{50}$  up to 11-fold for BACs with long alkyl chain lengths ( $\geq 12$  carbons), while medium constituents can increase the apparent  $EC_{50}$  up to 22-times. A more detailed determination of the actual amount of benzalkonium chloride that is active at the target site in cells may only be achievable by measuring membrane or cell-associated concentrations.

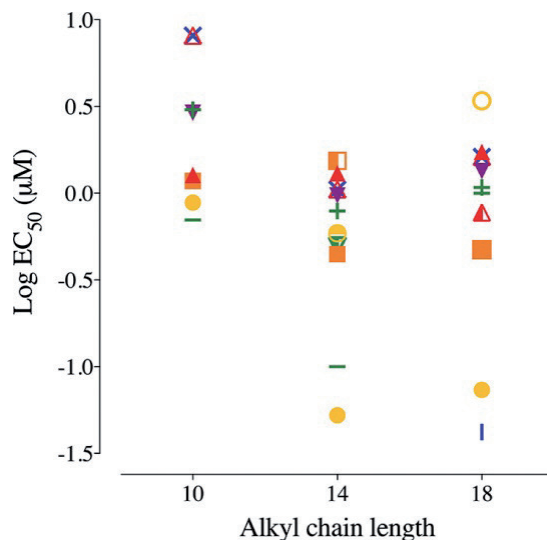
### Impact of assay setup on the cytotoxic potency

Depending on the assay conditions used, the observed toxic potency differs up to three orders of magnitude for BACs with long alkyl chain lengths (figure 4.7). The largest cytotoxic potency differences seem to be dose metric driven, e.g. median effect concentrations based on  $C_{t=48h}$  versus  $C_{nominal}$  and addition of serum or BSA to the medium. However, other assay setup conditions such as exposure time had an influence on observed cytotoxic potencies as well (figure 4.7).  $EC_{50}$  values after 48h of exposure are lower than after 24h exposure. These findings agree with those of Gülden et al. [236, 273] where  $EC_{50}$  values of various chemicals decreased with increasing exposure time in cultures of C6 glioma or Balb/c 3T3 cells until an “incipient”  $EC_{50}$  is reached. The incipient  $EC_{50}$  remains constant with longer exposure times. Understanding the effect of exposure duration is important to achieve accurate and reproducible cytotoxic potency determinations *in vitro*. [273] noted that using the incipient  $EC_{50}$  or at least 72h  $EC_{50}$ , instead of variable or arbitrary exposure times, will make comparisons to other *in vitro* assays, as well as extrapolations to *in vivo* experiments more meaningful. However, depending on the cell type and assay, it may not always be possible to expose the cells for 72h or longer, which is also the case for the RTgill-W1 studied. Toxicokinetic-Toxicodynamic (TK-TD) modelling may aid in determining a time independent measure of toxic potency [243, 274-276]. This could greatly improve applicability of *in vitro* toxicity data for extrapolation to *in vivo* and risk assessment.

Repeated dosing, fewer cells and slow shaking increased the observed toxic potency (figure 4.7). Together they increase the apparent toxic potency, while changing one of these factors alone did not necessarily lead to significantly different outcomes. Membrane affinity is higher for BACs with longer alkyl chain lengths [250, 271]. Therefore, the hydrophobicity is likely higher and diffusion through aqueous solutions and cellular uptake may be slower, compared to surfactants with shorter alkyl chain lengths, as is observed for other chemicals [277]. Considering this, the equilibrium time of the chemical distribution in the wells and particularly into the cells, will likely be slower for surfactants with long alkyl chain lengths [273]. In this case, 48h might not be enough for BAC18 to become equilibrated with all assay components and medium constituents. This might explain why the  $EC_{50}$  is higher than what is predicted based on the baseline toxic mechanism of action. It is speculated that increased flux into cells and other compartments caused by slow shaking of the system may increase the observed toxic potency, especially for more hydrophobic chemicals in assay systems where equilibrium is not reached within the exposure time. In addition, BSA and FBS likely facilitate the uptake kinetics into cells and distribution equilibrium as shown for other chemical groups [263, 277].

Different *in vitro* setups clearly can result in differing cytotoxic potencies. Chen et al. [54] reported effect concentrations for BAC12 that are higher compared to our results (20 fold higher) using the same RTgill-W1 cell line. However, the authors used shorter exposure times (24h) and 24 microtiter plates as opposed to 96WP in combination with a higher cell density (>60,000/cm<sup>2</sup> as opposed to 30,000/cm<sup>2</sup> in this study). Shorter exposure times can reduce the observed toxic potency as described earlier, while larger cell density can significantly reduce the observed toxic potency as well [235].





**Figure 4.7.** Impact of assay set-up on the observed cytotoxic potency of benzalkonium chlorides with 10, 14 or 18 carbons in the alkyl chain. The different experimental conditions result in up to three orders of magnitude differences in the observed toxic potency. Unless otherwise stated the setup was with 96 well plates, 48h exposure, 200,000 cells/ml, indirect and single dosing. The shown  $EC_{50}$  values were quantified using the nominal concentration ( $\blacktriangle$ ), measured concentration at the start of exposure ( $\blacksquare$ ), measured concentration in the wells after exposure ( $\bullet$ ), Measured total concentration in the presence of BSA ( $+$ ), measured concentration in the presence of FBS ( $\times$ ), Nominal concentration in the presence of BSA ( $\square$ ), Nominal concentration in the presence of FBS ( $\triangle$ ), Nominal concentration in L15/ex but after 24h of exposure ( $\blacksquare$ ), Nominal concentration but direct dosing ( $\circ$ ), Measured free concentration in L15/ex in 48WP ( $\text{—}$ ), analytically measured free concentration, slowly shaken after 24h exposure ( $\text{—}$ ), Repeatedly dosed nominal concentration after 24h of exposure ( $\triangle$ ), Nominal concentration in halved volume after 24h of exposure ( $\blacksquare$ ), Directly dosed nominal concentration with slow shaking ( $\bullet$ ), Nominal concentration in halved exposure medium and halved cell seeding density.

## Conclusions and Future Perspectives

As observed in this study, the toxic potency of BACs increases with increasing alkyl chain length. By using measured concentrations in medium after exposure rather than nominal concentrations to derive cytotoxic potency, the cytotoxic potency of BACs (BAC14 and up) increases with alkyl chain length. The extent of binding to well plate plastic is positively correlated with alkyl chain length. Thus with increasing chain length, plastic sorption plays an increasingly significant role in reducing the free concentration and the apparent cytotoxicity. The results illustrate the challenge of accurately describing the *in vitro* cytotoxic potency of BACs and, presumably, surfactants in general. As shown, factors such as sorption

to plastic and serum constituents can influence the apparent toxic potency. Conventional nominal concentrations are suitable to describe the toxic potency of benzalkoniums with short alkyl chain lengths (<10). For these chemicals, medium constituents have limited impact (<4 fold) on the observed toxic potency. However, for benzalkoniums with longer alkyl chain lengths, the fraction available for uptake into cells is reduced (4-30 fold) due to sorption to plastic and, if present, proteins. Other assay setup conditions such as cell density, repeated dosing, exposure time can influence the observed toxic potency as well.

Based on our results, we propose to use the free concentration in exposure medium to compare cytotoxic potencies of BACs between *in vitro* assays and between *in vitro* and *in vivo* bioassays when the BACs have a long alkyl chain length of more than 10 carbons, corresponding to a  $\log D_{MW}$  of 4 and higher [250]. Potencies based on intracellular or membrane concentration can further improve the comparability of toxicity values between assays. In fact, such concentrations may reduce the impact of other assay setup factors such as cell density. Additionally, using membrane concentrations may improve extrapolation to *in vivo* further if the cut-off point is caused by the surfactant distributive properties in aqueous solutions, which was not explainable by the dose metrics used in this study.

Although there are a few examples including the studies by Bernhard [278] and Fischer [277], it is currently difficult to quantify membrane or cell-associated concentrations of surfactants using analytical methods. The determination of free concentrations is often not considered feasible either since it also requires additional expertise, analytical equipment and time. Therefore, algorithms have been developed that model the distribution of chemicals *in vitro* including the free, intracellular and membrane concentrations. Armitage et al. [241] and Kramer et al. [230] have developed models that estimate the sorption of neutral organic chemicals to *in vitro* assay compartments once a chemical equilibrium has been established. Recently, Fischer et al. [242] extended the model by Armitage et al. [241] to include ionized chemicals. The prediction requires input of partition coefficients of the investigated chemicals to serum constituents, microtiter plate plastic. Often these are estimated using the octanol water partition coefficient,  $\log K_{OW}$ . Unfortunately, parameters such as the  $\log K_{OW}$  or  $\log D_{74}$  are not useful descriptors for surfactants because of their amphiphilic properties. The developed models are therefore not suitable to describe the *in vitro* distribution of surfactants and estimate the free or cell-associated concentration. The models are further limited by the fact that they have not been extensively validated with analytically determined free concentrations but were rather used to investigate the distribution characteristics of chemicals with a wide range of chemical properties. The accuracy of the models to estimate

free or cell-associated concentrations is therefore unclear. However, the current study sheds more light on the distribution characteristics of cationic surfactants and can therefore help to improve the modelling of *in vitro* concentrations in the future.

Using the free concentration for BACs with a log  $D_{MW}$  above 4 to calculate effect concentrations will likely improve the reproducibility and comparability of *in vitro* toxicity tests. This also implies an improved potential to successfully validate an *in vitro* test for use with these surfactants. Validation is important for regulators to know whether they can rely on the generated data for safety assessment. Finally, since the effect concentration *in vitro* is more a better representation of the target effect level, potential extrapolations to *in vivo* may be improved of which the performance will then depend more on the uncertainty of the extrapolation process itself.

## Acknowledgments

The authors would like to thank SEAC Unilever for funding this research. In addition, the authors would like to thank everyone who have contributed and commented to this work and in particular Theo Sinnige who has helped analyze some of the data.

## Abbreviations

BAC(s) Benzalkonium Chloride(s); BSA, Bovine Serum Albumin; HAS, Human Serum Albumin; QMIVE, FBS, fetal bovine serum; quantitative *in vitro in vivo* extrapolation; BAC6, Benzyltrimethylhexylammonium chloride; BAC8, Benzyltrimethyloctylammonium chloride; BAC10, Benzyldecyldimethylammonium chloride; BAC12, Benzyltrimethyloctylammonium chloride; BAC14, Benzyltrimethyltetradecylammonium chloride; BAC16, Benzyltrimethylhexadecylammonium chloride; BAC18, Benzyltrimethylstearyl ammonium chloride; Pyr-12, 1-dodecylpyridinium chloride monohydrate; CFDA-AM, 5-carboxyfluorescein diacetate acetoxymethyl ester; MP, ultrapure Millipore water; MeOH, methanol; LOQ, limit of quantification;  $K_{plastic}$ , sorption coefficient to plastic; tR, relative retention time;  $C_{t=0h}$ , analytically determined dosed concentrations;  $C_{nominal}$ , the nominal concentration;  $C_{t=48h}$ , analytically determined concentration at the end of exposure; PAH, polycyclic aromatic hydrocarbons; (Log)  $D_{MW}$ , distribution coefficient to (artificial) phospholipid membranes; logK, linearized percentage bound to 60  $\mu$ M BSA; L15/ex, exposure medium; DOC, dissolved organic carbon;  $EC_{50}$ , median effect concentration; TK-TD, Toxicokinetic-Toxicodynamic; CCB, critical cell burden.



# CHAPTER 5

---

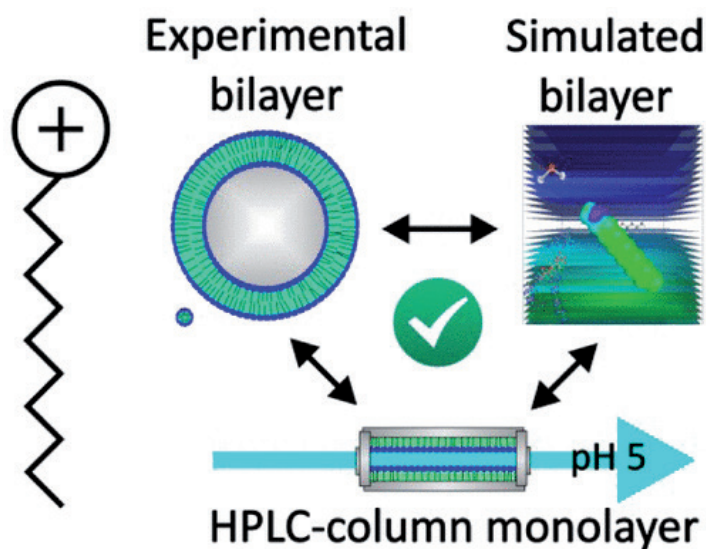
## **Sorption of Cationic Surfactants to Artificial Cell Membranes: Comparing Phospholipid Bilayers with Monolayer Coatings and Molecular Simulations**

Niels Timmer<sup>1</sup>, Steven T.J. Droge<sup>1</sup>

<sup>1</sup> Institute for Risk Assessment Sciences, Utrecht University, Utrecht, 3508 TD, The Netherlands

**Environmental Science and Technology, 51(5), 2890-2898 (2017)**

## Graphical Abstract



## Abstract

This study reports the distribution coefficient between phospholipid bilayer membranes and PBS medium ( $D_{MW,PBS}$ ) for 19 cationic surfactants. The method used a sorbent dilution series with solid supported lipid membranes (SSLMs). The existing SSLM protocol, applying a 96 well plate set-up, was adapted to use 1.5 mL glass autosampler vials instead, which facilitated sampling and circumvented several confounding loss processes for some of the cationic surfactants. About 1% of the phospholipids were found to be detached from the SSLM beads, resulting in nonlinear sorption isotherms for compounds with  $\log D_{MW}$  values above 4. Renewal of the medium resulted in linear sorption isotherms.  $D_{MW}$  values determined at pH 5.4 demonstrated that cationic surfactant species account for the observed  $D_{MW,PBS}$ .  $\log D_{MW,PBS}$  values above 5.5 are only experimentally feasible with lower LC-MS/MS detection limits and/or concentrated extracts of the aqueous samples. Based on the number of carbon atoms, dialkylamines showed a considerably lower sorption affinity than linear alkylamine analogues. These SSLM results closely overlapped with measurements on a chromatographic tool based on immobilized artificial membranes (IAM-HPLC), and with quantum-chemistry based calculations with COSMOmic. The SSLM data suggest that IAM-HPLC underestimates the  $D_{MW}$  of ionized primary and secondary alkylamines by 0.8 and 0.5 log units, respectively.

## Introduction

Phospholipid membranes separate (sub)cellular compartments from surrounding conditions, and play an important role in the uptake, distribution and toxicity of xenobiotics in multicellular organisms. Traditionally, the octanol-water partitioning coefficient ( $K_{OW}$ ) is used as a predictor for the uptake, distribution and accumulation of organic chemicals in various organisms and their tissues. However,  $K_{OW}$  does not adequately represent the partitioning of ionogenic organic chemicals (IOCs) between water and phospholipid membranes, because the ionic solute's interactions with octanol do not include ionic bonds that occur with the anionic phosphate groups and cationic choline groups in phosphatidylcholine phospholipids.[279-281] Cell membranes are expected to be the dominant sorption site for organic cations in tissue.[64, 282] Just like sorption coefficients to individual soil components are much more relevant for IOCs than  $K_{OW}$ [177, 218, 283-285] the membrane-water distribution coefficient ( $D_{MW}$ ) is a logical alternative for  $K_{OW}$  as the main model parameter to predict, for example, the tissue distribution and critical membrane burden in organisms.[64, 286] Many IOCs are highly relevant from an ecotoxicological perspective because of designed bioactive properties and/or continuous input via waste water streams.[287, 288] Cationic surfactants are hydrophobic IOCs with a relatively high potential to disrupt cell membranes.[289] Cationic surfactants are commonly used down-the-drain ingredients in personal care products, because of antistatic properties (hair conditioner, fabric softener). A variety of quaternary ammonium salt cationic surfactants are specifically used as biocide or disinfectants.[31, 36] Several cationic surfactants are regularly detected in various aquatic environments, particularly sediments.[31, 41, 42, 290, 291] Quaternary dialkylamines are highly adsorptive and therefore less accessible for biodegradation processes under certain conditions, and the longest chain structures such as DODMAC have subsequently been prohibited in several countries for certain uses. [292] This study aims to measure and model the  $D_{MW}$  for cationic surfactants with different alkyl chain lengths and head groups, in order to improve environmental and toxicological hazard/risk assessment for this class of IOCs. Since most common protocols to determine  $K_{OW}$  are considered to be impractical for surfactants, the assessment of  $D_{MW}$  would provide a representative alternative hydrophobicity parameter.

Several experimental methods exist to determine the  $D_{MW}$  of IOCs at physiological pH, such as liposome dispersions, specialized HPLC columns with phospholipid coatings, and solid supported phospholipid membranes (SSLM). Methods employing dispersions of freshly prepared liposomes are most realistic and accurate, but equilibrium dialysis requires

considerable effort and long equilibration times.[280, 293] Potentiometric titrations need substantial concentrations of chemical and phospholipids.[115] Recently, immobilized artificial membrane HPLC columns (IAM-HPLC) have been used to determine (relative) measures of lipophilicity in a number of frameworks.[119, 294-296] Confounding pH-dependent surface charges in IAM-HPLC have recently been recorded in detail.[120] These surface charges can considerably influence the retention capacity factors of IOCs on IAM-HPLC physiological pH.[120],[111, 297] At least for cationic compounds, confounding surface charges can be avoided by testing at low pH and highly saline eluent medium, and therewith one can specifically determine the IAM phospholipid-water distribution coefficient for the ionic form ( $K_{IAM,ion}$ ).[120] IAM-HPLC consists of an ordered monolayer of phospholipids covalently linked to a silica support,[298] instead of a dispersed double layer of phospholipids. This might reduce its relevance as a surrogate for the lipid bilayer cellular membrane. Solid supported phospholipid membranes (SSLMs) are available with macroporous spherical supports (e.g., silica beads) which are readily separated from the aqueous phase by mild centrifugation.[299]

Recently, IAM-HPLC was used to determine intrinsic sorption affinities to the IAM phospholipid monolayer  $K_{IAM,intr}$  for eighty different hydrocarbon-based monoprotic cations ( $C_xH_yN^+$ ).[119] Remarkably, these  $K_{IAM,ion}$  values did not differ between analogue structures of primary, secondary, and tertiary alkylamines with the same alkyl chain length, and were marginally lower for quaternary ammonium chloride (QAC) analogues ( $\sim 0.2$  log units). Quantum-chemistry based molecular calculations with a model DMPC bilayer (using the COSMOmic module within COSMOtherm software) of  $K_{DMPC-W}$  values for the ionic species closely aligned the full set of  $K_{IAM,ion}$  values, but predicted a stepwise decrease in  $K_{DMPC-W}$  with each methylation of the charged N, with primary amines at a log unit higher affinity than analogous QACs. Droge *et al.*[119] stated that only measurements on phospholipid bilayers would clarify if either the effect of N-methylation is over-predicted by molecular simulations, or under-predicted by the IAM monolayer.

The main goal of the present study was to measure partitioning of several series of cationic surfactants with the molecular formula  $C_xH_yN^+$  to phospholipid bilayers using a commercially available SSLM assay, for comparison with IAM-HPLC results and COSMOmic simulations. We thereby focused on the influence of the alkyl chain length and different types of charged head groups, but also on the difference between linear single chain alkylamines and dialkylamines. The applied SSLM assay (trademark TRANSIL) is sold as a



standardized sorbent dilution series assay in a 96 well plate format,[300] but was improved to facilitate measurements with hydrophobic organic cations.

## Materials and Methods

### Chemicals, sorbent and solutions

Nineteen amine based cationic surfactants compounds were selected. Their molecular structures, physicochemical properties, purities, and suppliers are listed in Table S1. Two secondary amines contained two linear alkyl chains of equal length (dihexylamine "S2-C<sub>6</sub>", dioctylamine "S2-C<sub>8</sub>"). Other moieties besides linear alkyl chains include benzyl in three benzalkonium chloride compounds (BAC), and dodecylpyridinium (C<sub>12</sub>-PYR) has the permanently charged nitrogen as part of an aromatic ring. All stock solutions were prepared as 100±10 mM solutions in methanol, further diluted with methanol as necessary. All solutions in methanol were stored at -20 °C until use.

TRANSIL<sup>XL</sup> Intestinal Absorption kits, and TRANSIL<sup>XL</sup> Intestinal Absorption kits for low affinity compounds, were purchased from Sovicell GmbH (Leipzig, Germany). These kits consist of a 96 wells plate made up of 12 strips with 8 wells each, individual strips containing two reference wells with phosphate buffered saline (PBS) and six wells with decreasing amounts (serial dilution factor of 1.8) of phosphatidylcholine coated macroporous silica beads ("beads") suspended in phosphate buffered solution (PBS). The pore diameter of the silica beads has been specified as 4000 Å in literature.[301] A 2012 paper by Hou et al. provides SEM images that give more insight into the three-dimensional structure of the beads.[302] PBS (Lonza BioWhittaker, Walkersville, USA; pH 7.4 ± 0.05, without Ca<sup>2+</sup> and Mg<sup>2+</sup>) was used as the test medium for all experiments, unless noted otherwise. To assess the contribution to the observed  $D_{MW}$  of the small neutral fraction present at pH 7.4 for the ionizable amines (<1%) the  $D_{MW}$  was also determined at pH 5.2 (<0.01% neutral) for several alkylamines. A 10 mM acetate buffer was used with analytical grade acetic acid (2.0 mM) and sodium acetate (8.0 mM), dissolved in Milli-Q pure water (>18.2 MΩ·cm<sup>-1</sup>, Millipore, Amsterdam, The Netherlands), and addition of 140 mM NaCl. Additions of all liquids were checked gravimetrically to record actual volumes.

## **Adapting the SSLM test protocol for cationic surfactants**

Cationic surfactants are notoriously difficult to work with due to relatively high adsorptive properties and accumulation at the water-air interface. Concentration dependent sorption to polystyrene well plate material was expected for several of the tested surfactants, as well as sorption to pipette tips when transferring supernatant to autosampler vials.[79] To partially avoid these adsorptive challenges, the SSLM beads were transferred quantitatively to 2 mL glass autosampler vials. After equilibration of the chemicals with the beads on a roller bank, the vials were centrifuged and the supernatant in the autosampler vials could be directly injected by the stainless steel needle of the autosampler. This reduces pipetting steps and allows for testing in a larger aqueous volume, of which the composition can be customized. Whereas the 96 well plate assay applies two PBS reference wells (without SSLM) serving as 100% references of dissolved concentrations, it was expected that for several cationic surfactants substantial binding to the walls of the test vials would compromise a mass balance approach. We therefore applied quadruplicate methanol solutions as 100% reference (as calibration standards) and assume that losses due to sorption to the wall of the test vials in the vials that contain the lipids does not affect the estimated membrane sorption coefficients. The validity of this assumption has been validated.

A Rainin Pipet-Lite XLS electronic multichannel pipette with adjustable spacer (Mettler Toledo BV, Tiel, The Netherlands) was used to transfer the contents of six wells from one strip with decreasing amounts of phospholipid coated beads to 2 mL autosampler vials. Wells were flushed six times with 50  $\mu$ L of PBS, to transfer all beads to the respective autosampler vials. Initially, autosampler vials were then filled with additional 400  $\mu$ L PBS, placed on a Stuart SRT9 roller mixer (Boom BV, Meppel, The Netherlands) for 15 minutes at 33 rpm, centrifuged at 750 g (20 °C) for 10 minutes. To these test vials, as well as to the four 500  $\mu$ L methanol references and four additional 500  $\mu$ L PBS controls (to verify the extent of glass binding), 20  $\mu$ L of spike solution was added. Overall, our tests were performed in the 1 nM – 1000 nM concentration range. We tried to cover isotherms with concentrations spanning at least a factor of 10, ideally a factor of 100. After addition of the spike, vials were transferred to a roller mixer for 15 minutes, centrifuged at 750 g (20 °C) for 10 minutes, and stored at 4 °C until LC-MS/MS analysis.

Pilot experiments with longer chain surfactants showed distinct nonlinear sorption isotherms, while the shorter chain surfactants showed linear isotherms. Several tests were performed to evaluate effects of spiking with solvent and bead density. Since

the phospholipid bilayer is not covalently bound to the beads, we considered that minute – but significant – fractions of phospholipids might leak from the beads into the test medium during storage and handling (e.g., thawing) and form small suspended liposomes. Especially for compounds with high  $D_{MW}$ , these liposomes could impact the  $D_{MW}$  measurements by artificially increasing measured concentrations in the aqueous phase being sampled. After transfer of the beads to the autosampler vials, we therefore added fresh PBS up to 1.8 mL, centrifuged, and carefully pipetted off 1.7 mL of supernatant to remove the majority of the detached phospholipids, and added 400  $\mu$ L of PBS and 20  $\mu$ L spike solution. Equilibration times of 5, 30, 60 and 240 minutes were compared with N-methyldodecylamine (“S<sub>12</sub>”). A test with dodecylpyridinium (“PYR<sub>12</sub>”) was performed to assess the tendency of phospholipids to leak from centrifuged beads while in the autosampler at room temperature, by injecting the same test series of six vials with washed beads 3 hours, 12 hours, and 21 hours after centrifugation.

### LC-MS/MS quantification and SSLM data analysis

All samples were analyzed using a PerkinElmer (Norwalk, USA) HPLC system with autosampler, coupled to an MDS Sciex API3000 triple quadrupole mass spectrometer (Applied Biosystems, Foster City, USA). Retention of test compounds from the saline test medium was achieved on a Kinetex 5  $\mu$ m XB-C18 column (50  $\times$  2.1 mm; 100 Å) with a C18 guard column. The mobile phase consisted of Milli-Q (pump A) and methanol (pump B), both containing 0.1% formic acid by volume. A solvent switch was employed to flush PBS salts into waste, at 10% B for 6 minutes, before eluting the surfactants from the column with 90% B. The autosampler needle depth was adjusted to prevent accidental injection of beads. External calibration standards in methanol had concentrations ranging from ~2 nM up to ~35  $\mu$ M. Detailed LC and MS/MS parameter settings for each compound can be found in Table S2.

The total spiked amount ( $A_{total}$ ) of surfactant in the autosampler will distribute between the aqueous phase ( $A_{water}$ ), the phospholipid coating on the beads ( $A_{lipid}$ ) and the glass/cap surfaces ( $A_{glass}$ ).  $A_{total}$  is obtained from the average concentrations in the methanol controls ( $C_{MeOH}$ ), and  $D_{MW}$  can then be calculated for each sample:

$$D_{MW} = \frac{C_{lipid}}{C_{water}} = \frac{\left( \frac{A_{total} - A_{water} - A_{glass}}{V_{lipid}} \right)}{C_{water}} = \frac{\left( \frac{C_{MeOH} \times V_{MeOH} - C_{water} \times V_{water} - A_{glass}}{V_{lipid}} \right)}{C_{water}} \quad (\text{eq. 1})$$

$V_{\text{lipid}}$  is the volume of phospholipids on the beads, as provided by the supplier. Because  $A_{\text{glass}}$  is in equilibrium with  $A_{\text{water}}$ , then  $A_{\text{glass}}$  can be considered negligible for the calculation of both  $A_{\text{lipid}}$  and  $D_{\text{MW}}$  if  $A_{\text{lipid}}$  is >90% of  $A_{\text{total}}$ , and if  $A_{\text{glass}} < A_{\text{water}}$ .  $A_{\text{glass}}$  was determined using the PBS reference samples, which demonstrated the level of equilibrium between glass-sorbed fractions and dissolved fractions (at the spiked concentration). Samples for decylbenzyltrimethylammonium ("BAC<sub>10</sub>") were emptied after analysis of  $C_{\text{water}}$ , flushed once with Milli-Q, and glass walls extracted with 90% B/10% A eluent mixture. Concentration independent  $\log D_{\text{MW}}$  values were obtained by fitting a linear curve on a double logarithmic plot with a forced slope of 1.

### **IAM-HPLC measurements of the phospholipid monolayer-water distribution coefficient $K_{\text{IAM,intr}}$ for cationic surfactants**

The IAM-HPLC procedure described for strongly sorbing  $C_xH_yN^+$  cationic amines without UV-absorbing moieties was followed as described previously.[119] Briefly, a solvent dilution series at pH 5 (10 mM acetate buffer) was tested in triplicate with LC-MS/MS detection. From a ~1-5 mg/L surfactant sample in 10% acetonitrile, 5  $\mu\text{L}$  was injected into an eluent mixtures of  $\leq 30\%$  acetonitrile, at flow rates of 1.0 mL/min. Multiplying the retention capacity factor  $k_{\text{IAM}}$  with the column's phase ratio of 18.9 gives the apparent distribution coefficient to the IAM phospholipid phase ( $K_{\text{IAM,app}}$ ) in each tested eluent mixture.[303] Extrapolation of the  $K_{\text{IAM,app}}$  values to fully aqueous medium buffered at pH 5 gives the intrinsic  $K_{\text{IAM,intr}}$ . For each surfactant at least 6 measurements were made.

### **COSMOmic calculations of the $K_{\text{DMPC-W}}$ for cationic surfactants**

COSMOmic was run within COSMOtherm Version C30\_1501, as described in the previous comparison between IAM-HPLC and COSMOmic.[119] However, instead of using COSMOmic's DMPC example micelle (1,2-dimyristoyl-sn-glycero-3-phosphocholine), we now used the same time averaged DMPC micelle file and TZVP-optimized structure of DMPC as used by Bittermann *et al.*[117] Briefly, the input file to represent a hydrated phospholipid bilayer is obtained with a molecular dynamics (MD) run with 128 DMPC molecules equilibrated with thousands of water molecules. COSMOmic divides the average atomic distribution in the MD simulated DMPC bilayer into 30 layers for one half of the hydrated bilayer, and uses the lowest free energy for each surfactant structure at 162 orientations at each layer to calculate the weighted DMPC-water partition coefficient ( $K_{\text{DMPC-W}}$ ). The three dimensional input structures for each cationic surfactant were

quantum-chemically optimized for calculations at TZVP level with COSMOmic, including different conformers (see Table S3 for information on conformers). COSMOconf Version 3.0 was used to create up to 6 of the most relevant conformers for all charged surfactants.

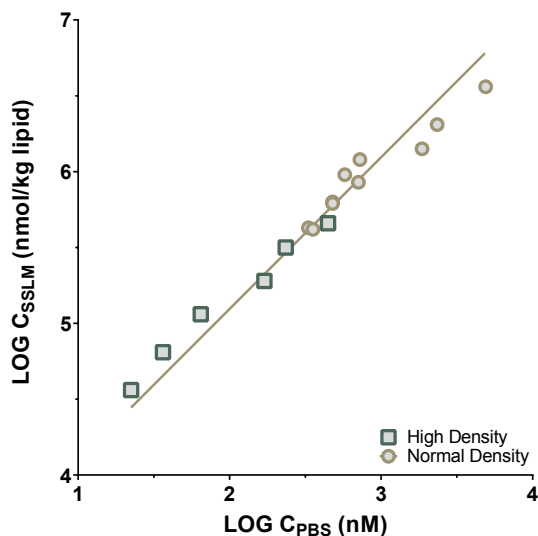
## Results and Discussion

### Measurements of $D_{MW}$ with adapted SSLM assays

Measured concentrations of the quadruplicate methanol control samples differed by less than 3.9% for all compounds tested. For  $C_8$ -alkylamines and  $C_{10}$ -alkylamines, the PBS controls showed 0-30% lower concentrations than the methanol controls, with exception of the larger  $C_{10}$ -benzalkonium ("C<sub>10</sub>-BAC" 39%). For  $C_{12}$  surfactants, losses to autosampler surfaces were between 20 and 60% in PBS. If PBS references would have been used for  $C_{10}$ -BAC as if they represented 100% of the available compound  $D_{MW}$  would have been 0.2 log units lower than with methanol control samples. Using methanol controls, measured extracts of the glass walls in vials with beads showed that the residual impact of glass binding on  $D_{MW}$  calculations was insignificant (0.011 log units).

Concentrations of test compound were aimed at keeping the phospholipid/sorbed compound molar ratio above 60 to prevent possible electrostatic effects due to the accumulated charge in the membranes.[304, 305] As shown in the full matrix of the final sorption isotherms for all tested compounds in figure S8, for nearly all of the selected surfactants, we have tested up to this maximum sorbed concentration in the membranes of ~40 mmol/kg to avoid electrostatic effects. Although the corresponding dissolved concentrations are orders of magnitude below the critical micelle concentrations (CMC, Table S1), the tested concentrations are most likely still well above highest environmental concentrations, but may be in the range of adverse effect concentrations. Concentrations of phospholipid in the test vial should result in sorbed fractions of at least 30%, to minimize effects of analytical uncertainties of  $C_{water}$  on the mass balance calculations. The adapted TRANSIL<sup>XL</sup> Intestinal Absorption kits allows for measuring  $D_{MW}$  values above 1000 with buffer volumes of ~525  $\mu$ L in the autosampler vials. The "TRANSIL<sup>XL</sup> Intestinal Absorption kits for low affinity compounds" contains a factor of ~20 higher levels of beads per well, thereby allowing for measurements of  $D_{MW} \geq 50$ . The results from these two kits show overlapping sorption isotherms and concentration independent  $D_{MW}$  as shown for dihexylamine ("S2-C<sub>6</sub>") in Figure 5.1. The sorption isotherms for  $C_8$ - and  $C_{10}$ -alkylamines

also showed concentration independent  $D_{MW}$  values, and overlapping sorption data with and without PBS renewal (Figure S1).



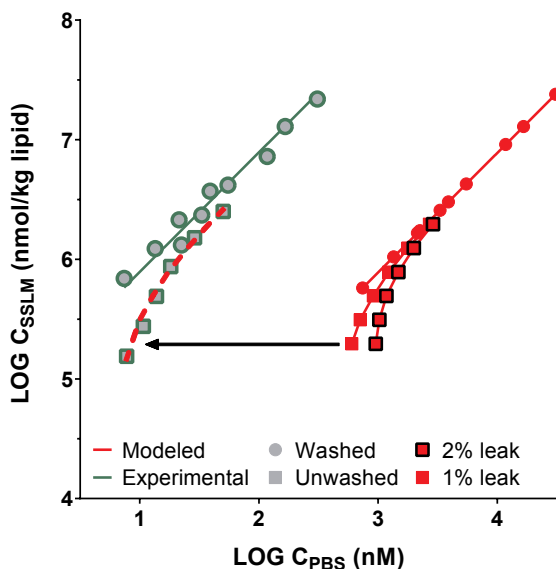
**Figure 5.1.** Sorption data for dihexylamine (S2-C6) obtained with two different sorbent dilution series and fit of a linear sorption isotherm (slope of 1), resulting in a  $\log D_{MW,PBS}$  of 3.15 (95% CI 3.10–3.20).

However, for the  $C_{12}$ -chain surfactants series measured without flushing off leaked phospholipids showed distinctly nonlinear isotherms, with higher  $D_{MW}$  values for the highest concentrations in a series (samples with lowest amounts of SSLM beads), and no correspondence between two series spiked at different initial concentrations (Figure S1). For each individual series, the slope of a linear isotherms on the double logarithmic plots was  $>1$ . This result would strongly cause doubt on the resulting  $K_{MW}$  from the SSLM assay, and an apparent concentration dependent sorption affinity over such a narrow tested concentration range would have considerable deviations of the  $K_{MW}$  at considerably lower (e.g., most environmental) and possibly higher concentrations (e.g., as applied, or at adverse effect levels). We found no evidence of influence of solvent from spiking solution, as data for secondary N-methyldodecylamine (“S<sub>12</sub>”) from methanol stock solutions overlapped with nonlinear results from stocks dissolved in water (Figure S2). Instead of a sorbent dilution series, we then tested primary dodecylamine (“P<sub>12</sub>”) with two series with constant concentration of SSLM material, spiked at six different concentrations (accompanied by six sets of methanol controls). Now, each series indicated concentration independent  $D_{MW}$  (slope of 1 on logarithmic plot), but again the series with higher amount of SSLM material

showed a lower sorption affinity (Figure S3). Evidently, higher SSLM material resulted in a higher detached amount of phospholipids from the beads leaking into the aqueous phase. If the sorbed amount of cationic surfactants to this phase significantly increases the measured  $C_{water}$ , this leads to underestimation of the  $D_{MW}$ . Using a common extension of Equation 1 for third phase systems [306], we modeled this effect by assuming a constantly leaked fraction ( $f_{leak}$ ) of the total amount of lipids coated on the beads, i.e., where the amount of lipids dispersed in the medium equals  $V_{lipid} \cdot f_{leak}$ :

$$C_{water} = \frac{\left(\frac{A_{total} \times V_{water}}{V_{water} + K_{PLIPW} \times V_{lipid}}\right) + \left(\frac{A_{total} \times D_{MW} \times V_{lipid}}{V_{water} + D_{MW} \times V_{lipid}}\right) \times f_{leak}}{V_{water}} \quad (\text{eq. 2})$$

Experimental and modeled results are plotted for dodecylpyridinium (“PYR<sub>12</sub>”) in Figure 5.2, combining data for ‘unwashed’ samples (still including medium from the well plate, thus with  $f_{leak}$  still present) with ‘washed’ samples (with  $f_{leak}$  mostly removed). As shown in Figure 5.2, the curve representing 1% of the phospholipids leaking from bilayers into the test medium ( $f_{leak} = 0.01$ ) approximated the observed experimental values that show a nonlinear curve. A modeled curve for  $f_{leak} = 0.02$  overestimated the observations. More plots comparing simulations for unwashed and washed beads for compounds with  $\log D_{MW}$  of 4.0, 4.5 and 5.0 can be found in the Figure S4. All experimental data and modeling output suggest a phospholipid leakage of approximately 1% from the bilayers on the beads into the medium, which – if not removed from the test medium – will influence the sorption isotherms for compounds with a  $D_{MW} > \log 4.0$ .



**Figure 5.2.** Experimental sorption data and simulated sorption data for dodecylpyridinium (PYR12) obtained with “unwashed” and “washed” sorbent dilution series, where unwashed still contains the medium from the well plates, whereas the medium was replenished with fresh PBS in “washed” samples. The simulated series show curves of a lipid leakage fraction of 0%, 1%, and 2%. The fitted linear curve for the experimental data indicates a  $\log D_{MW,PBS}$  of 4.89 (95% c.i. 4.84–4.95).

Varying the incubation time on the roller mixer (5–240 minutes) did not have a significant impact for fully dispersed SSLM solutions (Figure S5); 30 minutes was kept as standard. After centrifugation, the autosampler vials may stand for several hours in the autosampler before injection. The results of analysis after standing for 3, 12, or 21 h indicated no further leakage of phospholipids, as the measured surfactant concentrations and resulting sorption isotherm showed excellent overlap, whereas a significant fraction of leaked phospholipids would have increased the apparent concentrations in the medium (Figure S6). In test solution of pH 5.4 (“washed”), the  $D_{MW}$  values of an ionizable tertiary N,N-dimethyldecylamine (“T<sub>10</sub>”) as well as of a permanently charged QAC N,N,N-trimethyldecylammonium (“Q<sub>10</sub>”) were not statistically different from the  $D_{MW}$  in PBS (pH7.4), indicating that the <0.5% neutral fraction of T<sub>10</sub> is not contributing to the measured  $D_{MW}$  in PBS, and that there were no confounding pH-dependent surface charge effects of the SSLM material. In contrast, pH-dependent surface charge effects in IAM-HPLC confound the  $D_{MW}$  of organic cations in saline medium by ~0.7 log units between pH 5–7.4 [120]. As a result, the measurements of  $D_{MW}$  in PBS of cationic surfactants all relate to the partition



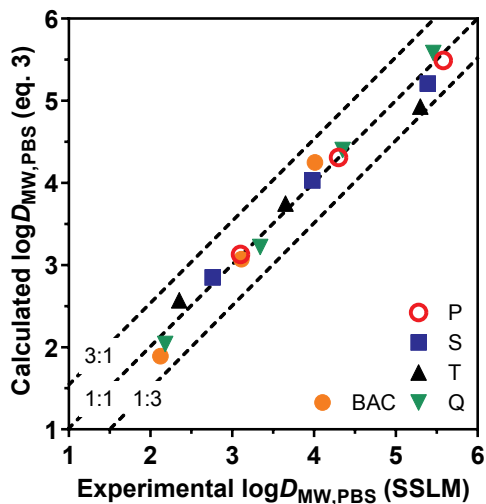
coefficient of the ionic form ( $K_{MW,ion}$ ), and can thus be directly compared to COSMOmic simulations with the ionized structures, and IAM-HPLC measurements made at pH5.

### Modeling the $D_{MW}$ by the structure of single chain cationic surfactants

Isotherms were fitted with a fixed slope of 1 for all data points from tests with washed medium, where  $f_{sorbed} \geq 0.3$  and the phospholipid/sorbate ratio was higher than 60 (Figure S8); an overview of all isotherm details can be found in Table S3. Standard errors were  $<0.05$  log units, and 95% confidence intervals were  $<0.17$  log units for all tested  $D_{MW}$  values. The resulting  $D_{MW}$  values (Table 5.1) were used to derive a simple quantitative structure activity relationship (QSAR) based on binary values for head group types and the length of the alkyl chain:

$$\log D_{MW} = -1.59(\pm 0.30) + 0.59(\pm 0.03) \cdot n_{carbon} - 0.28(\pm 0.16) \cdot N^{CC} - 0.56(\pm 0.16) \cdot N^{CCC} - 1.09(\pm 0.03) \cdot N^{CCCC} - 0.06(\pm 0.17) \cdot N^{Benz.}; \text{ (with s.e. between (), RMSE} = 0.16, \text{ d.f.} = 10, \text{ F} = 102.3) \quad (\text{eq. 3})$$

Where  $n_{carbon}$  denotes the number of carbon atoms in the alkyl chain,  $N^{Benz.}$  is a binary value indicating the presence (1) or absence (0) of a complete benzalkonium headgroup (3 compounds included), and  $N^{CC}$  (3 compounds included),  $N^{CCC}$  (3 compounds included),  $N^{CCCC}$  (4 compounds included) are binary values indicating the degree of N-alkylation. The  $N^{CCCC}$  value for benzalkonium compounds should be 0 by default.  $C_{12}$ -pyridinium was omitted as there was only one compound with this head group. Dialkylamines were omitted since they are expected to behave different because the dual alkyl chain influences their orientation in the phospholipid membrane.[119] Both types are discussed further on. As shown in Figure 5.3, the regression model of eq.3 fits all input compounds within a factor 3 of the experimental values (root mean square error of 0.20). Using binary values on only 3 or 4 compounds for each parameter in the QSARs of equation 3 results in a fairly low level of redundancy in the data. However, our main aim of this exercise was to obtain insight in these simplified head group properties (N-methylation), and not to provide a functional well validated QSAR to predict  $K_{MW}$  values for cationic surfactants. Considering that this dataset of cationic surfactants is still structurally relatively non-diverse and relatively small, no further efforts were made to refine a QSAR based on other physico-chemical or quantum-chemically derived parameters.



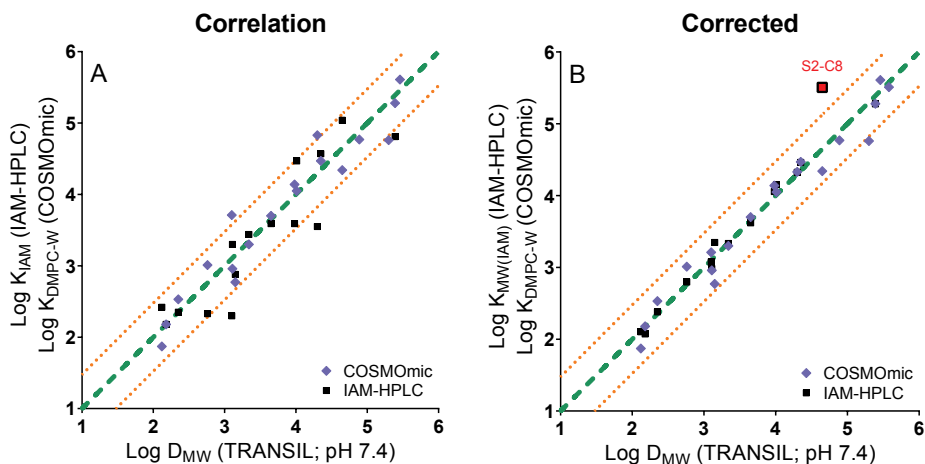
**Figure 5.3.** Observed and predicted  $\log D_{MW,PBS}$  values for single linear chain cationic surfactants using eq. 3 (P = primary amines, S = secondary amines, T = tertiary amines, Q = trimethylalkylammonium compounds, BAC = benzalkonium chloride compounds).

Obviously,  $D_{MW}$  increases with longer alkyl chains, with  $0.59 \pm 0.03$  log units per  $\text{CH}_2$  unit, which can be used to extrapolate  $D_{MW}$  predictions to longer chain surfactants. Comparing this fragment value with the tabulated  $D_{MW}$  values (Table 5.1) it seems to be slightly higher than expected based on the experimental values obtained for the quaternary ammonium compounds, and slightly lower than expected based on the secondary and tertiary  $\text{C}_{12}$  compounds. Although we expect a constant  $\text{CH}_2$  unit contribution for all single linear alkyl chains, the contributions of  $\text{CH}_2$  unit in the chain near the charged amine may be slightly lower, as these may not all reside in the hydrophobic core, and this is not defined in eq.3.[119] Effects of pH and possible neutral fraction for ionizable amines were ruled out based on additional tests at pH 5.4 (above, and Figure S7). A consistent trend of decreasing  $D_{MW}$  with increasing methylation of the N-atom is observed for the three analogue series of  $\text{C}_8$ -,  $\text{C}_{10}$ - and  $\text{C}_{12}$ -amines. Primary amines have  $0.28 \pm 0.16$  log unit higher  $D_{MW}$  than secondary amines, which are  $0.28 \pm 0.16$  log units higher than tertiary amines, which are  $0.53 \pm 0.16$  log units higher than QACs (excluding benzalkonium compounds). Taking the average over all the  $\text{C}_8$ -,  $\text{C}_{10}$ - and  $\text{C}_{12}$ -amines, primary amines sorbed 1.06 log units stronger than the QAC analogues. Considering that the quaternary amine has three more  $\text{CH}_2$  units than the primary analogue, this is a remarkable feature of IOCs. The benzalkonium compounds have a  $D_{MW}$  of  $1.0 \pm 0.17$  log units higher than trimethylalkylammonium compounds, which reflects the effect of an additional benzyl moiety. With an experimental

$\log D_{MW}$  of 4.89,  $\text{PYR}_{12}$  positions in between  $\text{BAC}_{12}$  and  $\text{Q}_{12}$  compounds, corresponding to the molecular volume differences. For 16 out of 19 compounds two or more conjoined series were tested, demonstrating both consistency of experimental results and steadiness over multiple orders of magnitude of the  $D_{MW}$  estimates.

## Correlation of SSLM data with IAM-HPLC measurements and COSMOmic predictions

The available  $K_{IAM}$  values obtained with IAM-HPLC (see detailed solvent series data in Figure S9, Table S3) and  $K_{DMPC-W}$  values from COSMOmic (Table S3) are plotted against the experimental  $D_{MW}$  results from the SSLM assay in Figure 5.4A. Overall, the alternative data sets and the SSLM data align reasonably well, with RMSE of 0.39 and 0.27 log units, for IAM-HPLC and COSMOmic, respectively. Instead of eq.3, now also dialkylamines and pyridinium compounds can be included. As discussed in Droge et al.,[119] IAM-HPLC data and COSMOmic predictions differed in the contributions of the N-methylations to the sorption affinity. The SSLM  $D_{MW}$  values confirm the ordering of primary > secondary > tertiary > quaternary amine analogues as predicted by COSMOmic, and indicate that IAM-HPLC accounts insufficiently for effects of N-methylation. Considering that the SSLM data are obtained with relatively fluid phospholipid bilayers, and IAM-HPLC applies a covalently bound monolayer, we suggest applying corrective increments for the N-methyl head group contributions to  $K_{IAM}$  values of IAM-HPLC, compared against the SSLM  $D_{MW}$  values ( $\delta_{IAM-SSLM}$ ). Multiple linear regression results in  $\delta_{IAM-SSLM}$  of  $0.78 \pm 0.07$  (s.e.) log units for primary alkylamines (i.e.,  $K_{IAM}$  values underestimate the  $K_{MW}$  in bilayers), and  $0.47 \pm 0.09$  log units for secondary amines. The  $\delta_{IAM-SSLM}$  for tertiary amines is insignificant ( $-0.03 \pm 0.10$  log units), and very small for quaternary alkyltrimethylamines  $-0.11 \pm 0.09$ . For COSMOmic  $\delta_{DMPC-SSLM}$  amine type corrective increments were derived similarly. Interestingly, primary amines tended to be slightly overestimated by COSMOmic ( $0.17 \pm 0.17$  log units), while the other amine types were slightly underestimated ( $0.2-0.4 \pm 0.16$  log units). COSMOmic seems to be capable of predicting the effect of N-methylation in phospholipid bilayers. Contrary to suggested correction of COSMOmic values reported previously,[119] the SSLM data support the notion that the IAM-HPLC monolayer is the most probable source of inconsistency, creating scatter between IAM-HPLC and COSMOtherm. Using these  $\delta_{IAM-SSLM}$  and  $\delta_{DMPC-SSLM}$  corrective increments, there is strong correspondence between SSLM  $D_{MW}$  values, the corrected IAM-HPLC  $K_{MW(IAM)}$  values, and corrected COSMOmic  $K_{DMPC-W}$  values, as shown in Figure 5.4B. All values are well within a factor 2 of the 1:1 line and the RMSE improved from 0.39 to 0.21 (IAM-HPLC) and from 0.27 to 0.18 (COSMOmic).



**Figure 5.4.** Experimental  $\log D_{MW,PBS}$  values with TRANSIL bilayers plotted against experimental  $\log K_{IAM}$  results from the IAM-HPLC monolayer and simulated  $\log K_{DMPC-w}$  values with DMPC bilayers using COSMOmic. In the graph on the right, IAM-HPLC values are corrected for 1° amines with +0.8 log units and 2° amines with +0.5 log units. COSMOmic values are corrected for 1° amines with -0.5 log units.

The three methods attribute similar effects of alkyl chain length, but also display a striking consistency in the difference between secondary dialkylamines and linear chain secondary alkylamine analogues. As discussed in Droge et al.,[119] COSMOmic provides a mechanistic explanation for the relatively lower contribution of  $CH_2$  units to the  $D_{MW}$  compared to single chain surfactants. Their design with two alkyl chains creates a steric effect, where the most favorable molecular position and orientation is mostly within the head group area of the phospholipid bilayer where – as a compromise – neither alkyl chain is aligned most favorably into the hydrophobic core region. The SSLM results confirm the difference in  $D_{MW}$  between secondary linear amine N-methyldodecylamine “S12” and secondary dihexylamine “S2-C6” by 2.24 log units, as was observed by Droge et al.[119] for IAM-HPLC (1.93 log units), and COSMOmic (2.43 log units). For all three methods the difference observed is much larger than expected with one extra  $CH_2$  fragment in  $S_{12}$ . Between S2-C6 and dioctylamine (S2-C8), the SSLM  $D_{MW}$  increased by 1.5 log units, while the regression model in equation 3 would predict a 2.36 log unit increase based on the addition of four  $CH_2$  units. COSMOmic also predicts a smaller value (1.73 log units) for the  $CH_2$  increment between S2-C6 and S2-C8, while IAM-HPLC showed a 2.16 log unit difference (Table S3).

## $D_{MW}$ values for cationic surfactants compared to $K_{OW}$ predictions

The most recent analysis of  $K_{MW}$  values of neutral compounds,[7] mostly obtained with liposomes, showed a strong correlation with  $K_{OW}$ :

$$\log K_{MW} = 1.01(\pm 0.02) \cdot \log K_{OW} + 0.12(\pm 0.07); n=156, SD=0.426, R^2= 0.948 \quad (\text{eq. 4})$$

There is only a poor correlation ( $R^2$  0.49) between the SSLM measured  $\log D_{MW}$  at pH 7.4 and the  $\log K_{OW}$  of the neutral primary, secondary, and tertiary amines, as shown in figure S10. The influence of the methyl units on the charged nitrogen are reversed for the two distribution coefficients. Each N-methyl unit increases the  $\log K_{OW}$  while it reduces the  $\log D_{MW}$ . Also, even though the sorption affinity of the protonated amines to the SSLM bilayer increases with linear alkyl chain length as the  $K_{OW}$  predicts, the  $\log D_{MW}$  of the dialkylamines is orders of magnitude lower than the  $\log K_{OW}$  (for S2-C8 4.61 and 7.01, respectively). Typically for studies on the toxicokinetic properties of ionizable chemicals, a  $\log D$  approach is followed, correcting the  $\log K_{OW}$  for speciation of the neutral amines at the tested pH 7.4 (99.9% ionic for primary and secondary amines, 99.7% for tertiary amines). To derive a  $\log D$ , however, the affinity of the ionic species for octanol needs to be known or predicted. In the absence of measurements, often a constant factor of  $\sim 3$  log units lower than  $\log P$  is applied, or the affinity of the ionic species are ignored and the  $K_{OW}$  is multiplied by the fraction of neutral species. As shown in Figure S10, both  $\log D$  approaches underestimate the sorption affinity to membranes up to a factor of 1000, and do not solve the poor correlation. Instead,  $\log K_{OW}$  could still be used to identify specific scaling factors to the difference in sorption affinity to a bilayer between neutral and ionic species, with the neutral affinity still based on equation 4. Table S3 lists the  $K_{MW}$  values for the neutral primary, secondary and tertiary amine species calculated via equation 4 ( $\log K_{OW}$  predicted by ACD/Labs). Accordingly, the average difference between charged  $D_{MW,PBS}$  and neutral  $K_{MW}$  species ( $\Delta_{MW}$ ) for primary amines is -0.05, so the affinity of charged primary amines is larger than the neutral species. For the three linear single chain N-methylalkylamines  $\Delta_{MW}$  is 0.44, for the linear N,N-dimethylalkylamines, the  $\Delta_{MW}$  is 1.25. These values closely correspond to the scaling factors suggested for the bioaccumulation model for ionogenic compounds (BIONIC) proposed by Armitage et al.,[64] which were 0.3, 0.5 and 1.25 for primary, secondary and tertiary amines, respectively, based on data sets of measured  $K_{MW}$  values for both ionic and neutral species. However, the  $\Delta_{MW}$  is 1.90 and 2.55 for the two dialkylamines S2-C6 and S2-C8, respectively, much higher than the 0.44 derived with the other secondary amines. The examples of the dialkylamines show that applying a single

$\Delta_{MW}$  scaling factor for all secondary amines to calculate the  $D_{MW,PBS}$  from the  $K_{OW}$  relationship in equation 4, can lead to erroneous values. Similarly, this exercise shows that  $K_{OW}$  is not an adequate single descriptor to model the  $D_{MW}$  values for ionized compounds. Measured  $K_{MW}$  values with TRANSIL,  $K_{PLIPW}$  values with IAM-HPLC, and even simulated  $K_{DMPC}$  values with COSMOmic, provide much more accurate and more mechanistically sound estimates compared to  $K_{OW}$ -based regressions.

### Perspective on SSLM assay measurements and associated $D_{MW}$ estimates

This study showed that the adapted SSLM protocol, with SSLM beads transferred from a well plate to autosampler vials, facilitated the analysis, improved recovery in methanol reference vials, and gained experimental control over the aqueous phase. The medium renewal removed third phase liposome artefacts, and allowed for altered pH of the test medium. The problem of detached phospholipids in the original SSLM medium became significant for all compounds with a  $D_{MW}$  higher than log 4, while using methanol controls instead of PBS controls seems mostly important for hydrophobic organic cations, and surfactants in general.[175] The experimental determination of  $D_{MW}$  becomes problematic above log 5.5, because with the required phospholipid/sorbate molar ratio >60, the aqueous phase concentrations obtained directly from the autosampler vials, are nearing LC-MS/MS detection limits. This means that to measure  $D_{MW}$  values for cationic surfactants with alkyl chains longer than  $C_{12}$ , and dialkylamines with alkyl chains longer than  $C_8$ , either cumbersome solid phase extraction steps from larger test volumes are required – which may include uncontrolled adsorption losses – or sorption affinities need to be extrapolated with the model, or from series of smaller analogues. Alternatively, COSMOmic seems to provide a realistic and accurate predictive tool for cationic surfactants, which allows for extrapolations to longer chain cationic surfactants (Table 5.1) and slight alterations of the head groups. For example, the  $\log K_{DMPC-W}$  for didecyldimethylammonium chloride (DDAC), a commonly used biocide,[307] and cetylpyridinium, a commonly used antiseptic, are 7.53 and 7.03 (Table 5.1), which are both experimentally not feasible to measure with currently applied IAM-HPLC and SSLM assays. The  $\log K_{DMPC-W}$  for behentrimonium, a trimethylalkylammonium compound with a chain length of  $C_{22}$  which is used in many hair care products and which has been detected in marine sediments,[37] is 10.3. The dialkylquat DODMAC (mixed chain length of  $C_{16}/C_{18}$ ), banned for certain uses in the EU,[292] has a predicted  $\log K_{DMPC-W}$  of 15.5. For these examples, the very high predicted sorption affinities to cell membrane should be considered in risk assessment models (e.g. for bioaccumulation [64]) alongside strong sorption affinities to environmental particles,[176, 177, 218, 283] which strongly reduces the bioavailability, and thus result in relatively low accumulation from the environment into tissues.[56, 57, 79, 171]

**Table 5.1.** Log $D_{MW}$  values for all compounds tested with the SSLM assay<sup>a</sup>, as well as uncorrected IAM-HPLC log $K_{PI,IPW}$  measurements and COSMOmic predicted log $K_{DMP,CW}$  values (no offset correction)

Alkyl chain	Method	Primary amine (P)	Secondary amines (S)	Tertiary amines (T)	Trimethyl ammonium (Q)	Benzalkonium cations (BAC)	Pyridinium cations (PYR)	Secondary dialkyl-amines (S2)	Quaternary dialkyl-ammonium (Q2)
<b>C<sub>6</sub></b>	SSLM					<b>2.12</b>		<b>3.15</b>	
	IAM	1.32				2.42		2.88	
<b>C<sub>8</sub></b>	COSMO	2.63	1.92	1.45	1.08	1.87		2.77	
	SSLM	<b>3.10</b>	<b>2.76</b>	<b>2.35</b>	<b>2.18</b>	<b>3.11</b>		<b>4.65</b>	
<b>C<sub>10</sub></b>	IAM	2.30	2.33	2.35	2.18	3.30		5.04	
	COSMO	3.71	3.01	2.53	2.18	2.96		4.34	
<b>C<sub>12</sub></b>	SSLM	<b>4.30</b>	<b>3.98</b>	<b>3.65</b>	<b>3.34</b>	<b>4.01</b>			
	IAM	3.55	3.59	3.59	3.44	4.47			
<b>C<sub>14</sub></b>	COSMO	4.83	4.14	3.70	3.30	4.05		6.26	
	SSLM	<b>5.58</b>	<b>5.39</b>	<b>5.30</b>	<b>4.35</b>		<b>4.89</b>		
<b>C<sub>16</sub></b>	IAM	4.81	4.81		4.57				
	COSMO	6.01	5.28	4.76	4.47	5.14	4.77	8.40	9.79
<b>C<sub>18</sub></b>	SSLM								
	COSMO	7.15	6.42	5.89	5.61	6.65	5.90		12.06
<b>C<sub>22</sub></b>	COSMO	8.31	7.56	7.07	6.72	7.90	7.03		<b>C16/C18</b>
	COSMO	9.43	8.74	8.29	7.94	9.01			15.51
	COSMO				10.1				

<sup>a</sup> details as # of data-points, standard errors and 95% confidence intervals are presented in table S3

## **Acknowledgements**

This study was funded by Unilever, Safety & Environmental Assurance Center (SEAC), Colworth Science Park, Sharnbrook, United Kingdom. We thank Joop Hermens for valuable suggestions and comments.



## Supporting Information

Sorption of Cationic Surfactants to Artificial Cell Membranes: Comparing Phospholipid Bilayers with Monolayers and Molecular Simulations

### Contents:

**Table S1:** *Test compounds*

**Table S2:** *LC-MS parameters*

**Table S3:** *Overview of KMW values and associated data for tested chemicals*

**Figure S1:** *Influence of KMW on significance of leaked phospholipids in medium*

**Figure S2:** *Comparison between aqueous spike solution and spike solution in methanol for N-methyldodecylamine (S12)*

**Figure S3:** *Comparison between B- and E-series for dodecylamine (P12), for which two constant SSLM amounts were spiked with six serially diluted stock solutions in methanol*

**Figure S4:** *Overview of the predicted influence of phospholipid leakage (no, 1% and 2% leakage from the SSLM material), at three different sorption affinities in the range log KMW 4-5*

**Figure S5:** *Influence of incubation time on measured KMW for N-methyldodecylamine (S12)*

**Figure S6:** *Influence of storage of centrifuged samples at room temperature in the autosampler on leaching of lipids as determined by KMW for N-methyl-dodecylamine (S12)*

**Figure S7:** *Influence of neutral fraction on KMW estimates*

**Figure S8:** *Matrix of all isotherm plots*

**Figure S9:** *Matrix of all solvent series measurements with IAM-HPLC*

**Figure S10:** *Comparison between logP/logD and the sorption affinity to bilayer membrane for ionizable cationic surfactants. LogP values are taken from ACD/Labs*

Table S1. Test compounds




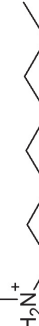




Compound	Code	pK <sub>a</sub>	Log P est. <sup>f</sup>	CMC (mM)	Supplier	CAS number	Purity (%)	Molecular structure
Octylamine	<b>P8</b>	10.7	3.06	400 <sup>a</sup>	Alfa Aesar	111-86-4	99	
Decylamine	<b>P10</b>	10.6	4.12	48 <sup>a</sup>	Sigma-Aldrich	2016-57-1	99.2	
Dodecylamine	<b>P12</b>	10.6	5.18	20 <sup>b</sup>	Sigma-Aldrich	124-22-1	>99.5	
N-methyl-1-octanamine	<b>S8</b>	10.9	3.29		Alfa Aesar	2439-54-5	98	
N-methyl-1-decanamine	<b>S10</b>		4.25		Angene	32509-42-5	95	
N-methyl-1-dodecanamine	<b>S12</b>		5.41		Sigma-Aldrich	7311-30-0	97	
N-hexyl-1-hexylamine	<b>S2-C6</b>		4.88		Sigma-Aldrich	143-16-8	97	
N-octyl-1-octanamine	<b>S2-C8</b>	±11	7.01		Alfa Aesar	1120-48-5	98	

Table S1. (Continued)

Compound	Code	pK <sub>s</sub>	Log P est. <sup>f</sup>	CMC (mM)	Supplier	CAS number	Purity (%)	Molecular structure
N,N-dimethyl-1-octanamine	<b>T8</b>	±9.9	3.78		Sigma-Aldrich	7378-99-6	95	
N,N-dimethyl-1-decanamine	<b>T10</b>		4.84		TCl	1120-24-7	>93	
N,N-dimethyl-1-dodecanamine	<b>T12</b>	10.0	5.91	0.3 <sup>c</sup>	TCl	112-18-5	>95	
N,N,N-trimethyl-1-octanaminium Br	<b>Q8</b>	N/A		260 <sup>d</sup>	Sigma-Aldrich	2083-68-3	>98	
N,N,N-trimethyl-1-decanaminium Br	<b>Q10</b>	N/A			Sigma-Aldrich	2082-84-0	>98	
N,N,N-trimethyl-1-dodecanaminium Cl	<b>Q12</b>	N/A		60 <sup>d</sup>	Sigma-Aldrich	112-00-5	>99	
N,N,N-trimethyl-1-tetradecanaminium Cl	<b>Q14</b>	N/A		5.6 <sup>e</sup>	Sigma-Aldrich	4574-04-3	>98s	

Table S1. (Continued)

Compound	Code	pK <sub>a</sub>	Log P est. <sup>f</sup>	CMC (mM)	Supplier	CAS number	Purity (%)	Molecular structure
N-benzyl-N,N-methyl-1-hexanaminium Cl	<b>BAQ6</b>	N/A			Sigma-Aldrich	22559-57-5	>96	
N-benzyl-N,N-methyl-1-octanaminium Cl	<b>BAQ8</b>	N/A			Sigma-Aldrich	959-55-7	>96	
N-benzyl-N,N-methyl-1-decanaminium Cl	<b>BAQ10</b>	N/A			Sigma-Aldrich	63449-41-2	>97	
1-dodecylpyridinium Cl·H <sub>2</sub> O	<b>PYR12</b>	N/A			Alfa Aesar	207234-02-4	98	

<sup>a</sup> [183], <sup>b</sup> [184], <sup>c</sup> [308], <sup>d</sup> [187], <sup>e</sup> [188], <sup>f</sup> log P values are log K<sub>ow</sub> values for neutral species estimated by ACD/Labs

**Table S2.** LC-MS parameters

The interface for the MS-MS was a Turbo Ion spray in positive ionization mode operated at 400 °C, except for P10 which was detected at 300 °C. The following settings were used for all compounds: nebulizer gas (NEB) = 8; collision cell gas (CAD) = 3; collision cell entrance potential (EP) = 10 V; collision cell exit potential (CXP) = 12 V. Compound-specific settings can be found in the table. (CUR = curtain gas; IS = ion spray voltage; DP = declustering potential; FP = focusing potential; CE = collision energy).

Compound	M1 m/z	M3 m/z	CUR	IS (V)	DP (V)	FP (V)	CE (V)
<b>P8</b>	130.1	70.9	7	4500	70	200	16
<b>P10</b>	158.3	57.1	6	4900	70	320	23
<b>P12</b>	186.4	70.9	7	4500	33	186	20
<b>S8</b>	144.1	71	7	4500	60	250	19
<b>S10</b>	172.3	57.1	7	4000	65	380	27
<b>S12</b>	200.2	70.9	7	4500	75	220	24
<b>S2-C6</b>	187.1	103	6	4500	70	400	22
<b>S2-C8</b>	243.4	131	6	4500	70	400	27
<b>T8</b>	158.4	46	7	4500	80	200	30
<b>T10</b>	185.9	57.1	7	4500	70	350	33
<b>T12</b>	214.2	57.1	7	4500	64	195	35
<b>Q8</b>	172.3	60	7	4500	43	292	34
<b>Q10</b>	200.3	60	8	3200	51	300	27
<b>Q12</b>	228.3	60	7	4500	58	292	39
<b>Q14</b>	256.5	60	7	4500	58	292	44
<b>BAQ6</b>	220	91	9	5500	38	292	33
<b>BAQ8</b>	248.2	91	9	5500	45	292	45
<b>BAQ10</b>	276.4	90.9	7	4500	51	292	47
<b>PYR12</b>	248.4	80.1	7	4500	45	270	33

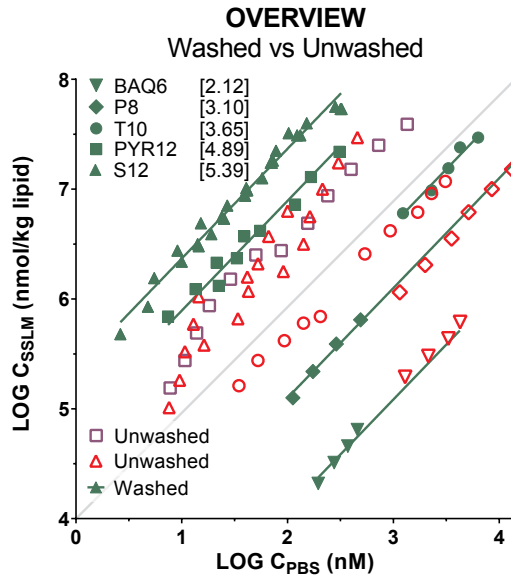
**Table S3.** Overview of  $K_{MW}$  values and associated data for tested chemicals

	Conc. Range (buffer, $\mu$ M)	Glass binding in ref.	$\log K_{MW}$ ( $\pm$ s.e.) TRANSIL PH7.4	N	95% c.i.	$\log K_{MW(IAM)}$ IAM-HPLC pH5.0 <sup>a</sup> corrected (nr. $k_{IAM}$ included)	$\log K_{DMPC-W}$ COSMOmic (cation) <sup>b</sup> incl. offset	maximum $\log K_{DMPC-W}$ difference between conformers (nr. conf.)	$\log K_{MW}$ <sup>c</sup> via $\log K_{OW}$ (neutral)
<b>P8</b>	0.11 - 13.2	25%	3.10 $\pm$ 0.03	12	3.04-3.17	3.10*	3.31	0.78 (5)	3.21
<b>P10</b>	0.010 - 2.3	29%	4.30 $\pm$ 0.04	12	4.23-4.38	4.35 (5)	4.43	0.84 (5)	4.28
<b>P12</b>	0.0013 - 0.036	57%	5.58 $\pm$ 0.04	11	5.49-5.66	-	5.61	0.35 (2)	5.35
<b>S8</b>	1.4 - 12.9	n.d.	2.76 $\pm$ 0.01	6	2.73-2.79	2.80*	2.61	0.87 (7)	3.44
<b>S10</b>	0.110 - 6.8	26%	3.98 $\pm$ 0.03	11	3.92-4.03	4.07 (7)	3.74	0.35 (2)	4.41
<b>S12</b>	0.0055 - 0.15	46%	5.39 $\pm$ 0.01	23	5.37-5.42	5.28*	4.88	0.46 (3)	5.58
<b>S2-C6</b>	0.022 - 0.71	5%	3.15 $\pm$ 0.02	14	3.10-3.20	3.35 (6)	2.37	0.35 (6)	5.05
<b>S2-C8</b>	0.074 - 1.26	-	4.65 $\pm$ 0.02	6	4.61-4.69	5.51 (6)	3.94	0.67 (4)	7.20
<b>T8</b>	2.46 - 17	n.d.	2.35 $\pm$ 0.02	6	2.31-2.40	2.35*	2.13	0.76 (5)	3.94
<b>T10</b>	0.035 - 6.3	26%	3.65 $\pm$ 0.02	15	3.61-3.68	3.59 (7)	3.30	0.78 (4)	5.01
<b>T12</b>	0.0026 - 0.20	46%	5.30 $\pm$ 0.02	12	5.25-5.34	-	4.36	0.44 (3)	6.09
<b>Q8</b>	1.78 - 27.5	n.d.	2.18 $\pm$ 0.04	12	2.10-2.26	2.07*	1.78	0.37 (2)	-
<b>Q10</b>	0.054 - 10.7	n.d.	3.34 $\pm$ 0.03	12	3.28-3.40	3.33 (7)	2.90	0.42 (2)	-
<b>Q12</b>	0.031 - 1.2	20%	4.35 $\pm$ 0.02	9	4.32-4.39	4.46 (6)	4.07	(1)	-
<b>Q14</b>	0.0052 - 0.180	56%	5.46 $\pm$ 0.03	9	5.39-5.54	-	5.21	(1)	-
<b>BAQ6</b>	0.20 - 4.3	n.d.	2.12 $\pm$ 0.02	8	2.08-2.16	2.31*	1.47	0.34 (4)	-
<b>BAQ8</b>	0.34 - 3.8	n.d.	3.11 $\pm$ 0.01	7	3.08-3.15	3.19*	2.56	0.44 (3)	-
<b>BAQ10</b>	0.010 - 2.0	39%	4.01 $\pm$ 0.02	12	3.97-4.06	4.36*	3.65	0.43 (2)	-
<b>PYR12</b>	0.0074 - 0.310	51%	4.89 $\pm$ 0.03	10	4.84-4.95	-	4.37	(1)	-

<sup>a</sup> $K_{MW(IAM)}$  is based on the retention capacity factor for the Immobilized Artificial Membrane column ( $k_{IAM}$ )  $\times$  18.9 phase ratio (water:phospholipids), and corrected for the  $\delta_{IAM-SSLM}$  corrective increments determined in this study: +0.78 log units for 1° amines, +0.48 log units for 2° amines, -0.03 log units for 3° amines, and -0.11 log units for QACs. Data with \* are from earlier work [119].

<sup>b</sup>COSMOmic calculations were performed with the same DMPC input structures and membrane potential settings as recommended by Bittermann et al. [117], with a recommended cation offset factor of -0.4 log units. Values are weighted averages of the most relevant conformers.

<sup>c</sup>using the regression by Endo et al. [7]:  $\log K_{MW} = 1.01 \times \log K_{OW} + 0.12$ .  $\log K_{OW}$  values are predicted by ACD/Labs



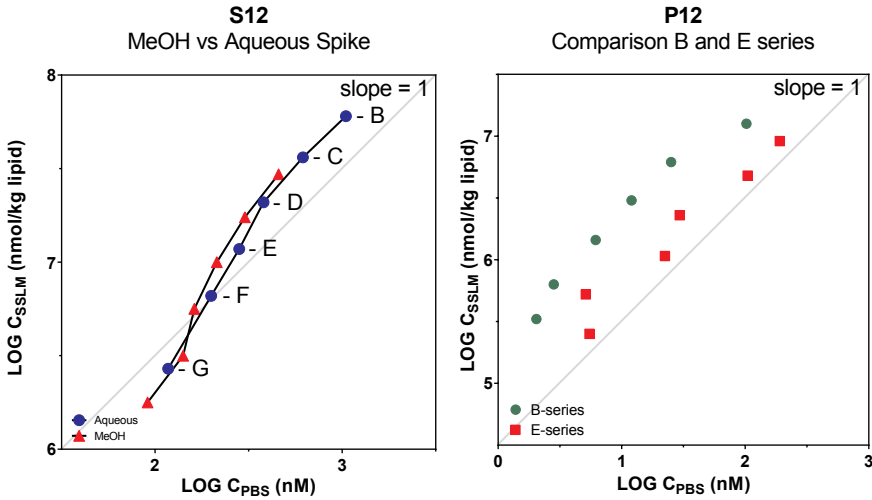
**Figure S1.** Influence of  $D_{MW}$  on significance of leaked phospholipids in medium

A series of cationic surfactants with different  $D_{MW}$  values were spiked to:

- HPLC autosampler vials that contained SSLM beads in their original test medium (transferred from the 96 well plate – “unwashed”, though diluted by a factor of 2);
- HPLC autosampler vials that contained SSLM beads without the original test medium (transferred from the 96 well plate – centrifuged, removal of supernatant and addition of fresh test medium – “washed”).

In accordance with the data modeled elsewhere (Figure S4), there is no influence of this washing step up to a  $D_{MW}$  of log 3.65 (e.g. the surfactant T10 plotted here).

For S12 (log  $D_{MW}$  of 5.39) the influence of renewing the test medium with fresh PBS, and thus removing the presence of leaked phospholipids, is up to factor 10 higher  $D_{MW}$  values and consistent linear isotherms instead of variable/nonlinear isotherms for unwashed beads.

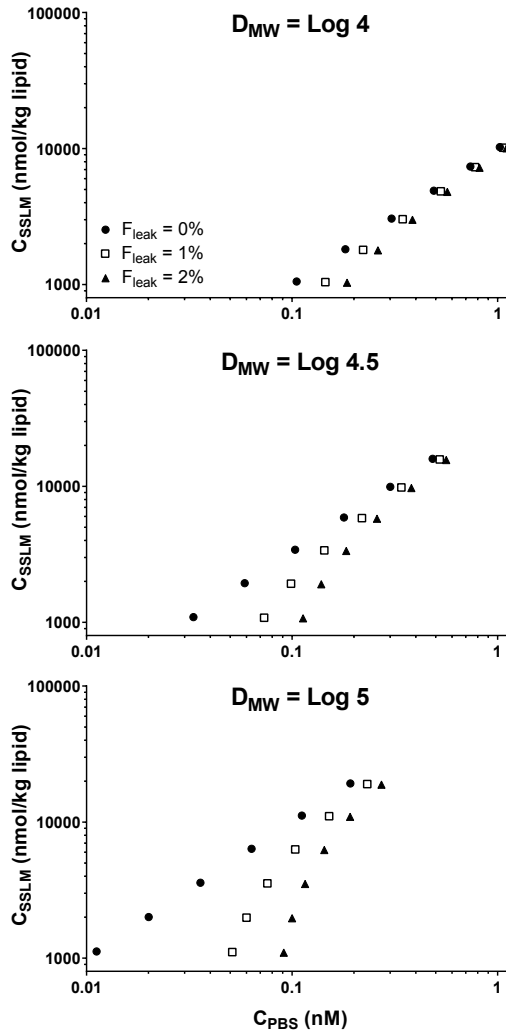


**Figure S2 (left).** Comparison between aqueous spike solution and spike solution in methanol for N-methyldodecylamine (S12). **Figure S3 (right).** Comparison between B- and E-series for dodecylamine (P12), for which two constant SSLM amounts were spiked with six serially diluted stock solutions in methanol.

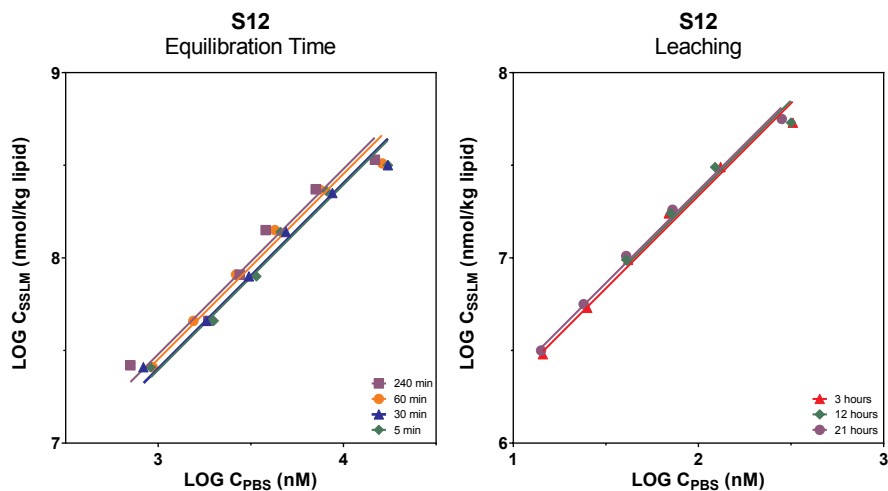
Figure S2 indicates that any influence of the composition of the spiking solution is minimal, if present at all, and no explanation for the non-linear shape of the sorption isotherm. Two SSLM test series were compared, of which one was spiked directly with a methanol dosing standard and one was spiked using a dosing standard made up of an aqueous solution. Both dosing standards did not have the same starting concentration, hence the downward shift of the isotherm based on the methanol-spiked series. The sorbent dilution series follow Vials B (lowest SSLM) – G (highest SSLM).

Figure S3 shows that when a consistent amount of TRANSIL beads were used in a series spiked with different concentrations of surfactant, a linear isotherm readily fits the data for each series. The B-series has the lowest bead content in a standard row of the 96 type well plate; the E-series has a 5.8 times higher bead content. Conform the nonlinear relationship within the standard sorbent dilution series (Figure S1), the  $D_{\text{mw}}$  for the E-series is consistently lower than for the B-series.





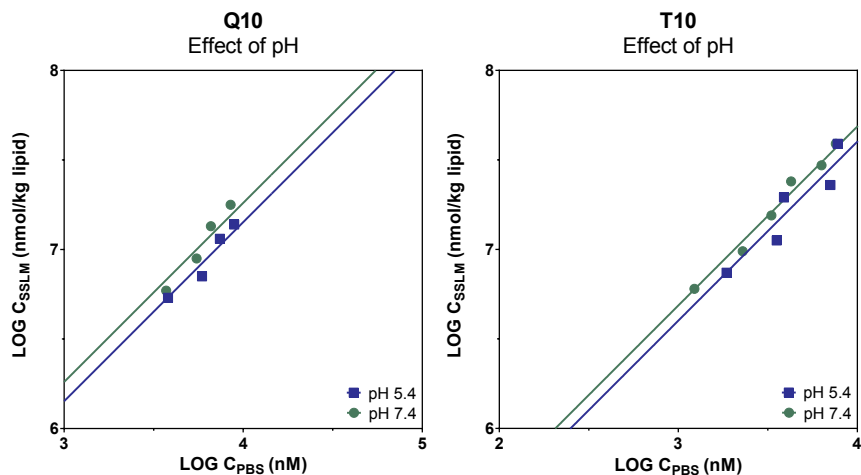
**Figure S4.** Overview of the predicted influence of phospholipid leakage (0%, 1% and 2% leakage from the SSLM material), at three different sorption affinities in the range  $\log D_{MW}$  4-5. The modeled values clearly show negligible deviations for a chemical with a  $\log D_{MW}$  of 4 at the vials with the lowest SSLM material (highest  $C_{PBS}$ ), up to a factor of 2 at the highest SSLM material (lowest  $C_{PBS}$ ) in the case of 2% leakage. For a chemical with a  $\log D_{MW}$  of 4.5 there is still negligible effect of leakage up to 2% lipids at the vials with the lowest SSLM material (highest  $C_{PBS}$ ), but this increases to a factor of 3 and factor of 8 at the highest SSLM material (lowest  $C_{PBS}$ ) in the case of 1% and 2% leakage, respectively. For a chemical with a  $\log D_{MW}$  of 5 there is still negligible effect of leakage up to 2% lipids at the vials with the lowest SSLM material (highest  $C_{PBS}$ ), but this increases to more than a factor of 3 at the highest SSLM material (lowest  $C_{PBS}$ ) in the case of only 1% leakage, and a factor of 10 with 2% lipids leaking into the test medium.



**Figure S5 (left).** Influence of incubation time on measured  $D_{MW}$  for N-methyldecylamine (S12). **Figure S6 (right).** Influence of storing centrifuged samples at room temperature in the autosampler on leaching of lipids, determined by  $D_{MW}$  for N-methyldecylamine (S12).

The results presented in figure S5 prove that incubation time has a very minor, if any, effect on measured  $D_{MW}$ . Four series of sorbent dilution series were placed on a roller mixer, each series spiked with the same methanol stock solution. The four different vials in each series were centrifuged (10 minutes) after 5, 30, 60 or 240 minutes on the roller mixer. No statistically significant differences in  $D_{MW}$  were observed when fitting with a log-linear sorption isotherm with a fixed slope of 1.

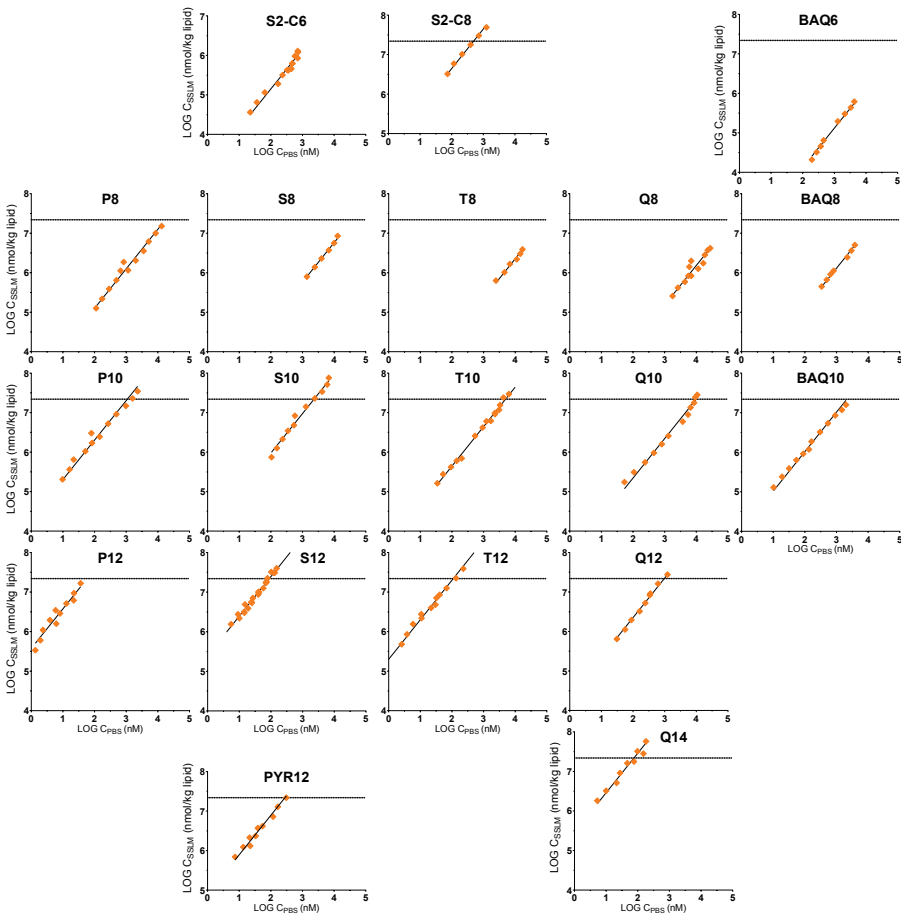
To produce the isotherms in figure S6, one series of beads was spiked (after washing as described in M&M) and left for 3 hours at room temperature before centrifugation and measurement. Vials with beads were then left at room temperature and measured again after a total of 12 and 21 hours at room temperature. The results between the three measurements are virtually identical, especially considering analytical uncertainty of LC-MS/MS measurements in general, indicating that lipids do not leak into the medium of the autosampler vial for centrifuged samples, as this would have increased the apparent  $C_{PBS}$ .



**Figure S7.** Influence of neutral fraction on  $D_{MW}$  estimates

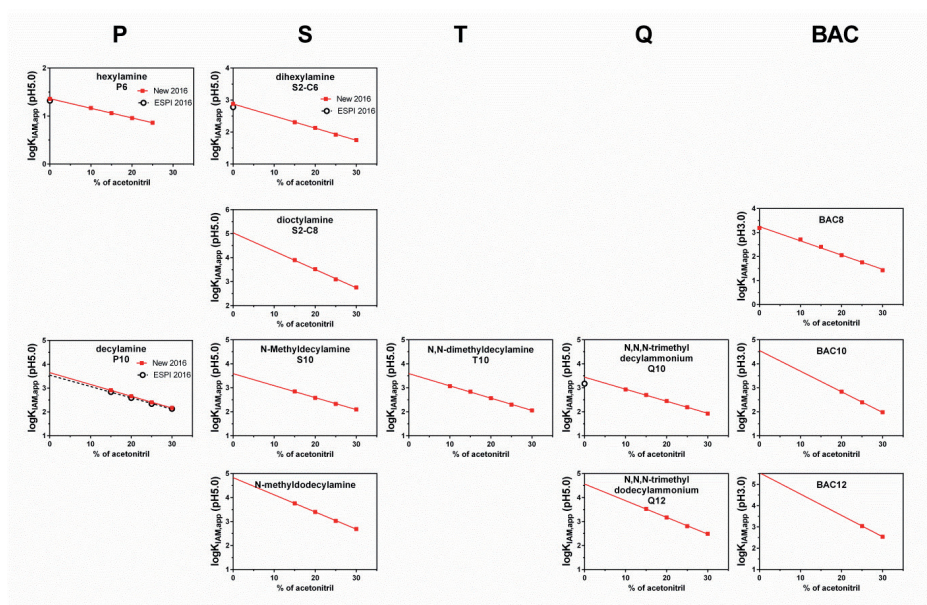
Comparison of a quaternary and tertiary amine at pH 5.4 and pH 7.4 provides evidence that there is negligible contribution of the neutral fraction of T10 at pH 7.4, where the tertiary amine T10 is >99.5% ionic ( $pK_a \sim 10$ , see Table S1). Q10 is of course 100% ionic at both pH values.

At pH 5.4 the neutral fraction should be 100-fold lower than at pH 7.4. Since only a slight (not statistically significant) decrease of 0.1 log units in  $D_{MW}$  is observed for both amines, virtually identical for a quaternary amine that – by definition – is not susceptible to contribution of a pH-dependent neutral fraction, any contribution of the small neutral fraction present at pH 7.4 can be assumed to be trivial.



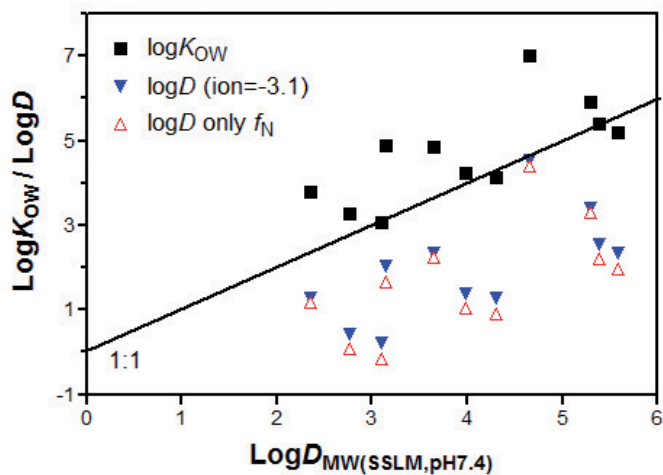
**Figure S8.** Matrix of all isotherm plots.

This matrix contains all data points and all isotherms used to calculate the  $D_{MW}$  values reported in the tables and the main body of this chapter. Both axes are identical for every graph. The dotted line at a sorbed concentration of approximately  $\log 7.3$  (nmol/kg lipid) indicates the maximum liposome loading as established in the main text.



**Figure S9.** Matrix of all solvent series measurements with IAM-HPLC

Performed in this study, and overlapping IAM-HPLC data from a previous study [119] [120]. The BAC series were performed for the ESPI study.



**Figure S10.** Comparison between  $\log P/\log D$  and the sorption affinity to bilayer membrane for ionizable cationic surfactants.  $\log P$  values are taken from ACD/Labs.



# CHAPTER 6

---

## Toxicity Mitigation and Bioaccessibility of the Cationic Surfactant Cetyltrimethylammonium Bromide in a Sorbent-Modified Biodegradation Study

Niels Timmer<sup>1</sup>, David Gore<sup>2</sup>, David Sanders<sup>2</sup>,  
Todd Gouin<sup>2</sup>, Steven T.J. Droge<sup>1,3</sup>

<sup>1</sup> Institute for Risk Assessment Sciences, Utrecht University, Utrecht, 3508 TD, The Netherlands

<sup>2</sup> Safety and Environmental Assurance Centre, Unilever, Colworth Science Park, Sharnbrook, Bedfordshire,  
MK44 1LQ, UK

<sup>3</sup> Department Freshwater and Marine Ecology, Institute for Biodiversity and Ecosystem Dynamics, University of Amsterdam, P.O. Box 94248, 1090 GE Amsterdam, The Netherlands

**Keywords:** Cationic Surfactant; Limited Bioaccessibility; Toxicity Mitigation; Ready Biodegradability; Environmental Risk Assessment; Cetyltrimethylammonium Bromide

**Chemosphere, 222, 461-468 (2019)**

## Abstract

Biodegradation potential of cationic surfactants may be hampered by inhibition of inoculum at concentrations required to accurately measure inorganic carbon. At >0.3 mg/L cetyltrimethylammonium bromide (CTAB) negatively impacted degradation of the reference compound aniline. We used silicon dioxide (SiO<sub>2</sub>) and illite as inorganic sorbents to mitigate toxicity of CTAB by lowering freely dissolved concentrations. In an OECD Headspace Test we tested whether 16.8 mg/L CTAB was readily biodegradable in presence of two concentrations of SiO<sub>2</sub> and illite. SiO<sub>2</sub> adsorbed 85% and 98% CTAB, resulting in concentrations of 2.5 and 0.34 mg/L, mineralized to CO<sub>2</sub> >60% within 16 and 23 d, respectively. With 89% and 99% sorbed to illite, 60% mineralization was reached within 9 and 23 d, respectively. However, higher sorbent concentrations increased time needed to reach >60% mineralization. Thus, desorption kinetics likely decreased bioaccessibility. It is therefore essential to determine appropriate concentration of mitigating sorbent to render a Headspace Test based on carbon analysis suitable to determine ready biodegradability of compounds which might inhibit inoculum. This would avoid use of expensive radiolabeled compounds. However, high sorbent concentrations can reduce bioaccessibility and limit degradation kinetics, particularly for relatively toxic substances that require strong mitigation.



## Introduction

Environmental persistence of potentially toxic chemicals is a key property in aquatic and terrestrial environmental risk assessment. Persistency may widespread occurrence and accumulation of concentrations near input streams. Evidence of significant biodegradation in standard test protocols, even without qualifying as readily biodegradable, is therefore of critical importance for routinely applied chemicals, such as ingredients of products for every-day consumer use, or commonly prescribed drugs that enter environmental systems via (treated) waste water effluent. Use in applications such as corrosion inhibitors or antifouling coatings may also generate fairly continuous environmental input. There are various types of standardized assays to determine biodegradability of a chemical by microbial communities, such as those present in activated sludge, sediment, or soil [139-144]. Ideally, these tests reproducibly determine the time needed to mineralize organic contaminants into CO<sub>2</sub>. CO<sub>2</sub> production due to biodegradation is routinely measured using inorganic carbon (IC) analysis, which is often restricted to limits of quantification (LOQ) around 0.5 mg/L, because of background respiration in the inoculum [145]. As a result, recommended test concentrations in biodegradation assays that depend on carbon analysis are in the range of 10-20 mg organic carbon per liter (mg C/L). Potential issues arise when these concentrations exceed solubility limits or toxic effect levels to critical micro-organisms in the inoculum [309, 310]. Dean-Raymond and Alexander (1977), tested ultimate degradation of ten cationic surfactants; eight were found to “resist attack by microorganisms” [311]. Only decyltrimethylammonium bromide and hexadecyltrimethylammonium bromide (cetyltrimethylammonium bromide; CTAB) were degraded by soil and sewage inocula, although CTAB was not degraded at the highest of three tested concentrations (100 mg/L), suggesting inhibitory effects prevented biodegradation for most compounds/concentrations.

The OECD 310 Guideline [140] describes how to measure aerobic mineralization of a chemical to CO<sub>2</sub> in inoculated medium, including stringent requirements to label a chemical as ‘readily biodegradable’ (>60% of maximum attainable theoretical IC production (ThIC) within 28 d of incubation, which has to be reached in a 10-d window that starts when biodegradation reaches 10%). The Guideline refers to a ring-test of five surfactants, including CTAB [140]. The addition of silica gel (SiO<sub>2</sub>) is specifically mentioned to “neutralize toxicity” of CTAB, referring to a 2003 study [146]. It is hypothesized that CTAB inhibits inoculum at the required concentration, although no references were provided. Adsorption of CTAB to silica gel reduced freely dissolved CTAB concentration to below inhibitory levels,

resulting in  $75\pm 13\%$  biodegradation (11 participating laboratories). CTAB adsorbed to  $\text{SiO}_2$  thus appeared to be bioaccessible, allowing for a potentially toxic concentration of CTAB to be degraded [146].

In 2008, another biodegradation study reported the use of 2 g/L  $\text{SiO}_2$  for octadecyltrimethylammonium chloride (ODTAC), a cationic surfactant with a longer alkyl chain than CTAB [145]. ODTAC was toxic to the inoculum, but could be classified as readily biodegradable with addition of  $\text{SiO}_2$ . In this study, other sorbents that enhanced biodegradation were humic acid and lignosulphonic acid, although biodegradation of ODTAC was fastest with  $\text{SiO}_2$  as mitigating adsorbent. A more recent paper by Sweetlove et al. provides some refinement of this work, aiming at high throughput screening [147]. The studies mentioned above provide rough guidelines on the use of adsorbents [145-147], but we argue that ideally a more systematic approach is required to determine the balance between toxicity, bioavailability and bioaccessibility of cationic surfactants in such critical biodegradation studies.

Our goal was to run a stepwise series of tests as a combined protocol to determine the biodegradation potential of CTAB in a sorbent-modified Headspace Test [140]. In previous studies it was identified that  $\text{SiO}_2$  formed a gel-like structure, hindering the use of magnetic stirring to aid gas exchange and increase interaction between sorbent and inoculated medium [145]. Cationic surfactants readily sorb to mineral surfaces such as clay minerals [177, 312, 313], and can cause analytical difficulties as they tend to sorb significantly to glassware and laboratory equipment [257]. Since clay minerals with a higher cation exchange capacity than  $\text{SiO}_2$  provide more adsorption sites, less sorbent material should be needed to mitigate toxicity. In addition, clay minerals do not form a viscous gel layer and might therefore offer faster desorption kinetics, enhancing bioaccessibility. We tested  $\text{SiO}_2$  and illite clay as sorbents unlikely to influence background respiration, since they contain no organic material. Previously, Illite clay was used in a systematic evaluation of the sorption affinity of organic cations [177]. This allows for close comparison between the sorption study by Droge and Goss and the conditions in the current biodegradation study. [177] Furthermore, illite is a 2:1 non-expanding clay mineral with only siloxane surfaces and therefore only has outer surfaces to adsorb organic cations, which should facilitate bioaccessibility through desorption. Compared to another non-expanding clay mineral such as kaolinite, illite has a relatively high cation-exchange capacity ( $\sim 200$  meq/g and  $\sim 20$  meq/g, respectively) [314].

First, we determined CTAB concentrations that maintain full inoculum activity, by determining the no observed effect concentration of CTAB at which biodegradation of a reference compound is inhibited. Degradation of aniline was followed for 14 d using the manometric respirometry method with the OxiTop respirometer system. Secondly, sorption isotherms with SiO<sub>2</sub> and illite were determined to calculate required sorbent loadings to achieve CTAB concentrations below the adverse effect level with a spiked CTAB concentration of 10 mg C/L (= 16.8 mg/L). The selected sorbents easily settled upon centrifugation, allowing for analysis of dissolved concentrations in supernatant and calculation of sorbed concentrations using a mass balance approach. Thirdly, we tested bioaccessibility of adsorbed CTAB, and whether employing these sorbents during a 28 d ready biodegradability study would serve to classify CTAB as readily biodegradable. Biodegradability is an intrinsic property of a chemical compound and has significant implications in environmental risk assessment. It is therefore highly relevant to pursue methodology preventing compounds from being incorrectly classified with respect to their biodegradability. We used radiolabeled [<sup>14</sup>C]CTAB to study biodegradation at a concentration of 16.8 mg/L, using the two mitigating sorbents at two different sorbent loadings that would amount to initially adsorbed fractions of 90% and 99%.

## Materials and methods

### Chemicals and sorbents

CTAB (analytical grade), sodium benzoate (analytical grade), aniline (analytical grade), and silicon dioxide (Davisil Grade 633, particle size 35-75 µm, surface area 480 m<sup>2</sup>/g), and all solvents (analytical grade) were obtained from Sigma-Aldrich (Gillingham, Dorset, UK). Illite clay was purchased as a fine powder and stems from Argiletz (France). [<sup>14</sup>C]CTAB (>98% by HPLC-PMT), was obtained from American Radiolabeled Chemicals Inc. (Saint Louis, MO, USA). [<sup>14</sup>C]CTAB was mixed with CTAB; production of radiolabeled CO<sub>2</sub> was a proxy for total biodegradation. A stock solution of [<sup>14</sup>C]CTAB was prepared in acetone and the exact concentration was determined using liquid scintillation counting (LSC), after which unlabeled CTAB was added to reach the desired ratio of labeled to unlabeled material. The stock solution was then kept at 4 ± 2 °C until use.

Salts used to prepare buffers and mineral media, potassium hydroxide (KOH), sodium hydroxide (NaOH), sulfuric acid (H<sub>2</sub>SO<sub>4</sub>), and trifluoroacetic acid were all analytical grade (Sigma-Aldrich). Scintillation cocktails (Hionic-Fluor, Pico-Fluor Plus and Permafluor E+),

Carbosorb and combustion cones for the sample oxidizer were purchased from PerkinElmer (Seer Green, Beaconsfield, UK). Each batch of mineral salts medium was prepared one hour before use with concentrated stock solutions and ultrapure water (PURELAB flex, ELGA LabWater, High Wycombe, UK), as described in the Guideline [140].

## **Inoculum**

Inoculum was extracted from activated sludge obtained from Broadholme Sewage Treatment Works (BSTW; Ditchford Road, Wellingborough & Irthling, UK), which treats sewage from approximately 80,000 household; <15% of the organic load is attributable to industrial discharge [315]. Sludge was sparged with CO<sub>2</sub> free air overnight at room temperature (21±1 °C) to remove inorganic carbon. The sparged suspension was then transferred to a flow-breaking beaker, and homogenized at 12,000 rpm for 5 min using a Polytron PT 3000 dispersion unit (Kinematica AG, Littau, Switzerland). The resulting suspension was centrifuged at 800 *g* for 10 min, after which remaining suspended solids were removed by slowly pouring through a funnel filled with laboratory grade glass wool (Sigma-Aldrich). Subsequently, the filtered inoculum was added to mineral salts medium (final inoculum concentration: 10 mL/L). Concentration of suspended solids in the activated sludge was generally 5±1 g/L, but it should be noted that only the filtered supernatant after centrifugation was used for inoculation.

## **CTAB toxicity test**

A 14 d manometric respirometry test [139] was used to determine the no observed effect concentration in activated sludge (NOEC-STP) of CTAB. Five CTAB concentrations were prepared in triplicate (0.3, 1.0, 3.0, 8.0 and 24 mg/L). All vessels were spiked with 9 mg/L aniline (theoretical oxygen demand (ThOD): 24 mg/L). Three control vessels containing only aniline and three blanks were included. Unlabeled CTAB stock solution in ultrapure water was added to 80 mL of medium, followed by 80 mL of medium containing 20 mL/L inoculum. Rubber inserts containing KOH were lodged into the vessels' opening. Manometric measuring heads (OxiTop, WTW, VWR, East Grinstead, UK) were tightly screwed onto each bottle to start the measurements. Vessels were maintained at 22 ± 1 °C in HT Multitron stackable incubators (Infors AG, Bottmingen, Switzerland), programmed for orbital shaking at 100 rpm. Measuring heads recorded pressure at 360 time points in equally spaced intervals for 14 d, which was automatically converted into oxygen consumption. Comparing oxygen consumption to the ThOD yields a percentage degradation. The NOEC-

STP of CTAB was considered to be the highest concentration at which  $\geq 60\%$  aniline was biodegraded within 14 d.

### CTAB sorption test

$\text{SiO}_2$  and illite clay form suspensions that readily settle upon standing still. Using 20 mL borosilicate scintillation vials (PerkinElmer), three CTAB concentrations (0.1, 1.0 and 10 mg/L) were exposed to three concentrations of sorbent (0.80, 4.0 and 20 g/L) in triplicate. Control vials without sorbent were also prepared to correct for sorption to the borosilicate surface. Vials were placed on a roller mixer (Thermo Fisher Scientific, Waltham, MA, USA), set at 30 rpm and  $20 \pm 1^\circ\text{C}$  overnight, centrifuged at 2,400 g for 30 minutes, after which three 4 mL aliquots of the supernatant were analyzed by LSC (Tri-Carb 2710TR, PerkinElmer). Sorbed amounts were calculated using a mass balance approach; a linear sorption isotherm was fitted to calculate average sorption coefficients. After determining the sorbent-water sorption coefficient ( $K_{\text{sorbent-water}}$ ) it is possible to calculate how much sorbent ( $V_{\text{sorbent}}$ ) to add to a certain amount of toxicant ( $A_{\text{toxicant}}$ ), in order to decrease the freely dissolved concentration to levels sufficiently below the NOEC-STP ( $C_{\text{aq, safe}}$ ):

$$A_{\text{toxicant, safe}} = C_{\text{aq, safe}} \times V_{\text{water}} + C_{\text{aq, safe}} \times K_{\text{sorbent-water}} \times V_{\text{sorbent}} \quad (\text{eq. 1})$$

, thus

$$V_{\text{sorbent}} = \frac{A_{\text{toxicant, safe}} - C_{\text{aq, safe}} \times V_{\text{water}}}{C_{\text{aq, safe}} \times K_{\text{sorbent-water}}} \quad (\text{eq. 2})$$

### CTAB biodegradability test

Biodegradability of a CTAB concentration exceeding the NOEC-STP was studied under variable sorbent additions during 35 d, using the design of the OECD Guideline [140]. Based on the obtained sorption coefficients sorbent concentrations were chosen to yield sorbed CTAB fractions of 0% (no sorbent),  $\sim 90\%$  and  $\sim 99\%$ . The spiked CTAB concentration of 16.8 mg/L in these three treatments was selected to be both in the inhibitory range determined in the toxicity test (8-24 mg/L) as well as comparable to spiking levels recommended for using IC analysis (i.e. 10-20 mg C/L; approximately 16-32 mg/L CTAB). Due to using [ $^{14}\text{C}$ ]CTAB relatively low freely dissolved concentrations of CTAB and  $\text{CO}_2$  could still be determined

accurately, while the mass balance could also be monitored, even in systems with high sorbent concentrations (see below).

For each sorbent-dosed CTAB treatment, triplicates were prepared for 10 measuring points in a 35 d test period. Six duplicates without sorbent were prepared to monitor the inhibition levels each week. Each 125 mL borosilicate serum vessel (Wheaton, New Jersey, USA) was filled with a total of 100 mL medium, resulting in a 64 mL headspace. Vessels were first spiked with [<sup>14</sup>C]CTAB acetone stock solution, loosely covered and left standing overnight at room temperature to allow acetone to evaporate. Gentle flushing with nitrogen gas removed residual acetone vapors. Dry sorbent was added, and a Perimatic Premier precision dispensing pump with a re-circulation loop (Jencons Scientific Ltd, VWR, East Grinstead, UK) delivered 50 mL mineral salts medium without inoculum. At least 2 h was allowed for interaction between dissolved CTAB and sorbent. Abiotic control vessels were filled with a second 50 mL aliquot of medium without inoculum. A 50 mL aliquot of medium with 20 mL/L of inoculum was added to all other vessels. Vessels were then tightly capped using 20 mm butyl rubber stoppers and aluminum crimp caps (Sigma-Aldrich), and incubated in HT Multitron stackable incubators at 22 ± 1 °C and an orbital shaking rate of 100 rpm.

Sodium benzoate was the reference compound in the CTAB biodegradability test. Benzoate is a more common reference than aniline and should be fully biodegraded within 14 d, usually ~90% biodegradation is reached within 7 d of incubation. Blanks should yield an IC content of <3 mg/L after 28 d. Supplementary controls with benzoate and sorbent (20 g/L SiO<sub>2</sub> or 4 g/L illite clay) were incorporated to rule out effects of sorbent on inoculum performance. These control vessels were all incubated and treated with 7 M NaOH as described below, but after opening the contents of each vessel were divided over three 20 mL vials compatible with a Shimadzu ASI-V autosampler (Shimadzu Ltd., Milton Keynes, UK). Vials were closed immediately after pouring in order to prevent uptake of atmospheric CO<sub>2</sub>. Within 24 h after initial sampling, IC content was determined using a Shimadzu TOC-V. IC production in the control vessels was corrected for background IC production in the blanks. Biodegradation was then quantified based on ThIC of the added benzoate.

## CTAB detection, analysis and mass balance

Before sampling, vessels were injected with 1 mL of 7 M NaOH, to solubilize all inorganic carbon, and left in the incubator for 60 min. After this time, suspended sorbent particles were allowed to settle if needed. Immediately after opening, three 3 mL aliquots were sampled to analyze the total carbon content (TC). Three additional 3 mL aliquots were acidified using 1 mL of 4 M H<sub>2</sub>SO<sub>4</sub> to convert HCO<sub>3</sub><sup>-</sup> to gaseous CO<sub>2</sub>, which was vented off by leaving samples uncapped overnight. Acidified samples therefore only contain organic carbon (TOC), and the difference between alkaline (TC) and acidified (TOC) samples represents mineralization i.e. the amount of IC (CO<sub>2</sub> and carbonates) formed. After adding 16 mL of Hionic-Fluor, followed by rigorous shaking for 5 s, samples were analyzed by LSC on a Tri-Carb 2710TR. Percentage biodegradation was then calculated by comparing the amount of radiolabeled CO<sub>2</sub> formed with the total applied dose of radioactivity. All biodegradation data was fitted using the '[Agonist] vs. response – Variable slope (four parameters)' model as included with GraphPad Prism 7.04 for Windows.

After sampling, vessels were emptied and sorbent was removed by rinsing the vessels with 10 mL MilliQ. To extract CTAB sorbed to the glass wall, 5 mL washing solution (90% (v/v) methanol and 0.1% (v/v) trifluoroacetic acid in MilliQ) was added to each vessel and left for 2.5 h at 30 rpm on a roller mixer (Thermo Fisher Scientific). The washing solution was then poured into a 20 mL liquid scintillation vial and mixed with 16 mL Hionic-Fluor for LSC.

On Day 22 the contents of the vessels were filtered under vacuum using a 100 mm Whatman GF/C glass fiber filter. If needed, vessels were rinsed twice with 6 mL of MilliQ to retrieve all sorbent. Filters were left to dry overnight, and stored at room temperature until further analysis. The residue on each filter was divided over multiple cellulose PerkinElmer combustion cones for use in a Packard Model 307 sample oxidizer (PerkinElmer). Empty filters were cut in halves and stuck into separate combustion cones. Before introduction into the sample oxidizer, combustion cones were enriched with 100 µL analytical grade hexadecane to increase the combustion temperature in order to volatilize any remaining [<sup>14</sup>C]CTAB. [<sup>14</sup>C]CO<sub>2</sub> formed during combustion was trapped in approximately 5 mL of Carbo-Sorb E, which was mixed with 7 mL of Permafluor E+. Combustion samples were then topped up with 8 mL of Pico-Fluor to decrease quenching, primarily caused by small soot particles from the combustion process. After LSC, measurements of glass extracts, combusted and alkaline samples were used to determine a mass balance, with abiotic control vessels as a 100% reference.

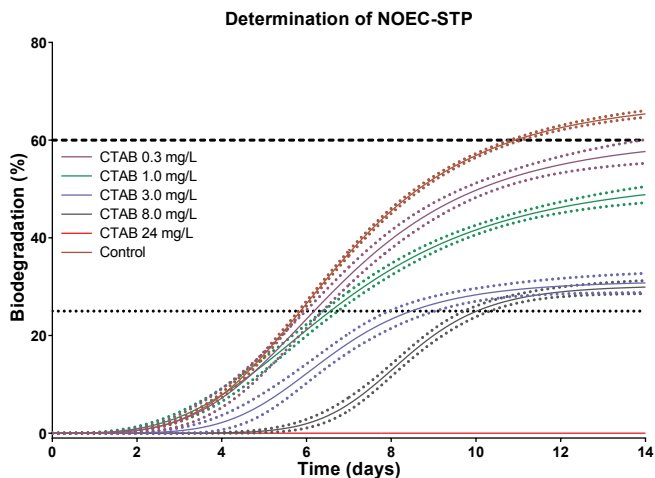
## Results and discussion

### CTAB no observed effect concentration

A manometric respirometry assay was used to determine the approximate concentration at which CTAB inhibits microbial degradation of aniline. The positive control containing only aniline showed close overlap between triplicate vials, and blanks showed no significant background oxygen consumption (Figure S1). A lag phase of approximately 4 d can be observed (Figure 6.1), and after 10 d 60% of ThOD is reached. Results obtained were suitable to estimate the no observed effect concentration in activated sludge (NOEC-STP). Only the CTAB treatment of 0.3 mg/L showed a biodegradation profile comparable with the positive control. At the highest CTAB concentration of 24 mg/L no biodegradation was recorded at all, indicating complete inoculum knockout. At 8.0 mg/L CTAB a prolonged lag phase was observed, in combination with significantly reduced biodegradation after 14 d, which was also observed at 3.0 mg/L. At 1.0 and 0.3 mg/L the lag phase was comparable with the positive control, but biodegradation at 1.0 mg/L reached only 50% after 14 d. These results indicate that inhibitory effects of CTAB on inoculum activity are likely to become significant above 1.0 mg/L, and stronger effects can be expected between 8.0 and 24 mg/L. A freely dissolved CTAB concentration of <1 mg/L through addition of sorbent should then be sufficient to mitigate inhibitory effects on the inoculum. The NOEC-STP for CTAB is up to two orders of magnitude lower than the recommended CTAB test concentration of 16-32 mg/L. Graphs showing mean raw data of all 360 measurement points per series can be found in figure S7.

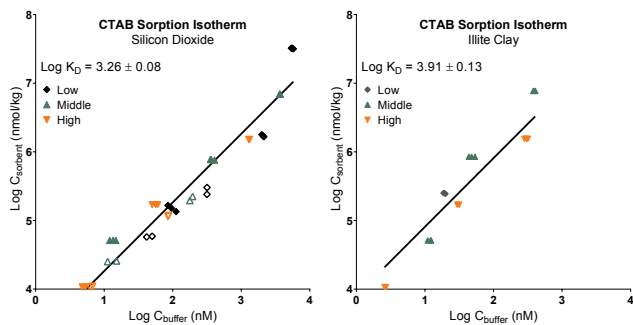
For optimal toxicity mitigation it is essential to accurately predict how addition of sorbent will influence freely dissolved concentrations of the inhibitory compound. CTAB sorption isotherms obtained for SiO<sub>2</sub> and illite clay are presented in Figure 6.2. For SiO<sub>2</sub> the isotherm is linear (fitted slope of 1) over the concentration range 2.2 µg/L to 2.4 mg/L, adequately covering concentrations exceeding the NOEC-STP (0.3 mg/L). Two independently performed series show good agreement; a second experiment was performed since the first measurement series shows signs of leveling off at its respective highest concentration (100 nM). Fit of the combined data results in a  $K_{\text{sorbent-water}}$  of 1820 L/kg SiO<sub>2</sub>. For illite clay the isotherm covered concentrations from 0.9 µg/L to 0.2 mg/L, ending slightly below the NOEC-STP. Obtaining a detailed sorption isotherm was beyond the scope of our study. Since the data acquired allowed for a reasonably realistic estimate of the sorption affinity, we therefore decided not to perform a second measurement series.





**Figure 6.1** Biodegradation of aniline by itself and in combination with different concentrations of CTAB, measured using the automated OxiTop respirometer assay, to determine the no observed effect concentration of CTAB. Fitted curves based on 360 measurements; dotted lines represent the 95% confidence bands for each curve, fitted using a four parameter variable slope agonist/response model; the dotted line at 60% indicates the required level to satisfy one of the conditions for ready biodegradability. The curve of CTAB 24 mg/L lies on the X-axis as no mineralization to  $\text{CO}_2$  was measured.

### CTAB sorption affinity to $\text{SiO}_2$ and illite clay



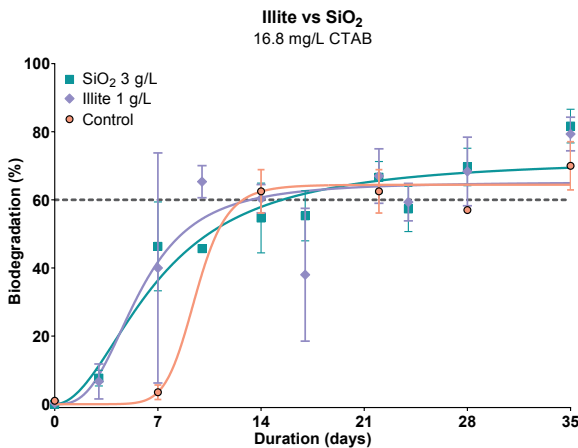
**Figure 6.2** CTAB isotherms for sorption to  $\text{SiO}_2$  (left) and illite clay (right); symbols have been color coded to relate them with associated sorbent concentrations; open symbols for  $\text{SiO}_2$  are to distinguish between the first (open symbols) and second (closed symbols) series

The data indicate a  $K_{\text{sorbent-water}}$  of 8130 L/kg, about 4.5 times higher than for  $\text{SiO}_2$ . Interestingly, the calculated sorption coefficient of CTAB to illite clay is in agreement with predicted  $K_{\text{illite-water}}$  based on a cation exchange model proposed by Droge & Goss in 2013 [177]. Applying

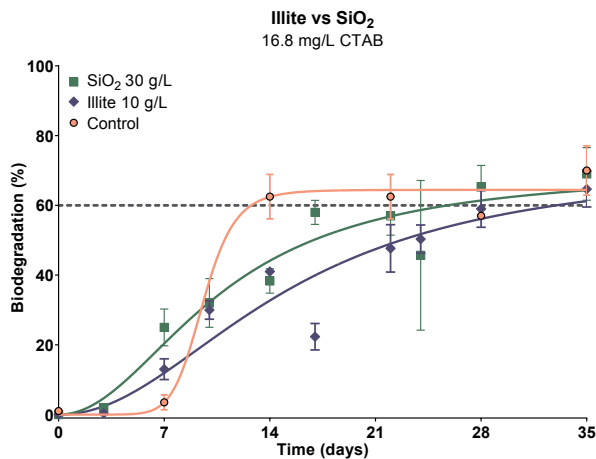
eq.2 for (i) the recommended concentration of 16.8 mg/L in the OECD Headspace test [ $A_{\text{toxicant, safe}}$ ], (ii) the NOEC-STP of 0.3 mg/L [ $C_{\text{aq, safe}}$ ], in (iii) the volume of medium applied (0.1 L) [ $V_{\text{water}}$ ], and (iv) the derived sorption coefficients [ $K_{\text{sorbent-water}}$ ], suggests required sorbent concentrations of 31.1 g  $\text{SiO}_2/\text{L}$  and 7 g illite/L.

### CTAB biodegradation in Headspace Test without sorbent

Abiotic controls showed stable (<2% variation) concentrations of [ $^{14}\text{C}$ ]CTAB throughout the 35 d incubation period, providing a mass balance reference. Adequate inoculum activity was demonstrated in the benzoate controls (Figure S2), also in the presence of sorbents; 80-90% biodegradation within 7 d for controls without sorbent and with  $\text{SiO}_2$ . Results for illite clay, however, surprisingly reached 250% biodegradation. We suspect IC release from clay particles might be the cause for this, as clay minerals are known to sorb  $\text{CO}_2$  and carbonates [316], and illite clay used in this experiment had not undergone any pretreatment. Sorbent controls were included to rule out inhibitory effects of added sorbent, which can be considered successful. For the biodegradation test with [ $^{14}\text{C}$ ]CTAB, possible release of IC from illite clay should have no impact, since [ $^{14}\text{C}$ ]  $\text{CO}_2$  will be analyzed.



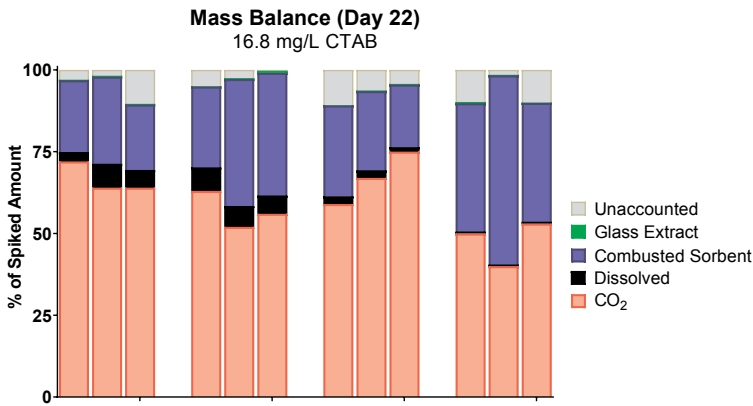
**Figure 6.3** CTAB biodegradation profile with sorbent concentrations resulting in sorbed fractions of ~90% (3 g/L  $\text{SiO}_2$  - squares; 1 g/L illite - diamonds), compared to controls without sorbent (control - circles); the dotted line at 60% indicates the required level to satisfy one of the conditions for ready biodegradability; biodegradation (%) is calculated by comparing radioactive  $\text{CO}_2$  with total applied radioactivity, and was fitted using a four parameter variable slope agonist/response model



**Figure 6.4** CTAB biodegradation profile with sorbent concentrations resulting in sorbed fractions of ~99% (30 g/L SiO<sub>2</sub> - squares; 10 g/L illite - diamonds), compared to controls without sorbent (control - circles); the dotted line at 60% indicates the required level to satisfy one of the conditions for ready biodegradability; biodegradation (%) is calculated by comparing radioactive CO<sub>2</sub> with total applied radioactivity, and was fitted using a four parameter variable slope agonist/response model

The high rate of biodegradation at 16.8 mg/L CTAB (Figure S3, also visible in Figure 6.3 and 4) was unexpected in comparison with the results of the NOEC-STP determination (Figure 6.1). After at least a 7-d lag phase, measurements from Day 14 onwards show biodegradation of ~60%. This suggests CTAB was actually not inhibitory in the current experiment, whereas previously 8.0 mg/L strongly reduced biodegradation of aniline, and 24 mg/L caused full inoculum knockout (Figure 6.1). These differences might be partially explained by several factors. Firstly, while CTAB impacted microorganisms that degrade aniline in the toxicity tests, it may be that microorganisms able to convert CTAB are different species, less sensitive to CTAB. Secondly, inoculum in the toxicity test was obtained from the same source (BSTW), but sampled at a different time point, and activated sludge samples are known to lack in reproducibility [317]. Thirdly, different vessels and volumes were used, which may result in different fractions sorbed to glass surfaces, although the mass-balance (see Figure 6.5) indicates only a minute fraction of [<sup>14</sup>C]CTAB was actually sorbed to the glass surface on Day 22. Fourthly, the manometric respirometry method can be a less direct assessment of biodegradation, since CO<sub>2</sub> might be present in the aqueous phase as carbonate while gaseous CO<sub>2</sub> does not react with the KOH instantaneously. Nonetheless, the CTAB concentration that would inhibit microbial activity was underestimated, so full toxicity mitigation of CTAB cannot be investigated with the current data. However,

the sorbent-modified biodegradation studies focus on lag phase delay instead and are informative on the effect of bioaccessibility.



**Figure 6.5.** Day 22 mass balance, determined based on mean of three samples. Glass extract accounts for <0.6% of total

### CTAB biodegradation in Headspace Test with additions of SiO<sub>2</sub> or illite clay

Sorbent levels were chosen to yield freely dissolved CTAB concentrations slightly below and somewhat above the NOEC-STP of 0.3 mg/L. Based on the obtained  $K_{\text{sorbent-water}}$  values, the 3 and 30 g/L SiO<sub>2</sub> or 1 and 10 g/L illite applied in the Headspace Test currently performed resulted in respective sorbed fractions of 84.5% and 98.2% for SiO<sub>2</sub> and 89.0% and 98.8% for illite, and respective freely dissolved CTAB concentrations of 2.6 and 0.3 mg/L for SiO<sub>2</sub>, and 1.9 and 0.2 mg/L for illite.

Figure 6.3 shows the biodegradation profile of CTAB with low concentrations of the two sorbents. Although it was expected this would still result in moderately inhibitory effects based on the toxicity test with aniline, biodegradation was already initiated on Day 3, and was >40% within 7 d. On Day 7 IC production in controls without sorbent was <5%, indicating that sorbent additions shortened the lag phase and had a positive effect on inoculum activity. During the last three weeks no differences between controls and sorbent treated groups were observed. This would suggest that the freely dissolved CTAB concentrations in the low sorbent concentration treatments were non-inhibitory to the inoculum fraction responsible for degradation of CTAB.

Results of the high sorbent concentration (30 g/L SiO<sub>2</sub> and 10 g/L illite clay) are presented in Figure 6.4. Dissolved CTAB concentrations below the NOEC-STP were expected. Just as with the lower sorbent concentration treatments, the lag phase was shorter in the sorbent groups, with an average biodegradation after 7 d of 25% for SiO<sub>2</sub> and 14% for illite, compared to <5% in the controls. However, whereas the lower sorbent concentrations reached approximately 60% between Day 7 and 10, the higher sorbent concentration treatments showed a slower biodegradation rate between Day 7 and 21. For both sorbent treatments, CTAB biodegradation leveled off at 60%. Graphs showing all measurement points can be found in figure S8 and S9.

The shorter lag phase in all sorbent groups is indicative of mitigation of moderately inhibitory effects of the applied CTAB concentration. The slower increase of biodegradation in high concentration sorbent treatments compared to lower concentration treatments (See also Figure S4 and S5) could be explained by larger sorbed fractions that need to fully desorb in order to reach the inoculum and be biodegraded, which makes bioaccessibility the rate-limiting factor. In high concentration sorbent groups freely dissolved fractions were considerably smaller (1.8% with 30 g/L SiO<sub>2</sub> and 1.2% with 10 g/L illite clay) than in the low concentration sorbent treatments, requiring a higher flux of CTAB from sorbent to medium in order to maintain a constant freely dissolved concentration assuming a fixed biodegradation rate. Note that the amount of CTAB freely dissolved in the high concentration sorbent treatments was < 2% of that available in the control group without sorbent, although the freely dissolved concentration is likely maintained more rapidly at higher sorbent loadings.

Comparing concentrations of both sorbents, it becomes clear that bioaccessibility of CTAB is mainly shaped by sorption affinity of CTAB, not by nature or morphological structure of these sorbents. Orbital shaking sufficiently suspends Illite particles, maximizing interaction between inoculated mineral medium and sorbent particles, while SiO<sub>2</sub> can form a gel-like precipitate. Although this gel is hydrated, interaction with the inoculum suspended in the mineral medium is presumably smaller than for fully suspended illite clay. However, both sorbent types show similar kinetics at comparable sorbed fractions, indicating that in SiO<sub>2</sub> treatments inoculum activity may have been concentrated on the settled particles.

## CTAB mass balance in the Headspace Test

Sorbent containing vessels sampled on Day 22 were used to determine a mass balance (see Figure 6.5). Average mass balance was >90% for all treatment conditions, although two of the twelve vessels sampled scored slightly lower (89.6% and 89.2%). Since complete oxidation of samples containing biomass and sorbent was not expected, this was considered to be an excellent mass balance. Measured freely dissolved CTAB in the low concentration sorbent treatments was in the same order of magnitude as calculated using sorption coefficients, which was also true for the high concentration of illite. However, for unknown reasons the high concentration of  $\text{SiO}_2$  showed freely dissolved CTAB comparable to the low concentration of  $\text{SiO}_2$ . This might be due to the formation of silica gel at high sorbent loading, while at low  $\text{SiO}_2$  concentration a higher percentage of sorbent remained in suspension.

Amounts extracted from inside glass surfaces of vessels with sorbent were generally <1% (see also Table S1), although this fraction is significant when compared with the freely dissolved concentration, with which it should theoretically be in equilibrium. For vessels with  $\text{SiO}_2$ , the average amount of CTAB extracted from glass vessels accounted for approximately 5% of the freely dissolved amount. These percentages were 8% and 39% for 1 g/L and 10 g/L illite clay, respectively. However, freely dissolved concentrations were a factor 3 and 10 lower, respectively, while absolute amounts of CTAB extracted from glass vessels were comparable. Overall, glass binding was lower than what was expected based on previous work [257], although results are within the same order of magnitude.

Combustions of the sorbent indicated that significant portions of CTAB were still sorbed on Day 22 (~23% for both low sorbent concentrations, ~34% for 30 g/L  $\text{SiO}_2$  and ~44% for 10 g/L illite), while for low sorbent concentrations ~67% was already biodegraded. This raises the question if this sorbed fraction is bioaccessible or if it represents a strongly or irreversibly sorbed, or perhaps a microbially incorporated fraction of the radiolabeled carbon [318, 319]. Combustion of sorbent samples was difficult and it is therefore plausible that actual sorbed fraction (and therefore the mass balance) would turn out higher if a more thorough extraction method would have been available. Interestingly, for one 10 g/L vessel sorbent was divided in smaller aliquots over a larger number of combustion cones. This sample showed ~8% higher recovery than its replicate samples and the highest recovery from sorbent overall (~58%), indicating that more extensive subsampling could increase recovery of sorbent combustion and improve mass balance. We have provided

a comparison between mass balance on Day 22 with sorbent combustion and on Day 35 without sorbent combustion in figure S6, illustrating the likelihood of a >90% mass balance at the end of the experiment.

## Conclusion

CTAB met the criteria for ready biodegradability without sorbent, which signifies the relevance of reducing the lag phase through addition of inert sorbent. The most important element of this study was verifying that with a balanced amount of sorbent, unlabeled CTAB and carbon analysis could have been used to test biodegradability at freely dissolved concentrations below the NOEC-STP. It has been clearly demonstrated that CTAB inhibits inoculum activity by different metrics, such as impact on biodegradation of the reference substrate aniline, a significant lag phase in the current Headspace Test (which decreased after addition of sorbent), and absence of biodegradation in literature [311]. Findings presented in this chapter clearly illustrate that addition of inorganic sorbents can potentially mitigate toxicity of a broad range of well-adsorbing compounds in the Headspace Test. A stepwise approach was followed where NOEC-STP and sorption affinity of the test compound were determined first, in order to calculate the amount of sorbent needed to keep a specific concentration of test chemical below the NOEC-STP. Results suggest that 1 g/L illite clay, resulting in an initially sorbed fraction of 89% and freely dissolved CTAB concentrations a factor 2 above the NOEC-STP, provided adequate bioaccessibility for a successful ready biodegradability classification. However, sorbent dosing resulting in initially sorbed fractions of ~99%, and corresponding bioavailable concentrations below the NOEC-STP, may have resulted in retardation of biodegradation rate by decreasing bioaccessibility. Future research might benefit from more closely elucidating the desorption kinetics, apparent bioaccessibility, and biodegradation kinetics at various sorbent and substrate concentrations. Using [<sup>14</sup>C]CTAB we confirmed mass balance >90% after 3 weeks of exposure with mitigating sorbents, and identified that 20-60% of [<sup>14</sup>C]CTAB-related 'material' was still sorbed to sorbent after 22 d, while 40-70% was already fully mineralized. Minor freely dissolved fractions and negligible sorption to glass surfaces were confirmed. Table 6.1 summarizes the biodegradability classification of CTAB under different conditions in the current study. Addition of an amount of sorbent sufficient to reduce inhibitory effects of CTAB to the inoculum had a significant impact on satisfying the 10-d window criterion. This is an important finding, since satisfying the criteria for ready biodegradability has significant consequences for environmental risk assessment and it is

therefore important that readily biodegradable compounds are not incorrectly labelled as poorly biodegradable and vice versa.

**Table 6.1.** Classification of biodegradability of CTAB (tested at 16.8 mg/L) based on results obtained in the OECD 310 Headspace Test presently performed.

Conditions	Classification	Remarks
no sorbent	Readily biodegradable	Lag phase >7 d; 14 d to reach 60%
SiO <sub>2</sub> 3 g/L	Inherently biodegradable	Lag phase <3 d; 16 d to reach 60%
SiO <sub>2</sub> 30 g/L	Inherently biodegradable	Lag phase <3 d; 23 d to reach 60%
illite 1 g/L	Readily biodegradable	Lag phase <3 d; 9 d to reach 60%
illite 10 g/L	Inherently biodegradable	Lag phase 3-7 d; 23 d to reach 60%

The Argiletz illite clay, sold as “cosmetic green clay”, was available relatively cheap in large volumes in powdered form, making it directly suitable as adsorbent for (labelled) cationic surfactants in biodegradation studies. However, care should be taken with this material when using IC analysis, since the IC signal from the reference substrate reached 250% of theoretical maximum IC production. Finally, the use of automated OxiTop respirometer assay in the toxicity tests, where we demonstrated that CTAB affected the biodegradation of the reference substrate aniline, showed to be a promising efficient tool in biodegradability studies. It lacks the need of sacrificial sampling, reducing sample load and associated lab work, and provided detailed time profiles of all vessels tested for each condition. The use of toxicity mitigating adsorbents and such automated respirometer samplers may become even more valuable, expressed in time/cost-efficiency and relevance in biodegradation studies, for cationic surfactants that have a higher intrinsic toxicity to inoculum, and for which no radiolabeled compounds are available. The two sorbents employed during this work resemble sorbing surfaces encountered by sewage when traveling from the point of discharge to the sewage treatment plant, during treatment at the plant itself, and if inadvertently entering the environment. Therefore, the concept of toxicity mitigation is ecologically relevant, can be translated to environmental settings, and should be deemed permissible in biodegradability studies.

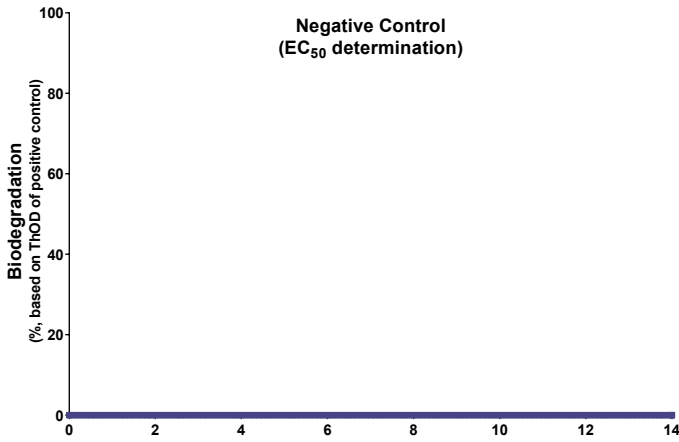
## Acknowledgements

This study was funded by Unilever, Safety & Environmental Assurance Centre (SEAC), Colworth Science Park (United Kingdom) under project CH-2012-0283. Geoff Hodges (Unilever) and Joop L.M. Hermens (Utrecht University) provided many useful comments and fruitful discussions on this work.

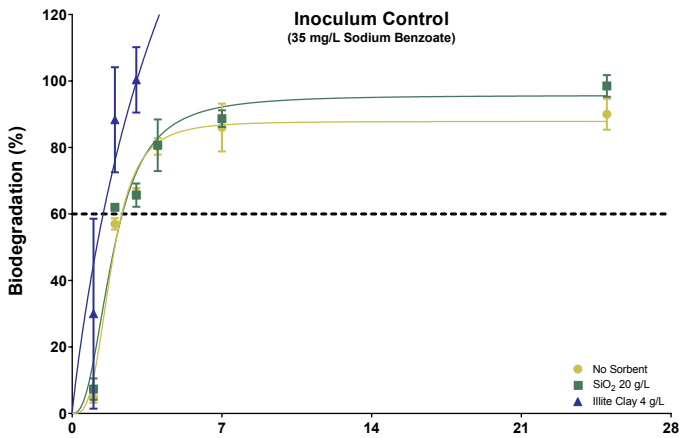


## Supporting Information

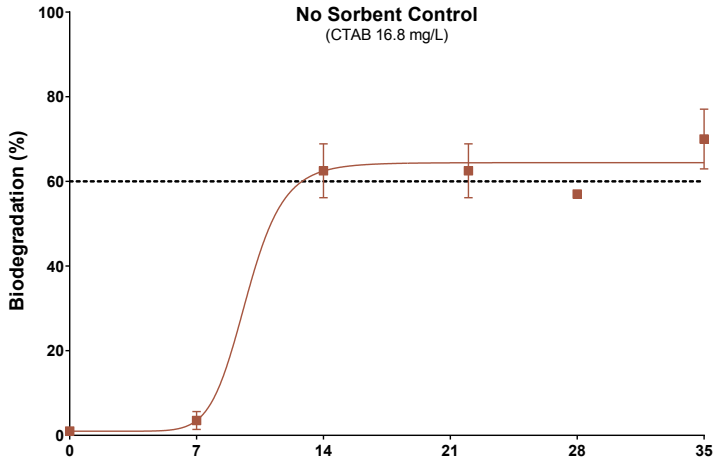
Toxicity Mitigation and Bioaccessibility of the Cationic Surfactant Cetyltrimethylammonium Bromide in a Sorbent-Modified Biodegradation Study



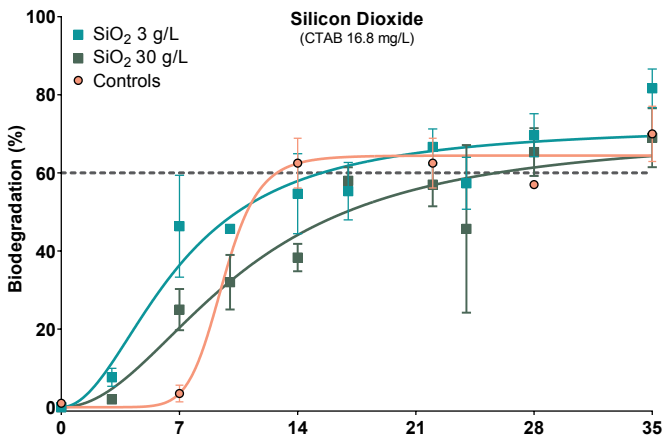
**Figure S1.** Results for the negative control in the manometric respirometry experiment. There was no oxygen consumption in the negative control



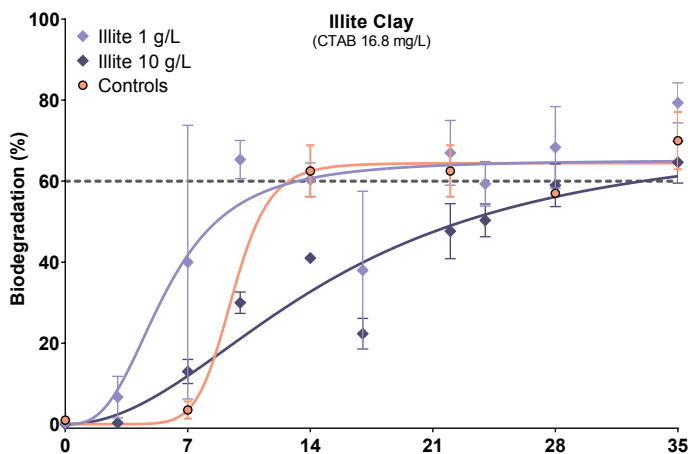
**Figure S2.** Results of the positive control in the 28d Headspace test. Without sorbent the reference item is >80% biodegraded in 14 days. Furthermore, SiO<sub>2</sub> as well as illite clay do not have a negative impact.



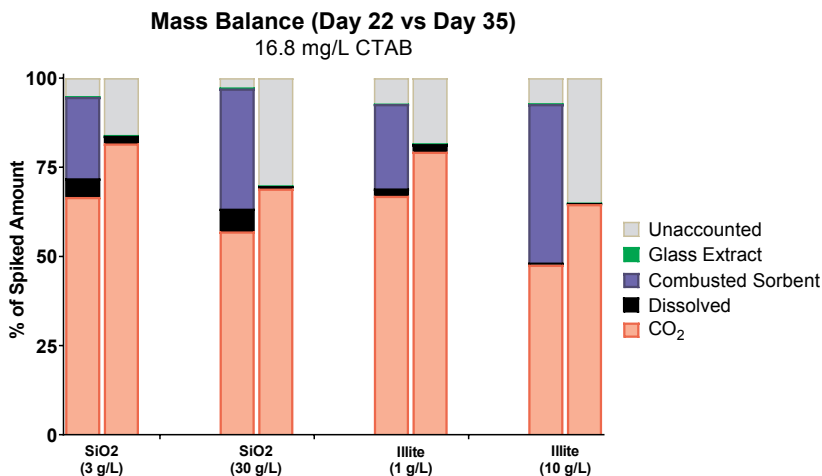
**Figure S3.** Biodegradation in the control without sorbent (28d Headspace test); biodegradation (%) is calculated by comparing radioactive  $\text{CO}_2$  with total applied radioactivity, and was fitted using a four parameter variable slope agonist/response model. CTAB satisfied the criteria for ready biodegradability. The high biodegradation of CTAB was somewhat unexpected based on the results of the 14d study of aniline degradation in the presence of CTAB.



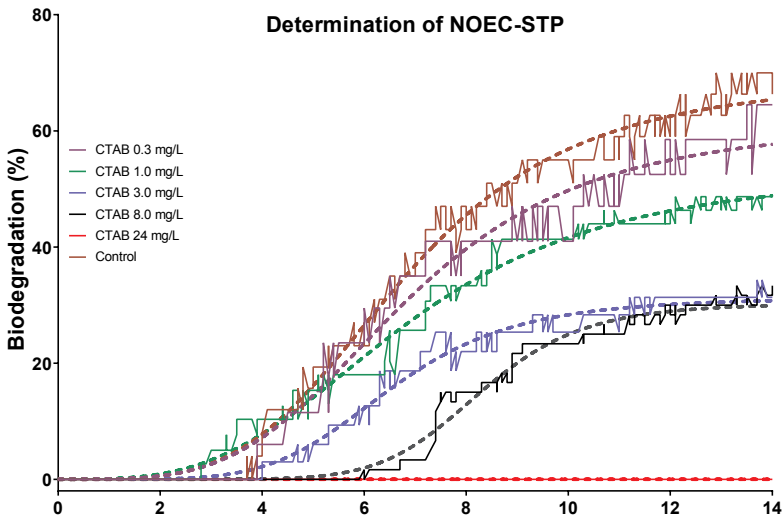
**Figure S4.** Comparison between low (light squares) and high (dark squares) concentration of  $\text{SiO}_2$ , showing that the initial rate of biodegradation is slightly lower with a tenfold higher amount of  $\text{SiO}_2$  added; biodegradation (%) is calculated by comparing radioactive  $\text{CO}_2$  with total applied radioactivity, and was fitted using a four parameter variable slope agonist/response model



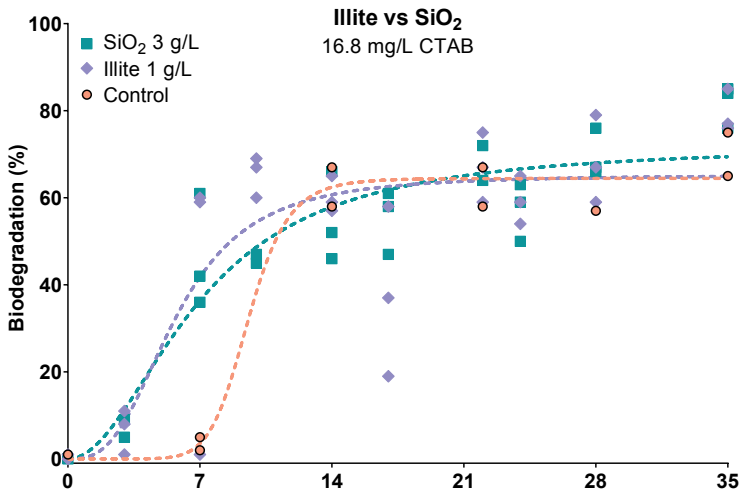
**Figure S5.** Comparison between low (light diamonds) and high (dark diamonds) concentration of illite clay; biodegradation profile is different and slower with a tenfold higher amount of illite clay added; biodegradation (%) is calculated by comparing radioactive  $\text{CO}_2$  with total applied radioactivity, and was fitted using a four parameter variable slope agonist/response model



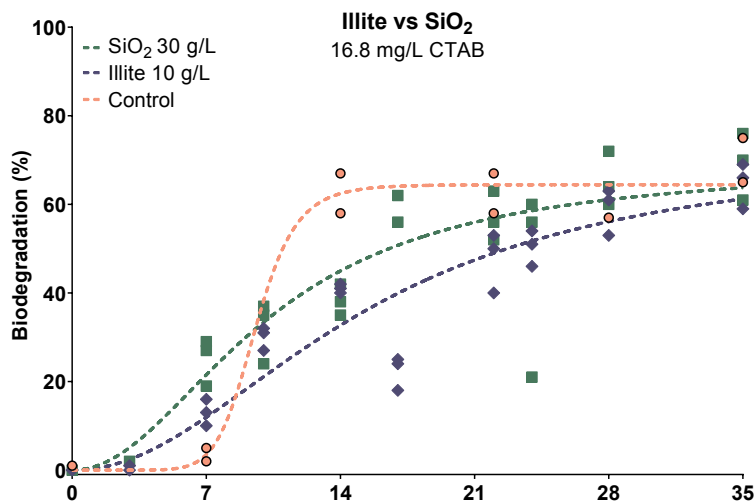
**Figure S6.** Comparison between mean mass balance on Day 22 (left bar) and on Day 35 (without combustion; right bar), to illustrate the increased  $\text{CO}_2$  production and decreased freely dissolved fraction. It is reasonable to assume sorbent combustion on Day 35 would have led to a mass balance of >90%.



**Figure S7.** Dotted lines are the plots as shown in Figure 6.1; continuous lines represent mean of raw measurements. Since 360 triplicate measurements were used for each concentration inclusion of all data points would create an undistinguishable graph.



**Figure S8.** Graph including the raw measurement data; dotted lines are the plots as shown in Figure 6.3.



**Figure S9.** Graph including the raw measurement data; dotted lines are the plots as shown in Figure 6.4.

**Table S1:** Glass vessels were extracted on each sampling day. Average sorption of CTAB to glassware is presented below; SD = standard deviation. The general trend is low glass binding (<1%) in vessels with sorbent. Measurements in the control without sorbent generally show higher glass binding, while measurements in the control without inoculum show a consistent increase in glass binding over the course of the experiment.

Day	No sorbent		SiO <sub>2</sub> (3 g/L)		SiO <sub>2</sub> (30 g/L)		Illite (1 g/L)		Illite (10 g/L)		No inoculum	
	Glass sorbed	SD	Glass sorbed	SD	Glass sorbed	SD	Glass sorbed	SD	Glass sorbed	SD	Glass sorbed	SD
0	2.0%	0.1	8.2%	2.4	1.3%	0.3	0.8%	0.3	0.5%	0.2	2.0%	0.1
3			1.2%	0.2	0.8%	0.2	3.0%	1.1	1.0%	0.6	2.9%	0.1
7	3.9%	0.2	0.6%	0.4	0.6%	0.2	0.5%	0.5	0.1%	0.0		
10			0.9%	0.1	0.5%	0.0	1.5%	0.3	0.6%	0.1	4.0%	1.1
14	0.9%	0.0	0.5%	0.1	0.3%	0.0	0.2%	0.0	0.1%	0.0		
17			0.5%	0.2	0.2%	0.0	0.1%	0.0	0.1%	0.1	4.5%	0.7
22	0.4%	0.0	0.3%	0.1	0.4%	0.2	0.2%	0.0	0.3%	0.2		
24			0.5%	0.1	0.3%	0.1	0.3%	0.1	0.1%	0.0	4.8%	0.3
28	5.2%	4.2	1.1%	0.6	1.3%	1.5	0.2%	0.1	0.1%	0.1		
35	2.2%	0.6	0.3%	0.0	0.2%	0.0	0.3%	0.0	0.1%	0.0	5.2%	0.2



# CHAPTER 7

---

## Sorbent-Modified Biodegradation Studies of the Biocidal Cationic Surfactant Cetylpyridinium Chloride

Niels Timmer,<sup>a</sup> David Gore,<sup>b</sup> David Sanders,<sup>b</sup>  
Todd Guoin,<sup>b</sup> Steven T.J. Droge<sup>a, c</sup>

<sup>a</sup>Institute for Risk Assessment Sciences, Utrecht University, Utrecht, 3508 TD, The Netherlands

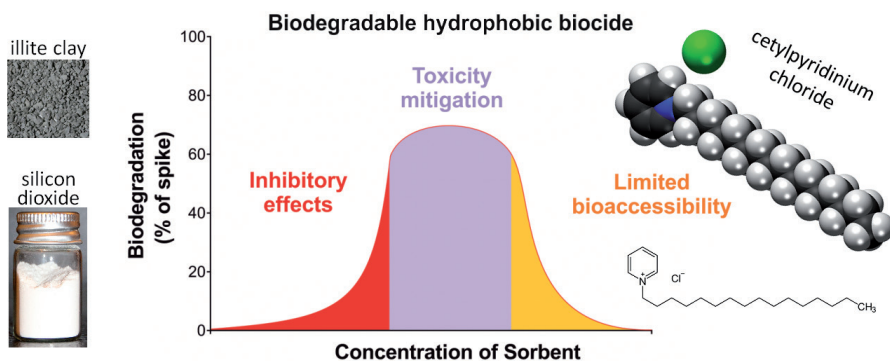
<sup>b</sup>Safety and Environmental Assurance Centre, Unilever, Colworth Science Park, Sharnbrook, MK44 1LQ,  
Bedfordshire, UK

<sup>c</sup>Department Freshwater and Marine Ecology, Institute for Biodiversity and Ecosystem Dynamics, University  
of Amsterdam, PO Box 94248, 1090 GE Amsterdam, The Netherlands

**Keywords:** Cationic Surfactant; Environmental Risk Assessment; Toxicity Mitigation;  
Ready Biodegradability Testing; Cetylpyridinium Chloride; Bioaccessibility

**Ecotoxicology and Environmental Safety, 182, #109417 (2019)**

## Graphical Abstract



## Abstract

Biodegradability studies for the cationic surfactant cetylpyridinium chloride (CPC) are hampered by inhibitory effects on inoculum at prescribed test concentrations (10–20 mg C/L). In this study, we used <sup>14</sup>C labeled CPC in the 28 d Headspace Test (OECD 310) and demonstrated that CPC was readily biodegradable (10–>60% mineralization within a 10 day window) at test concentrations 0.006–0.3 mg/L with CPC as single substrate. Biodegradation efficiency was comparable over this concentration range. CPC inhibited degradation at 1 mg/L and completely suppressed inoculum activity at 3 mg/L. In an extensive sorbent modified biodegradation study we evaluated the balance between CPC bioaccessibility and toxicity. A non-inhibitory concentration of 0.1 mg/L CPC was readily biodegradable with 83% sorbed to SiO<sub>2</sub>, while biodegradation was slower when 96% was sorbed. SiO<sub>2</sub> mitigated inhibitory effects of 1 mg/L CPC, reaching >60% biodegradation within 28 d; inhibitory effects were also mitigated by addition of commercial clay powder (illite) but this was primarily reflected by a reduced lag phase. At 10 mg/L CPC SiO<sub>2</sub> was still able to mitigate inhibitory effects, but bioaccessibility seemed limited as only 20% biodegradation was reached. Illite limited bioaccessibility more strongly and was not able to sustain biodegradation at 10 mg/L CPC.



## Introduction

Environmental risk assessment compares likely exposure scenarios with associated hazards. Assessment of the overall hazard profile of a chemical includes information on persistency, bioaccumulation potential and toxicity, combined with available information on actual environmental exposure levels. For most chemicals, persistency depends largely on microbial biodegradation rates ultimately resulting in full mineralization to inorganic carbon (IC) [320]. For many chemicals biodegradation by microbial communities present in sewage sludge is the major process to reduce environmental exposure levels. Measuring biodegradation is complicated for chemicals that are toxic to the inoculum at required testing levels [321], and for highly sorptive chemicals with insufficient bioaccessibility [322, 323]. Certain cationic surfactants combine these properties: relatively toxic to microorganisms, with several being used as biocides or antiseptics, and adsorptive properties due to favorable electrostatic and hydrophobic interactions with sorbents [24, 43, 324-327]. Specific microbial strains capable of metabolizing these surfactants have been identified [328].

Metabolites resulting from the primary degradation of most cationic surfactants can be identified using liquid chromatography/mass spectrometry on aqueous samples from a biodegradation study, but formation of metabolites provides limited evidence for complete mineralization potential. Therefore, most standardized biodegradation test methods aim to measure complete mineralization using e.g. standard IC analysis [140]. However, to generate IC levels significantly above inoculum background IC production, recommended test concentrations are 10-20 mg organic carbon/L ( $\text{mg}_C/\text{L}$ ) [139, 140]. For  $^{14}\text{C}$ -radiolabeled substrates, mineralization to  $^{14}\text{C-CO}_2$  can be detected at much lower ( $<1 \mu\text{g}/\text{L}$ ) and potentially non-inhibitory test concentrations, but labeled compounds are expensive and not readily available.

Recently, we evaluated biodegradability of the cationic surfactant cetyltrimethylammonium bromide (CTAB), spiking potentially inhibitory concentrations with introduction of mitigating adsorbents silicon dioxide ( $\text{SiO}_2$ ) and illite [329]. The concept of toxicity mitigation of CTAB while maintaining adequate bioaccessibility was also demonstrated in the OECD 310 ring test and other studies [140, 145, 146]. However, in our recent study there were indications that higher adsorbent doses limited bioaccessibility, reducing biodegradation efficiency [329]. This is in agreement with studies suggesting ultimate biodegradability of surfactants and polycyclic aromatic hydrocarbons is determined by desorption rates

[152, 330]. In the current study, we aimed to further elucidate the balance between toxicity, bioavailability and bioaccessibility using cetylpyridinium chloride (CPC). CPC is a common antiseptic, and is also used in various organoclay processes [331-334], and as a key component of ionic liquids [335, 336]; and detectable levels are present in the environment [337]. CPC has been widely studied: a search for literature with 'cetylpyridinium' as keyword in Scopus resulted in 4385 hits (March 2019). However, no studies on ready biodegradability of CPC were identified, although in a recent study Nguyen & Oh explored the removal by and impact on activated sludge of environmentally relevant levels of CPC [338]. Ready biodegradability of the structurally related surfactant benzalkonium chloride received more attention [154, 326, 339].

The first aim was to determine whether  $^{14}\text{C}$ -labeled CPC ( $^{14}\text{C}$ -CPC) was readily biodegradable (definition in Supporting Information) by sewage treatment plant (STP) inoculum in a standard 28 d Headspace Test [140]. Since ready biodegradability experiments are very stringent, compounds that pass will likely be degraded rapidly under environmental conditions. Hence, it is desirable for high production volume chemicals to be classified as readily biodegradable, as they will not be persistent. The second aim was to determine whether biodegradation efficiency with CPC as a single source of carbon had a threshold level in the non-inhibitory  $\mu\text{g/L}$  range [340, 341]. With the knowledge that CPC was toxic at concentrations below the recommended  $10\text{ mg}_\text{C}/\text{L}$  spiking level, we then explored biodegradation efficiency enhancement of a mixture of labelled and non-labelled surfactant through addition of sorbent. Based on the premise that increased sorbent levels reduce bioavailable concentrations, we also aimed to define under which conditions bioaccessibility could become rate limiting. Systematic series of biodegradation studies were performed with addition of two inert inorganic sorbents ( $\text{SiO}_2$  and illite) at different surfactant spiking levels (non-inhibitory, inhibitory,  $\sim 10\text{ mg}_\text{C}/\text{L}$ ). This should clarify whether a biodegradation study following a stepwise sorbent addition approach (determine inhibitory threshold concentration, sorption studies, perform sorbent modified biodegradation test) has applicability boundaries or is applicable to multiple potentially inhibitory cationics. It should be noted that the methods proposed were specifically designed to remain within the boundaries of OECD Guidelines. Ultimately, this should lead to a defensible decision regarding biodegradability of surfactants under more realistic field conditions where sorptive substrates are available, e.g. sand and sludge itself in a STP, contaminated sediment, or soil on which sewage sludge is applied. In addition, it would be more relevant to employ test item concentrations close to the predicted environmental

concentration; recommended test concentrations are generally unrealistically high and proposed matrices lack sorptive substrates.

## Materials and Methods

### Chemicals and Sorbents

CPC ( $M_w$  340 g/mol), sodium benzoate (reference substrate), silicon dioxide ( $\text{SiO}_2$ ; Davisil Grade 633, particle size 35-75  $\mu\text{m}$ , surface area 480  $\text{m}^2/\text{g}$ ), and buffer salts were analytical grade and obtained from Sigma-Aldrich (Gillingham, Dorset, UK). Illite (fine powder; Argiletz, France), was comparable as in related sorption studies with surfactants [177, 342]. Potassium hydroxide (KOH), sodium hydroxide (NaOH), sulfuric acid ( $\text{H}_2\text{SO}_4$ ) and trifluoroacetic acid (TFA) were analytical grade (Sigma-Aldrich). Scintillation cocktails (Hionic-Fluor, Pico-Fluor Plus, Permafluor E+), Carbosorb, and combustion cones for the sample oxidizer (Packard Model 307) were purchased from PerkinElmer (Seer Green, Beaconsfield, UK).

$^{14}\text{C}$ -CPC was obtained from Quotient Bioresearch Ltd. (Cardiff, UK); the molecule contained two  $^{14}\text{C}$  atoms within the pyridinium, which is likely the last moiety to be biodegraded. Radiochemical purity was 99.8% (Radio-HPLC). A 20.62 mg/L  $^{14}\text{C}$ -CPC stock solution was prepared in acetone; concentration was confirmed by LSC (TriCarb 2810TR, PerkinElmer). Higher concentrations were prepared by supplementing with unlabeled CPC; formation of  $^{14}\text{C}\text{-CO}_2$  is a proxy for total mineralization.

### Inoculum

Activated sludge was obtained from Broadholme Sewage Treatment Works (BSTW; Ditchford Road, Wellingborough & Irthingborough, UK). The BSTW treats sewage from approximately 80,000 households and <15% of the organic load is attributable to industrial discharge [315]. Sludge was treated as described previously [329]. Suspended solids concentration of activated sludge was  $5\pm 1$  g/L; filtered supernatant after centrifugation was used as inoculum.

## Sorption Test

Three doses of illite and SiO<sub>2</sub> (0.80, 4.0 and 20 g/L) were exposed to three concentrations of <sup>14</sup>C-CPC (13.5 mg/L, 1.35 mg/L, and 135 µg/L) in 20 mL borosilicate vials (PerkinElmer), and placed overnight on a roller mixer at 30 rpm (Thermo Fisher Scientific, Waltham, MA, USA), at room temperature. Control vials without sorbent were also prepared. All vials were centrifuged at 2,400 g for 30 min, followed by visual inspection for absence of suspended particles and sampling of three 2 mL aliquots of supernatant. Kerr et al. successfully applied centrifugation combined with LSC to determine sorption coefficients using radiolabeled cationic surfactants of comparable alkyl chain length (CTAB), sorbed to activated sludge [343]. Concentration of <sup>14</sup>C-CPC was determined by LSC, followed by calculation of sorbed amounts by assuming 100% - supernatant = sorbed amount; possible sorption to glassware was disregarded as affinity for sorbent is theoretically much higher and the aim was to provide an estimated sorption coefficient. Measurements were used to fit linear sorption isotherms and calculate sorption coefficients.

## Preparation of Headspace Test

The OECD 310 Guideline was used to design the biodegradation experiments performed [140], as outlined in more detail in the Supporting Information. In brief, <sup>14</sup>C-CPC was added to 50 mL mineral medium in 125 mL borosilicate glass serum bottles containing appropriate amounts of sorbent. Vessels were left standing for 2 h to allow CPC to equilibrate between medium and sorbent. Thereafter, 50 mL of mineral medium containing 20 mL/L of inoculum was added to all test vessels, resulting in a 64 mL headspace and an inoculum concentration of 10 mL/L. Vessels were incubated under orbital shaking (100 rpm) in HT Multitron incubators (Infors AG, Bottmingen, Switzerland) at 22.0±1.0 °C.

Sodium benzoate (C<sub>7</sub>H<sub>5</sub>O<sub>2</sub>.Na) was used as reference substrate at a concentration of 17 mg/L, corresponding with ~10 mg<sub>C</sub>/L. After incubation bottles were injected with 1 mL 7 M NaOH and shaken for 60 min, after which contents of each bottle were divided over three 20 mL vials. Benzoate biodegradation was quantified by triplicate IC measurements on a TOC-V total organic carbon analyzer (Shimadzu Ltd., Milton Keynes, UK). IC in blanks was subtracted from IC in test vessels to control for background IC production. Biodegradation was determined by comparing IC production with organic carbon in the spiked concentration.

## Biodegradation Studies without Sorbent

Six  $^{14}\text{C}$ -CPC concentrations (6.0-3,000  $\mu\text{g/L}$ ) were tested without sorbent to assess influence of freely dissolved concentration ( $C_{\text{free}}$ ) on biodegradability. This also allowed determination of a non-inhibitory effect concentration for STP inoculum (NIEC-STP). Three concentrations (6, 25, and 300  $\mu\text{g/L}$ ) were sampled at seven time points (see Table S1), which was sufficient to assess kinetics and presence of inhibitory effects. Ten and eight time points (see Table S1) were prepared in duplicate for 100  $\mu\text{g/L}$  and 1.0  $\text{mg/L}$ , respectively. These concentrations were tested in more detail since they were the nominal concentrations to be added in the experiments with sorbent. Based on inconclusive replicates at high test concentrations in previous work [329] and the expectation of full inoculum knockout at 3  $\text{mg/L}$ , twelve replicates were prepared to be sampled on Day 28. Upon sacrificial sampling, vessels were injected with 1 mL of 7 M NaOH and further treated as described previously.

## Biodegradation Studies with Sorbent

For sorbent modified biodegradation series two different sorbents were used ( $\text{SiO}_2$  and illite) at doses of 0.8, 4.0 and 20  $\text{g/L}$ . Only  $\text{SiO}_2$  was employed at 100  $\mu\text{g/L}$  CPC, as  $\text{SiO}_2$  was the chosen sorbent in literature [145, 146]. For the 1  $\text{mg/L}$  CPC treatment both sorbents were applied to assess suitability of illite and to allow comparison with  $\text{SiO}_2$  at this inhibitory concentration. At 10  $\text{mg/L}$  CPC only the highest sorbent dose was tested, based on sorption coefficients and expected NIEC-STP. Before sampling, designated vessels were injected with 1 mL of 7 M NaOH and further treated as described previously. Benzoate controls were incubated at three concentrations of  $\text{SiO}_2$  to evaluate sorbent effects on inoculum activity; due to a significant IC content (1.7%) illite was not suitable for use with standard IC analysis and could not be tested with benzoate.

## Detection and Analysis of $^{14}\text{C}$ -CPC

After shaking with NaOH (60 min), vessels were left standing for 5 min to settle suspended sorbent. Six 3 mL aliquots were sampled; 1 mL of 4 M  $\text{H}_2\text{SO}_4$  (sulfuric acid) was added to three aliquots. These acidified samples were left uncapped in a fume hood overnight to vent off  $\text{CO}_2$ . Mineralization, calculated from the difference between alkaline (containing  $^{14}\text{CO}_2$ ) and acidified (without  $^{14}\text{CO}_2$ ) samples, was then compared with applied radioactivity to calculate biodegradation percentages.  $^{14}\text{C}$ -CPC potentially sorbed to the glass surface was extracted. Vessels were emptied after sampling, while shaken vigorously if necessary

to re-suspend and pour out residual sorbent. Vessels still containing visible amounts of sorbent were quickly rinsed twice with 5 mL MilliQ. A 5 mL aliquot of washing solution (0.1% TFA in 90/10 MeOH/MilliQ v/v) was added, after which vessels were capped and put on a roller mixer (Thermo Fisher Scientific) at 30 rpm for 150 min. This extract was collected in a 20 mL liquid scintillation vial. All samples were prepared for LSC by adding 16 mL of Hionic-Fluor followed by forceful shaking for 5 seconds.

## **Mass Balance**

The contents of all Day 7 vessels without sorbent (0.1, 1.0 and 10 mg/L CPC) were filtered under vacuum using 100 mm Whatman GF/C filters. This was repeated for all vessels sampled on Day 28. Sorbent was flushed onto the filter by rinsing vessels twice with 5 mL MilliQ. Filters were carefully placed on marked pieces of aluminum foil, which were left overnight in a fume hood to dry and were subsequently analyzed by combustion. Filter residue was distributed over multiple cellulose combustion cones, after which the emptied filters were divided over two combustion cones. Shortly before combustion the contents of every combustion cone were enriched with 100  $\mu$ L analytical grade hexadecane to increase combustion temperature and efficiency. CO<sub>2</sub> formed during combustion was trapped in ~5 mL Carbo-Sorb E, which was mixed with 7 mL Permafluor E+ and 8 mL Pico-Fluor to prevent quenching, which was observed during a trial run and was likely caused by soot particles in the samples. LSC measurements of alkaline samples, glass extracts, and combusted samples were used to determine the mass balance; control vessels without inoculum served as 100% reference.

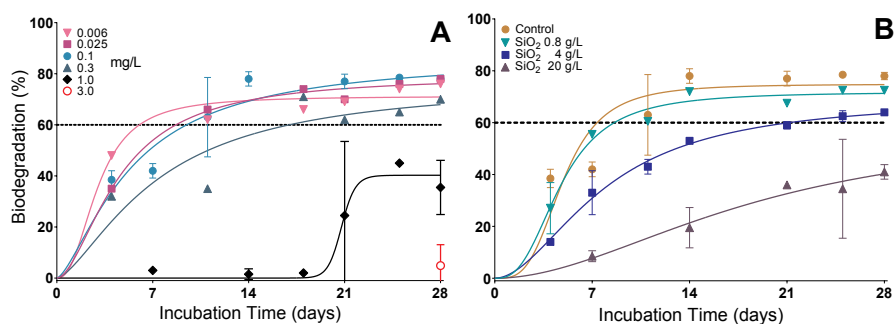
## **Statistics**

Curves presenting biodegradation results were fitted using the '[Agonist] vs. response – Variable slope (four parameters)' model included with GraphPad Prism 7.04 for Windows.

## Results and Discussion

### Biodegradation Studies without Sorbent

BSTW inoculum was shown to be of adequate activity using a positive control with benzoate. Results after 4 d and 7 d of incubation indicate >80% biodegradation in all vessels (Figure S1). This confirms that SiO<sub>2</sub> has no negative impact on inoculum activity. Rapid biodegradation without apparent lag phase was observed for the three lowest CPC concentrations (Figure 7.1), reaching >30% biodegradation after 4 d, >60% biodegradation within 10 d, and a maximum biodegradation of 70–80%, satisfying the criteria for ready biodegradability. Biodegradation at 300 µg/L was slightly slower and failed to meet the criteria for ready biodegradability, although >60% biodegradation was reached after 18 d. Larger differences in biodegradation efficiency became apparent at 1 mg/L, with a three-week lag phase and some inconsistency between replicates in further measurements, especially on Day 21. At 1 mg/L, an average biodegradation of 40% was reached after 25 d. Only two of the twelve 3 mg/L replicates showed >5% biodegradation after 28 d. This not only reflects the strong inhibitory effect of CPC at this concentration, but simultaneously illustrates that results obtained in this kind of biodegradability experiments can be variable. Even at inhibitory test item concentrations significant biodegradation can occasionally occur in individual replicates.

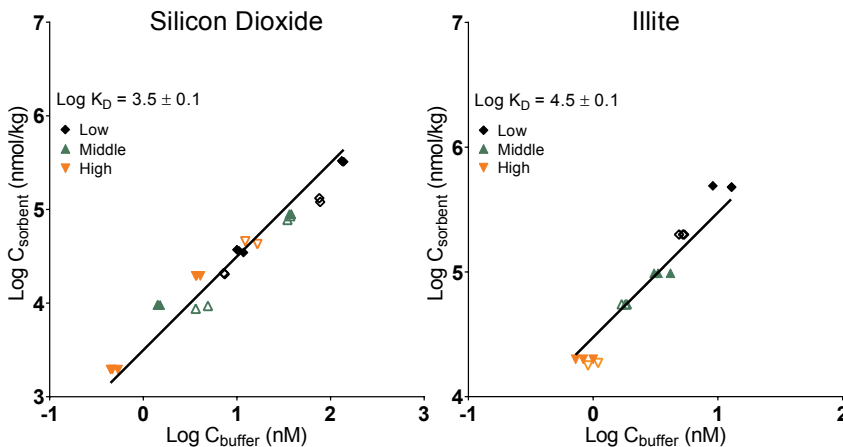


**Figure 7.1.** (A) CPC biodegradation without sorbent. Single replicates for 6, 25, and 300 µg/L. Duplicates for 0.1 and 1 mg/L (averages + error bars). Twelve 3 mg/L replicates were sampled after 28 d. (B) Influence of SiO<sub>2</sub> on biodegradation at non-inhibitory CPC concentration (0.1 mg/L).

Overall, results indicate CPC induced inoculum inhibition at 1 mg/L with partial recovery in the fourth week. There is complete inoculum knock-out at 3 mg/L, while signs of inhibition were already apparent at 300  $\mu\text{g/L}$ . The NIEC-STP of CPC was 100  $\mu\text{g/L}$ , at least 100 times lower than recommended concentrations in most ready biodegradability studies [139, 140]. Inconsistent replicates in 1 and 3 mg/L groups are likely caused by inoculum heterogeneity and variability in developmental rate of micro-organisms capable of degrading CPC. Optimal toxicity mitigation can be achieved by assessing the NIEC-STP, as this allows estimating the amount of sorbent needed to reduce freely dissolved concentrations ( $C_{\text{free}}$ ) to non-inhibitory levels, especially if data on sorbent affinity is available or determined experimentally.

### Sorption Coefficients

Isotherms for sorption of CPC to  $\text{SiO}_2$  and illite were plotted with a fixed slope of 1 (Figure 7.2), as sorption is expected to be linear at concentrations well below the cation-exchange capacity (CEC) [177, 285, 344]. Two independent experiments using  $\text{SiO}_2$  were in good agreement; the fitted curve indicates a  $\log K_D$  of 3.5 and spans two orders of magnitude, with highest concentration (47  $\mu\text{g/L}$ ) close to the NIEC-STP (100  $\mu\text{g/L}$ ). Although used concentrations were sometimes above this concentration range the  $K_D$  can still be used to predict  $C_{\text{free}}$  as previous work with a surfactant of comparable alkyl chain length (CTAB) demonstrated linear sorption up to 1 mg/L, using the same batch of  $\text{SiO}_2$  ( $\log K_D$  3.3) [329].



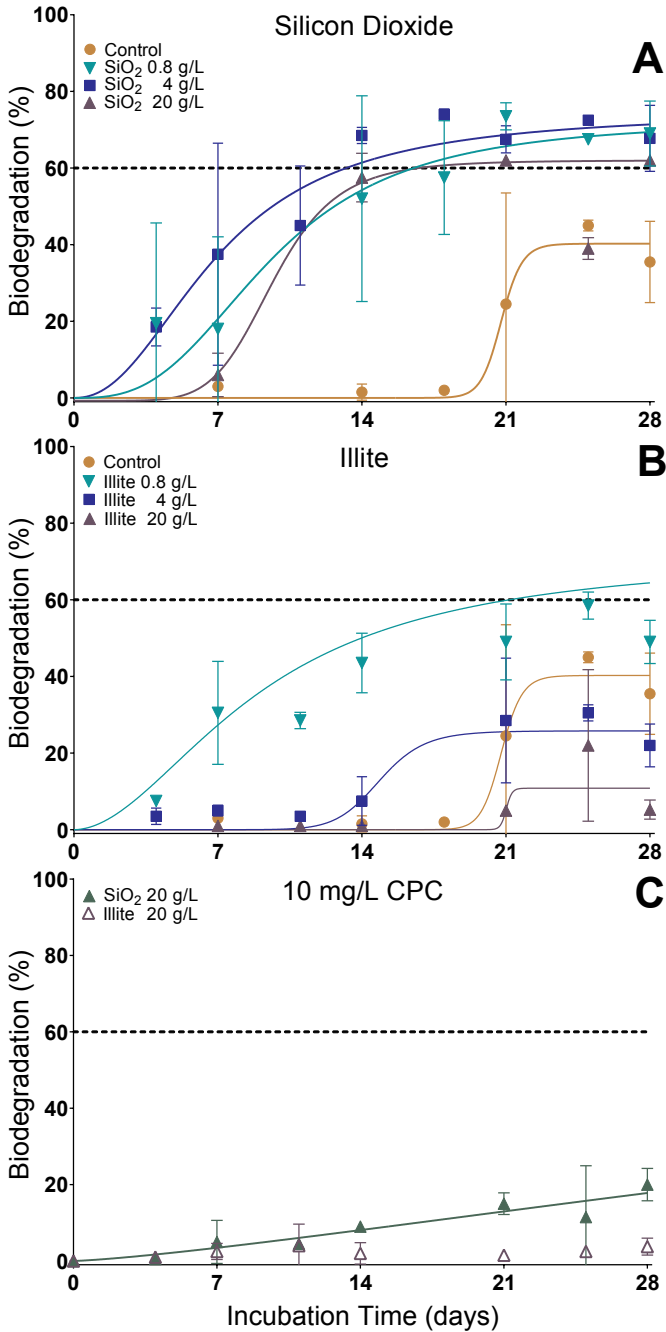
**Figure 7.2.** Isotherms for CPC sorption to  $\text{SiO}_2$  (left) and illite (right). Symbols correspond with associated sorbent dosages and distinguish between a first (open symbols) and second (closed symbols) measurement series.



The isotherm for illite covered a 20-fold concentration range, with highest concentration a factor 20 below the NIEC-STP and ~500 times lower than the reported CEC of 288 mmol/kg [345]. The calculated  $\log K_D$  of 4.5 was used as a representative sorption affinity; establishing a sorption isotherm encompassing all test concentrations was not within the scope of our work. Furthermore, this experimentally determined  $K_D$  (mineral medium; pH 7.4; divalent cation concentration ~0.1 mM  $Mg^{2+}$ ) was in agreement with predicted  $K_D$  ( $\log 4.18$ ) based on a cation-exchange model for  $C_xH_yN^+$  amines as derived by Droge & Goss (pH 7; medium with 5 mM  $Ca^{2+}$ ) [176]. Measurements of actual  $C_{free}$  on Day 0 were used to estimate initially sorbed fractions in the biodegradation study. Figure S2 compares measurements with predictions based on experimentally determined  $K_D$ , and shows these are in good agreement for 1 mg/L groups and at the two highest sorbent dosages in particular.

### Bioaccessibility and Biodegradability with Sorbent

At 0.1 mg/L CPC was readily biodegradable without sorbent, as well as with the lowest sorbent dose at which ~83% was initially adsorbed (Figure 7.1B). Interestingly, biodegradation rates seemed to decrease with increasing sorbent concentration. At 4 g/L (sorbed fraction ~88%) biodegradation was slower and reached 60% after 21 d. At 20 g/L (sorbed fraction ~96%;  $C_{free}$  ~4  $\mu g/L$ ) biodegradation slowed down further and total mineralization after 28 d was half of control, while  $C_{free}$  in these vessels was comparable to the lowest concentration without sorbent, which showed rapid and extensive biodegradation (Figure 7.1A). However, nominal amount of CPC in these vessels was 17 times higher. This supports the notion of bioaccessibility limitations, with highest  $SiO_2$  dose associated with lowest bioaccessibility. Availability of carbon (in the form of CPC) is apparently sufficient to maintain degrading microorganisms, but might be insufficient to allow for the exponential growth necessary to degrade all CPC within 28 d.



**Figure 7.3.** Influence of SiO<sub>2</sub> (A) and illite (B) on biodegradation at inhibitory CPC concentration (1 mg/L). Influence of both sorbents on biodegradation at 10 mg/L CPC (C); measured  $C_{\text{free}}$  was <0.1 mg/L, which should not be inhibitory to the inoculum.

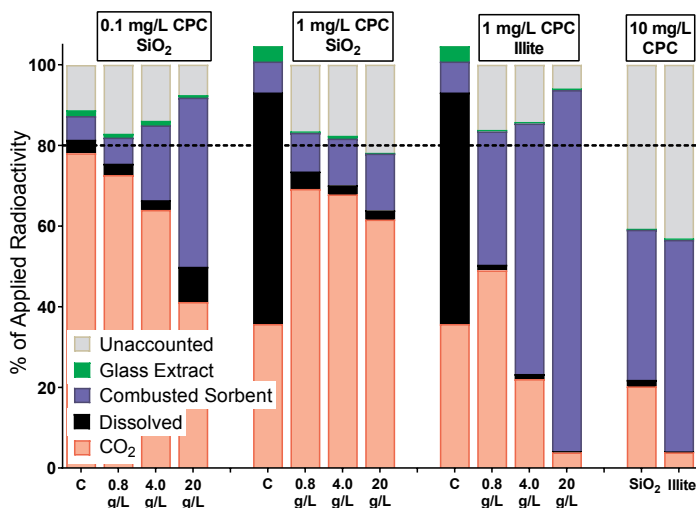
Results observed with 1 mg/L CPC were different than those obtained with 0.1 mg/L CPC. As discussed previously, controls without sorbent showed a three-week lag phase (Figures 7.1A, 7.3A and 7.3B), indicating inhibitory effects. This lag phase was strongly reduced with SiO<sub>2</sub> as mitigating sorbent. All three SiO<sub>2</sub> doses show comparable results during the last two weeks of the experiment (Figure 7.3A), with 60-70% of CPC mineralized. Apparently, at these concentrations CPC was sufficiently bioaccessible to allow exponential growth of CPC-degrading microorganisms. The delayed onset of biodegradation at 20 g/L SiO<sub>2</sub> is indicative of lower bioaccessibility initially impairing exponential growth. During the first three weeks a number of replicates at 0.8 g/L showed lower biodegradation. This suggests inhibitory effects still might occur at relatively high C<sub>free</sub> associated with the lowest sorbent concentration (sorbed fraction ~85%, reducing C<sub>free</sub> to 150 µg/L, a factor 1.5 above the NIEC-STP). Overall, these results support the hypothesis that SiO<sub>2</sub> is a suitable sorbent to mitigate inhibitory effects of CPC, although at a concentration below the 10-20 mg<sub>c</sub>/L recommended for IC analysis.

As shown in Figure 7.3B, results with illite differed from those discussed for SiO<sub>2</sub>. Highest biodegradation levels were observed at the lowest sorbent concentration (adsorbed fraction ~93%), with decreasing biodegradation for increasing sorbent concentrations. While equal doses of illite and SiO<sub>2</sub> had been used, C<sub>free</sub> will be significantly lower because of the 10 times higher sorption affinity to illite (Figure 7.2). However, despite – or perhaps because of – lower bioavailable concentrations in the illite treatments, none of the illite dosed groups reached >60% biodegradation. Thus, addition of illite did not result in a readily biodegradable classification. On average, the highest illite dose (>99.6% adsorbed) showed ~10% mineralization after 28 d, six times lower than the respective SiO<sub>2</sub> treatment.

In the 10 mg/L CPC treatment, in line with Guideline recommendations of 10 mg<sub>c</sub>/L [139, 140], sorbents were tested only at 20 g/L, as this high CPC concentration requires considerable sorptive capacity to decrease C<sub>free</sub> below the NIEC-STP. Measurements on Day 0 (Figure S2) confirmed that C<sub>free</sub> was below the NIEC-STP. As shown in Figure 7.3C, addition of SiO<sub>2</sub> results in linear biodegradation with a relatively short lag phase, but at a seemingly slow rate compared to the 20 g/L dose at 1 mg/L CPC. However, converted to absolute amount of CPC (Figure S5) approximately four times more has been mineralized at 10 mg/L than at 1 mg/L. Results for illite show virtually no biodegradation over the 28 d period. Since inhibitory effects can be ruled out based on C<sub>free</sub> of <100 µg/L, this supports the bioaccessibility hypothesis.

Limited biodegradation at high CPC concentrations with high adsorbed fractions indicates microbes might not degrade sorbed fractions directly, and require release to the aqueous phase for sustenance and exponential growth [340]. It appears that desorption and subsequent diffusion can be rate-limiting, whereby influx of chemical substrate is insufficient to act as the sole carbon source during exponential growth. Similar findings were reported by Scow & Alexander for decreased biodegradation kinetics of phenol by *Pseudomonas* in the presence of spherical kaolinite aggregates, where microbes were considered to have limited access to substrate aggregates [346]. Such findings could be explained by a diffusion-sorption-biodegradation (DSB) model [346-348]. Ugochukwu et al. demonstrated limited substrate bioaccessibility caused by strong sorption/limited desorption were using organoclay and other clay additions to influence biodegradation rate of crude oil hydrocarbons [349, 350], and Smith et al. found that quinoline sorbed to smectite was degraded 30 times slower than dissolved quinoline [351]. Future studies could consider accurate desorption or diffusion rate measurements combined with qualitative and quantitative measurements of inoculum microorganism development, in order to fit experimental data to such DSB models.

Based on a lower degradation rate at 10 mg/L CPC compared to 1 mg/L CPC with similar sorbent doses, it can be argued that the flux micro-organisms can handle optimally has a (Michaelis-Menten) maximum, a notion supported by Lo et al. in their *in vitro* research using rainbow trout liver enzymes [352]. Micelle formation can be ruled out, as the highest CPC concentration applied is still a factor 40 below the critical micelle concentration (~370 mg/L) [198]. Compared to porous and rapidly settling SiO<sub>2</sub> particles, which were observed to partially form a gel-like precipitate, it was expected that the flat (non-expanding) platelet structure and suspensibility of illite would facilitate desorption, thereby enhancing bioaccessibility. Contrastingly, our findings indicate SiO<sub>2</sub> bioaccessibility outperformed that of illite. We currently do not have clear explanations for this difference, although illite sedimentation was observed at high sorbent loadings. We hypothesize, though, that the porous SiO<sub>2</sub> structure could facilitate microbial growth near pores [353], providing benefits from nanoscale distances over which desorption allows for acquiring CPC as carbon substrate, although Johnsen et al. suggest a minimum pore size of 200 nm for microbial colonization [354].



**Figure 7.4.** Day 28 mass balance. 0.1 mg/L CPC at three SiO<sub>2</sub> doses; 1 mg/L CPC at three SiO<sub>2</sub> doses; 1 mg/L CPC at three illite doses; 10 mg/L CPC with 20 g/L of both sorbents. Combusted sorbent fraction might also contain <sup>14</sup>C assimilated by biomass (C = control).

## Mass Balance

Controls without inoculum were used as 100% reference to calculate a mass balance for Day 7 (Figure S3) and Day 28 (Figure 7.4). Mass balance for 0.1 mg/L CPC on Day 7 is 103%, with 3.5% glass-bound and 42% mineralized. Biodegradation on Day 7 in the 1.0 mg/L treatment is 3.0% and indicative of inoculum inhibition (see Figure 7.1B), while a high (>90%) mass balance was retrieved. Mass balance after 28 d was >80% (replicate average), except for the 10 mg/L CPC groups (~60%). The poor mass balance in the 10 mg/L group is likely caused by incomplete recovery during sorbent combustion. Fraction of dissolved organic <sup>14</sup>C (CPC and/or metabolites) for sorbent additions ranged between 0.2% (10 mg/L CPC with 20 g/L illite) and 8.8% (0.1 mg/L CPC with 20 g/L SiO<sub>2</sub>). At 1.0 mg/L CPC, dissolved fraction decreases with increasing sorbent concentration. The dissolved fraction is 2-8 times lower in illite vessels, demonstrating the 10 times higher sorption coefficient. Glass wall extracts are insignificant, except for vessels without sorbent which have a higher  $C_{free}$ .

Combustion of filter residue at 0.1 mg/L CPC retrieved 6-42% of applied radioactivity, which is likely partially due to assimilation of <sup>14</sup>C into biomass. Although this fraction might still contain adsorbed radioactivity, particularly for the 20g/L dose, this is not necessarily solely non-metabolized <sup>14</sup>C-CPC. Results were more variable within 1 mg/L CPC treatments,

especially for filter residues and CO<sub>2</sub> determination. Nevertheless, C<sub>free</sub> (or rather dissolved organic <sup>14</sup>C) was higher than in the 0.1 mg/L group (8.8-30.1 µg/L vs. 4.4 µg/L). Different vessels with SiO<sub>2</sub> had comparable fractions in filter residue and mineralized to CO<sub>2</sub>. This might be an indication that radioactivity in filter residue consists primarily of assimilated <sup>14</sup>C. For vessels with illite, filter residue increased with sorbent dose, and most likely indicates presence of <sup>14</sup>C-CPC and partially metabolized <sup>14</sup>C-CPC. Overall mass balance was 83.8-93.7% for illite treated groups at 1.0 mg/L CPC.

### **Toxicity Mitigation Assessment**

Toxicity is caused by exposure of an actual target site to a chemical, which is mechanistically closely related to C<sub>free</sub> [286, 355, 356]. Therefore, the potential for toxicity mitigation is logically expressed by evaluating how sorbents influence C<sub>free</sub>. During the biodegradation experiments, fractions in acidified samples were closely related to C<sub>free</sub> because inorganic <sup>14</sup>C was vented off as CO<sub>2</sub>. As shown in Figure S4, there is a clear relationship between C<sub>free</sub> and sorbent concentration for 0.1 and 1 mg/L CPC treatments. Highest C<sub>free</sub> was observed in controls, while increasing sorbent concentrations lead to incrementally decreased C<sub>free</sub>. Lower C<sub>free</sub> for illite spiked with identical CPC concentration as SiO<sub>2</sub> was supported by the higher sorption coefficient. Comparison between illite and SiO<sub>2</sub> in the 10 mg/L group further confirms this, as C<sub>free</sub> is consistently lower in vessels with illite.

A distinct influence of incubation time was also observed. C<sub>free</sub> increases notably for most groups after 4 to 7 days. Day 0 samples are within range of expectations based on the sorption test, so C<sub>free</sub> increases by Day 4 may relate to the formation of less sorptive <sup>14</sup>C-CPC metabolites. Following the initially increasing C<sub>free</sub> a gradual decrease of C<sub>free</sub> was observed, indicative of ultimate mineralization. Higher amounts of sorbent are more likely to release a continuous flux, which would translate to gradually decreasing C<sub>free</sub> under the assumption of steady-state biodegradation. The 0.1 mg/L data is a straightforward illustration of this effect, showing rapid decrease in control group, somewhat slower decrease at low sorbent concentration, while C<sub>free</sub> remains relatively constant at 20 g/L. For 0.1 and 1 mg/L CPC treatments with SiO<sub>2</sub>, there is overlap between C<sub>free</sub> reaching a minimum (Figure S4) and biodegradation reaching plateau (Figures 7.1B and 7.3A). This correlation is lacking for illite, which supports the hypothesis that bioaccessibility is limited by desorption kinetics.

## Classification of CPC Biodegradability with Different Test Modifications

No reduction in biodegradation efficiency was observed with CPC as sole carbon source for concentrations as low as 6  $\mu\text{g/L}$ . Table 7.1 provides an overview of biodegradability results discussed in this section. Inhibitory effect of 1 mg/L CPC could be mitigated by appropriate doses of  $\text{SiO}_2$ , rendering CPC to satisfy Guideline criteria for ready biodegradability [140]. These results carry significant environmental relevance, as CPC and other pyridinium-based surfactants are a key component in various organoclays and ionic liquids [331-336], while several authors highlight the limited biodegradability and potential toxicity [357-359].

It was unexpected that, while illite reduced  $C_{\text{free}}$  from 1 mg/L to below the NIEC-STP, bioaccessibility was apparently too low to reach ready biodegradability. At 3 mg/L, CPC was found to be toxic to STP inoculum, but a nominal CPC concentration of 10 mg/L could be reduced to below NIEC-STP using  $\text{SiO}_2$  and illite. Although more CPC was actually mineralized than in the 1 mg/L treatment, the highly sorbed fractions were not adequately bioaccessible within the experimental time frame of 28 days. Lower dosing of a stronger adsorbent is thus not a universal solution to mitigate inhibitory effects when testing biodegradability of non-labeled compounds.

The balance between toxicity mitigation and bioaccessibility would probably need to come from combining a sufficiently high adsorbed fraction with adequate desorption kinetics. Most likely, this can be achieved in the form of a higher dose of a sorbent that would still allow for high mobility of microbes, but sorbs weaker ( $K_d < 1000 \text{ L/kg}$ ) than the porous  $\text{SiO}_2$  we applied. It should be noted that a concentration of 10 mg/L CPC is unrealistically high from an environmental perspective [337]. The sorbents used resemble sorbing surfaces encountered in the environment, e.g. by sewage en route to the STP, while undergoing processing at the STP, and in sewage sludge itself e.g. when applied as fertilizer. Addition of inorganic sorbents is, therefore, not only a means to mitigate potential inhibitory effects but also serves to decrease  $C_{\text{free}}$  to predicted environmental levels, increasing relevance of test results. This is supported by findings such as those by Nguyen & Oh, who found approximately 50-80% sorption to activated sludge at environmentally relevant concentrations [338]. Related surfactants such as benzalkonium are also known to have strong sorption to activated sludge [360].

**Table 7.1.** Biodegradability classification of CPC at multiple test and sorbent concentrations.

Sorbent	Sorbent Dose	CPC Concentration	Classification <sup>1</sup>	Remarks
No sorbent	-	0.006 mg/L	Readily biodegradable	No lag phase; <7 d to reach 60%
	-	0.025 mg/L	Readily biodegradable	No lag phase; <9 d to reach 60%
	-	0.1 mg/L	Readily biodegradable	No lag phase; 10 d to reach 60%
	-	0.3 mg/L	Inherently biodegradable	No lag phase; 17 d to reach 60%
	-	1.0 mg/L	Inherently biodegradable	Lag phase 18 d; does not reach 60%
	-	3.0 mg/L	Slowly biodegradable	Does not reach >10%
Silicon dioxide	0.8 g/L		Readily biodegradable	No lag phase; <9 d to reach 60%
	4.0 g/L	0.1 mg/L	Inherently biodegradable	No lag phase; 21 d to reach 60%
	20 g/L		Inherently biodegradable	Lag phase ~3 d; does not reach 60%
	0.8 g/L		Inherently biodegradable	Lag phase ~2 d; 17 d to reach 60%
	4.0 g/L	1.0 mg/L	Readily biodegradable	No lag phase; 13 d to reach 60%
	20 g/L		Readily biodegradable	Lag phase ~5 d; 17 d to reach 60%
Illite	20 g/L	10 mg/L	Inherently biodegradable	No lag phase; does not reach 60%
	0.8 g/L		Inherently biodegradable	No lag phase; 28 d to reach 60%
	4.0 g/L	1.0 mg/L	Inherently biodegradable	Lag phase 12 d; does not reach 60%
	20 g/L		Slowly biodegradable	Lag phase 21 d; does not reach 60%
	20 g/L	10 mg/L	Slowly biodegradable	Lag phase unclear; does not reach 60%

<sup>1</sup>Classifications 'readily biodegradable' and 'inherently biodegradable' do not imply Guideline criteria are met definitively, but indicate results provide support for such classification.

Taking into account *in situ* sorption effects, CPC will under most circumstances be degradable by microorganisms at a certain rate. The question remains how this contributes to or counteracts the degree of persistency of cationic surfactants, should desorption kinetics indeed hamper rapid biodegradation. Bergero & Lucchesi explored the biodegradability of cationic surfactant sorbed to sterilized activated sludge after addition of specifically selected micro-organisms, and found 90% biodegradation within 24 hours [361]. Furthermore, biodegradability of numerous ammonium-based cationic surfactants has been evaluated in surface water, sediment, sludge, and sludge-amended soil. Findings indicate relatively good degradability of sorbed surfactants, although some types can be persistent under anaerobic conditions [36, 362]. Biodegradability classification can have significant environmental and commercial implications, and high amounts of resources are invested in biodegradability experiments. Therefore, we should progress towards more realistic testing methodology to obtain the most environmentally relevant results.



## **Acknowledgements**

We thank Joop L.M. Hermens (Utrecht University) and Geoff Hodges (Unilever) for fruitful discussions and valuable suggestions regarding this work.

## **Abbreviations**

CEC, cation exchange capacity; CPC, cetylpyridinium chloride; CTAB, cetyltrimethylammonium bromide; DSB, diffusion-sorption-biodegradation; IC, inorganic carbon;  $\text{mg}_c/\text{L}$ ,  $\text{mg}$  carbon per liter; NIEC-STP, non-inhibitory effect concentration for sewage treatment plant inoculum; STP, sewage treatment plant.

## Supporting Information

### Balancing Bioaccessibility and Inhibitory Effects of Cationic Surfactant Cetylpyridinium Chloride in Sorbent-Modified Biodegradation Studies

#### **Additional information on the methods**

Concentrated stock solutions to prepare mineral salts medium were always prepared  $\leq 5$  days before the start of the incubation period. Each batch of mineral salts medium was prepared  $< 1$  h before use, using freshly dispensed ultrapure water (MilliQ; PURELAB flex, ELGA LabWater, High Wycombe, UK) and the required volumes of the four stock solutions. Details on preparation of the mineral salts medium can be found in the OECD 310 guideline [140]. Freshly prepared mineral salts medium always had a pH of  $7.4 \pm 0.2$ , a buffer capacity of 4 mM, and a divalent cation concentration (as  $Mg^{2+}$ ) of approximately 0.1 mM.

#### **Details for spiking the test medium.**

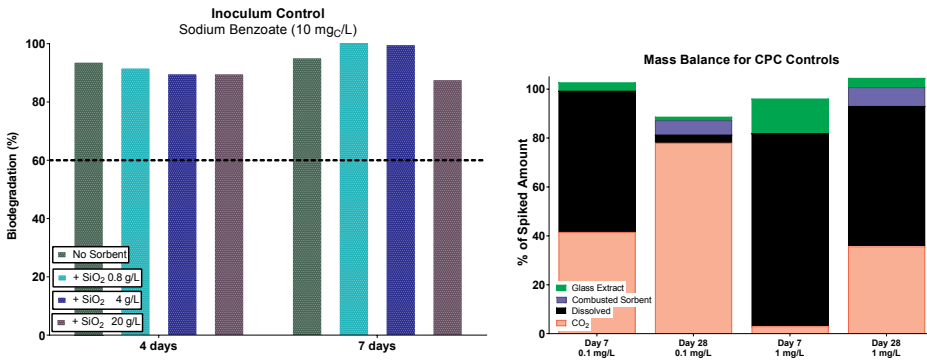
Borosilicate glass serum bottles (125 mL; Wheaton, New Jersey, USA) were spiked with  $^{14}C$ -CPC stock solution in acetone, loosely covered with analytical tissue paper, and left standing overnight to allow the acetone to evaporate. Nitrogen gas was used to gently flush out remaining acetone vapor. Bottles for the positive control were spiked directly with sodium benzoate stock solution. Weighed amounts of dried sorbent were then transferred to appropriate bottles, followed by the addition of 50 mL mineral medium using a Perimatic Premier precision dispensing pump (Jencons Scientific Ltd, VWR, East Grinstead, UK), fitted with a re-circulation loop. Bottles were loosely capped with 20 mm butyl rubber stoppers (Sigma-Aldrich) and left to stand at room temperature ( $20.0 \pm 1.0$  °C) for at least two h to allow the CPC to dissolve and interact with the sorbent material. Dummy vessels were filled with a second 50 mL aliquot of mineral medium, while other vessels were filled with 50 mL of mineral medium inoculated with 20 mL/L of inoculum treated as described above, resulting in a 64 mL headspace. Each vessel was then capped using butyl rubber stoppers and aluminum crimp caps (Sigma-Aldrich), after which the bottles were transferred to HT Multitron stackable incubators (Infors AG, Bottmingen, Switzerland). These incubators were set for orbital shaking at 100 rpm at  $22.0 \pm 1.0$  °C.

### **Details for the OECD 310 biodegradability criteria.**

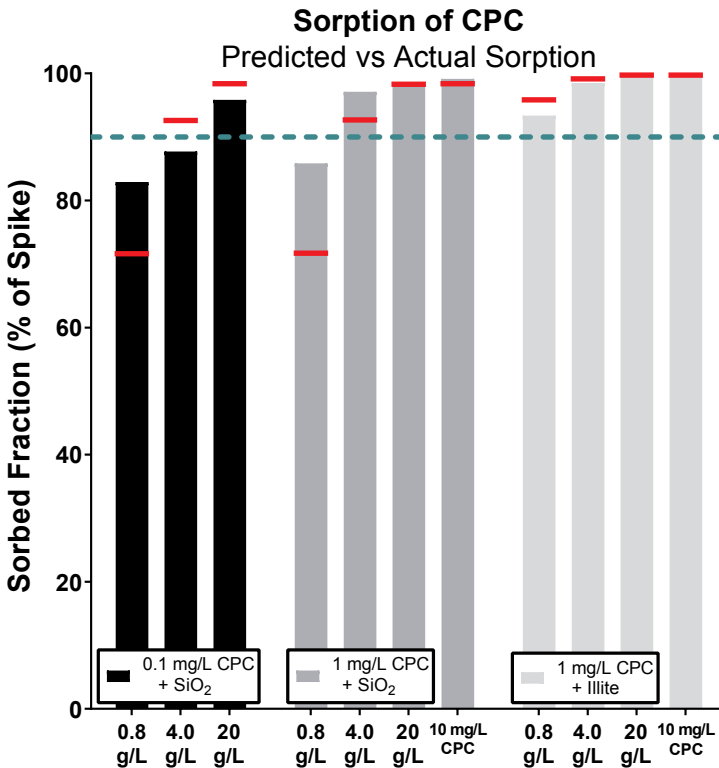
Conclusions on the biodegradability of a compound from the OECD 310 test are based on comparisons between observed biodegradation (mineralization of organic carbon to  $\text{CO}_2$ ) and the Theoretical  $\text{CO}_2$  production ( $\text{ThCO}_2$ ), which can be attained when all organic carbon is fully metabolized to  $\text{CO}_2$ . In order for a compound to be readily biodegradable, 60% of  $\text{ThCO}_2$  has to be reached within 10 days of reaching 10% of  $\text{ThCO}_2$ . An adequate sampling schedule to assess this so-called 10-day window should be defined prior to incubation, with replicate vessels at each sampling point. The OECD recommends at least 60% degradation of a reference substance (based on  $\text{ThCO}_2$ ) after 14 days of incubation, to confirm there is adequate microbial activity in the inoculum for biodegradation to occur. A healthy inoculum should be able to metabolize benzoate within 7 days. Biodegradation of benzoate can be adequately quantified using a standard carbon analyzer equipped to measure inorganic carbon (IC). In this study, we furthermore confirmed that the addition of sorbent had no impact on the microbial degradation of a reference substance (see Figure S1).

### **Details on the alkaline and acidified samples.**

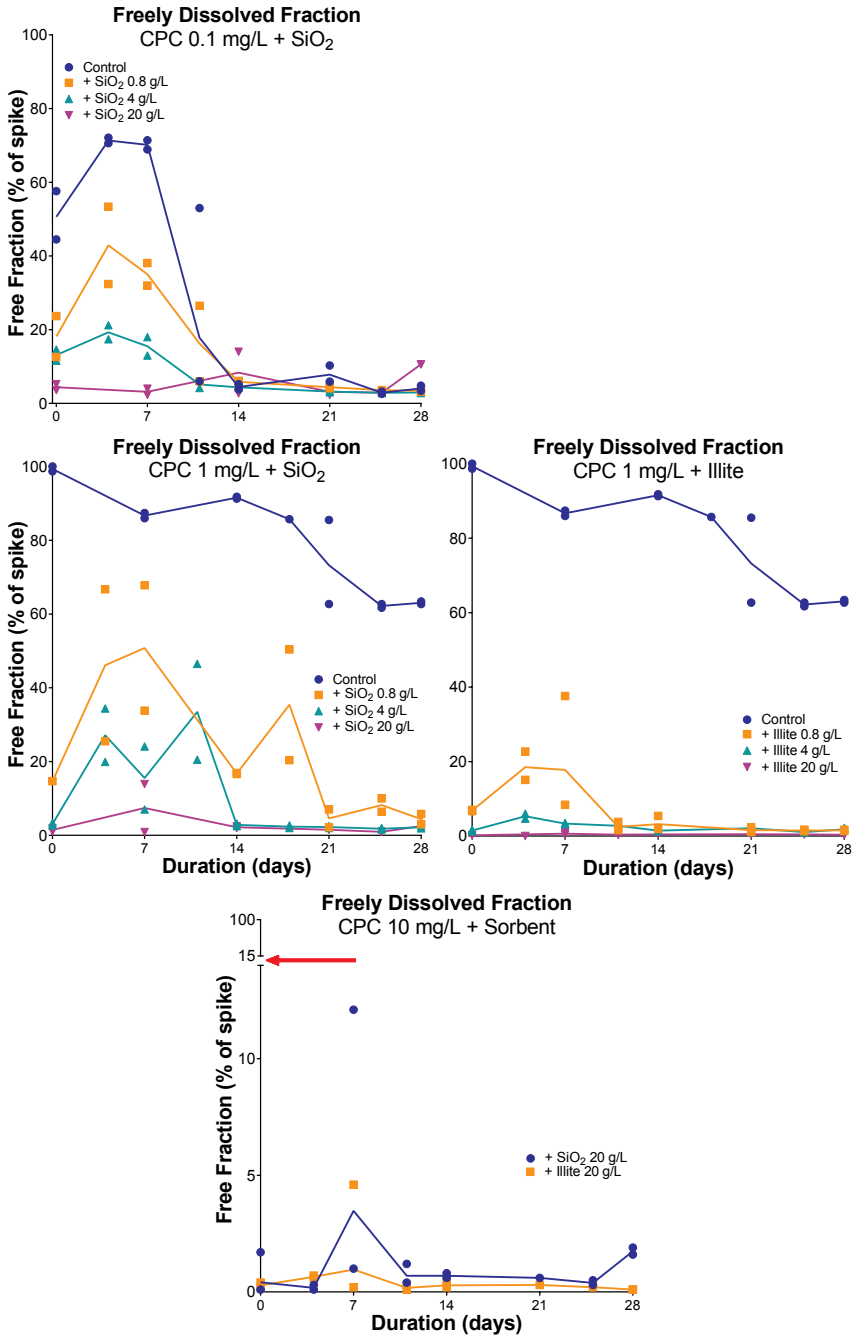
During the 60 min treatment with NaOH all (radioactive)  $\text{CO}_2$  should have reacted with the  $\text{OH}^-$ , forming soluble  $\text{HCO}_3^-$ . The low pH of the sulfuric acid treatment should subsequently convert all  $\text{HCO}_3^-$  to  $\text{CO}_2$ . As  $\text{CO}_2$  was allowed to disperse from the acidified samples overnight, the difference in radioactivity between alkaline and acidified samples represents mineralization of  $^{14}\text{C}$ -CPC to radioactive  $\text{CO}_2$  and carbonates. The relative amount of mineralization determined from the comparison between alkaline and acidified samples was then compared with the  $\text{ThCO}_2$  to calculate the percentage of biodegradation. It can be assumed that microbial degradation of CPC and  $^{14}\text{C}$ -CPC will be equivalent, which means production of radioactive  $\text{CO}_2$  is a proxy for total production of  $\text{CO}_2$ .



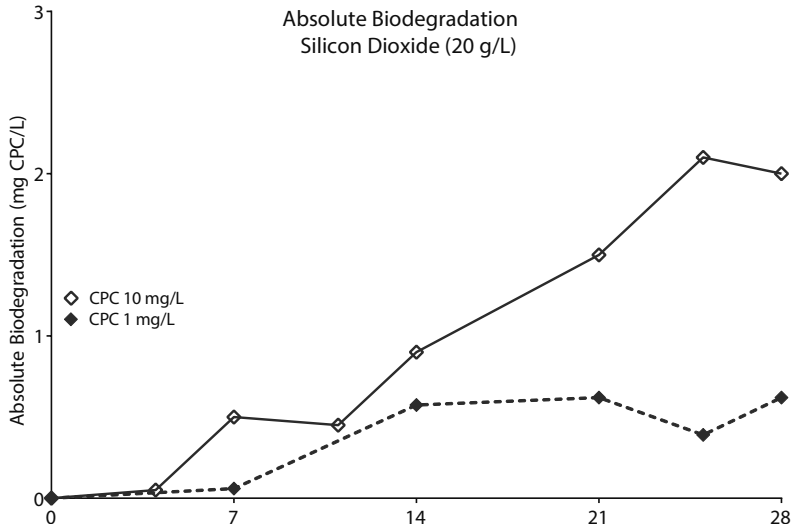
**Figure S1 (left).** Biodegradation of sodium benzoate (positive control). **Figure S2 (right).** Comparison of mass balances on day 7 and day 28 for vessels without sorbent for two different CPC treatments. The freely dissolved fraction ( $C_{free}$ ; black bar) is much higher at 1 mg/L CPC. The filter residue accounts for approximately 6% of total spiked radioactivity. This is probably largely caused by uptake and assimilation of <sup>14</sup>C by biomass.



**Figure S3.** Comparison of predicted sorption based on  $K_D$  (red dashes) with actual sorption estimated based on measured samples (bars).



**Figure S4.** Attempt to quantify toxicity mitigation by comparing the freely dissolved fraction of different treatment groups. Freely dissolved fraction is based on <sup>14</sup>C analysis in acidified samples.



**Figure S5.** Comparison of absolute biodegradation at initially spiked CPC concentration of 1 and 10 mg/L, both treated with 20 g/L  $\text{SiO}_2$ .

**Table S1.** Overview of time points used for biodegradation experiments without sorbent. The number of replicates sampled at each time point are listed; - means no replicates were sampled.

Time	6 $\mu\text{g/L}$	25 $\mu\text{g/L}$	100 $\mu\text{g/L}$	300 $\mu\text{g/L}$	1 mg/L	3 mg/L
4 d	1	1	2	1	-	-
7 d	-	-	2	-	2	-
11 d	1	1	2	1	-	-
14 d	-	-	2	-	2	-
18 d	1	1	-	1	2	-
21 d	1	1	2	1	2	-
25 d	1	1	2	1	2	-
28 d	1	1	2	1	2	12

**Table S2.** Overview of time points used for biodegradation experiments with sorbent. The number of replicates sampled at each time points are listed; - means no replicates were sampled.

Time	100 $\mu\text{g/L}$ ( $\text{SiO}_2$ )			1 mg/L ( $\text{SiO}_2$ )			1 mg/L (illite)			10 mg/L	
	0.8 g/L	4 g/L	20 g/L	0.8 g/L	4 g/L	20 g/L	0.8 g/L	4 g/L	20 g/L	$\text{SiO}_2$	Illite
4 d	2	2	-	2	2	-	2	2	-	2	2
7 d	2	2	2	2	2	2	2	2	2	2	2
11 d	2	2	-	-	-	-	2	2	2	2	2
14 d	2	2	2	2	2	2	2	2	2	2	2
18 d	-	-	-	2	2	-	-	-	-	-	-
21 d	2	2	2	2	2	2	2	2	2	2	2
25 d	2	2	2	2	2	2	2	2	2	2	2
28 d	2	2	2	4	4	2	4	4	4	2	4







# CHAPTER 8

---

## Application of Seven Different Clay Types in Sorbent-Modified Biodegradability Studies with Cationic Biocides

Niels Timmer<sup>a,b</sup>, David Gore<sup>c</sup>, David Sanders<sup>c</sup>,  
Todd Gouin<sup>c</sup>, Steven T.J. Droge<sup>a,d</sup>

<sup>a</sup>Institute for Risk Assessment Sciences, Utrecht University, Utrecht, 3508 TD, The Netherlands.

<sup>b</sup>Department Discovery and Environmental Sciences, Charles River Laboratories Den Bosch BV,  
s-Hertogenbosch, 5231 DD, The Netherlands

<sup>c</sup>Safety and Environmental Assurance Centre, Unilever, Colworth Science Park, Sharnbrook, MK44 1LQ,  
Bedfordshire, UK.

<sup>d</sup>Department Freshwater and Marine Ecology, Institute for Biodiversity and Ecosystem Dynamics, University  
of Amsterdam, P.O. Box 94248, 1090 GE Amsterdam, The Netherlands.

**Keywords:** Cationic Surfactant; Environmental Risk Assessment; Bioaccessibility;  
Toxicity Mitigation; Ready Biodegradability Testing; Clay Minerals

**Chemosphere, 245, #125643 (2020)**

## Abstract

The cationic surfactants cetyltrimethylammonium bromide (CTAB) and cetylpyridinium chloride (CPC) can exert inhibitory effects on micro-organisms responsible for their biodegradation. However, under environmentally relevant exposure scenarios the presence of and sorption to organic and inorganic matter can lead to significant reduction of inhibitory effects. In our studies we investigated silica gel and seven clays as inert sorbents to mitigate these inhibitory effects in a 28 day manometric respirometry biodegradation test. CTAB was not inhibitory to the used inoculum, but we did observe that seven out of eight sorbents increased maximum attainable biodegradation, and four out of eight decreased the lag phase. The strongly inhibitory effect of CPC was successfully mitigated by most sorbents, with five out of eight allowing >50% biodegradation within 28 days. Results further indicate that bioaccessibility of the sorbed fractions in the stirred manometric test systems was higher than in calmly shaken headspace test systems. Bioaccessibility might also be limited depending on characteristics of test chemical and sorbent type, with montmorillonite and bentonite apparently providing the lowest level of bioaccessibility with CPC. Clay sorbents can thus be used as environmentally relevant sorbents to mitigate potential inhibitory effects of test chemicals, but factors that impede bioaccessibility should be considered. In addition to apparently increased bioaccessibility due to stirring, the automated manometric respirometry test systems give valuable and highly cost-effective insights into lag phase and biodegradation kinetics; information that is especially relevant for test chemicals of gradual biodegradability.

## Introduction

There is an increased appreciation of studies on biodegradability in the environment and chemical persistence. Today, both consumers and regulators are increasingly urging for assurance that chemicals in consumer products can be demonstrated to degrade in sewers or waste water treatment facilities, before they reach receiving environments. Numerous standard laboratory studies exist to assess the biodegradability of chemicals and mixtures. The Organization for Economic Co-operation and Development (OECD), for example, provides several guidelines that are globally recognized by regulatory agencies to assess the fate and behavior of chemicals.[139, 140, 143] These include relatively stringent screening studies to assess ready biodegradability in an aqueous, aerobic medium. The stringency of these screening studies is important, as numerous potentially harmful chemicals have continuous emissions into the environment and will be detectable in the environment, even if they are indeed readily biodegradable. Should such continuously emitted, potentially hazardous chemicals not be biodegradable (i.e. persistent), their levels in the environment would increase over time, as would the risk for negative effects on the environment.

Depending on the specific guideline, chemicals are generally considered to be readily biodegradable if biodegradation, based on formation of inorganic carbon (CO<sub>2</sub>) or consumption of oxygen, exceeds 60% within 10 days after reaching 10% biodegradation. The 10-day window criterion is not applicable for mixtures of structurally related chemicals. Due to the natural origin of the raw materials used to produce surfactants they are generally available as technical mixtures with several alkyl chain lengths. Surfactants are therefore exempt from the 10-day window criterion.[363, 364] Results that do not meet these aforementioned criteria but show unequivocal biodegradation within 60 days can be used to claim classification as non-persistent, based on inherent or ultimate biodegradability. Due to the stringency of these criteria, any chemical that passes can be assumed to degrade rapidly in the environment, which lowers the potential environmental impact for chemicals that may be toxic and/or bioaccumulative. However, there are several limitations with the methods described. In particular, in order to identify degradation of the test chemical above background metabolism of the test inoculum, recommended test concentrations are relatively high, ranging from 1 to 20 mg organic carbon/L.[139, 140] These high concentrations add to the stringency of the test method. However, for certain chemicals employing such high concentrations can lead to inhibitory effects on the microbial inoculum. As described in Annex II of the OECD 301 Guideline,[139] chemicals

with potential inhibitory effects should be tested at 10% of the  $EC_{50}$  for microorganisms. However, this information is not always readily available and testing at concentrations much lower than those suggested in the guideline will lead to analytical limitations when quantifying biodegradation. In addition, matrices proposed in these guidelines are usually aqueous and lack sorptive capacity to mitigate inhibitory effects by reducing bioavailability of the test chemical. The environmental relevance of clay minerals and their intuitively favorable properties for cationic biocides have led us to elucidate the efficacy and limitations of their application in biodegradability testing to better represent environmentally relevant conditions.[329, 365] [366]

In the context of biodegradation studies with added mitigating sorbent (e.g. clay, soil, or technical material such as silica gel ( $SiO_2$ )) it is important to distinguish between bioavailability and bioaccessibility of the test chemical.[140, 145, 146, 152, 330] The fraction of a chemical that is freely dissolved – the bioavailable fraction – drives chemical equilibrium in the cells of (micro-)organisms, directly influencing toxic potential and possibilities for metabolism.[286, 356, 367] The bioaccessible fraction is the fraction that can reasonably be expected to become bioavailable (i.e. the fraction that remains accessible) in a given time frame under applicable conditions e.g. undissolved crystals or reversibly sorbed fractions. [368] Bioaccessibility is important with respect to the extent of degradation attainable,[369] especially for prolonged experiments. Impaired bioaccessibility can limit biodegradation rates such that criteria for classifying a chemical as biodegradable are not met. Therefore, the aim of toxicity mitigation will be preventing or diminishing inhibitory effects, while simultaneously maintaining adequate bioaccessibility.[147, 370]

Due to inhibitory effects at recommended test concentrations (2-100 mg/L),[139, 140] or losses through strong sorption,[321-323, 371, 372] biodegradation potential may be underestimated. Certain cationic surfactants combine inhibitory effects on microorganisms with high adsorption capacity.[24, 43, 324-327] Still, several strains of microorganisms have demonstrated the ability to metabolize these surfactants.[157, 328, 339] In two recent studies,[329, 365] we have evaluated biodegradability of  $^{14}C$ -labeled cationic surfactants cetyltrimethylammonium bromide (CTAB) and cetylpyridinium chloride (CPC) at potentially inhibitory concentrations in a 28-d Headspace Test (HST).[140] As described in the OECD 301 Guideline,[139] it is difficult to test biodegradability of chemicals with an  $EC_{50}$  for microorganisms exceeding 20 mg/L. The  $EC_{50}$  as determined for CTAB and CPC are 19 mg/L and 20.7 mg/L, respectively.[373, 374] Inhibitory effects were therefore mitigated by addition of the inorganic sorbents silica gel ( $SiO_2$ ) and commercial illite

(C-ill); both surfactants sorbed weaker to SiO<sub>2</sub> than to C-ill, and bioaccessibility of SiO<sub>2</sub>-sorbed fractions was generally higher. Under test conditions that rendered non-inhibitory dissolved concentrations, both CTAB and CPC could potentially satisfy the criteria for ready biodegradability. However, at concentrations of 10-20 mg/L these surfactants could not be classified as readily biodegradable at sorbent concentrations >10 g/L. The high sorbed fractions (>99.9%) of surfactant appeared to be insufficiently bioaccessible, with biodegradability probably limited by unfavorable desorption kinetics.

In our CTAB HST study, we employed automated manometric respirometers (AutMR) to evaluate potential inhibitory effects (but not full inoculum toxicity) of CTAB in a 14 day setup with reference substrate.[329] The AutMR method works by adding CO<sub>2</sub>-sorbent to hermetically sealed vessels, so that CO<sub>2</sub> produced as a result of biodegradation of the test chemical is removed (Figure S1).[139] Built-in manometers detect and log decreases in air pressure due to O<sub>2</sub>-consumption, generating a series of consecutive measurements in unaffected systems, thereby increasing efficiency and consistency.

The primary aim of this study was to use AutMR to determine biodegradability of CTAB and CPC exposed with SiO<sub>2</sub> and C-ill, in order to compare with results from our previous studies using the HST design. The AutMR method is specifically included in the OECD 301 F Guideline, and is thus an established method to determine ready biodegradability. [139] Furthermore, we wanted to investigate whether other phyllosilicate clays besides C-ill could be more effective (and more standardized) sorbents for cationic surfactants, in terms of mitigation efficiency and desorption kinetics. In comparison with other inorganic soil constituents, clay minerals have a relatively high specific surface area (SSA), surface charge density, and cation exchange capacity (CEC).[375, 376] Theoretically, these factors all contribute to their suitability for application as sorbents in an environmental context,[159, 377] where especially the high SSA (increased surface area providing sorption sites; decreased likelihood of steric hindrance when the number of occupied sorption sites increases) and high CEC (increased number of sorption sites for organic cations) can be valuable. Therefore, several reference clays obtained from the Clay Minerals Society (CMS), encompassing a range of properties (SSA, CEC, interlayer accessibility), were used as inert sorbents for CTAB and CPC in a series of AutMR tests. Due to the stronger sorption characteristics addition of clay may more readily lead to bioaccessibility limitations than e.g. SiO<sub>2</sub>, although Van Ginkel et al. noted that SiO<sub>2</sub> tends to form a gel-like structure,[145] which could potentially decrease interaction between sorbent and medium in experimental settings without sufficient magnetic stirring.

## Materials and Methods

### Chemicals and Sorbents

Analytical grade CPC (pure C<sub>16</sub> homolog), CTAB (pure C<sub>16</sub> homolog), sodium benzoate, and solvents were obtained from Sigma-Aldrich (Gillingham, Dorset, UK). Use of SiO<sub>2</sub> has been described in literature,[145, 152] while C-ill and commercial bentonite (C-ben) were included since they could be easily obtained in large quantities from industrial sources. Clay types obtained from the Clay Minerals Society (CMS) were of interest since they have been characterized extensively, providing insight into how clay characteristics might be translated to expected efficacy of industrially sourced clays. SiO<sub>2</sub> (Davisil Grade 633, particle size 35-75 µm, SSA 480 m<sup>2</sup>/g), was obtained from Sigma-Aldrich. Comparable illite was used as in related sorption studies with surfactants,[177, 342] purchased as fine powder (Argiletz, France). Commercial fine powder bentonite was obtained from Keramikos (Haarlem, The Netherlands). CMS clays were received as coarse clay: montmorillonites SAz-2 and SCa-3, illite clays IMt-1 and IMt-2, and kaolinite KGa-2. These were treated to obtain the approximate 2 µm fraction using a CMS protocol.[378] Buffer salts and potassium hydroxide were analytical grade and obtained from Sigma-Aldrich. For AutMR tests a WTW OxiTop Control system was used, except for the test with CPC and CMS clays, where we used Lovibond BD600 GLP systems. All measuring heads were calibrated and checked visually before use. Details on the radiolabeled chemicals used in previous work referenced throughout this chapter, and associated methods, can be found in previous publications:[329, 365] the methods are briefly described in the Supporting Information.

### Inoculum

Activated sludge was obtained from Broadholme Sewage Treatment Works (BSTW; Ditchford Road, Wellingborough & Irthingborough, UK). BSTW treats waste water from ~80,000 households; <15% of organic load is attributable to industrial discharge.[315] Sludge was sparged with CO<sub>2</sub> free air overnight to allow habituation to lab conditions and to remove inorganic carbon. Subsequently, sludge was transferred to a flow-breaking glass vessel and homogenized using a Polytron PT 3000 dispersion unit (Kinematica AG, Littau, Switzerland) at 12,000 rpm for 5 min. The resulting fine-grained suspension was centrifuged at 800 g for 10 min, after which supernatant was filtered over analytical grade glass wool (Sigma-Aldrich) and used as inoculum. Before treatment the suspended solids concentration in activated sludge was 5 ± 1 g/L.

## Preparation of Automated Manometric Respirometry (AutMR) Tests

AutMR tests were performed using vendor-supplied amber glass bottles. Weighed amounts of sorbent were added to respective bottles, followed by spiking with sodium benzoate (positive control), CTAB, or CPC using aqueous stock solutions, brought up to a volume of 180 mL per vessel using mineral medium as described in the OECD 301 Guideline.[139] Bottles were left standing for 2 hours to allow interaction with sorbents. Thereafter, mineral medium with inoculum (10 mL/L) was added to each bottle to obtain the required headspace-to-volume ratio, as specified by the AutMR manufacturer. Total medium volume in AutMR tests was 360 mL, allowing to measure oxygen consumption up to 80 mg O<sub>2</sub>/L. Rubber gaskets containing two KOH-pellets (CO<sub>2</sub>-sorbent) were inserted and bottles were tightly closed by screwing on measuring heads. Bottles were then placed on magnetic induction stirrers (320 rpm) inside temperature-controlled incubators (22.0 °C). Internal pressure measurements were stored automatically at each sampling interval and converted to oxygen consumption (mg O<sub>2</sub>/L). In AutMR tests, biodegradation is calculated by subtracting endogenous oxygen consumption from measured oxygen consumption, and dividing the resulting value by the theoretical oxygen demand (ThOD), which is the amount of oxygen required to fully oxidize all test chemical in the system. The ThOD with full oxidation of nitrogen to NO<sub>3</sub> (ThOD<sub>NO<sub>3</sub></sub>) for CPC and CTAB was calculated using equation 1, and was determined to be 2.99 and 2.70 mg O<sub>2</sub>/mg, respectively.

$$\text{ThOD}_{\text{NO}_3} = \frac{16 \times (2 \times C + 1/2 \times H + 5/2 \times N)}{\text{Molecular weight}} \text{ mg O}_2/\text{mg} \quad (\text{eq. 1})$$

### AutMR Test with Sorbent

Sorption affinity to C-ill and SiO<sub>2</sub> and data on inhibitory effect concentrations for CTAB and CPC were used as established in previous work.[329, 365] Biodegradation of 13.6 mg/L CPC was determined without addition of sorbent and with addition of seven types of clay (triplicate, inoculum batch #6), 20 g/L C-ill (six replicates, inoculum batch #3), and 20 g/L SiO<sub>2</sub> (six replicates, inoculum batch #3). Biodegradation of 20 mg/L CTAB was determined without sorbent (duplicate, inoculum batch #4), and with addition of SiO<sub>2</sub> and seven types of clay (four replicates, inoculum batch #4 and #5, respectively). An overview of the most relevant details for each experiment, including experiments published previously, can be found in Table 8.1. For each experiment, vessels with medium and inoculum were incubated to determine endogenous respiration; dedicated blanks with sorbent were

not included. Dosing of all clay types is described in Table 2. We aimed to dose amounts of clay resulting in a CEC of ~500  $\mu\text{mol}$  charge equivalents per liter ( $\mu\text{eq/L}$ ), which at a sorbed fraction of ~90-99% would reach less than 10% saturation of the charged sorption sites. Exceptions were for IMt-1 and IMt-2 which were both dosed based on the higher CEC of IMt-2 in order to gain insight in the actual contribution of an equal added CEC. We assumed CEC of G-ben was comparable to that of SAz-2 and SCa-3, as montmorillonite is the major constituent of bentonite. However, the CEC for G-ben was a factor 2.5 lower than expected (40 meq/100 g; see also Table 2).

**Table 8.1.** Relevant details on performed experiments.

Experiment type	HST	HST	AutMR	AutMR	AutMR	AutMR
Inoculum batch	#1	#2	#3	#4	#5	#6
CTAB/CPC	CPC	CTAB	CPC	CTAB	CTAB	CPC
Concentration	1-10 mg/L	16.8 mg/L	13.6 mg/L	20 mg/L	20 mg/L	13.6 mg/L
Replicates	2	3	6	4	4	3
Duration	28 d	28 d	30 d	27 d	27 d	30-120 d
Sorbents	C-ill + SiO <sub>2</sub>	C-ill + SiO <sub>2</sub>	C-ill + SiO <sub>2</sub>	C-ill + SiO <sub>2</sub>	CMS clays	CMS clays
Sorbent concentration	0.8-20 g/L	1-30 g/L	4-20 g/L	1.8-6 g/L	See Table 2	See Table 2
Figures	2A + 2B	2C + 2D	1A + 2A + 2B + 3A	1B + 2C + 2D + 4A	4A + 4B	3A + 3B
Published previously	Yes	Yes	No	No	No	No

## Graphs

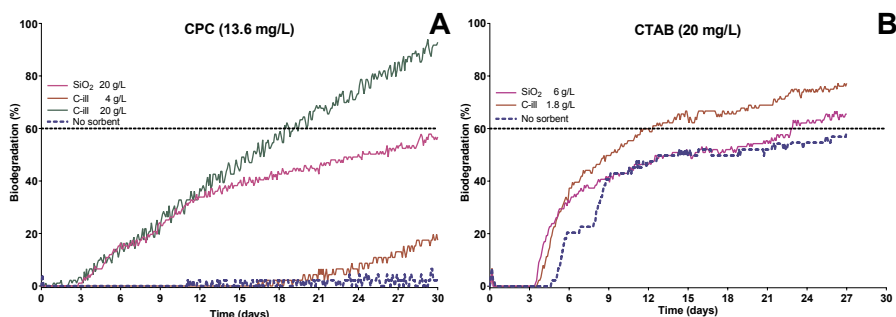
All figures of AutMR results show mean values of all replicates. Figures in Supporting Information include error margins to allow assessment of variability and statistical relevance of apparent differences. All graphs were constructed using GraphPad Prism 8.2.0.435 for Windows.



## Results and Discussion

### AutMR Test with Illite and SiO<sub>2</sub> for CPC

Blanks containing only inoculum and medium (triplicate) were used to determine endogenous respiration, which was minor (<5 mg O<sub>2</sub>/L after 28 days of incubation). Sodium benzoate (reference; 15 mg/L) was degraded >60% after ~7 days of incubation, indicating adequate microbial activity (Figure S2 and S3). Test vessels were spiked with 13.6 mg/L CPC. Vessels containing CPC without sorbent showed 2% biodegradation (based on oxygen consumption) after 30 days (Figure 8.1A), indicative of strong inhibition of microbial activity by CPC, as noted previously in HSTs.[365] For both SiO<sub>2</sub> and C-ill at 20 g/L, rapid biodegradation was observed, up to 55% (SiO<sub>2</sub>) and 95% (C-ill) within 30 days. In the treatment with a lower amount of C-ill (4 g/L) a lag phase of ~18 days was observed, followed by relatively slow biodegradation. The 4 g/L C-ill group reached only ~17% after 30 d, indicating that the increased lag phase is likely caused by inhibitory effects and a microbial adaptation period. Until Day 10 biodegradation rates are similar between the 20 g/L sorbent groups, after which it levels off gradually in the SiO<sub>2</sub> group while remaining steady in the 20 g/L C-ill group. Since the curves match perfectly during the first 12 days of incubation (Figure S10) it is unlikely inhibitory effects cause leveling off in the SiO<sub>2</sub> vessels, and differences between C-ill and SiO<sub>2</sub> might very well be related to bioaccessibility of sorbed CPC.



**Figure 8.1. A:** Biodegradation profile (AutMR; mean of six replicates) of 13.6 mg/L CPC with C-ill (two concentrations) and SiO<sub>2</sub>. Full inoculum inhibition in control (dashed line), minor mitigation at 4 g/L C-ill. SiO<sub>2</sub> and 20 g/L C-ill perform similarly during first 12 days; 20 g/L C-ill reaches highest biodegradation. **B:** Biodegradation profile (AutMR; mean of four replicates) of 20 mg/L CTAB with C-ill and SiO<sub>2</sub>. Both sorbents perform similarly during first 6 days; SiO<sub>2</sub> performs better than control (dashed line); C-ill reaches highest plateau.

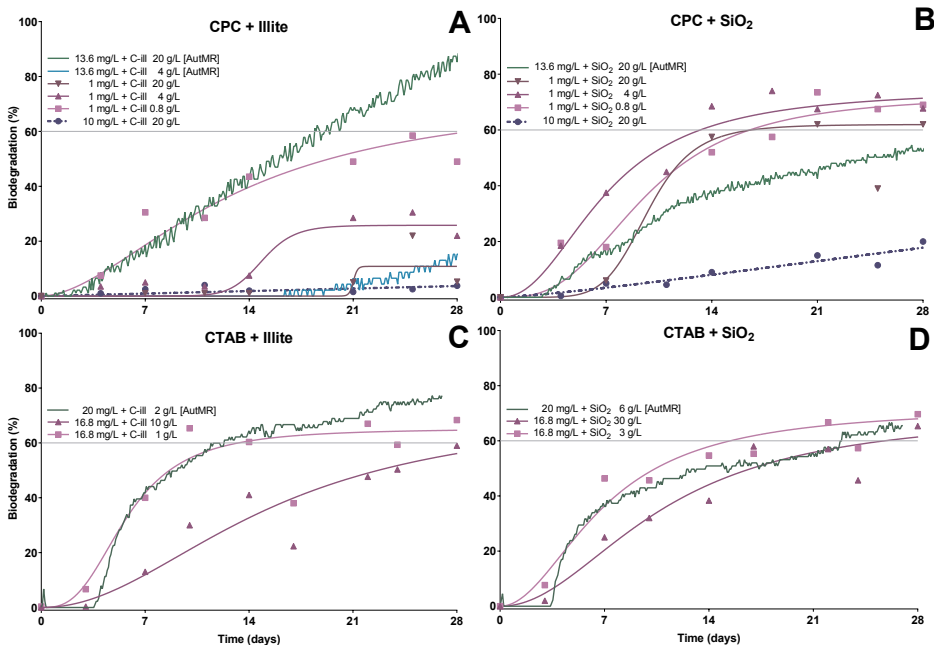
## AutMR Test with Illite and SiO<sub>2</sub> for CTAB

A second series of vessels was spiked with 20 mg/L CTAB (Figure 8.1B). Duplicate blanks with only medium and inoculum showed minor endogenous respiration (<5 mg O<sub>2</sub>/L after 28 days). Although inhibitory effects were expected at this concentration, based on CTAB concentrations inhibiting aniline biodegradation in previous work,[329] we observed a 4 day lag phase followed by relatively fast biodegradation, reaching an apparent maximum of ~55% after 18 days. CTAB vessels were incubated with C-ill at 2 g/L and SiO<sub>2</sub> at 6 g/L, which were calculated to achieve dissolved concentrations below the threshold of inhibitory effects.[329] In both sorbent groups, the lag phase was somewhat shorter than in vessels without sorbent. Although substantial biodegradation was observed in the no sorbent group within a relatively short incubation time, these results indicate that the lag phase might still be caused by inhibitory effects to which microbes need to adjust. Comparable to the CPC experiment (Figure 8.1A), biodegradation evolves similarly between C-ill and SiO<sub>2</sub> groups initially (up to Day 5), after which the rate levels off in the SiO<sub>2</sub> group. In contrast to the CPC experiment, the rate of biodegradation in the C-ill group levels off as well; the plateau reached is 17% higher than for the SiO<sub>2</sub> group (60% vs. 77%). These results suggest that differences between C-ill and SiO<sub>2</sub> might indeed be related to bioaccessibility.

## Comparison of Biodegradability in Headspace Test and AutMR Test

Relevant AutMR results are plotted in Figure 8.2 alongside data from previous HSTs,[329, 365] that were run with 1 or 10 mg/L CPC and different C-ill (2A) or SiO<sub>2</sub> (2B) treatments. Virtually no degradation was observed in the HST with 10 mg/L CPC and 20 g/L C-ill, while biodegradation is >90% in the AutMR test at 13.6 mg/L CPC with 20 g/L C-ill. Remarkably, in the HST 1 mg/L CPC showed low biodegradation with addition of 4 and 20 g/L C-ill, while with 0.8 g/L C-ill biodegradation rate was similar as in the AutMR. C-ill was also used at 4 g/L with 13.6 mg/L CPC in the AutMR test, which resulted in low biodegradation (20%) with a 15 day lag phase. Bioaccessibility seems rate limiting in the HST, to the extent that apparent effectiveness of sorbent is opposed to what is observed with AutMR. This might be explained by stirring in AutMR which increases turbulence, thereby reducing thickness of unstirred boundary layers surrounding the particles,[379] enhancing desorption kinetics. However, in light of AutMR results it seems unlikely CPC could not degrade at all with 20 g/L C-ill in the HST (Figure 8.2A). The mild shaking applied was probably insufficient to facilitate effective desorption.

In the AutMR test 13.6 mg/L CPC with 20 g/L  $\text{SiO}_2$  is degraded much faster than 10 mg/L CPC in the HST (Figure 8.2B), which is in line with our hypothesis of increased bioaccessibility through stirring. In the three 1 mg/L CPC groups in the HST biodegradation is faster overall and reaches a higher plateau, except for the lag phase at 20 g/L  $\text{SiO}_2$  which is consistent with the bioaccessibility hypothesis and comparable with observations for the two highest C-ill concentrations. Interpreting differences between the two test methods is more difficult with CTAB, partly because CTAB did not show inoculum inhibition without sorbent. Concentrations between both methods differed by <20%. Biodegradation rate in the 2 g/L C-ill group (AutMR) is approximately the same as in the 1 g/L C-ill HST (Figure 8.2C). The HST with 10 g/L C-ill, however, showed a reduced biodegradation rate, indicative of lower bioaccessibility without stirring. In the CTAB groups with  $\text{SiO}_2$  (Figure 8.2D) there are no obvious differences between AutMR and HST. All vessels reach a level of ~60% degradation within 28 days.



**Figure 8.2. A:** Comparison of biodegradability of different concentrations of CPC and illite in AutMR and HST; results suggest limited bioaccessibility in the HST. **B:** Comparison of biodegradability of different concentrations of CPC and  $\text{SiO}_2$  in AutMR and HST; results suggest higher biodegradability in the AutMR if corrected for CPC concentration. **C:** Comparison of biodegradability of different concentrations of CTAB and illite in AutMR and HST; results suggest comparable bioaccessibility at 1-2 g/L C-ill. **D:** Comparison of biodegradability of different concentrations of CTAB and  $\text{SiO}_2$  in AutMR and HST; results suggest comparable bioaccessibility at 3-6 g/L  $\text{SiO}_2$ .

The results shown in Figure 8.2 provide compelling evidence that the AutMR test is a suitable alternative for the HST, and that magnetic stirring in sorbent enriched vessels appears to increase bioaccessibility substantially. Although C-ill proved to be a suitable sorbent in AutMR, its relatively strong sorption capacity compared to SiO<sub>2</sub> resulted in limited desorption kinetics, reducing biodegradation in the absence of stirring. AutMR systems generally provide a sampling resolution that is difficult to achieve using other standardized biodegradation assays and can easily be extended beyond the original end date, for example to determine inherent biodegradability over longer exposure periods.

**Table 8.2.** Details and applied amounts of clay sorbents; clay coding according to CMS.

Clay Type	CEC (meq/100g)	SSA (m <sup>2</sup> /g)	CTAB (20 mg/L = 55 µM)		CPC (13.6 mg/L = 44 µM)	
			Dose (g/L)	CEC (µeq/L)	Dose (g/L)	CEC (µeq/L)
			Commercial illite (C-ill)	29 [380]	n.d.	1.80
IMt-1 (illite)	15 [381]	34.2 <sup>a</sup> [382]	1.80	270	1.90	290
IMt-2 (illite)	25 [383]	24.2 <sup>a</sup> [384]	1.80	450	1.90	475
SAz-2 (Ca-montmorillonite)	120 [385-387]	820 <sup>b</sup> [388]	0.40	480	0.44	530
SCa-3 (montmorillonite)	120 [389, 390]	750 <sup>c</sup> [390]	0.50	600	0.40	480
KGa-2 (kaolinite)	3.7 [387]	21.6 <sup>a</sup> [391]	20.0	740	12.0	440
Commercial bentonite (C-ben)	40	n.d.	0.50	200	0.52	210

CEC: Cation Exchange Capacity ; SSA: Specific Surface Area ; <sup>a</sup>: SSA determined using N<sub>2</sub> and Brunauer-Emmett-Teller method ; <sup>b</sup>: SSA determined using EGME ; <sup>c</sup>: SSA determined by theoretical means.

## Effectiveness of Different Clay Sorbents with CPC

Clays are phyllosilicates that are built of tetrahedral silicate sheets and octahedral hydroxide sheets. Clay minerals can carry a permanent negative charge due to isomorphic substitution, where atoms in the crystal lattice are replaced by atoms of similar size but different valence.[392] Clays can consist of one tetrahedral sheet and one octahedral sheet (1:1 clay), or of two tetrahedral sheets with one octahedral sheet in between (2:1 clay). Kaolinite would be the classical example of a 1:1 clay. Several 2:1 clays, such as montmorillonite, are expansive or swelling clays, which means they can become hydrated by taking up water through cation exchange, in the interlayer between clay mineral sheets. [393-396] Such expansive clays can be significant in the context of our work, as interlayer sorption in some hydrated expanding clays can reduce desorption kinetics.[368, 397] Illites are well-known and ubiquitous non-expandable 2:1 clays. Differences in CEC and SSA between the clay types used for this study are described in Table 2.

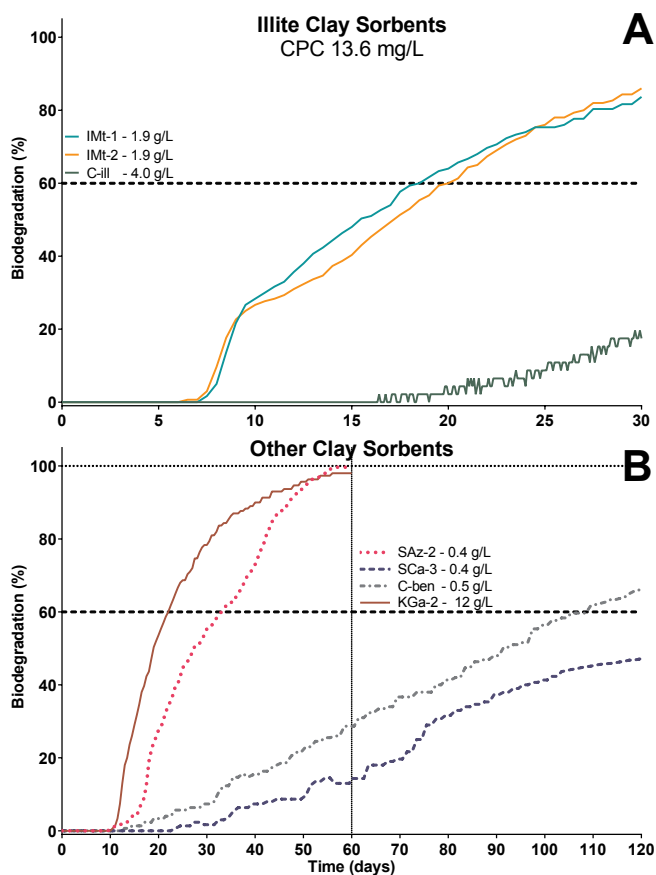
Seven clay sorbents (Table 2) were exposed to 13.6 mg/L CPC (Figure 8.3), a fully inhibiting concentration if no sorbent was added (Figure 8.1). Endogenous respiration was  $<5$  mg  $O_2/L$ . This CPC concentration required a sorbed fraction of  $>98\%$  in order to not inhibit inoculum metabolic performance.[365] Sorbent amounts were in the range of 210–1160  $\mu\text{eq/L}$ . The tested CPC concentration yields 40  $\mu\text{eq}$  of positive charge, which is 5–29 times lower than the CEC of the added sorbents. Therefore, sorbed surfactant levels should be well below sorption site saturation, which is relevant as sorption can become less efficient near saturation. C-ill provided the highest CEC and biodegradation tests performed with C-ill demonstrate a comparatively long lag phase and slow biodegradation rate. Despite this, the results with 20 g/L C-ill (Figure 8.1A) in the first AutMR series indicate that a high concentration of this sorbent does not necessarily lead to lower biodegradation rates attributable to reduced bioaccessibility. It should be noted that C-ill was tested using a different inoculum and test system (OxiTop vs. BD600), which could be the cause for some of the variability as sludge is known to be a variable inoculum source.[317, 398] IMt-1 and IMt-2 provide the optimal mitigation/bioaccessibility equilibrium, evidenced by the short lag phase (Figure 8.3A). Overall, results obtained with these two types of illite are very similar, although their characteristics (40% difference in CEC and 30% difference in SSA) are not. Although addition of kaolinite (KGa-2) resulted in a longer lag phase than the standard illites (Figure 8.3B), biodegradation was actually faster. KGa-2 and IMt-1 both satisfy the criteria to label CPC as readily biodegradable at recommended concentrations.

Addition of commercial bentonite (C-ben) and CMS montmorillonite (SCa-3) results in a relatively long lag phase, followed by gradual biodegradation over multiple weeks (Figure 8.3B). Both sorbents are expandable 2:1 clay minerals and attained only  $<10\%$  biodegradation after 28 days. Total CEC of added SCa-3 and IMt-2 in the test system was comparable, which highlights the fact that CEC alone is not sufficient to predict or explain sorbent efficacy. The Ca-montmorillonite SAZ-2, on the other hand, had a longer lag phase than both standard illites, but once started biodegradation rate was similar, reaching 60% within 32 days of incubation. Incubation with KGa-2 and SAZ-2 was terminated after 60 days, while C-ben and SCa-3 were incubated for 120 days. Single replicates with KGa-2 and SAZ-2 reach a biodegradation of  $>100\%$  (107% and 110%, respectively), which is technically not possible. However, these replicates reached their plateau at least 7 days before the experiment was terminated. Percentages up to 110% in ready biodegradability tests are not unheard of, and could be due to natural variation as well as small dosing errors.

It seems not all clay types tested are equally suitable as mitigants for cationic surfactants that bind as strong as CPC. The commercial clays C-ill and C-ben performed quite poor in comparison with four of the CMS clays (IMt-1, IMt-2, KGa-2, and SAz-2). However, total biodegradation and biodegradation rate increased with all tested clay sorbents, although these effects are limited for C-ben and SCa-3. While these two sorbents could mitigate inhibitory effects, desorption rates were insufficient to maintain adequate bioaccessibility. This raises the question if the high CEC and SSA of SCa-3 and C-ben directly impacted bioaccessibility, although KGa-2 and SAz-2 have comparable or higher CEC and SSA at the applied dosage. These results might be explained by the fact that bentonite is an expansive clay type, which could also be a factor in the results for SAz-2, although SAz-2 is more in line with the non-expansive clay types. Interpretation of the results for CPC and CTAB might have benefitted from sorption data (e.g.  $K_p$ ) of both chemicals for each clay type, as bioaccessibility is likely related more directly to sorption affinity than to descriptors such as CEC or SSA.

### **Effectiveness of Different Clay Sorbents with CTAB**

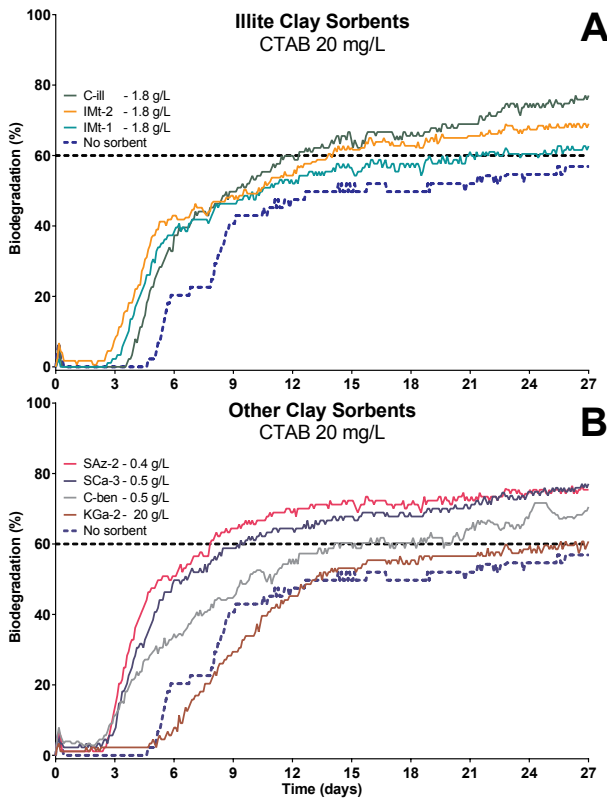
The same seven clay sorbents (Table 2) were also exposed in quadruplicate to 20 mg/L CTAB. Endogenous respiration was  $<5$  mg  $O_2/L$ . As there was extensive biodegradation in vessels without sorbent, sorbent efficacy and desorption efficiency were mainly evaluated by considering lag phase and plateau height (Figure 8.4). It should be kept in mind that  $>98\%$  of CTAB was sorbed initially. At 20 mg/L CTAB provides 55  $\mu\text{eq}$  of positive charge, 4-13 times lower than CEC of added sorbents (Table 2). The standard illite clays, IMt-1 and IMt-2, impact CTAB biodegradation similarly as the commercial illite C-ill. CTAB biodegradation with these three illites is faster, particularly in the first 9 days. On average, these vessels reach a 5.1 ( $\pm 4.3$ ) %, 11.7 ( $\pm 4.5$ ) %, and 19.2 ( $\pm 9.1$ ) % higher plateau than the no-sorbent control, respectively (Figure 8.4A). The SSA of IMt-1 is 30% higher while CEC is 40% lower than for IMt-2; it is unclear how SSA and CEC are related in terms of toxicity mitigation. The amount of KGa-2 used provided the highest CEC but barely influences lag phase and plateau height (Figure 8.4B).



**Figure 8.3. A:** Biodegradation profile (AutMR; mean of three replicates) of 13.6 mg/L CPC with the three illite clay sorbent C-ill, IMt-1, and IMt-2. Study was terminated after 30 days; both IMt clays reach >60% biodegradation. **B:** Biodegradation profile (AutMR; mean of three replicates) of 13.6 mg/L CPC with four clay types, with experimental duration of 60 and 120 days. SAz-2 and KGa-2 reach ~100% biodegradation; SCa-3 and C-ben lead to slow and gradual biodegradation.

The montmorillonites SAz-2 and SCa-3 show even more rapid biodegradation in the first 9 days than the illite clays, and reach a  $18.5 (\pm 4.7) \%$  and  $19.2 (\pm 14.9) \%$  higher plateau than no-sorbent control, respectively (Figure 8.4B). Due to their high CEC with exchange sites residing mainly in the interlayer, it was expected montmorillonites would result in slower desorption kinetics and biodegradation rates in comparison with illite clays. So either CTAB sorbed mainly to external clay surfaces, or the interlayer sorbed fraction is readily bioaccessible. The commercially available bentonite (C-ben) consists of montmorillonite and illite, but final degradation results ( $12.5 (\pm 9.4) \%$  higher plateau) compare better to the illite

sorbents. Overall results indicate that SAz-2 and SCa-3 might be most suitable to enhance or maintain bioaccessibility of CTAB-like chemicals, while potentially mitigating inhibitory effects. However, commercially available powdered illite and bentonite might be more cost efficient. We have shown that apparent biodegradability and biodegradation rate could be increased with the seven clay sorbents tested, proving adequate bioaccessibility with all tested sorbents. In addition, biodegradation curves are steeper and the lag-phase is shorter; important factors to satisfy the 10-day window criterion. Although the 10-day window is not applicable for industrially produced surfactants, it could be argued the 10-day window remains applicable for our experiments since pure homologs were tested.



**Figure 8.4. A:** Biodegradation profile (AutMR; mean of four replicates) of 20 mg/L CTAB with the three illite clay sorbent C-ill, IMt-1, and IMt-2. Study was terminated after 27 days; compared with control (dashed line) all illite clays improve plateau height and biodegradation rate in the first week of the study. **B:** Biodegradation profile (AutMR; mean of four replicates) of 20 mg/L CTAB with four clay types. Study was terminated after 27 days; KGa-2 shows no clear improvement over control (dashed line), C-ben performs better than control, and SAz-2 and SCa-3 lead to highest plateau and fastest biodegradation.



## Comparing AutMR Results for CTAB and CPC

Results obtained in the AutMR test show considerable differences in behavior for CTAB and CPC between clay types. Some chemicals show lower biodegradability with stronger sorbing clay types,[366, 399] while other chemicals degrade more efficient with stronger sorbents.[400] In some instances, biodegradability can be impaired in presence of clay sorbents,[401, 402] although this is sometimes linked to other effects than bioaccessibility limitations.[403] Some studies even suggest a protective mechanism, selective for cationic chemicals, against degradation by hydroxyl radicals.[404] Overall, available literature is mostly in line with the findings we observed with CPC, where montmorillonite and montmorillonite-containing bentonite showed less efficient biodegradation than illite and kaolinite. In conclusion, the present results indicate there is no clearly defined best clay type for all test chemicals.

## Factors Governing Sorption Potential of Different Clay Types

Figure 8.3 and Figure 8.4 clearly illustrate that clays are promising candidates to achieve toxicity mitigation while maintaining bioaccessibility. However, in order to identify the most appropriate clay type, understanding how clay characteristics influence bioaccessibility is needed. SSA and CEC both follow the general order montmorillonite > bentonite > illite > kaolinite, which complicates differentiation.[405, 406] Sorption to montmorillonite might also be dependent on hydration of the interlayer, which has been linked to decreased bioaccessibility.[368, 393-397] Due to their relatively flat and thin structure, aromatic systems within a molecule can be expected to interact favorably with sorption sites within the interlayer. This has been shown in scientific studies with phenol and quinoline as specific examples, which were shown to enter the montmorillonite interlayer. [397, 407, 408] Interlayer sorption of aromatic amines was also investigated in detail, with attempts to take into account the contribution of specific interactions of the aromatic systems with cation exchange sites in the interlayer.[409, 410]

## Other Beneficial Effects of Clays on Biodegradation

Clay minerals may also provide a functional habitat for microorganisms, since they can act as a practical support material, providing a protective environment through biofilm formation.[159, 160] This has been described rather extensively for kaolinite,[411, 412] zeolite,[413] montmorillonite,[414, 415] and smectite in general.[414] Clay minerals may also

stimulate microbial activity by providing a microhabitat with optimum pH, by exchanging  $H^+$  resulting from metabolic activity with counter-ions at the mineral surface.[160, 400] As a result of these combined properties, microorganisms could potentially degrade substrates adsorbed onto clay particles more effectively. However, bioaccessibility is also influenced by desorption and subsequent diffusion of substrate,[416] although there is evidence sorbed substrate can be taken up by microorganisms directly, albeit less efficient than freely dissolved molecules.[417] While formation of such biofilms could not be evaluated in our study, it would be interesting to further elucidate the extent of biofilm formation in clay-amended biodegradability studies. If biofilm formation is observed in such studies, this would add further weight to the environmental relevance of introducing clay minerals.

### **Environmental Relevance of CTAB and CPC**

Although clearly indicating pure homologs of CPC and CTAB are readily biodegradable, while even satisfying the 10-day window criterion, the results in Figure 8.4 and especially Figure 8.3 also show there can be a lag-phase before significant biodegradation levels are reached, a feature described previously for numerous surfactants and detergent mixtures.[418] This lag-phase might be linked to the fact that surfactants can have concentration-dependent inhibitory effects on microorganisms, although such effects are not observed at environmentally relevant concentrations.[138, 419-428] Due to large-scale application in down-the-drain products (e.g. mouthwash, fabric softener, cleaning products), biodegradability of surfactants is carefully assessed and surfactants with poor biodegradability have limited application.[1, 428, 429]

More specifically, CPC and other pyridinium-based surfactants, as well as CTAB, are a key component in ionic liquids and are also used in the preparation of organoclays,[331-336, 430] while several studies highlight the limited biodegradability and potential toxicity. [357-359] Detectable levels of CPC and CTAB are present in the environment, with levels detected in river water ranging from 2.0-102  $\mu\text{g/L}$  for CPC and from 0.4-138  $\mu\text{g/L}$  for CTAB. [337, 431-433] Higher concentrations are usually associated with industrial areas; lower concentrations are measured in Western countries. We have concluded that, although detectable levels might be present in the environment, CPC is readily biodegradable under environmentally relevant conditions.[365]

## **Relevance of Sorbent Addition for Proper Environmental Risk Assessment**

Altogether, the work presented in this chapter further improves the stepwise sorbent addition approach postulated previously.[329, 365] Sorptive surfaces are readily encountered under realistic field conditions e.g. activated sludge and suspended solids within a STP, sand and sediment in natural water bodies, and soil on which dried sewage sludge, river water, or STP effluent might be applied. We conclude that addition of inert sorbents will lead to more environmentally relevant methods to determine biodegradability of (cationic) biocides, by mitigating the toxicity of concentrations well above environmentally relevant dissolved concentrations and a controlled presence of inert strongly sorptive phases under defined conditions, which release the sorbed fraction and allow microbial degradation. In addition, continuous measurements provided by AutMR systems give valuable and cost-effective insight into biodegradation kinetics and lag phase.

## **Acknowledgements**

We are grateful to Charles River Laboratories, 's Hertogenbosch, The Netherlands, for offering their facilities and resources to carry out part of the AutMR work. We thank Joop L.M. Hermens (Utrecht University) and Geoff Hodges (Unilever) for fruitful discussions and valuable suggestions regarding this work.

## **Abbreviations**

AutMR, automated manometric respirometer; C-ben, commercial bentonite; CEC, cation exchange capacity; G-ill, commercial illite; CMS, clay minerals society; CPC, cetylpyridinium chloride; CTAB, cetyltrimethylammonium bromide; IC, inorganic carbon; IMt-1, illite from Silver Hill, Montana, USA; IMt-2, illite from Silver Hill, Montana, USA; KGa-2, kaolinite from Warren, Georgia, USA; SSA, specific surface area; SAz-2, calcium-montmorillonite from Apache, Arizona, USA; SCa-3, bentonite from Otay, California, USA

## Supporting Information

Application of Seven Different Clay Types in Sorbent-Modified Biodegradability Studies with Cationic Biocides

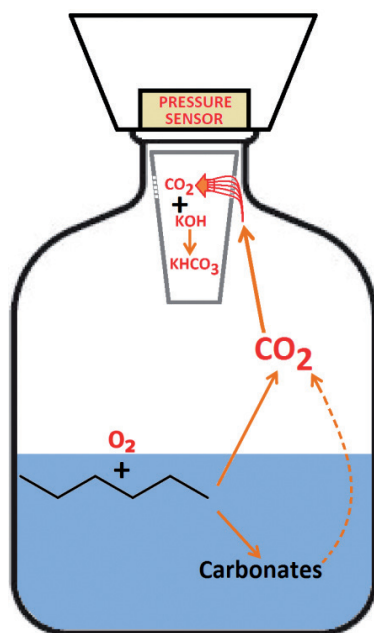
### Additional information on experimental procedures

The OECD 310 Headspace Test can be used to determine the extent to which a chemical is mineralized to CO<sub>2</sub> by microbial action in an inoculated medium.[140] Concentrated stock solutions to prepare mineral salts medium were always prepared ≤5 days before the start of the incubation period. Each batch of mineral salts medium was prepared <1 h before use, using freshly dispensed ultrapure water (MilliQ; PURELAB flex, ELGA LabWater, High Wycombe, UK) and respective volumes of the four stock solutions; preparation is described in the OECD Guidelines.[139, 140] Freshly prepared mineral salts medium always had a pH of 7.4±0.2, a buffer capacity of 4 mM, and a divalent cation concentration (as Mg<sup>2+</sup>) of approximately 0.1 mM.

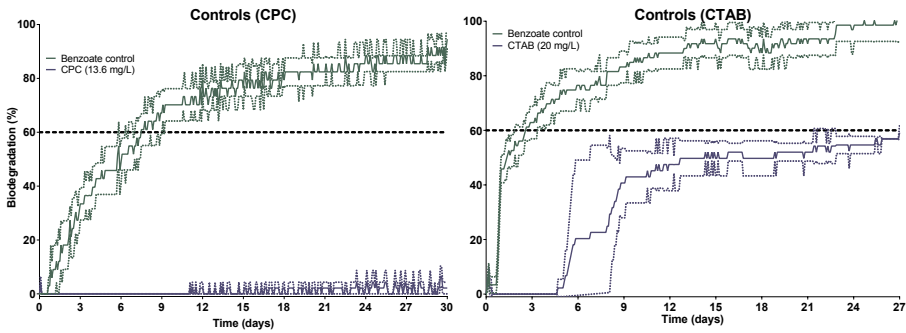
Borosilicate glass serum bottles (125 mL; Wheaton, New Jersey, USA) were spiked with stock solution in acetone, loosely covered with analytical tissue paper, and left standing overnight to allow the acetone to evaporate. Nitrogen gas was used to gently flush out remaining acetone vapor. Bottles for the positive control were spiked directly with sodium benzoate stock solution. Weighed amounts of dried sorbent were then transferred to appropriate bottles, followed by the addition of 50 mL mineral medium using a Perimatic Premier precision dispensing pump (Jencons Scientific Ltd, VWR, East Grinstead, UK), fitted with a re-circulation loop. Bottles were loosely capped with 20 mm butyl rubber stoppers (Sigma-Aldrich) and left to stand at room temperature (20.0±1.0 °C) for at least two h to allow the CPC to dissolve and interact with the sorbent material. Dummy vessels were filled with a second 50 mL aliquot of mineral medium, while other vessels were filled with 50 mL of mineral medium inoculated with 20 mL/L of inoculum treated as described above, resulting in a 64 mL headspace. Each vessel was capped using butyl rubber stoppers and aluminum crimp caps (Sigma-Aldrich), after which bottles were transferred to HT Multitron stackable incubators (Infors AG, Bottmingen, Switzerland). These incubators were set for orbital shaking at 100 rpm at 22.0±1.0 °C.

## Background of OECD 301F

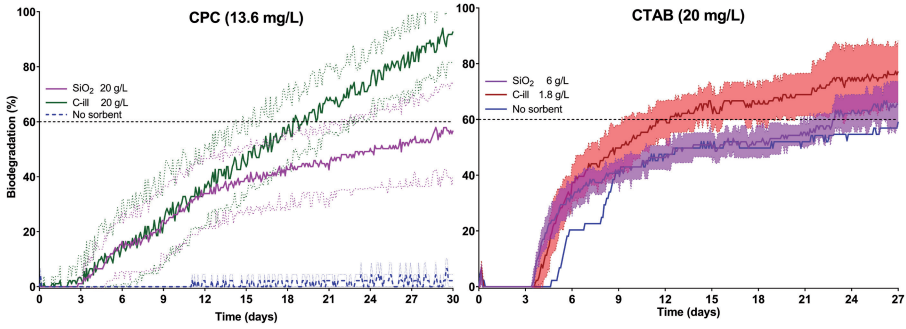
The molecular formula of the substrate can be used to determine the Theoretical Oxygen Demand (ThOD), which indicates how much oxygen is needed to fully mineralize the whole molecule. Together with substrate concentration the ThOD can be used to convert measured oxygen consumption into percentage biodegradation. The OECD 301F Manometric Respirometry Test describes how biodegradation can be quantified by a change in pressure when the resulting  $\text{CO}_2$  is absorbed by a suitable adsorbent e.g. sodium or potassium hydroxide.[139] The OECD 301F relies on a manometer built into a measurement device which can be directly screwed onto suitable vessels, sealing the contents (see Figure S1). Biodegradation of an organic molecule consumes oxygen and produces  $\text{CO}_2$  which is released from solution or converted further into carbonates ( $\text{CO}_3^{2-}$ ).  $\text{CO}_2$  in the headspace eventually comes into contact with e.g.  $\text{KOH}$ , which reacts with the  $\text{CO}_2$  to form  $\text{KHCO}_3$  and, ultimately,  $\text{K}_2\text{CO}_3$ . The net effect is a decrease in air pressure, as gaseous oxygen is converted into solid carbonates. The measuring head contains a pressure sensor and automatically converts measurements of decreasing air pressure into oxygen consumption.



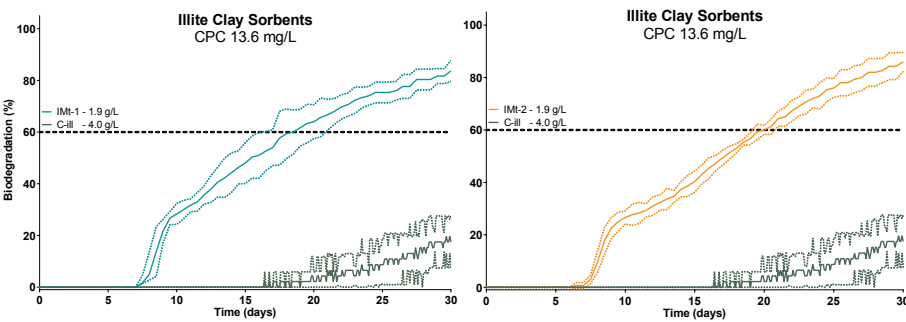
**Figure S1:** Schematic representation of AutMR system.



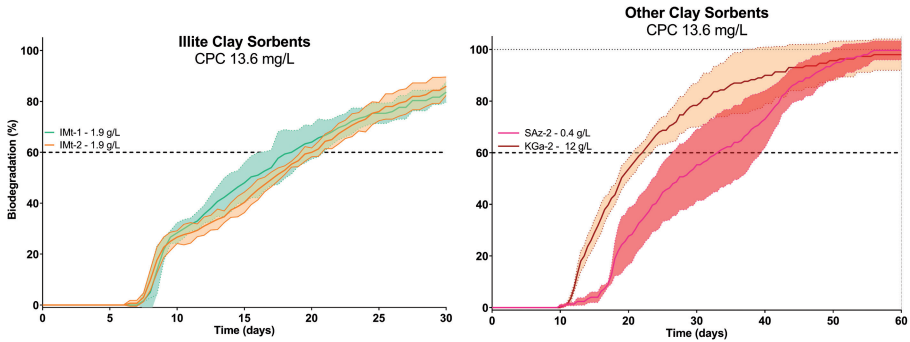
**Figure S2 (left):** Benzoate control and 13.6 mg/L CPC without sorbent. Mean  $\pm$  SD. **Figure S3 (right):** Benzoate control and 20 mg/L CTAB without sorbent. Mean  $\pm$  SD.



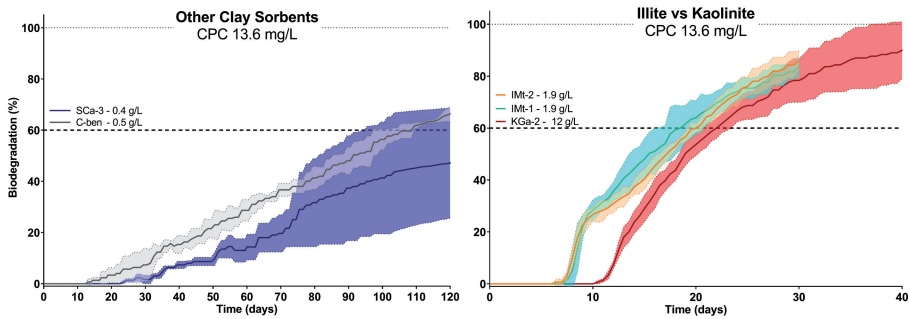
**Figure S4 (left):** Results of 13.6 mg/L CPC with no sorbent and at 20 g/L SiO<sub>2</sub> or 20 g/L C-ill (Illite). Mean  $\pm$  SD. **Figure S5 (right):** Results of 20 mg/L CTAB with no sorbent and at 6 g/L SiO<sub>2</sub> or 1.8 g/L C-ill (Illite). Mean  $\pm$  SD. SD area fill has been applied to SiO<sub>2</sub> and C-ill to emphasize overlap.



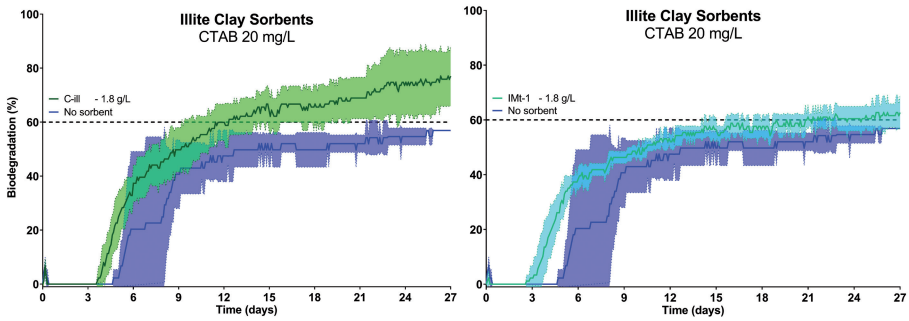
**Figure S6 (left):** Results of 13.6 mg/L CPC with 1.9 g/L IMt-1 (Illite) and 4 g/L C-ill (Illite). Mean  $\pm$  SD. **Figure S7 (right):** Results of 13.6 mg/L CPC with 1.9 g/L IMt-2 (Illite) and 4 g/L C-ill (Illite). Mean  $\pm$  SD.



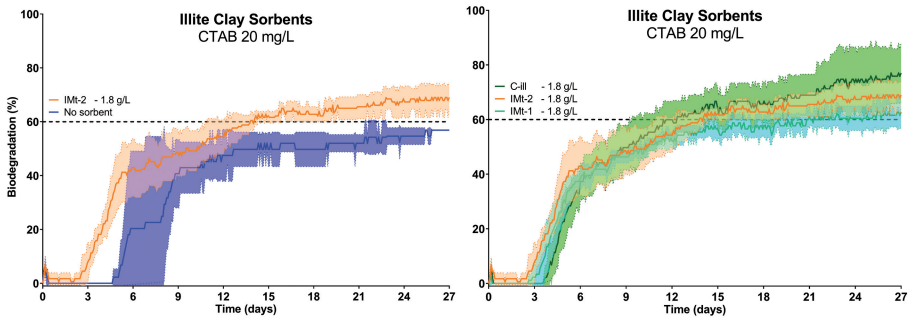
**Figure S8 (left):** Results of 13.6 mg/L CPC with 1.9 g/L IMt-1 (Illite) and 1.9 g/L IMt-2 (Illite). Mean  $\pm$  SD. SD area fill has been applied to emphasize overlap. **Figure S9 (right):** Results of 13.6 mg/L CPC with 12 g/L KGa-2 (Kaolinite) and 0.4 g/L SAz-2 (Ca-Montmorillonite). Mean  $\pm$  SD. SD area fill has been applied to emphasize overlap. It can be observed variability is highest in the second half of the biodegradation phase, and decreases again when plateau is approached.



**Figure S10 (left):** Results of 13.6 mg/L CPC with 0.4 g/L SCa-3 (Montmorillonite) and 0.5 g/L C-ben (Bentonite). Mean  $\pm$  SD. SD area fill has been applied to emphasize overlap. Variability is low for C-ben and the first 60 days for SCa-3, but increases significantly in the second half of the SCa-3 curve. This could be indicative of inoculum instability after prolonged incubation in a sealed system. **Figure S11 (right):** Results of 13.6 mg/L CPC with 1.9 g/L IMt-1 (Illite) and 1.9 g/L IMt-2 (Illite), compared with 12 g/L KGa-2 (Kaolinite). Mean  $\pm$  SD. SD area fill has been applied to emphasize overlap.

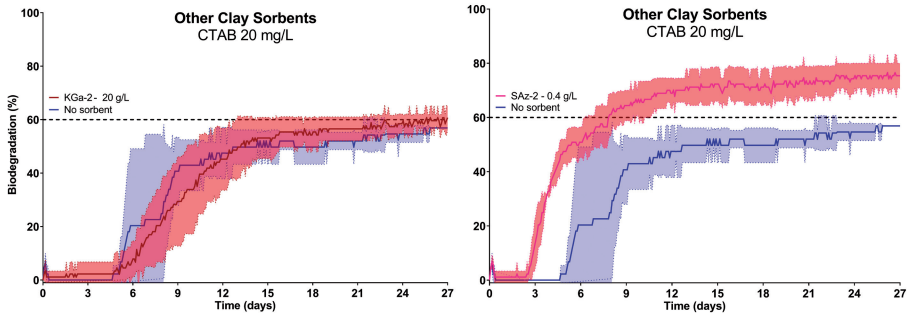


**Figure S12 (left):** Results of 20 mg/L CTAB with 1.8 g/L C-III (Illite) and no sorbent. Mean  $\pm$  SD. SD area fill has been applied to emphasize overlap. **Figure S13 (right):** Results of 20 mg/L CTAB with 1.8 g/L IMt-1 (Illite) and no sorbent. Mean  $\pm$  SD. SD area fill has been applied to emphasize overlap.

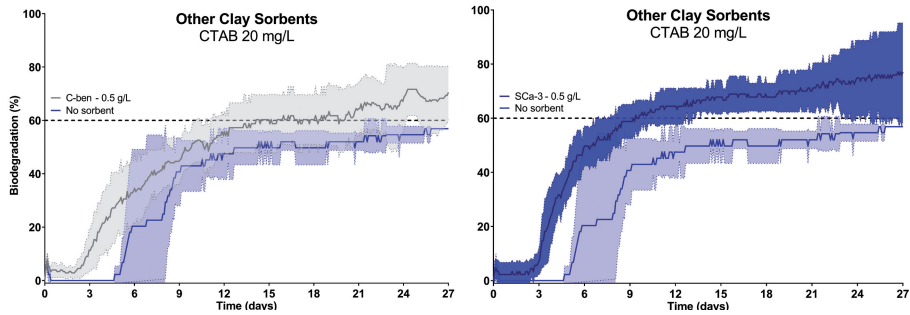


**Figure S14 (left):** Results of 20 mg/L CTAB with 1.8 g/L IMt-2 (Illite) and no sorbent. Mean  $\pm$  SD. SD area fill has been applied to emphasize overlap. **Figure S15 (right):** Results of 20 mg/L CTAB with 1.8 g/L C-III (Illite), 1.8 g/L IMt-1 (Illite), and 1.8 g/L IMt-2 (Illite). Mean  $\pm$  SD. SD area fill has been applied to emphasize overlap.

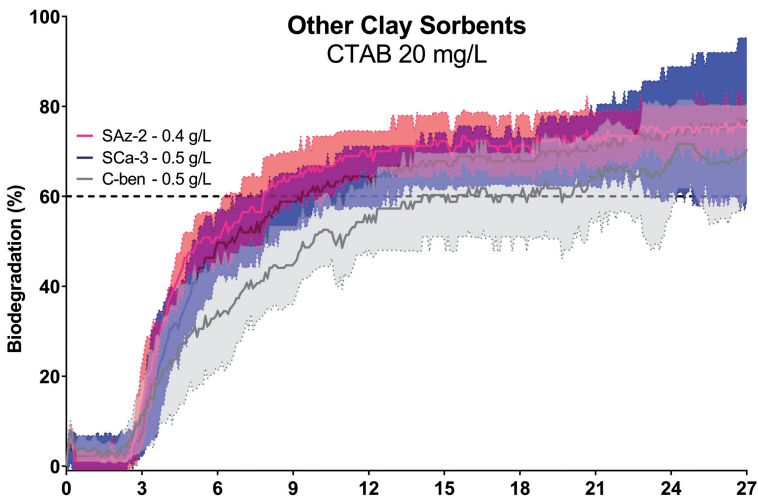




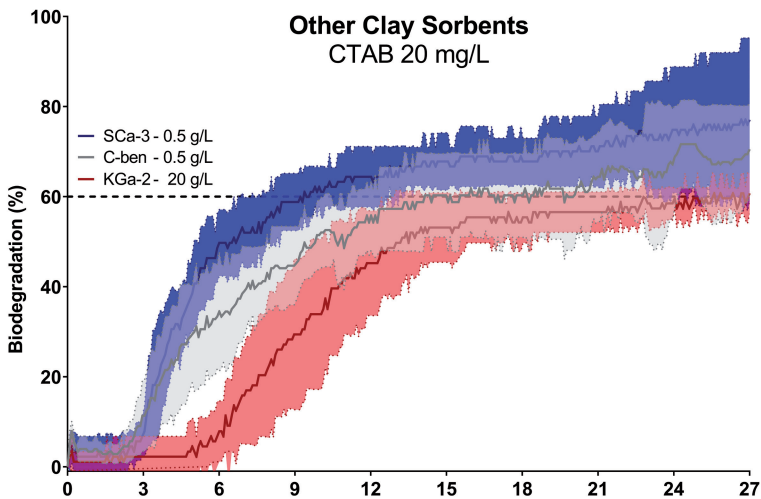
**Figure S16 (left):** Results of 20 mg/L CTAB with 20 g/L KGa-2 (Kaolinite) and no sorbent. Mean  $\pm$  SD. SD area fill has been applied to emphasize overlap. **Figure S17 (right):** Results of 20 mg/L CTAB with 0.4 g/L SAz-2 (Ca-Montmorillonite) and no sorbent. Mean  $\pm$  SD. SD area fill has been applied to emphasize overlap.



**Figure S18 (left):** Results of 20 mg/L CTAB with 0.5 g/L C-ben (Bentonite) and no sorbent. Mean  $\pm$  SD. SD area fill has been applied to emphasize overlap. **Figure S19 (right):** Results of 20 mg/L CTAB with 0.5 g/L SCa-3 (Montmorillonite) and no sorbent. Mean  $\pm$  SD. SD area fill has been applied to emphasize overlap.



**Figure S20:** Results of 20 mg/L CTAB with 0.4 g/L SAz-2 (Ca-Montmorillonite), 0.5 g/L SCa-3 (Montmorillonite), and 0.5 g/L C-ben (Bentonite). Mean  $\pm$  SD. SD area fill has been applied to emphasize overlap.



**Figure S21:** Results of 20 mg/L CTAB with 0.5 g/L SCa-3 (Montmorillonite), 0.5 g/L C-ben (Bentonite), and 20 g/L KGa-2 (Kaolinite). Mean  $\pm$  SD. SD area fill has been applied to emphasize overlap.





# CHAPTER 9

---

## Summary and General Discussion

The scope of my project was to improve environmental risk assessment of cationic chemicals, specifically looking at cationic surfactants. In order to achieve this, I tried to improve understanding of the behavior of cationic surfactants and the mechanisms that underlie their sorption to environmentally relevant matrices. In addition, I devoted a significant portion of my project to elucidate the impact of sorption on bioavailability, bioaccessibility, and toxicity in biodegradability studies as well as *in vitro* toxicity assays. The summary and discussion below will illustrate how the various objectives associated with the scope of this project were handled, placing my findings in perspective of environmental risk assessment.

### **Analytical Challenges: Avoiding Losses in Aqueous Samples**

As described in **Chapter 1**, one of the main goals of my project was to identify analytical limitations and the challenges when using typical laboratory techniques to analyze cationic surfactants in various samples. In order to evaluate these challenges, first analytical methods for the selected cationic surfactants needed to be developed. For most cationic surfactants the LC-MS/MS performed best for concentrations between 5 nM and 20  $\mu$ M. Since all aqueous samples were diluted 1:4 with an acidic eluent solvent mixture (90% methanol with 0.1% (v/v) TFA), the effective LOQ for aqueous samples was approximately 20 nM (**Chapter 2**). For analysis by LC-MS/MS, samples should contain virtually no inorganic salts or suspended colloidal material. In order to properly isolate and concentrate cationic surfactants from aqueous samples, the performance of a weak-cation exchange (WCX) based solid phase extraction (SPE) column was evaluated in detail. Oasis WCX-SPE columns displayed a recovery  $\geq 80\%$  for all 30 cationic surfactants tested, and  $\geq 90\%$  for 16 of these (**Chapter 2**). These relatively high recoveries prove my SPE protocol can thus be used to extract cationic surfactants from aqueous samples. I was also able to prove strong retention of analyte when flushing the SPE columns with solvents at neutral pH to remove organic neutral components, and flushing the SPE columns with acidified water to remove inorganic salts. My results further indicate that WCX material is also effective for complex technical cationic surfactant mixtures and environmental samples, as long as the ion-exchange capacity of the WCX material is not exceeded.

Glass binding of simple primary and quaternary amines was found to correlate with alkyl chain length, and increases considerably above a certain alkyl chain length. Losses from the aqueous phase to the glass surface were highest in small volume autosampler vials (1.5 mL), which is probably related to the higher surface-to-volume ratio for small volume

vials. At a nominal concentration of 0.3  $\mu\text{M}$  I observed binding of 40% at an alkyl chain length of 12 carbon atoms for QACs, while for primary amines binding approached 60%. However, losses in larger volume vessels can still be considerable (20-60%) for alkyl chain lengths of  $\geq 16$  carbon atoms (**Chapter 2**). As expected based on the charge delocalizing effect of methylated headgroups, the sorptive effects appear to be more challenging for ionizable amines in comparison with analogue quaternary ammonium compounds (QACs), and are concentration dependent due to saturation of surface sorption sites. This means that for small volume vials such as autosampler vials, relative losses become smaller at higher concentrations, and are generally lower for QACs of comparable alkyl chain lengths. Obviously, if these effects are not taken into consideration, actual freely dissolved concentrations in either test systems or samples for analysis may be up to an order of magnitude lower than intended.

I also found significant binding of cationic surfactants to the outside of pipette tips, which might be co-extracted upon transferring samples to solvent containing vials. Pipette tip binding was only significant for longer alkyl chain lengths – with sorption of 10-20%, I expect issues for alkyl chain lengths  $\geq 18$  carbon atoms – and showed a more pronounced concentration dependency than glass binding (**Chapter 2**). Still, the combination of pipette tip binding and sorption to glassware can significantly decrease the freely dissolved concentration in aqueous samples and interfere with mass balance based calculations. The impact of surfactants sorbing to the outside of pipette tips can be diminished by not submerging the pipette tip in the sample solution during pipetting. The impact of surfactant sorbing to the inside of pipette tips can be minimized by always transferring samples to solvent, flushing the pipette tip several times with this solvent. This would simultaneously serve to prevent binding of cationic surfactant to the glass wall of sample vials.

### **Suitability of SPME to Sample Cationic Surfactants**

Recent studies from our lab indicated that freely dissolved cationic surfactants were readily equilibrating with polyacrylate solid-phase microextraction (PA-SPME) samplers [78, 79, 172]. This should allow for accurate measurements of dissolved concentrations in all kinds of suspensions used in sorption or toxicity studies, without pipetting aqueous samples or using WCX-SPE columns, as long as partitioning coefficients between PA-SPME fibers and dissolved concentrations are constant and well-established. I thus aimed to establish PA-SPME sorption coefficients for a wide range of cationic surfactants by testing various

structural families. However, when performing passive sampling experiments with PA-SPME for the series of cationic surfactants described previously, I found relatively large (>1 order of magnitude) variability, seemingly dependent on alkyl chain length as well as number of alkyl chains (**Chapter 2**). The used batch of PA-SPME fibers was therefore deemed unsuitable to determine freely dissolved concentrations for compounds with an alkyl chain length  $\geq 14$  carbon atoms, and I strongly advise to include calibration sets within each experiment.

PA-SPME uptake kinetics for a QAC and a primary amine, both with an alkyl chain length of 12 carbon atoms, were sufficiently rapid to use overnight exposure, although uptake of the neutral form of the primary amine was slower; an effect that increases in significance with increasing coating thickness, supporting my hypothesis that the neutral form is absorbed rather than adsorbed. I therefore advise that implementation of the PA coating at alkaline pH should be subject to additional testing, although it should be noted that the impact of coating thickness was much less significant at alkaline pH. Ionic composition of exposure medium was also investigated, and I conclude that shifting from 100 mM Na<sup>+</sup> to 10 mM Ca<sup>2+</sup> leads to an order of magnitude decrease of apparent affinity for the PA-SPME fiber for both the QAC and the primary amine. Since I also found minor pH-dependence of fiber affinity with the QAC, the number of ion-exchange groups on the PA coating surface may not be constant, as surface acid groups with pK<sub>a</sub> values between 6 and 10 likely exist. This further underscores our advice to always include a calibration set in the exact same media as applied in the test samples. However, the observed high variation in SPME replicates – up to 0.8 log units between fibers exposed to the same aqueous concentration – should be taken into account when using this sampling material. Since the surface properties of PA remain unclear, we suggest that other ion-exchange based samplers may prove to have more consistent sampling efficiency.

### **Further Passive Sampler Evaluations with Organic Cations**

In the quest for a suitable SPME sorbent material for cationic surfactants, I determined sorption affinity to the alternative ion-exchange sampler material C18/SCX (based on propylsulfonate) for several series of cationic C<sub>x</sub>H<sub>y</sub>N structures, mostly smaller compounds with an alkyl chain length up to 12 carbon atoms. These simple cationic structures allowed for straightforward evaluation of the influence amine type, alkyl chain length, presence of an aromatic ring, and alkyl chain branching on sorption affinity. Aqueous concentrations used to construct sorption isotherms spanned at least two orders of magnitude, and show



nonlinear sorption above fiber concentrations of 10 mmol/L, hinting at competition effects when sorption sites become saturated. I conclude sorption to the C18/SCX fiber is linear up to a fiber concentration of 1 mmol/L, as slopes of the resulting isotherms were close to 1 on a logarithmic scale (**Chapter 3**). Using the sorption affinities as extracted from these isotherms, I was able to estimate fragment contribution values for aliphatic carbons, aromatic carbons, and charged nitrogen moieties. Lower sorption affinity of QACs due to the more extensive charge localization around the nitrogen atom could also be explained with my data set. Significant contribution of neutral species could be ruled out, since all amines were tested as  $\geq 99.9\%$  ionized.

The cationic surfactant with the longest alkyl chain tested with the C18/SCX fiber was a diethanolamine with an alkyl chain length of 12 carbon atoms (C12-DEA). C12-DEA had a fiber/water distribution coefficient of  $\sim 35,000$ . This leads me to hypothesize that the applicability domain of the C18/SCX fiber for cationic surfactants is limited to alkyl chain lengths of 14 or perhaps 16 carbon atoms. In case of longer alkyl chain lengths SPME with C18/SCX fibers will become exhaustive. For such analytes, a large polymer backbone with a lower density of SCX groups or utilization of weak cation exchange material might be better. The use of porous coatings can significantly increase the exposed surface area, which will enhance sorption efficiency, especially for cationic surfactants. However, for longer alkyl chain lengths this might be counterproductive, as sorption affinity will likely become too high.

Together with several environmental toxicologists and exposure scientists from IRAS that were all interested in developing a sampler tool for organic cations, I then tested a set of 14 different pharmaceuticals, most of which were  $\geq 98\%$  cationic at test pH, and found relatively high sorption affinities to the C18/SCX fiber (**Chapter 3**). Considering the fact that ionized compounds have relatively high aqueous solubility, most cationic species sorbed stronger than expected. Especially for neutral benzodiazepine compounds, sorption affinity appears to be unrelated to  $K_{OW}$ . This underscores the importance of relevant molecular descriptors as an alternative for  $K_{OW}$ , as further described and elucidated in **Chapter 5**. Interestingly, the anionic diclofenac also showed substantial sorption to the C18/SCX fiber, while it was expected the negatively charged SCX groups would repulse anionic molecules. Testing nicotine, difenzoquat, and verapamil we were able to obtain similar or better results with the C18/SCX fiber than with ion exchange membranes [219], although the cation exchange capacity is lower and sorption therefore levels off at lower sorbed concentrations. I hypothesize that these improved results might be due to the porosity of

the C18/SCX fiber coating, which allows increased accessibility for high molecular weight compounds (**Chapter 3**). However, this increased porosity may also have disadvantages such as fouling with serum albumin, which was indeed found to be higher than for ion exchange membranes at high serum albumin concentrations.

### **Cytotoxic Potency Ranking of Cationic Surfactants with Increasing Alkyl Chain Lengths**

The sorption of cationic surfactants to laboratory equipment and other surfaces can also cause difficulties when interpreting the results of *in vitro* toxicity assays. Sorption to well plate plastic, pipette tips (during dosing as well as sampling; **Chapter 2**), and medium constituents such as serum albumin (**Chapter 4**) can significantly decrease the freely dissolved exposure concentration, while nominal concentrations are regularly used to extract toxicity parameters. I therefore decided to use a series of benzalkonium chloride surfactants with increasing alkyl chain length to evaluate and quantify how nominal concentrations correspond with actual exposure concentrations. I decided to use a cell assay that does not require the use of serum-enriched medium during exposure. This allowed using a simple and clear medium containing mostly dissolved salts and nutrients, absolving the need to employ SPME or sample clean up techniques.

By using measured exposure concentrations rather than nominal concentrations, I was able to determine that toxic potency of benzalkonium chlorides increases with alkyl chain length, while the extent of binding to well plate plastic is also dependent on alkyl chain length. Thus, the impact of plastic sorption on apparent cytotoxicity increases significantly for more hydrophobic compounds. My results further show that sorption to serum constituents can also influence apparent toxic potency. For alkyl chain lengths  $\leq 10$  carbon atoms nominal concentrations are suitable to describe toxic potency, as sorption to well plate plastic and serum constituents is limited. However, with longer alkyl chain lengths the freely dissolved fraction can be reduced by a factor 30 due to these sorptive losses. I also conclude that assay conditions such as cell density, exposure time, and repeated dosing can influence apparent toxic potency as well.

I propose that, based on these findings, the free concentration in exposure medium should be used to evaluate cytotoxic potency of benzalkonium chlorides, and possibly all cationic surfactants, with an alkyl chain length of  $>10$  carbon atoms. The analytical challenges associated with determination of the free concentration far outweigh the impact of

reporting unverified exposure concentrations in toxicity assays, especially if these data are used in further risk assessment. Using intracellular or membrane concentrations to evaluate cytotoxic potency may further improve comparability of results between assays, and allows for accurate extrapolation from *in vitro* results to *in vivo* effects. While it is obviously difficult to quantify intracellular or membrane concentrations of surfactants analytically, some algorithms have been developed that can model distribution of chemicals in *in vitro* systems. However, since these models usually ultimately rely on a conversion factor based on  $K_{ow}$ , we conclude such models are not yet very well applicable to surfactants with their amphiphilic properties. Once future studies gather more data for cationic compounds (e.g. surfactants, biocides, and pharmaceuticals) on sorption to well plate plastic and medium constituents, it may also be possible to predict or model the extent of sorption using an appropriate input parameter.

### Membrane Water Partitioning Coefficients As Replacement For $K_{ow}$

As  $K_{ow}$  is not a suitable parameter to model the sorptive behavior of cationic surfactants (**Chapter 1**), it is necessary to identify a feasible alternative hydrophobicity parameter, which can directly support risk assessment modeling. Phospholipid-water partitioning is a likely candidate to be a suitable input parameter for all kinds of models, especially models concerning binding to cell membranes of all living organisms. In order to determine sorption to membrane lipids, I used a commercially available solid-supported lipid membrane (SSLM) test kit, in which macroporous silica beads are coated with a phospholipid bilayer. Due to the high density of the fused silica core, these beads can be easily separated from the aqueous phase by centrifugation, rendering the aqueous compartment accessible for sampling. In order to apply the SSLM approach for cationic surfactants, I first optimized the existing SSLM protocol in order to overcome observed artefacts, as well as potential issues when applying SSLM to cationic surfactants. By transferring SSLM beads from well plate to autosampler vials, I was able to facilitate analysis and gain more control over the aqueous phase constituents (e.g. use of different buffer). An incubation time of 30 minutes was deemed sufficient to obtain sorption equilibrium. Overnight stability of centrifuged sample solution in autosampler vials was also confirmed, allowing for HPLC injections directly from the supernatant in the autosampler, which circumvents possible pipetting artefacts (**Chapter 1**). The pH dependent surface charge effects observed with silica-based stationary phases in immobilized artificial membrane (IAM) HPLC columns were ruled out for SSLM,[120] ensuring measurements in PBS relate to the partitioning coefficient of the ionic species into phospholipid bilayers only.

My first series of experimental data with SSLM, however, suggested phospholipid leakage of approximately 1% in the well plate strips after thawing, influencing sorption isotherms for compounds with  $D_{MW} > 10,000$  L/kg (**Chapter 5**). This was observed in distinct sorption nonlinearity in original SSLM test solutions in the sorbent dilution series. Comparing a model assuming 1% leakage with these nonlinear isotherms confirmed my hypothesis, and confirmed that leakage increased the phospholipid content in the SSLM supernatant in a series with increasing sorbent. By renewing the original test kit medium with new medium, I was also able to simply remove third phase liposome artefacts caused by leaching of detached SSLM phospholipid material. I believe this finding of phospholipid leaching to be quite important, and my suggested solution of medium/buffer renewal will be of high significance for future experiments testing molecules with expected  $D_{MW} > 10,000$  L/kg, which is in the range of cationic surfactants with alkyl chain lengths of more than 10 carbon atoms.

### **Limitations of the SSLM Assay**

I was able to demonstrate consistent and reproducibly constant phospholipid partitioning over multiple orders of magnitude by testing two or more conjoined SSLM dilution series using 16 different cationic surfactants, which were all tested well below their critical micelle concentration. By using methanol controls and extracts I could also prove that impact of glass binding did not contribute significantly to resulting  $D_{MW}$  values. With the two SSLM sorbent dilution series obtained as commercially available kits, I was able to test  $D_{MW}$  values above 1000 and 50 L/kg, respectively. At  $D_{MW}$  values above 300,000 L/kg ( $\log D_{MW} \geq 5.5$ ), however, the balance between maximum allowable sorbed membrane concentration and the detection limit becomes critical, as the resulting aqueous concentration in the sorbent dilution series approaches the limit of detection at such high sorption affinities. In practice, this means that most single chain alkylamines and benzalkonium compounds can be tested up to an alkyl chain length of 12 carbon atoms, trimethylalkylammonium compounds up to an alkyl chain length of 14 carbon atoms, and secondary dialkylamines up to 8 carbon atoms per alkyl chain. It should be noted that the applicability domain of SSLM is not limited to cationic surfactants; recent developments have shown high-quality results with anionic surfactants and perfluoroalkyl anions.[118]

## Deriving QSARs and Comparison with Molecular Simulations

Ultimately, I used the data obtained for 19 compounds to derive a simple QSAR, taking into account head group type and alkyl chain length (**Chapter 5**). The QSAR was able to fit all compounds within a factor 3 of their experimental value, which is likely stemming from the fact that most cationic surfactants have relatively simple molecular structures with one or more alkyl chains. Development of a more broadly applicable QSAR would benefit from inclusion of more poly-alkyl compounds, and perhaps headgroups supplemented with additional hydrophilic moieties e.g. ethanolamine. The fragment value for  $\text{CH}_2$  units of 0.6 log units seemed to be higher than expected based on analogue series of neutral compounds, although I expect  $\text{CH}_2$  units closer to the headgroup to contribute less to overall  $D_{\text{MW}}$ . Also, consistently decreasing  $D_{\text{MW}}$  with increasing methylation of the headgroup was observed, contrasting typical  $D_{\text{OW}}$  based predictions. On the other hand, the benzalkonium headgroup increases  $D_{\text{MW}}$  by an order of magnitude. I also found that IAM-HPLC likely accounts insufficiently for the observed effect of headgroup methylation on  $D_{\text{MW}}$ . Considering the SSLM bilayer is relatively fluid and mobile while IAM-HPLC consists of covalently bound monolayers, we suggest applying corrective increments on IAM-HPLC results.

Recent advancements in computer simulations using COSMOmic software provide for another alternative way of deriving  $D_{\text{MW}}$  values for cationic surfactants, for example in the absence of adequate testing material or as a relatively inexpensive pre-screening phase. An important advantage of the COSMOmic approach is that it accounts for both ionic properties of a chemical and the chemical's three dimensional structure in its ideal position in the anisotropic membrane phase. Although slight differences between COSMOmic and SSLM data were observed, we conclude COSMOmic is able to correctly predict the effect of headgroup methylation on  $D_{\text{MW}}$ . Scaling factors extracted from the QSAR model I constructed also correspond closely with commonly used  $K_{\text{OW}}/D_{\text{OW}}$  based approaches used for organic bases, although my results with dialkylamines indicate that a single scaling factor cannot be applied to all secondary amines, as the presence of a second alkyl chain will impact  $D_{\text{MW}}$  very differently from that of a  $D_{\text{OW}}$  approach. For example, the  $D_{\text{MW}}$  of dihexylamine (total  $\text{C}_{12}$ ) is 2.2 log units lower than that of the single chain analogue N-methyldodecylamine ( $\text{C}_{12+\text{N}}$ ), while a difference in  $D_{\text{OW}}$  of only 0.5 log units is expected (based on one additional  $\text{CH}_2$ ). Dialkylamines are therefore of unique value to cross-validate different tools, as only the tools with truly high predictive value for actual

sorption to naturally occurring phospholipid membranes will be able to correctly predict sorption behavior of dialkylamines.

### **Sorbent-Modified Biodegradation of CTAB**

Biodegradability studies are usually not supported with specific analyses, but employ various methods to determine production of CO<sub>2</sub> or consumption of O<sub>2</sub>. The relatively high test concentrations required for such analyses can be problematic for chemicals that can exert toxic or inhibitory effects, such as long-chain cationic surfactants. I hypothesized this issue could be tackled in a stepwise approach, first determining a non-toxic concentration, then finding a suitable sorbent and determining the required sorbent concentration to mitigate potential inhibitory effects, and lastly running a biodegradability study employing a suitable amount of sorbent. I decided to first perform these steps with CTAB, as this compound has been used previously in an OECD ring trial where inhibitory effects were mitigated using silicon dioxide.[140]

I first determined the approximate concentration at which CTAB inhibits degradation of the reference compound aniline, which is 0.3 mg/L and up to two orders of magnitude lower than the recommended test concentration in standard biodegradation test protocols. Combining this data with sorption coefficients determined for SiO<sub>2</sub> and illite clay, I was able to calculate how much sorbent to add to test systems to render freely dissolved concentrations below the threshold of inhibition. However, when testing this approach in a degradation experiment a high biodegradation rate of CTAB at 16.8 mg/L was observed. This might have been caused by CTAB selectively inhibiting aniline degrading microbes in the first experiment, or heterogeneity between the batches of inoculum prepared for these two experiments. As toxicity mitigation could not be evaluated in the absence of inhibitory effects, I decided to focus on lag-phase and bioaccessibility instead. In all sorbent groups the lag-phase was decreased, although some bioaccessibility effects were apparent at high sorbent concentrations. Average mass-balances were >90% for all treatment conditions. Sorbed fractions were in the same order of magnitude as what was expected based on the sorption experiment. However, glass binding was lower than what was expected based on the work described in **Chapter 2**. I also found that more extensive subsampling could increase recovery of sample combustion. Overall, I was able to demonstrate that with addition of a carefully determined amount of sorbent, it is possible to decrease freely dissolved concentration of a potentially inhibitory substrate to levels below the threshold of inhibitory effects. More specifically, for CTAB I can conclude that addition of a suitable

amount of sorbent had a substantial impact on the likelihood of satisfying the criteria for ready biodegradability.

### **Sorbent-Modified Biodegradation of CPC**

I observed ready biodegradability for CPC at concentrations  $\leq 100 \mu\text{g/L}$ , with indications of slight inhibitory effects at  $300 \mu\text{g/L}$  and strong inhibitory effects at higher concentrations (**Chapter 7**). Together with the experimentally determined  $\log K_D$  for  $\text{SiO}_2$  and illite clay (3.5 and 4.5, respectively), I decreased the freely dissolved concentration to below  $100 \mu\text{g/L}$  with additions of  $\text{SiO}_2$  and illite, when incubating CPC at nominal concentrations of  $1 \text{ mg/L}$  and  $10 \text{ mg/L}$ . CPC at  $100 \mu\text{g/L}$  was also incubated with  $\text{SiO}_2$  to assess bioaccessibility limitations, which I found at  $4 \text{ g/L}$  and  $20 \text{ g/L}$  and seemed to be concentration-dependent. At  $1 \text{ mg/L}$  I observed a three week lag-phase, which could be reduced significantly by applying  $\text{SiO}_2$  as a mitigating sorbent, although I still observed bioaccessibility limitations at  $20 \text{ g/L SiO}_2$ . With illite as mitigating sorbent bioaccessibility seemed to hinder biodegradation already at  $4 \text{ g/L}$ , while inhibitory effects were successfully mitigated at  $0.8 \text{ g/L}$ . CPC at  $10 \text{ mg/L}$  was not sufficiently bioaccessible with  $20 \text{ g/L}$  illite, while gradual biodegradation was observed with  $20 \text{ g/L SiO}_2$ . Except for the  $10 \text{ mg/L}$  CPC samples, mass balances after 28 days of incubation were  $>80\%$ ; freely dissolved concentrations and amounts associated with sorbents were generally in agreement with expectations, which supports the suitability of my stepwise approach. However, I conclude there is a balance between mitigating effects and bioaccessibility limitations, which means appropriate sorbents and sorbent concentrations need to be established to maximize efficacy.

### **Optimizing the Sorbent-Modified Biodegradation Approach**

Using automated manometric respirometry (AutMR) test systems, I exposed  $13.6 \text{ mg/L}$  CPC and  $20 \text{ mg/L}$  CTAB to seven clays sorbents, most of which were obtained from the Clay Minerals Society (CMS). Some of these clays were expansive or swelling clays, which can take up water in the interlayer between clay mineral sheets, causing them to increase in size significantly. Two batches of CMS illite (IMt-1 and IMt-2) and CMS kaolinite (KGa-2) provided optimal equilibrium between toxicity mitigation and bioaccessibility. Application of IMt-1 and KGa-2 successfully mitigated inhibitory effects and biodegradation was sufficient to satisfy the criteria required to label CPC as readily biodegradable. With commercial bentonite (C-ben) and CMS montmorillonite (SCa-3), two swelling clays, I found a lag-phase followed by gradual biodegradation. This is indicative of bioaccessibility limitations,

potentially caused by sorption of CPC in the poorly accessible interlayer. This effect was not observed for the CMS montmorillonite SAz-2; for this specific clay type the replacement of  $K^+$  and  $Na^+$  with  $Ca^{2+}$  might have impacted sorption behavior in the interlayer, which could have helped to maintain bioaccessibility. Overall, I observed mitigation of CPC inhibitory effects with all clay types tested, with increases in biodegradability and biodegradation rates in all instances (**Chapter 8**). Significant differences with results obtained with previous biodegradation experiments in **Chapter 7** are likely due to the application of stirring in the manometric respirometry test systems, which is likely to have enhanced desorption kinetics [379].

When exposing the same seven clay sorbents to 20 mg/L CTAB, I found extensive biodegradation in the control vessels without sorbent. Sorbent efficacy was therefore evaluated by considering effects on lag-phase and plateau height. IM-1 and IMt-2 as well as the commercial illite C-ill all lead to faster biodegradation of CTAB. The observed plateau was 5-19% higher than control, which strongly indicates there were no bioaccessibility limitations. KGa-2 barely influenced plateau height or lag-phase duration, which is a remarkable difference with the results for CPC and KGa-2. The results I obtained for CTAB with SAz-2 and SCa-3 also indicate sufficient bioaccessibility, and with 19% higher plateau than control provide additional evidence that addition of suitable clay types can impact apparent biodegradability. Lastly, C-ben leads to a 13% higher plateau, with kinetics that are more comparable to the illite clays. Overall, for CTAB I conclude that, with addition of sorbents, biodegradation curves are steeper and lag-phases are shorter (**Chapter 8**). Although my results indicate different efficacy per clay type when comparing CPC with CTAB, available literature suggests these findings are not uncommon [366, 399-404, 434]. In my opinion the beneficial effects observed with application of clays could also be driven by biofilm formation. Although biofilm formation could not be evaluated in my thesis, elucidation of the extent and impact of biofilm formation in clay-amended biodegradability studies would help to further advance understanding of the underlying mechanisms. The sampling resolution and flexibility offered using AutMR systems makes them an excellent test system for biodegradability testing, especially for challenging compounds – such as cationic surfactants – which may require specifically designed test methods or prolonged test designs.



## General Conclusion

Altogether, the work presented in this thesis is relevant to improve environmental risk assessment of cationic surfactants. Insights from **Chapter 2 and 3** are undoubtedly relevant and are vital to understand the general behavior of cationic molecules, although not all aspects will be applicable for all cationic molecules. All cationic surfactants with an alkyl chain length of  $\geq 16$  carbon atoms are analytically very challenging. Exposure concentrations in experiments with these compounds should be verified if possible. The fact that many molecules are cationic, including pharmaceuticals and high-volume discharged industrial chemicals (**Chapter 1 and 3**), further underscores the significance of improving environmental risk assessment for this group of chemicals. Analytical tools to isolate and/or sample organic cations are available, but require careful calibration at applied testing conditions. Although toxicity and environmental behavior of these chemicals remains to be understood in more detail, the work performed in **Chapter 4 and 5** helps to advance understanding of their behavior within *in vitro* toxicity assays and to identify suitable molecular descriptors (i.e. phospholipid distribution coefficients) for modeling purposes. Phospholipid distribution coefficients appear to be a key molecular descriptor to replace  $K_{ow}$  removing the uncertainties associated with  $K_{ow}$  in risk assessment of cationic surfactants and potentially all cationic molecules. The work on sorbent-modified biodegradation assays allowed us to propose and improve a stepwise sorbent addition approach (**Chapter 6, 7, and 8**). Since negatively charged sorptive surfaces are encountered throughout the environment (e.g. activated sludge, sediment, biomass, dissolved organic carbon), applying a negatively charged but otherwise inert sorbent should increase environmental relevance of the obtained results of biodegradability studies. Automated manometric respirometry systems appear to be most suitable when applying mitigating sorbents in biodegradability studies.

Taken together, this thesis has provided several key insights that should be considered vital to properly handle, sample, and assess cationic surfactants. Since most methods ultimately depend on reliable analytical quantification, my evaluation of analytical challenges and their solutions is a critical addition to existing literature. Correctly applying my findings can prevent order-of-magnitude miscalculations of exposure concentration, (environmental) sample concentration, and apparent *in vitro* toxicity. Equally relevant in the context of environmental risk assessment is the proposed methodology to determine biodegradability using a stepwise sorbent-addition approach, which again can prevent order-of-magnitude underestimation of biodegradability.

## References

- [1] A. Kumar, Global Market for Surfactant Chemicals and Materials, BCC Research, (2018) 1-188.
- [2] Paracelsus, *dritte defensio*, (1538).
- [3] N.R. Council, *Toxicity Testing in the 21st Century: A Vision and a Strategy*, The National Academies Press, Washington, DC, 2007, pp. 216.
- [4] N. Bhogal, C. Grindon, R. Combes, M. Balls, Toxicity testing: Creating a revolution based on new technologies, *Trends in Biotechnology*, 23 (2005) 299-307.
- [5] F.A. Groothuis, M.B. Heringa, B. Nicol, J.L. Hermens, B.J. Blaauboer, N.I. Kramer, Dose metric considerations in in vitro assays to improve quantitative in vitro-in vivo dose extrapolations, *Toxicology*, 332 (2015) 30-40.
- [6] E.P.a. Council, Regulation (EC) No 1907/2006 of the European Parliament and of the Council of 18 December 2006 concerning the Registration, Evaluation, Authorisation and Restriction of Chemicals (REACH), establishing a European Chemicals Agency, amending Directive 1999/45/EC and repealing Council Regulation (EEC) No 793/93 and Commission Regulation (EC) No 1488/94 as well as Council Directive 76/769/EEC and Commission Directives 91/155/EEC, 93/67/EEC, 93/105/EC and 2000/21/EC, *Official Journal of the European Union*, L396 (2006) 1-849.
- [7] S. Endo, B.I. Escher, K.U. Goss, Capacities of membrane lipids to accumulate neutral organic chemicals, *Environmental science & technology*, 45 (2011) 5912-5921.
- [8] S. Trapp, Plant Uptake and Transport Models for Neutral and Ionic Chemicals, *Environmental Science and Pollution Research*, 11 (2004) 33-39.
- [9] D.R.J. Moore, R.L. Breton, D.B. MacDonald, A comparison of model performance for six quantitative structure-activity relationship packages that predict acute toxicity to fish, *Environ Toxicol Chem*, 22 (2003) 1799-1809.
- [10] M. Kah, C.D. Brown, Adsorption of Ionisable Pesticides in Soils, in: G.W. Ware, D.M. Whitacre, L.A. Albert, P. de Voogt, C.P. Gerba, O. Hutzinger, J.B. Knaak, F.L. Mayer, D.P. Morgan, D.L. Park, R.S. Tjeerdema, R.S.H. Yang, F.A. Gunther (Eds.) *Reviews of Environmental Contamination and Toxicology: Continuation of Residue Reviews*, Springer New York, New York, NY, 2006, pp. 149-217.
- [11] O.S.A. Al-Khazrajy, A.B.A. Boxall, Impacts of compound properties and sediment characteristics on the sorption behaviour of pharmaceuticals in aquatic systems, *Journal of Hazardous Materials*, 317 (2016) 198-209.
- [12] B.O. Clarke, S.R. Smith, Review of 'emerging' organic contaminants in biosolids and assessment of international research priorities for the agricultural use of biosolids, *Environ Int*, 37 (2011) 226-247.
- [13] D.J. Lapworth, N. Baran, M.E. Stuart, R.S. Ward, Emerging organic contaminants in groundwater: A review of sources, fate and occurrence, *Environmental Pollution*, 163 (2012) 287-303.
- [14] J.V. Tarazona, B.I. Escher, E. Giltrow, J. Sumpter, T. Knacker, Targeting the environmental risk assessment of pharmaceuticals: Facts and fantasies, *Integrated environmental assessment and management*, 6 (2010) 603-613.
- [15] A. Franco, A. Ferranti, C. Davidsen, S. Trapp, An unexpected challenge: ionizable compounds in the REACH chemical space, *The International Journal of Life Cycle Assessment*, 15 (2010) 321-325.

- [16] S. Rayne, K. Forest, Dow and Kaw,eff vs. Kow and Kaw degrees: acid/base ionization effects on partitioning properties and screening commercial chemicals for long-range transport and bioaccumulation potential, *J Environ Sci Health A Tox Hazard Subst Environ Eng*, 45 (2010) 1550-1594.
- [17] T. Ivanković, J. Hrenović, Surfactants in the environment, *Arhiv za Higijenu Rada i Toksikologiju*, 61 (2010) 95-110.
- [18] E.S. Williams, J. Panko, D.J. Paustenbach, The European Union's REACH regulation: A review of its history and requirements the EU REACH regulation: A review E. S. Williams et al, *Critical Reviews in Toxicology*, 39 (2009) 553-575.
- [19] A. Franco, A. Ferranti, C. Davidsen, S. Trapp, An unexpected challenge: ionizable compounds in the REACH chemical space, *The International Journal of Life Cycle Assessment*, (2010).
- [20] D.T. Manallack, The pK(a) Distribution of Drugs: Application to Drug Discovery, *Perspect Medicin Chem*, 1 (2008) 25-38.
- [21] S. Rayne, K. Forest, pH dependent partitioning behaviour of food and beverage aroma compounds between air-aqueous and organic-aqueous matrices, *Flavour and Fragrance Journal*, 31 (2016) 228-234.
- [22] H. Li, L.S. Lee, J.R. Fabrega, C.T. Jafvert, Role of pH in partitioning and cation exchange of aromatic amines on water-saturated soils, *Chemosphere*, 44 (2001) 627-635.
- [23] G. Könnecker, J. Regelmann, S. Belanger, K. Gamon, R. Sedlak, Environmental properties and aquatic hazard assessment of anionic surfactants: Physico-chemical, environmental fate and ecotoxicity properties, *Ecotoxicology and Environmental Safety*, 74 (2011) 1445-1460.
- [24] B.J. Brownawell, H. Chen, J.M. Collier, J.C. Westall, Adsorption of Organic Cations to Natural Materials, *Environmental science & technology*, 24 (1990) 1234-1241.
- [25] T.L. Ter Laak, M. Van der Aa, C.J. Houtman, P.G. Stoks, A.P. Van Wezel, Relating environmental concentrations of pharmaceuticals to consumption: A mass balance approach for the river Rhine, *Environment international*, 36 (2010) 403-409.
- [26] M. Matsuda, A. Kaminaga, K. Hayakawa, N. Takisawa, T. Miyajima, Surfactant binding by humic acids in the presence of divalent metal salts, *Colloids & Surfaces A*, 347 (2009) 45-49.
- [27] M. Ishiguro, W. Tan, L.A. Koopal, Binding of Cationic Surfactants to Humic Substances, *Colloids and Surfaces A: Physicochem. Eng. Aspects*, 306 (2007) 29-39.
- [28] G.G. Ying, Fate, behavior and effects of surfactants and their degradation products in the environment, *Environ Int*, 32 (2006) 417-431.
- [29] R.S. Boethling, Environmental fate and toxicity in wastewater treatment of quaternary ammonium surfactants, *Water research*, 18 (1984) 1061-1076.
- [30] L.H. Huber, Ecological behavior of cationic surfactants from fabric softeners in the aquatic environment, *Journal of the American Oil Chemists' Society*, 61 (1984) 377-382.
- [31] O. Nunez, E. Moyano, M.T. Galceran, Determination of quaternary ammonium biocides by liquid chromatography-mass spectrometry, *J Chromatogr A*, 1058 (2004) 89-95.
- [32] C. Wegner, M. Hamburger, Occurrence of stable foam in the upper Rhine River caused by plant-derived surfactants, *Environmental Science and Technology*, 36 (2002) 3250-3256.
- [33] C.A. Moody, J.A. Field, Perfluorinated surfactants and the environmental implications of their use in fire-fighting foams, *Environmental Science and Technology*, 34 (2000) 3864-3870.

- [34] J.H. Harwell, D.A. Sabatini, R.C. Knox, Surfactants for ground water remediation, *Colloids and Surfaces A: Physicochemical and Engineering Aspects*, 151 (1999) 255-268.
- [35] M.R. Taha, I.H. Soewarto, Y.B. Acar, R.J. Gale, M.E. Zappi, Surfactant enhanced desorption of TNT from soil, *Water, Air, and Soil Pollution*, 100 (1997) 33-48.
- [36] G.G. Ying, Fate, behavior and effects of surfactants and their degradation products in the environment, *Environment international*, 32 (2006) 417-431.
- [37] P.A. Lara-Martin, X. Li, R.F. Bopp, B.J. Brownawell, Occurrence of Alkyltrimethylammonium Compounds in Urban Estuarine Sediments: Behentrimonium As a New Emerging Contaminant, *Environmental science & technology*, 44 (2010) 7569-7575.
- [38] J. Waters, T.C.J. Feijte, AIS+/CESIO+ Environmental surfactant monitoring programme: Outcome of five national pilot studies on linear alkylbenzene sulphonate (LAS), *Chemosphere*, 30 (1995) 1939-1956.
- [39] M. Stalmans, E. Matthijs, N.T. de Oude, Fate and effect of detergent chemicals in the marine and estuarine environment, *Water Science and Technology*, 24 (1991) 115-126.
- [40] T. Ruan, S. Song, T. Wang, R. Liu, Y. Lin, G. Jiang, Identification and composition of emerging quaternary ammonium compounds in municipal sewage sludge in China, *Environmental Science and Technology*, 48 (2014) 4289-4297.
- [41] W.H. Ding, Y.H. Liao, Determination of alkylbenzyltrimethylammonium chlorides in river water and sewage effluent by solid-phase extraction and gas chromatography/mass spectrometry, *Anal Chem*, 73 (2001) 36-40.
- [42] X.L. Li, B.J. Brownawell, Analysis of Quaternary Ammonium Compounds in Estuarine Sediments by LC-ToF-MS: Very High Positive Mass Defects of Alkylamine Ions as Powerful Diagnostic Tools for Identification and Structural Elucidation, *Anal Chem*, 81 (2009) 7926-7935.
- [43] X. Li, B.J. Brownawell, Quaternary ammonium compounds in urban estuarine sediment environments - A class of contaminants in need of increased attention?, *Environmental science & technology*, 44 (2010) 7561-7568.
- [44] D.M. Di Toro, C.S. Zarba, D.J. Hansen, W.J. Berry, R.C. Swartz, C.E. Cowan, S.P. Pavlou, H.E. Allen, N.A. Thomas, P.R. Paquin, Technical basis for establishing sediment quality for nonionic organic-chemicals using equilibrium partitioning, *Environ Toxicol Chem*, 10 (1991) 1541-1583.
- [45] I. Van Zandvoort, Y. Wang, C.B. Rasrendra, E.R.H. Van Eck, P.C.A. Bruijninx, H.J. Heeres, B.M. Weckhuysen, Formation, molecular structure, and morphology of humins in biomass conversion: Influence of feedstock and processing conditions, *ChemSusChem*, 6 (2013) 1745-1758.
- [46] A.J. Simpson, G. Song, E. Smith, B. Lam, E.H. Novotny, M.H.B. Hayes, Unraveling the structural components of soil humin by use of solution-state nuclear magnetic resonance spectroscopy, *Environmental Science and Technology*, 41 (2007) 876-883.
- [47] A.W.P. Vermeer, J.K. McCulloch, W.H. Van Riemsdijk, L.K. Koopal, Metal ion adsorption to complexes of humic acid and metal oxides: Deviations from the additivity rule, *Environmental Science and Technology*, 33 (1999) 3892-3897.
- [48] H. Azejjel, C. del Hoyo, K. Draoui, M.S. Rodríguez-Cruz, M.J. Sánchez-Martín, Natural and modified clays from Morocco as sorbents of ionizable herbicides in aqueous medium, *Desalination*, 249 (2009) 1151-1158.

- [49] Q. Zhao, S.E. Burns, Molecular dynamics simulation of secondary sorption behavior of montmorillonite modified by single chain quaternary ammonium cations, *Environmental Science and Technology*, 46 (2012) 3999-4007.
- [50] G. Sheng, S. Xu, S.A. Boyd, Cosorption of organic contaminants from water by hexadecyltrimethylammonium-exchanged clays, *Water research*, 30 (1996) 1483-1489.
- [51] J.R. Fábrega, C.T. Jafvert, H. Li, L.S. Lee, Modeling competitive cation exchange of aromatic amines in water-saturated soils, *Environmental science & technology*, 35 (2001) 2727-2733.
- [52] J.R. Fábrega, C.T. Jafvert, H. Li, L.S. Lee, Modeling short-term soil-water distribution of aromatic amines, *Environmental science & technology*, 32 (1998) 2788-2794.
- [53] C.C. Ainsworth, J.M. Zachara, R.L. Schmidt, Quinoline Sorption on Na-Montmorillonite - Contributions of the Protonated and Neutral Species, *Clays and Clay Minerals*, 35 (1987) 121-128.
- [54] Y. Chen, M. Geurts, S.B. Sjollem, N.I. Kramer, J.L.M. Hermens, S.T.J. Droge, Acute toxicity of the cationic surfactant C12-benzalkonium in different bioassays: How test design affects bioavailability and effect concentrations, *Environmental Toxicology and Chemistry*, 33 (2014) 606-615.
- [55] K. Bittermann, L. Linden, K.U. Goss, Screening tools for the bioconcentration potential of monovalent organic ions in fish, *Environmental Science: Processes and Impacts*, 20 (2018) 845-853.
- [56] P.C. Thomas, K. Velthoven, M. Geurts, D. van Wijk, Bioavailability and detoxification of cationics: II. Relationship between toxicity and CEC of cationic surfactants on *Caenorhabditis elegans* (Nematoda) in artificial and natural substrates, *Chemosphere*, 75 (2009) 310-318.
- [57] D. van Wijk, M. Gyimesi-van den Bos, I. Garttner-Arends, M. Geurts, J. Kamstra, P. Thomas, Bioavailability and detoxification of cationics: I. Algal toxicity of alkyltrimethyl ammonium salts in the presence of suspended sediment and humic acid, *Chemosphere*, 75 (2009) 303-309.
- [58] G. Cornelissen, Ö. Gustafsson, T.D. Bucheli, M.T.O. Jonker, A.A. Koelmans, P.C.M. Van Noort, Extensive sorption of organic compounds to black carbon, coal, and kerogen in sediments and soils: Mechanisms and consequences for distribution, bioaccumulation, and biodegradation, *Environmental Science and Technology*, 39 (2005) 6881-6895.
- [59] N.J. Diepens, G.H.P. Arts, T.C.M. Brock, H. Smidt, P.J. Van Den Brink, M.J. Van Den Heuvel-Greve, A.A. Koelmans, Sediment toxicity testing of organic chemicals in the context of prospective risk assessment: A review, *Critical Reviews in Environmental Science and Technology*, 44 (2014) 255-302.
- [60] M.T.D. Cronin, J.D. Walker, J.S. Jaworska, M.H.I. Comber, C.D. Watts, A.P. Worth, Use of QSAR in international decision-making frameworks to predict ecologic effects and environmental fate of chemical substances, *Environmental Health Perspectives*, 111 (2003) 1376-1390.
- [61] IHCP, Technical Guidance Document on Risk Assessment, 2003.
- [62] M.W. Verhaar H.J.M., Hermens J.L.M., QSARs for Ecotoxicity, Overview of Structure-Activity Relationships for Environmental Endpoints, (1995).
- [63] W. Fu, A. Franco, S. Trapp, Methods for estimating the bioconcentration factor of ionizable organic chemicals, *Environ Toxicol Chem*, 28 (2009) 1372-1379.
- [64] J.M. Armitage, J.A. Arnot, F. Wania, D. Mackay, Development and evaluation of a mechanistic bioconcentration model for ionogenic organic chemicals in fish, *Environ Toxicol Chem*, 32 (2013) 115-128.
- [65] S.J. Singer, G.L. Nicolson, The fluid mosaic model of the structure of cell membranes, *Science*, 175 (1972) 720-731.

- [66] J. Neuwoehner, B.I. Escher, The pH-dependent toxicity of basic pharmaceuticals in the green algae *Scenedesmus vacuolatus* can be explained with a toxicokinetic ion-trapping model, *Aquatic Toxicology*, 101 (2011) 266-275.
- [67] X. Zhang, K.D. Oakes, S. Cui, L. Bragg, M.R. Servos, J. Pawliszyn, Tissue-specific in vivo bioconcentration of pharmaceuticals in rainbow trout (*Oncorhynchus mykiss*) using space-resolved solid-phase microextraction, *Environmental Science and Technology*, 44 (2010) 3417-3422.
- [68] R.J. Erickson, J.M. McKim, G.J. Lien, A.D. Hoffman, S.L. Batterman, Uptake and elimination of ionizable organic chemicals at fish gills: I. Model formulation, parameterization, and behavior, *Environ Toxicol Chem*, 25 (2006) 1512-1521.
- [69] T. Jimbo, P. Ramirez, A. Tanioka, S. Mafe, N. Minoura, Passive transport of ionic drugs through membranes with pH-dependent fixed charges, *Journal of colloid and interface science*, 225 (2000) 447-454.
- [70] A.P. Van Wezel, A. Opperhuizen, Narcosis due to environmental pollutants in aquatic organisms: Residue-based toxicity, mechanisms, and membrane burdens, *Critical Reviews in Toxicology*, 25 (1995) 255-279.
- [71] A.P. Van Wezel, G. Cornelissen, J. Van Kees Miltenburg, A. Opperhuizen, Membrane burdens of chlorinated benzenes lower the main phase transition temperature in dipalmitoyl-phosphatidylcholine vesicles: Implications for toxicity by narcotic chemicals, *Environ Toxicol Chem*, 15 (1996) 203-212.
- [72] M. Holmstrup, H. Bouvrais, P. Westh, C. Wang, S. Slotsbo, D. Waagner, K. Enggrob, J.H. Ipsen, Lipophilic contaminants influence cold tolerance of invertebrates through changes in cell membrane fluidity, *Environmental Science and Technology*, 48 (2014) 9797-9803.
- [73] G. Oros, T. Cserhádi, E. Forgács, Inhibitory effect of nonionic surfactants on sunflower downy mildew. A quantitative structure–activity relationship study, *Chemometrics and Intelligent Laboratory Systems*, 47 (1999) 149-156.
- [74] U. Kragh-Hansen, Transitional steps in the solubilization of protein-containing membranes and liposomes by nonionic detergent, *Biochemistry*, 32 (1993) 1648-1656.
- [75] T. Thorsteinsson, M. Másson, K.G. Kristinsson, M.A. Hjálmarsdóttir, H. Hilmarsson, T. Loftsson, Soft antimicrobial agents: Synthesis and activity of labile environmentally friendly long chain quaternary ammonium compounds, *Journal of Medicinal Chemistry*, 46 (2003) 4173-4181.
- [76] R.L. Grant, C. Yao, D. Gabaldon, D. Acosta, Evaluation of surfactant cytotoxicity potential by primary cultures of ocular tissues: I. Characterization of rabbit corneal epithelial cells and initial injury and delayed toxicity studies, *Toxicology*, 76 (1992) 153-176.
- [77] A. Hrabák, F. Antoni, M.T. Szabó, Damaging effect of detergents on human lymphocytes, *Bulletin of Environmental Contamination and Toxicology*, 28 (1982) 504-511.
- [78] Y. Chen, S.T. Droge, J.L. Hermens, Analyzing freely dissolved concentrations of cationic surfactant utilizing ion-exchange capability of polyacrylate coated solid-phase microextraction fibers, *J Chromatogr A*, 1252 (2012) 15-22.
- [79] Y. Chen, M. Geurts, S.B. Sjollem, N.I. Kramer, J.L. Hermens, S.T. Droge, Acute toxicity of the cationic surfactant C12-benzalkonium in different bioassays: how test design affects bioavailability and effect concentrations, *Environ Toxicol Chem*, 33 (2014) 606-615.

- [80] E. Boyaci, C. Sparham, J. Pawliszyn, Thin-film microextraction coupled to LC-ESI-MS/MS for determination of quaternary ammonium compounds in water samples, *Analytical and bioanalytical chemistry*, 406 (2014) 409-420.
- [81] A. Muwamba, P. Nkedi-Kizza, R.D. Rhue, J.J. Keaffaber, Use of mixed solvent systems to eliminate sorption of strongly hydrophobic organic chemicals on container walls, *Journal of Environmental Quality*, 38 (2009) 1170-1176.
- [82] D.C. Leggett, L.V. Parker, Modeling the equilibrium partitioning of organic contaminants between PTFE, PVC, and groundwater, *Environmental Science and Technology*, 28 (1994) 1229-1233.
- [83] K. Bester, Quantification with HPLC-MS/MS for environmental issues: Quality assurance and quality assessment, *Analytical and bioanalytical chemistry*, 391 (2008) 15-20.
- [84] J. Wang, B. Han, M. Dai, H. Yan, Z. Li, R.K. Thomas, Effects of chain length and structure of cationic surfactants on the adsorption onto Na-kaolinite, *Journal of colloid and interface science*, 213 (1999) 596-601.
- [85] I.E. Stas, B.P. Shipunov, I.N. Pautova, Y.V. Sankina, A study of adsorption of lead, cadmium, and zinc ions on the glass surface by stripping voltammetry, *Russian Journal of Applied Chemistry*, 77 (2004) 1487-1490.
- [86] J.C. Westall, B.J. Brownawell, H. Chen, J.M. Collier, J. Hatfield, Adsorption of organic cations to soils and subsurface materials, *USEPA Res. Dev.*, (1990).
- [87] OECD, OECD Guidelines for the Testing of Chemicals. Test No. 106: Adsorption -- Desorption Using a Batch Equilibrium Method, Organisation for Economic Cooperation and Development, Paris, France, 2000.
- [88] C.L. Arthur, J. Pawliszyn, Solid-Phase Microextraction with Thermal-Desorption Using Fused-Silica Optical Fibers, *Anal Chem*, 62 (1990) 2145-2148.
- [89] J.L.M. Hermens, A.P. Freidig, E.U. Ramos, W.H.J. Vaes, W.M.G.M. Van Loon, E.M.J. Verbruggen, H.J.M. Verhaar, Application of Negligible Depletion Solid-Phase Extraction (nd-SPE) for Estimating Bioavailability and Bioaccumulation of Individual Chemicals and Mixtures, *ACS Symposium Series*, 2001, pp. 64-74.
- [90] W.H.J. Vaes, C. Hamwijk, E. Urrestarazu Ramos, H.J.M. Verhaar, J.L.M. Hermens, Partitioning of organic chemicals to polyacrylate-coated solid phase microextraction fibers: kinetic behavior and quantitative structure-property relationships, *Anal Chem*, 68 (1996) 4458-4462.
- [91] J. Pawliszyn, 2 - Theory of Solid-Phase Microextraction, *Handbook of Solid Phase Microextraction*, Elsevier, Oxford, 2012, pp. 13-59.
- [92] S. Endo, S.T.J. Droge, K.U. Goss, Polyparameter Linear Free Energy Models for Polyacrylate Fiber-Water Partition Coefficients to Evaluate the Efficiency of Solid-Phase Microextraction, *Anal Chem*, 83 (2011) 1394-1400.
- [93] M.B. Heringa, J.L.M. Hermens, Measurement of free concentrations using negligible depletion-solid phase microextraction (nd-SPME), *Trends Anal. Chem.*, 22 (2003) 575-587.
- [94] H. Lord, J. Pawliszyn, Evolution of solid-phase microextraction technology, *J. Chromatogr. A*, 885 (2000) 153-193.
- [95] P. Mayer, W.H.J. Vaes, F. Wijnker, K.C.H.M. Legierse, R.H. Kraaij, J. Tolls, J.L.M. Hermens, Sensing dissolved sediment porewater concentrations of persistent and bioaccumulative pollutants using disposable solid-phase microextraction fibers, *Environ. Sci. Technol.*, 34 (2000) 5177-5183.

- [96] W.H.J. Vaes, E.U. Ramos, H.J.M. Verhaar, W. Seinen, J.L.M. Hermens, Measurement of the free concentration using solid-phase microextraction: Binding to protein, *Anal. Chem.*, 68 (1996) 4463-4467.
- [97] F. Wang, Y. Chen, J.L.M. Hermens, S.T.J. Droge, Evaluation of passive samplers with neutral or ion-exchange polymer coatings to determine freely dissolved concentrations of the basic surfactant lauryl diethanolamine: Measurements of acid dissociation constant and organic carbon-water sorption coefficient, *J. Chromatogr. A*, 1315 (2013) 8-14.
- [98] E. Boyaci, A. Rodriguez-Lafuente, K. Gorynski, F. Mirnaghi, E.A. Souza-Silva, D. Hein, J. Pawliszyn, Sample preparation with solid phase microextraction and exhaustive extraction approaches: Comparison for challenging cases, *Anal Chim Acta*, 873 (2015) 14-30.
- [99] D. Sijm, R. Kraaij, A. Belfroid, Bioavailability in soil or sediment: Exposure of different organisms and approaches to study it, *Environmental Pollution*, 108 (2000) 113-119.
- [100] X. Cui, P. Mayer, J. Gan, Methods to assess bioavailability of hydrophobic organic contaminants: Principles, operations, and limitations, *Environmental Pollution*, 172 (2013) 223-234.
- [101] M. Pavan, A.P. Worth, T.I. Netzeva, Review of QSAR Models for Bioconcentration, 2006.
- [102] J. Saarikoski, R. Lindström, M. Tyynelä, M. Viluksela, Factors affecting the absorption of phenolics and carboxylic acids in the guppy (*Poecilia reticulata*), *Ecotoxicology and Environmental Safety*, 11 (1986) 158-173.
- [103] R.J. Erickson, J.M. McKim, G.J. Lien, A.D. Hoffman, S.L. Batterman, Uptake and elimination of ionizable organic chemicals at fish gills: I. Model formulation, parameterization, and behavior, *Environ Toxicol Chem*, 25 (2006) 1512-1521.
- [104] R.J. Erickson, J.M. McKim, G.J. Lien, A.D. Hoffman, S.L. Batterman, Uptake and elimination of ionizable organic chemicals at fish gills: II. Observed and predicted effects of pH, alkalinity, and chemical properties, *Environ Toxicol Chem*, 25 (2006) 1522-1532.
- [105] C.T. Jafvert, J.C. Westall, E. Grieder, R.P. Schwarzenbach, Distribution of hydrophobic ionogenic organic compounds between octanol and water: organic acids, *Environmental science & technology*, 24 (1990) 1795-1803.
- [106] A. Geisler, S. Endo, K.U. Goss, Partitioning of Organic Chemicals to Storage Lipids: Elucidating the Dependence on Fatty Acid Composition and Temperature, *Environ Sci Technol*, (2012).
- [107] M.C. Yarema, C.E. Becker, Key concepts in postmortem drug redistribution, *Clinical Toxicology*, 43 (2005) 235-241.
- [108] M. Kah, C.D. Brown, Log D: Lipophilicity for ionisable compounds, *Chemosphere*, 72 (2008) 1401-1408.
- [109] J. Hammer, J.J.H. Haftka, P. Scherpenisse, J.L.M. Hermens, P.W.P. de Voogt, Fragment-based approach to calculate hydrophobicity of anionic and nonionic surfactants derived from chromatographic retention on a C18 stationary phase, *Environ Toxicol Chem*, 36 (2017) 329-336.
- [110] A. Avdeef, *Absorption and Drug Development: Solubility, Permeability, and Charge State*, Wiley, 2012.
- [111] B.I. Escher, R.P. Schwarzenbach, J.C. Westall, Evaluation of liposome-water partitioning of organic acids and bases. 2. Comparison of experimental determination methods, *Environmental science & technology*, 34 (2000) 3962-3968.
- [112] B.I. Escher, R.P. Schwarzenbach, J.C. Westall, Evaluation of liposome-water partitioning of organic acids and bases. 1. Development of a sorption model, *Environmental science & technology*, 34 (2000) 3954-3961.



- [113] R.P. Austin, A.M. Davis, C.N. Manners, Partitioning of Ionizing Molecules between Aqueous Buffers and Phospholipid-Vesicles, *Journal of pharmaceutical sciences*, 84 (1995) 1180-1183.
- [114] M.J. Moreno, M. Bastos, A. Velazquez-Campoy, Partition of amphiphilic molecules to lipid bilayers by isothermal titration calorimetry, *Analytical biochemistry*, 399 (2010) 44-47.
- [115] A. Avdeef, K.J. Box, J.E. Comer, C. Hibbert, K.Y. Tam, pH-metric logP 10. Determination of liposomal membrane-water partition coefficients of ionizable drugs, *Pharm Res*, 15 (1998) 209-215.
- [116] D. Yordanova, E. Ritter, T. Gerlach, J.H. Jensen, I. Smirnova, S. Jakobtorweihen, Solute Partitioning in Micelles: Combining Molecular Dynamics Simulations, COSMOmic, and Experiments, *Journal of Physical Chemistry B*, 121 (2017) 5794-5809.
- [117] K. Bittermann, S. Spycher, S. Endo, L. Pohler, U. Huniar, K.U. Goss, A. Klamt, Prediction of Phospholipid-Water Partition Coefficients of Ionic Organic Chemicals Using the Mechanistic Model COSMOmic, *J Phys Chem B*, 118 (2014) 14833-14842.
- [118] S.T.J. Droge, Membrane-Water Partition Coefficients to Aid Risk Assessment of Perfluoroalkyl Anions and Alkyl Sulfates, *Environmental Science and Technology*, 53 (2019) 760-770.
- [119] S.T. Droge, J.L. Hermens, J. Rabone, S. Gutsell, G. Hodges, Phospholipophilicity of CHN amines: chromatographic descriptors and molecular simulations for understanding partitioning into membranes, *Environ Sci Process Impacts*, (2016).
- [120] S.T. Droge, Dealing with Confounding pH-Dependent Surface Charges in Immobilized Artificial Membrane HPLC Columns, *Anal Chem*, 88 (2016) 960-967.
- [121] M.R. Ledbetter, S. Gutsell, G. Hodges, J.C. Madden, P.H. Rowe, M.T.D. Cronin, Robustness of an immobilized artificial membrane high-performance liquid chromatography method for the determination of lipophilicity, *J Chem Eng Data*, 57 (2012) 3696-3700.
- [122] C. Giaginis, A. Tsantili-Kakoulidou, Alternative measures of lipophilicity: From octanol-water partitioning to IAM retention, *Journal of pharmaceutical sciences*, 97 (2008) 2984-3004.
- [123] K. Bittermann, S. Spycher, K.U. Goss, Comparison of different models predicting the phospholipid-membrane water partition coefficients of charged compounds, *Chemosphere*, 144 (2016) 382-391.
- [124] G.D. Veith, D.J. Call, L.T. Brooke, Structure - toxicity relationships for the fathead minnow, *Pimephales promelas*: narcotic industrial chemicals, *Canadian Journal of Fisheries and Aquatic Sciences*, 40 (1983) 743-748.
- [125] W.H.J. Vaes, E.U. Ramos, H.J.M. Verhaar, J.L.M. Hermens, Acute toxicity of nonpolar versus polar narcosis: Is there a difference?, *Environ Toxicol Chem*, 17 (1998) 1380-1384.
- [126] H.J.M. Verhaar, E.U. Ramos, J.L.M. Hermens, Classifying environmental pollutants. 2: Separation of class 1 (baseline toxicity) and class 2 ('polar narcosis') type compounds based on chemical descriptors, *Journal of Chemometrics*, 10 (1996) 149-162.
- [127] S.P. Bradbury, R.W. Carlson, G.J. Niemi, T.R. Henry, Use of respiratory-cardiovascular responses of rainbow trout (*Oncorhynchus mykiss*) in identifying acute toxicity syndromes in fish: Part 4. Central nervous system seizure agents, *Environ Toxicol Chem*, 10 (1991) 115-131.
- [128] S.P. Bradbury, T.R. Henry, G.J. Niemi, R.W. Carlson, V.M. Snarski, Use of respiratory-cardiovascular responses of rainbow trout (*Salmo gairdneri*) in identifying acute toxicity syndromes in fish: Part 3. Polar narcotics, *Environ Toxicol Chem*, 8 (1989) 247-261.

- [129] N.C. Bols, A. Barlian, M. Chirino-Trejo, S.J. Caldwell, P. Goegan, L.E.J. Lee, Development of a cell line from primary cultures of rainbow trout, *Oncorhynchus mykiss* (Walbaum), gills, *Journal of Fish Diseases*, 17 (1994) 601-611.
- [130] B.I. Escher, J.L.M. Hermens, Modes of action in ecotoxicology: Their role in body burdens, species sensitivity, QSARs, and mixture effects, *Environmental Science and Technology*, 36 (2002) 4201-4217.
- [131] M. Manaargadoo-Catin, A. Ali-Cherif, J.L. Pougna, C. Perrin, Hemolysis by surfactants - A review, *Advances in Colloid and Interface Science*, 228 (2016) 1-16.
- [132] P. Balgavý, F. Devinsky, Cut-off effects in biological activities of surfactants, *Advances in Colloid and Interface Science*, 66 (1996) 23-63.
- [133] S. Przystalski, J. Sarapuk, H. Kleszczyska, J. Gabrielska, J. Hładyszowski, Z. Trela, J. Kuczera, Influence of amphiphilic compounds on membranes, *Acta Biochimica Polonica*, 47 (2000) 627-638.
- [134] B. Isomaa, H. Hägerstrand, G. Paatero, A.C. Engblom, Permeability alterations and antihemolysis induced by amphiphiles in human erythrocytes, *BBA - Biomembranes*, 860 (1986) 510-524.
- [135] M. Sandbacka, I. Christianson, B. Isomaa, The acute toxicity of surfactants on fish cells, *Daphnia magna* and fish - a comparative study, *Toxicology in vitro : an international journal published in association with BIBRA*, 14 (2000) 61-68.
- [136] S.T. Giolando, R.A. Rapaport, R.J. Larson, T.W. Federle, M. Stalmans, P. Masscheleyn, Environmental fate and effects of DEEDMAC: A new rapidly biodegradable cationic surfactant for use in fabric softeners, *Chemosphere*, 30 (1995) 1067-1083.
- [137] J. Waters, K.S. Lee, V. Perchard, M. Flanagan, P.E. Clarke, Monitoring of diester cationic surfactant residues in UK and Dutch sewage treatment effluents, *Tenside, Surfactants, Detergents*, 37 (2000) 161-X.
- [138] J. Menzies, K. Casteel, K. Wehmeyer, M. Lam, K. McDonough, Probabilistic exposure assessment of DEEDMAC using measured effluent and sludge concentrations from 41 wastewater treatment plants across the United States, *Sci Total Environ*, 684 (2019) 247-253.
- [139] OECD, Test No. 301: Ready Biodegradability, OECD Publishing 1992.
- [140] OECD, Test No. 310: Ready Biodegradability - CO<sub>2</sub> in sealed vessels (Headspace Test), OECD Publishing 2014.
- [141] OECD, Test No. 303: Simulation Test - Aerobic Sewage Treatment -- A: Activated Sludge Units; B: Biofilms, 2001.
- [142] OECD, Test No. 314: Simulation Tests to Assess the Biodegradability of Chemicals Discharged in Wastewater, 2008.
- [143] OECD, Test No. 302B: Inherent Biodegradability: Zahn-Wellens / EMPA Test, 1992.
- [144] OECD, Test No. 302A: Inherent Biodegradability: Modified SCAS Test, 1981.
- [145] C.G. van Ginkel, C. Gancet, M. Hirschen, M. Galobardes, P. Lemaire, J. Rosenblom, Improving ready biodegradability testing of fatty amine derivatives, *Chemosphere*, 73 (2008) 506-510.
- [146] H.A. Painter, P. Reynolds, S. Comber, Application of the headspace CO<sub>2</sub> method (ISO 14 593) to the assessment of the ultimate biodegradability of surfactants: results of a calibration exercise, *Chemosphere*, 50 (2003) 29-38.
- [147] C. Sweetlove, J.C. Chenèble, Y. Barthel, M. Boualam, J. L'Haridon, G. Thouand, Evaluating the ready biodegradability of two poorly water-soluble substances: comparative approach of bioavailability improvement methods (BIMs), *Environmental Science and Pollution Research*, 23 (2016) 17592-17602.

- [148] C.G. van Ginkel, M. Kolvenbach, Relations between the structure of quaternary alkyl ammonium salts and their biodegradability, *Chemosphere*, 23 (1991) 281-289.
- [149] C.G. Van Ginkel, A. Haan, M.L.G.C. Luijten, C.A. Stroo, Influence of the size and source of the inoculum on biodegradation curves in closed-bottle tests, *Ecotoxicology and Environmental Safety*, 31 (1995) 218-223.
- [150] A.R. Tehrani-Bagha, H. Oskarsson, C.G. van Ginkel, K. Holmberg, Cationic ester-containing gemini surfactants: Chemical hydrolysis and biodegradation, *Journal of colloid and interface science*, 312 (2007) 444-452.
- [151] A.R. Tehrani-Bagha, K. Holmberg, C.G. van Ginkel, M. Kean, Cationic gemini surfactants with cleavable spacer: Chemical hydrolysis, biodegradation, and toxicity, *Journal of colloid and interface science*, 449 (2014) 72-79.
- [152] C.G. Van Ginkel, A. Hoenderboom, A.M. Van Haperen, M.G.J. Geurts, Assessment of the biodegradability of dialkyldimethylammonium salts in flow through systems, *Journal of Environmental Science and Health - Part A Toxic/Hazardous Substances and Environmental Engineering*, 38 (2003) 1825-1835.
- [153] C.G. van Ginkel, C.A. Stroo, Simple method to prolong the closed bottle test for the determination of the inherent biodegradability, *Ecotoxicology and Environmental Safety*, 24 (1992) 319-327.
- [154] R. Geerts, C.G. van Ginkel, C.M. Plugge, Accurate assessment of the biodegradation of cationic surfactants in activated sludge reactors (OECD TG 303A), *Ecotoxicology and Environmental Safety*, 118 (2015) 83-89.
- [155] C. Dick, S. Rey, A. Boschung, F. Miffon, M. Seyfried, Current limitations of biodegradation screening tests and prediction of biodegradability: A focus on fragrance substances, *Environmental Technology and Innovation*, 5 (2016) 208-224.
- [156] C.G. Van Ginkel, Ultimate Biodegradation of Ingredients Used in Cleaning Agents, *Handbook for Cleaning/Decontamination of Surfaces 2007*, pp. 655-694.
- [157] A.G.M. Kroon, C.G. Van Ginkel, Complete mineralization of dodecyldimethylamine using a two-membered bacterial culture, *Environmental Microbiology*, 3 (2001) 131-136.
- [158] P.D. Nguyen, C.G. Van Ginkel, C.M. Plugge, Anaerobic degradation of long-chain alkylamines by a denitrifying *Pseudomonas stutzeri*, *FEMS Microbiology Ecology*, 66 (2008) 136-142.
- [159] B. Biswas, B. Sarkar, R. Rusmin, R. Naidu, Bioremediation of PAHs and VOCs: Advances in clay mineral-microbial interaction, *Environment international*, 85 (2015) 168-181.
- [160] Z. Filip, Clay minerals as a factor influencing the biochemical activity of soil microorganisms, *Folia Microbiologica*, 18 (1973) 56-74.
- [161] J. Cross, E.J. Singer, *Cationic Surfactants: Analytical and Biological Evaluation*, Marcel Dekker, New York, USA, 1994.
- [162] N. Desbenoit, I. Schmitz-Afonso, C. Baudouin, O. Lapr evote, D. Touboul, F. Brignole-Baudouin, A. Brunelle, Localisation and quantification of benzalkonium chloride in eye tissue by TOF-SIMS imaging and liquid chromatography mass spectrometry, *Analytical and bioanalytical chemistry*, 405 (2013) 4039-4049.
- [163] D. van Wijk, M.G.V. den Bos, I. Garttner-Arends, M. Geurts, J. Kamstra, P. Thomas, Bioavailability and detoxification of cationics: I. Algal toxicity of alkyltrimethyl ammonium salts in the presence of suspended sediment and humic acid, *Chemosphere*, 75 (2009) 303-309.

- [164] W. Giger, Hydrophilic and amphiphilic water pollutants: Using advanced analytical methods for classic and emerging contaminants, *Analytical and bioanalytical chemistry*, 393 (2009) 37-44.
- [165] B.I. Escher, J.L.M. Hermens, Internal exposure: Linking bioavailability to effects, *Environ. Sci. Technol.*, 38 (2004) 455A-462A.
- [166] M. Gulden, H. Seibert, Influence of protein binding and lipophilicity on the distribution of chemical compounds in in vitro systems, *Toxicology in vitro: an international journal published in association with BIBRA*, 11 (1997) 479-483.
- [167] D.J. Paustenbach, The practice of exposure assessment: A state-of-the-art review (Reprinted from *Principles and Methods of Toxicology*, 4th edition, 2001), *Journal of Toxicology and Environmental Health-Part B-Critical Reviews*, 3 (2000) 179-291.
- [168] E. Boyaci, C. Sparham, J. Pawliszyn, Thin-film microextraction coupled to LC-ESI-MS/MS for determination of quaternary ammonium compounds in water samples, *Analytical and Bioanalytical Chemistry*, 406 (2014) 409-420.
- [169] S. Hultgren, N. Larsson, B.F. Nilsson, J.A. Jönsson, Ion-pair hollow-fiber liquid-phase microextraction of the quaternary ammonium surfactant dicocodimethylammonium chloride, *Analytical and bioanalytical chemistry*, 393 (2009) 929-937.
- [170] J.J.H. Haftka, P. Scherpenisse, M.T.O. Jonker, J.L.M. Hermens, Using Polyacrylate-Coated SPME Fibers To Quantify Sorption of Polar and Ionic Organic Contaminants to Dissolved Organic Carbon, *Environmental science & technology*, 47 (2013) 4455-4462.
- [171] S.D.W. Comber, K.L. Rule, A.U. Conrad, S. Höss, S.F. Webb, S. Marshall, Bioaccumulation and toxicity of a cationic surfactant (DODMAC) in sediment dwelling freshwater invertebrates, *Environmental Pollution*, 153 (2008) 184-191.
- [172] Y. Chen, J.L. Hermens, S.T. Droge, Influence of organic matter type and medium composition on the sorption affinity of C12-benzalkonium cation, *Environ. Poll.*, 179 (2013) 153-159.
- [173] J.H. Canton, W. Slooff, Toxicity and accumulation studies of cadmium (cd-2+) with fresh-water organisms of different trophic levels, *Ecotoxicol. Environ. Saf.*, 6 (1982) 113-128.
- [174] P. Jandera, T. Hájek, M. Staňková, Monolithic and core-shell columns in comprehensive two-dimensional HPLC: A review, *Analytical and bioanalytical chemistry*, 407 (2015) 139-151.
- [175] S.T.J. Droge, T.L. Sinnige, J.L.M. Hermens, Analysis of freely dissolved alcohol ethoxylate homologues in various seawater matrixes using solid-phase microextraction, *Anal Chem*, 79 (2007) 2885-2891.
- [176] S.T. Droge, K.U. Goss, Development and evaluation of a new sorption model for organic cations in soil: contributions from organic matter and clay minerals, *Environmental science & technology*, 47 (2013) 14233-14241.
- [177] S.T.J. Droge, K.U. Goss, Sorption of Organic Cations to Phyllosilicate Clay Minerals: CEC-Normalization, Salt Dependency, and the Role of Electrostatic and Hydrophobic Effects, *Environmental science & technology*, 47 (2013) 14224-14232.
- [178] A. Rico-Rico, S.T.J. Droge, D. Widmer, J.L.M. Hermens, Freely dissolved concentrations of anionic surfactants in seawater solutions: Optimization of the non-depletive solid-phase microextraction method and application to linear alkylbenzene sulfonates, *J Chromatogr A*, 1216 (2009) 2996-3002.
- [179] A. Rico-Rico, S.T.J. Droge, J.L.M. Hermens, Predicting Sediment Sorption Coefficients for Linear Alkylbenzenesulfonate Congeners from Polyacrylate-Water Partition Coefficients at Different Salinities, *Environmental science & technology*, 44 (2010) 941-947.

- [180] J.J.H. Haftka, J. Hammer, J.L.M. Hermens, Mechanisms of Neutral and Anionic Surfactant Sorption to Solid-Phase Microextraction Fibers, *Environmental Science and Technology*, 49 (2015) 11053-11061.
- [181] F. Wang, Y. Chen, J.L. Hermens, S.T. Droge, Evaluation of passive samplers with neutral or ion-exchange polymer coatings to determine freely dissolved concentrations of the basic surfactant lauryl diethanolamine: Measurements of acid dissociation constant and organic carbon-water sorption coefficient, *J Chromatogr A*, 1315 (2013) 8-14.
- [182] H. Peltenburg, F.A. Groothuis, S.T.J. Droge, I.J. Bosman, J.L.M. Hermens, Elucidating the sorption mechanism of "mixed-mode" SPME using the basic drug amphetamine as a model compound, *Anal Chim Acta*, 782 (2013) 21-27.
- [183] C.W. Hoerr, A.W. Ralston, Studies on high molecular weight aliphatic amines and their salts. XI. Transference numbers of some primary amine hydrochlorides in aqueous solution and their significance in the interpretation of the micelle theory, *Journal of the American Chemical Society*, 65 (1943) 976-983.
- [184] E.J. Hoffman, G.E. Boyd, A.W. Ralston, Studies on high molecular weight aliphatic amines and their salts. V. Soluble and insoluble films of the amine hydrochlorides, *Journal of the American Chemical Society*, 64 (1942) 498-503.
- [185] A.W. Ralston, D.N. Eggenberger, Conductivities of alkylammonium chlorides in aqueous solutions of their homologs, *Journal of the American Chemical Society*, 70 (1948) 2918-2921.
- [186] A.W. Ralston, C.W. Hoerr, The electrical conductivities of aqueous solutions of mixtures containing alkylammonium chlorides, *Journal of the American Chemical Society*, 69 (1947) 883-886.
- [187] D. Gómez-Díaz, J.M. Navaza, B. Sanjurjo, Density, kinematic viscosity, speed of sound, and surface tension of hexyl, octyl, and decyl trimethyl ammonium bromide aqueous solutions, *J Chem Eng Data*, 52 (2007) 889-891.
- [188] A. Kroflič, B. Šarac, M. Bešter-Rogač, Influence of the alkyl chain length, temperature, and added salt on the thermodynamics of micellization: Alkyltrimethylammonium chlorides in NaCl aqueous solutions, *Journal of Chemical Thermodynamics*, 43 (2011) 1557-1563.
- [189] B. Šarac, M. Bešter-Rogač, Temperature and salt-induced micellization of dodecyltrimethylammonium chloride in aqueous solution: A thermodynamic study, *Journal of colloid and interface science*, 338 (2009) 216-221.
- [190] D. Gómez-Díaz, J.M. Navaza, B. Sanjurjo, Density, kinematic viscosity, speed of sound, and surface tension of tetradecyl and octadecyl trimethyl ammonium bromide aqueous solutions, *J Chem Eng Data*, 52 (2007) 2091-2093.
- [191] J. Baxter-Hammond, C.R. Powley, K.D. Cook, T.A. Nieman, Determination of critical micelle concentrations by bipolar pulse conductance, *Journal of colloid and interface science*, 76 (1980) 434-438.
- [192] H. Sifaoui, K. Ługowska, U. Domańska, A. Modaressi, M. Rogalski, Ammonium ionic liquid as modulator of the critical micelle concentration of ammonium surfactant at aqueous solution: Conductimetric and dynamic light scattering (DLS) studies, *Journal of colloid and interface science*, 314 (2007) 643-650.
- [193] K.H. Kang, H.U. Kim, K.H. Lim, Effect of temperature on critical micelle concentration and thermodynamic potentials of micellization of anionic ammonium dodecyl sulfate and cationic octadecyl trimethyl ammonium chloride, *Colloids and Surfaces A: Physicochemical and Engineering Aspects*, 189 (2001) 113-121.

- [194] G. Rauwel, L. Leclercq, J. Criquelion, J.M. Aubry, V. Nardello-Rataj, Aqueous mixtures of di-n-decyldimethylammonium chloride/polyoxyethylene alkyl ether: Dramatic influence of tail/tail and head/head interactions on co-micellization and biocidal activity, *Journal of colloid and interface science*, 374 (2012) 176-186.
- [195] L.M. Bergström, M. Aratono, Synergistic effects in mixtures of two identically charged ionic surfactants with different critical micelle concentrations, *Soft Matter*, 7 (2011) 8870-8879.
- [196] A. González-Pérez, J.L. Del Castillo, J. Czapkiewicz, J.R. Rodríguez, Micellization of decyl- and dodecyldimethyl-benzylammonium bromides at various temperatures in aqueous solutions, *Colloid and Polymer Science*, 280 (2002) 503-508.
- [197] J.R. Rodríguez, A. González-Pérez, J.L. Del Castillo, J. Czapkiewicz, Thermodynamics of micellization of alkyl dimethylbenzylammonium chlorides in aqueous solutions, *Journal of colloid and interface science*, 250 (2002) 438-443.
- [198] A. Safavi, M.A. Karimi, Flow injection determination of cationic surfactants by using N-bromosuccinimide and N-chlorosuccinimide as new oxidizing agents for luminol chemiluminescence, *Anal Chim Acta*, 468 (2002) 53-63.
- [199] P.A. Lambert, A.R.W. Smith, The mode of action of N (n Dodecyl)diethanolamine with particular reference to the effect of protonation on uptake by *Escherichia coli*, *Journal of General Microbiology*, 103 (1977) 367-374.
- [200] C.L. Arthur, J. Pawliszyn, Solid phase microextraction with thermal desorption using fused silica optical fibers, *Anal Chem*, 62 (1990) 2145-2148.
- [201] R. Xu, H.K. Lee, Application of electro-enhanced solid phase microextraction combined with gas chromatography-mass spectrometry for the determination of tricyclic antidepressants in environmental water samples, *J Chromatogr A*, 1350 (2014) 15-22.
- [202] F. Augusto, E. Carasek, R.G.C. Silva, S.R. Rivellino, A.D. Batista, E. Martendal, New sorbents for extraction and microextraction techniques, *J Chromatogr A*, 1217 (2010) 2533-2542.
- [203] A. Spietelun, M. Pilarczyk, A. Kloskowski, J. Namieśnik, Current trends in solid-phase microextraction (SPME) fibre coatings, *Chemical Society Reviews*, 39 (2010) 4524-4537.
- [204] E.A. Souza Silva, S. Risticovic, J. Pawliszyn, Recent trends in SPME concerning sorbent materials, configurations and in vivo applications, *TrAC - Trends in Analytical Chemistry*, 43 (2013) 24-36.
- [205] A. Kabir, H. Holness, K.G. Furton, J.R. Almirall, Recent advances in micro-sample preparation with forensic applications, *TrAC - Trends in Analytical Chemistry*, 45 (2013) 264-279.
- [206] H. Kataoka, K. Saito, Recent advances in SPME techniques in biomedical analysis, *J Pharmaceut Biomed*, 54 (2011) 926-950.
- [207] F.M. Musteata, Recent progress in in-vivo sampling and analysis, *TrAC - Trends in Analytical Chemistry*, 45 (2013) 154-168.
- [208] D. Vuckovic, J. Pawliszyn, Systematic evaluation of solid-phase microextraction coatings for untargeted metabolomic profiling of biological fluids by liquid chromatography-mass spectrometry, *Anal Chem*, 83 (2011) 1944-1954.
- [209] B. Bojko, K. Gorynski, G.A. Gomez-Rios, J.M. Knaak, T. Machuca, V.N. Spetzler, E. Cudjoe, M. Hsin, M. Cypel, M. Selzner, M. Liu, S. Keshavjee, J. Pawliszyn, Solid phase microextraction fills the gap in tissue sampling protocols, *Anal Chim Acta*, 803 (2013) 75-81.

- [210] B. Bojko, K. Gorynski, G.A. Gomez-Rios, J.M. Knaak, T. MacHuca, E. Cudjoe, V.N. Spetzler, M. Hsin, M. Cypel, M. Selzner, M. Liu, S. Keshjavee, J. Pawliszyn, Low invasive in vivo tissue sampling for monitoring biomarkers and drugs during surgery, *Laboratory Investigation*, 94 (2014) 586-594.
- [211] E. Cudjoe, B. Bojko, I. Delannoy, V. Saldivia, J. Pawliszyn, Solid-phase microextraction: A complementary InVivo sampling method to microdialysis, *Angewandte Chemie - International Edition*, 52 (2013) 12124-12126.
- [212] B. Bojko, M. Wąsowicz, J. Pawliszyn, Metabolic profiling of plasma from cardiac surgical patients concurrently administered with tranexamic acid: DI-SPME-LC-MS analysis, *Journal of Pharmaceutical Analysis*, 4 (2014) 6-13.
- [213] E. Cudjoe, J. Pawliszyn, Optimization of solid phase microextraction coatings for liquid chromatography mass spectrometry determination of neurotransmitters, *J Chromatogr A*, 1341 (2014) 1-7.
- [214] E. Boyaci, K. Gorynski, A. Rodriguez-Lafuente, B. Bojko, J. Pawliszyn, Introduction of solid-phase microextraction as a high-throughput sample preparation tool in laboratory analysis of prohibited substances, *Anal Chim Acta*, 809 (2014) 69-81.
- [215] H. Peltenburg, S.T.J. Droge, J.L.M. Hermens, I.J. Bosman, Sorption of amitriptyline and amphetamine to mixed-mode solid-phase microextraction in different test conditions, *J Chromatogr A*, 1390 (2015) 28-38.
- [216] H. Peltenburg, I.J. Bosman, J.L.M. Hermens, Sensitive determination of plasma protein binding of cationic drugs using mixed-mode solid-phase microextraction, *J Pharmaceut Biomed*, 115 (2015) 534-542.
- [217] S.D. Sibley, J.A. Pedersen, Interaction of the macrolide antimicrobial clarithromycin with dissolved humic acid, *Environmental science & technology*, 42 (2008) 422-428.
- [218] S.T.J. Droge, K.-U. Goss, Effect of sodium and calcium cations on the ion-exchange affinity of organic cations for soil organic matter, *Environ. Sci. Technol.*, 46 (2012) 5894-5901.
- [219] L. Oemisch, K.U. Goss, S. Endo, Ion exchange membranes as novel passive sampling material for organic ions: Application for the determination of freely dissolved concentrations, *J Chromatogr A*, 1370 (2014) 17-24.
- [220] ChemAxon.
- [221] D. Vrakas, C. Giaginis, A. Tsantili-Kakoulidou, Electrostatic interactions and ionization effect in immobilized artificial membrane retention A comparative study with octanol-water partitioning, *J Chromatogr A*, 1187 (2008) 67-78.
- [222] Anesthetic Structure Database.
- [223] EPA, Estimation Programs Interface Suite™ for Microsoft® Windows, V4.11, United States Environmental Protection Agency, Washington, DC, USA, (2012).
- [224] E.L. DiFilippo, R.P. Eganhouse, Assessment of PDMS-Water Partition Coefficients: Implications for Passive Environmental Sampling of Hydrophobic Organic Compounds, *Environmental science & technology*, (2010).
- [225] NRC, National Research Council, Committee on Toxicity Testing and Assessment of Environmental Agents.; Toxicity testing in the 21st century: A vision and a strategy, The National Academies Press, (2007).
- [226] NAC, National Academies of Sciences, Engineering, and Medicine.; Using 21st Century Science to Improve Risk-Related Evaluations, The National Academies Press, (2017).

- [227] F.A. Groothuis, M.B. Heringa, B. Nicol, J.L.M. Hermens, B.J. Blaauboer, N.I. Kramer, Dose metric considerations in in vitro assays to improve quantitative in vitro-in vivo dose extrapolations, *Toxicology*, 332 (2015) 30-40.
- [228] M.B. Heringa, R.H.M.M. Schreurs, F. Busser, P.T. van der Saag, B. van der Burg, J.L.M. Hermens, Toward more useful in vitro toxicity data with measured free concentrations, *Environmental science & technology*, 38 (2004) 6263-6270.
- [229] M. Gülден, H. Seibert, Influence of protein binding and lipophilicity on the distribution of chemical compounds in in vitro systems, *Toxicology in Vitro*, 11 (1997) 479-483.
- [230] N.I. Kramer, M. Krismartina, A. Rico-Rico, B.J. Blaauboer, J.L.M. Hermens, Quantifying Processes Determining the Free Concentration of Phenanthrene in Basal Cytotoxicity Assays, *Chemical research in toxicology*, 25 (2012) 436-445.
- [231] H. Seibert, S. Morchel, M. Gülден, Factors influencing nominal effective concentrations of chemical compounds in vitro: medium protein concentration, *Toxicology in Vitro*, 16 (2002) 289-297.
- [232] B.I. Escher, J.L.M. Hermens, Internal exposure: Linking bioavailability to effects, *Environmental science & technology*, 38 (2004) 455A-462A.
- [233] J.L.M. Hermens, M.B. Heringa, T.L. ter Laak, Bioavailability in dose and exposure assessment of organic contaminants in (Eco)toxicology, *Journal of Toxicology and Environmental Health-Part A-Current Issues*, 70 (2007) 727-730.
- [234] J. Riedl, R. Altenburger, Physicochemical substance properties as indicators for unreliable exposure in microplate-based bioassays, *Chemosphere*, 67 (2007) 2210-2220.
- [235] M. Gülден, S. Morchel, H. Seibert, Factors influencing nominal effective concentrations of chemical compounds in vitro: cell concentration, *Toxicology in Vitro*, 15 (2001) 233-243.
- [236] M. Gülден, A. Jess, J. Kammann, E. Maser, H. Seibert, Cytotoxic potency of H<sub>2</sub>O<sub>2</sub> in cell cultures: Impact of cell concentration and exposure time, *Free Radical Biology and Medicine*, 49 (2010) 1298-1305.
- [237] N.I. Kramer, E. Di Consiglio, B.J. Blaauboer, E. Testai, Biokinetics in repeated-dosing in vitro drug toxicity studies, *Toxicology in Vitro*, (2015).
- [238] N.I. Kramer, Measuring, Modeling, and Increasing the Free Concentration of Test Chemicals in Cell Assays, Institute for Risk Assessment Sciences, PhD Dissertation, Utrecht University, Utrecht, 2010, pp. 170.
- [239] M. Gülден, J. Schreiner, H. Seibert, In vitro toxicity testing with microplate cell cultures: Impact of cell binding, *Toxicology*, 332 (2015) 41-51.
- [240] M. Gülден, S. Morchel, S. Tahan, H. Seibert, Impact of protein binding on the availability and cytotoxic potency of organochlorine pesticides and chlorophenols in vitro, *Toxicology*, 175 (2002) 201-213.
- [241] J.M. Armitage, F. Wania, J.A. Arnot, Application of mass balance models and the chemical activity concept to facilitate the use of in vitro toxicity data for risk assessment, *Environ. Sci. Technol.*, 48 (2014) 9770-9779.
- [242] F.C. Fischer, L. Henneberger, M. König, K. Bittermann, L. Linden, K.-U. Goss, B.I. Escher, Modeling Exposure in the Tox21 In Vitro Bioassays, *Chemical Research in Toxicology*, 30 (2017) 1197-1208.
- [243] J. Stadnicka-Michalak, K. Tanneberger, K. Schirmer, R. Ashauer, Measured and modeled toxicokinetics in cultured fish cells and application to in vitro - In vivo toxicity extrapolation, *PLoS ONE*, 9 (2014).



- [244] H. Mielke, E. Di Consiglio, R. Kreutz, F. Partosch, E. Testai, U. Gundert-Remy, The importance of protein binding for the in vitro–in vivo extrapolation (IVIVE)—example of ibuprofen, a highly protein-bound substance, *Archives of Toxicology*, 91 (2017) 1663-1670.
- [245] W. Pfaller, P. Prieto, W. Dekant, P. Jennings, B.J. Blaauboer, The Predict-IV project: Towards predictive toxicology using in vitro techniques, *Toxicology in Vitro*, 30 (2015) 1-3.
- [246] K. Tanneberger, M. Knöbel, F.J.M. Busser, T.L. Sinnige, J.L.M. Hermens, K. Schirmer, Predicting fish acute toxicity using a fish gill cell line-based toxicity assay, *Environ. Sci. Technol.*, 47 (2013) 1110-1119.
- [247] J. Stadnicka, K. Schirmer, R. Ashauer, Predicting Concentrations of Organic Chemicals in Fish by Using Toxicokinetic Models, *Environmental science & technology*, 46 (2012) 3273-3280.
- [248] G. Ma, Q. Yuan, H. Yu, H. Lin, J. Chen, H. Hong, Development and evaluation of predictive model for bovine serum albumin-water partition coefficients of neutral organic chemicals, *Ecotoxicology and Environmental Safety*, 138 (2017) 92-97.
- [249] S.D.L.M. Proenca, A. Paini, E. Joossens, S. Benito Jose, E. Berggren, A. Worth, P. Peraita Maria Del Pilar, Application of the Virtual Cell Based Assay for Simulation of in vitro Chemical fate following Acute Exposure, 2017.
- [250] N. Timmer, S.T.J. Droge, Sorption of Cationic Surfactants to Artificial Cell Membranes: Comparing Phospholipid Bilayers with Monolayer Coatings and Molecular Simulations, *Environmental Science & Technology*, 51 (2017) 2890-2898.
- [251] D.T. Manallack, The pK(a) Distribution of Drugs: Application to Drug Discovery, *Perspectives in Medicinal Chemistry*, 1 (2007) 25-38.
- [252] A. Franco, A. Ferranti, C. Davidsen, S. Trapp, An unexpected challenge: Ionizable compounds in the REACH chemical space, *Int. J. Life Cycle Assess.*, 15 (2010) 321-325.
- [253] G.G. Ying, Fate, behavior and effects of surfactants and their degradation products in the environment, *Environ. Int.*, 32 (2006) 417-431.
- [254] Y. Chen, J.L.M. Hermens, S.T.J. Droge, Influence of organic matter type and medium composition on the sorption affinity of C12-benzalkonium cation, *Environ. Pollut.*, 179 (2013) 153-159.
- [255] L.E.J. Lee, V.R. Dayeh, K. Schirmer, N.C. Bols, Applications and potential uses of fish gill cell lines: Examples with RTgill-W1, *In Vitro Cellular and Developmental Biology - Animal*, 45 (2009) 127-134.
- [256] A. Behrens, K. Schirmer, N.C. Bols, H. Segner, Polycyclic aromatic hydrocarbons as inducers of cytochrome P4501A enzyme activity in the rainbow trout liver cell line, RTL-W1 and in primary cultures of rainbow trout hepatocytes, *Environmental Toxicology and Chemistry*, 20 (2001) 632-643.
- [257] N. Timmer, P. Scherpenisse, J.L.M. Hermens, S.T.J. Droge, Evaluating solid phase (micro-) extraction tools to analyze freely ionizable and permanently charged cationic surfactants, *Analytica Chimica Acta*, 1002 (2018) 26-38.
- [258] K. Schirmer, A.G.J. Chan, B.M. Greenberg, D.G. Dixon, N.C. Bols, Methodology for demonstrating and measuring the photocytotoxicity of fluoranthene to fish cells in culture, *Toxicology in Vitro*, 11 (1997) 107-119.
- [259] C.L. Gemmill, An Introduction to Pharmacology, *Journal of Medicinal Chemistry*, 9 (1966) 982-983.
- [260] M.B. Heringa, D. Pastor, J. Algra, W.H.J. Vaes, J.L.M. Herment, Negligible depletion solid-phase microextraction with radiolabeled analytes to study free concentrations and protein binding: An example with [3H]estradiol, *Analytical Chemistry*, 74 (2002) 5993-5997.

- [261] J. Moulin, Effect of protein binding on the determination of intrinsic clearance of hydrophobic compounds, Master Thesis, Utrecht University, 2012.
- [262] S. Endo, K.U. Goss, Serum albumin binding of structurally diverse neutral organic compounds: Data and models, *Chemical research in toxicology*, 24 (2011) 2293-2301.
- [263] N.I. Kramer, J.C.H. van Eijkeren, J.L.M. Hermens, Influence of albumin on sorption kinetics in solid-phase microextraction: Consequences for chemical analyses and uptake processes, *Analytical Chemistry*, 79 (2007) 6941-6948.
- [264] N.I. Kramer, F.J.M. Busser, M.T.T. Oosterwijk, K. Schirmer, B.I. Escher, J.L.M. Hermens, Development of a partition-controlled dosing system for cell assays, *Chemical research in toxicology*, 23 (2010) 1806-1814.
- [265] K. Tanneberger, A. Rico-Rico, N.I. Kramer, F.J.M. Busser, J.L.M. Hermens, K. Schirmer, Effects of Solvents and Dosing Procedure on Chemical Toxicity in Cell-Based in Vitro Assays, *Environmental science & technology*, 44 (2010) 4775-4781.
- [266] K. Valko, S. Nunhuck, C. Bevan, M.H. Abraham, D.P. Reynolds, Fast Gradient HPLC Method to Determine Compounds Binding to Human Serum Albumin. Relationships with Octanol/Water and Immobilized Artificial Membrane Lipophilicity, *Journal of Pharmaceutical Sciences*, 92 (2003) 2236-2248.
- [267] F.A. Groothuis, B. Nicol, N.I. Kramer, E. Stammler, Distribution of Benzalkonium Chlorides in Aqueous Solutions: A Comparison of Methods to Estimate Binding Affinity to Bovine Serum Albumin, (manuscript in preparation).
- [268] K. Schirmer, D.G. Dixon, B.M. Greenberg, N.C. Bols, Ability of 16 priority PAHs to be directly cytotoxic to a cell line from the rainbow trout gill, *Toxicology*, 127 (1998) 129-141.
- [269] J.E. Springer, R.D. Azbill, S.L. Carlson, A rapid and sensitive assay for measuring mitochondrial metabolic activity in isolated neural tissue, *Brain Research Protocols*, 2 (1998) 259-263.
- [270] B.I. Escher, J.L.M. Hermens, Modes of action in ecotoxicology: Their role in body burdens, species sensitivity, QSARs, and mixture effects, *Environmental science & technology*, 36 (2002) 4201-4217.
- [271] S.T.J. Droge, J.L.M. Hermens, J. Rabone, S. Gutsell, G. Hodges, Phospholipophilicity of C: XHyN+ amines: Chromatographic descriptors and molecular simulations for understanding partitioning into membranes, *Environ. Sci. Process. Impacts*, 18 (2016) 1011-1023.
- [272] M. Sandbacka, I. Christianson, B. Isomaa, The acute toxicity of surfactants on fish cells, *Daphnia magna* and fish - A comparative study, *Toxicology in Vitro*, 14 (2000) 61-68.
- [273] M. Gülден, D. Kähler, H. Seibert, Incipient cytotoxicity: A time-independent measure of cytotoxic potency in vitro, *Toxicology*, 335 (2015) 35-45.
- [274] J. Stadnicka-Michalak, K. Schirmer, R. Ashauer, Toxicology across scales: Cell population growth in vitro predicts reduced fish growth, *Science Advances*, 1 (2015).
- [275] J.J.W. Broeders, C. Parmentier, G.L. Truise, R. Jossé, E. Alexandre, C.C. Savary, P.G. Hewitt, S.O. Mueller, A. Guillouzo, L. Richert, J.C.H. van Eijkeren, J.L.M. Hermens, B.J. Blaauboer, Biokinetics of chlorpromazine in primary rat and human hepatocytes and human HepaRG cells after repeated exposure, *Toxicology in Vitro*, 30 (2015) 52-61.
- [276] J.M.Z. Comenges, E. Joossens, J.V.S. Benito, A. Worth, A. Paini, Theoretical and mathematical foundation of the Virtual Cell Based Assay – A review, *Toxicology in Vitro*, 45 (2017) 209-221.

- [277] F.C. Fischer, C. Abele, S.T.J. Droge, L. Henneberger, M. König, R. Schlichting, S. Scholz, B.I. Escher, Cellular Uptake Kinetics of Neutral and Charged Chemicals in *in vitro* Assays Measured by Fluorescence Microscopy, *Chemical Research in Toxicology*, 31 (2018) 646-657.
- [278] M.J. Bernhard, S.D. Dyer, Fish critical cellular residues for surfactants and surfactant mixtures, *Environmental Toxicology and Chemistry*, 24 (2005) 1738-1744.
- [279] A. Taillardat-Bertschinger, P.A. Carrupt, F. Barbato, B. Testa, Immobilized artificial membrane HPLC in drug research, *J Med Chem*, 46 (2003) 655-665.
- [280] G.M. Pauletti, H. Wunderli-Allenspach, Partition coefficients *in vitro*: artificial membranes as a standardized distribution model, *European Journal of Pharmaceutical Sciences*, 1 (1994) 273-282.
- [281] B.I. Escher, R.P. Schwarzenbach, Partitioning of substituted phenols in liposome-water, biomembrane-water, and octanol-water systems, *Environmental science & technology*, 30 (1996) 260-270.
- [282] L. Henneberger, K.U. Goss, S. Endo, Partitioning of Organic Ions to Muscle Protein: Experimental Data, Modeling, and Implications for *in Vivo* Distribution of Organic Ions, *Environmental Science and Technology*, 50 (2016) 7029-7036.
- [283] S.T.J. Droge, K.U. Goss, The ion-exchange process for cationic amines to soil organic matter also depends on nonionic interactions, Poster presentation, SETAC 2009Seville, 2010.
- [284] S.T.J. Droge, K.U. Goss, Ion-exchange of cationic organic compounds with monovalent and divalent inorganic cations in soil organic matter, to be submitted, (2011).
- [285] W.C. Jolin, J. Sullivan, D. Vasudevan, A.A. MacKay, Column Chromatography to Obtain Organic Cation Sorption Isotherms, *Environmental Science and Technology*, 50 (2016) 8196-8204.
- [286] B.I. Escher, J.L. Hermens, Internal exposure: linking bioavailability to effects, *Environmental science & technology*, 38 (2004) 455A-462A.
- [287] T. Heberer, Occurrence, fate, and removal of pharmaceutical residues in the aquatic environment: a review of recent research data, *Toxicol Lett*, 131 (2002) 5-17.
- [288] T.A. Ternes, Occurrence of drugs in German sewage treatment plants and rivers, *Water research*, 32 (1998) 3245-3260.
- [289] W.J. Xia, H. Onyuksel, Mechanistic studies on surfactant-induced membrane permeability enhancement, *Pharm Res*, 17 (2000) 612-618.
- [290] E. Martínez-Carballo, C. González-Barreiro, A. Sitka, N. Kreuzinger, S. Scharf, O. Gans, Determination of selected quaternary ammonium compounds by liquid chromatography with mass spectrometry. Part II. Application to sediment and sludge samples in Austria, *Environmental Pollution*, 146 (2007) 543-547.
- [291] I. Ferrer, E.T. Furlong, Identification of alkyl dimethylbenzylammonium surfactants in water samples by solid-phase extraction followed by ion trap LC/MS and LC/MS/MS, *Environmental science & technology*, 35 (2001) 2583-2588.
- [292] P. Fernandez, A.C. Alder, M.J.F. Suter, W. Giger, Determination of the quaternary ammonium surfactant ditallowdimethylammonium in digested sludges and marine sediments by supercritical fluid extraction and liquid chromatography with postcolumn ion-pair formation, *Anal Chem*, 68 (1996) 921-929.
- [293] S.D. Kramer, A. Braun, C. Jakits-Deiser, H. Wunderli-Allenspach, Towards the predictability of drug-lipid membrane interactions: the pH-dependent affinity of propranolol to phosphatidylinositol containing liposomes, *Pharm Res*, 15 (1998) 739-744.

- [294] F. Tsopeias, T. Vallianatou, A. Tsantili-Kakoulidou, Advances in immobilized artificial membrane (IAM) chromatography for novel drug discovery, *Expert Opinion on Drug Discovery*, 11 (2016) 473-488.
- [295] L. Grumetto, G. Russo, F. Barbato, Relationships between human intestinal absorption and polar interactions drug/phospholipids estimated by IAM-HPLC, *International Journal of Pharmaceutics*, 489 (2015) 186-194.
- [296] M.R. Ledbetter, S. Gutsell, G. Hodges, J.C. Madden, S. O'Connor, M.T.D. Cronin, Database of published retention factors for immobilized artificial membrane HPLC and an assessment of the effect of experimental variability, *Environ Toxicol Chem*, 30 (2011) 2701-2708.
- [297] C. Ottiger, H. Wunderli-Allenspach, Immobilized artificial membrane (IAM)-HPLC for partition studies of neutral and ionized acids and bases in comparison with the liposomal partition system, *Pharm Res*, 16 (1999) 643-650.
- [298] S. Ong, H. Liu, C. Pidgeon, 19th International Symposium on Column Liquid Chromatography and Related Techniques Immobilized-artificial-membrane chromatography: measurements of membrane partition coefficient and predicting drug membrane permeability, *J Chromatogr A*, 728 (1996) 113-128.
- [299] T.M. Bayerl, M. Bloom, Physical properties of single phospholipid bilayers adsorbed to micro glass beads. A new vesicular model system studied by  $^2\text{H}$ -nuclear magnetic resonance, *Biophys J*, 58 (1990) 357-362.
- [300] A. Loidl-Stahlhofen, T. Hartmann, M. Schottner, C. Rohring, H. Brodowsky, J. Schmitt, J. Keldenich, Multilamellar liposomes and solid-supported lipid membranes (TRANSIL): screening of lipid-water partitioning toward a high-throughput scale, *Pharm Res*, 18 (2001) 1782-1788.
- [301] W.C. Hou, B.Y. Moghadam, C. Corredor, P. Westerhoff, J.D. Posner, Distribution of functionalized gold nanoparticles between water and lipid bilayers as model cell membranes, *Environmental Science and Technology*, 46 (2012) 1869-1875.
- [302] A. Loidl-Stahlhofen, A.S. Ulrich, S. Kaufmann, T.M. Bayerl, Protein binding to supported lecithin bilayers controlled by the lipid phase state: A new concept for highly selective protein purification, *European Biophysics Journal*, 25 (1996) 151-153.
- [303] S. Ong, D. Pidgeon, Thermodynamics of solute partitioning into immobilized artificial membranes, *Anal Chem*, 67 (1995) 2119-2128.
- [304] R.P. Austin, P. Barton, A.M. Davis, R.E. Fessey, M.C. Wenlock, The thermodynamics of the partitioning of ionizing molecules between aqueous buffers and phospholipid membranes, *Pharmaceutical Research*, 22 (2005) 1649-1657.
- [305] A. Seelig, P.R. Allegrini, J. Seelig, Partitioning of local anesthetics into membranes: surface charge effects monitored by the phospholipid head-group, *Biochim Biophys Acta*, 939 (1988) 267-276.
- [306] S.M. Schrap, A. Opperhuizen, On the contradictions between experimental sorption data and the sorption partitioning model, *Chemosphere*, 24 (1992) 1259-1282.
- [307] L. Juergensen, J. Busnarda, P.-Y. Caux, R.A. Kent, Fate, behavior, and aquatic toxicity of the fungicide DDAC in the canadian environment, *Environmental Toxicology*, 15 (2000) 174-200.
- [308] M. Thorsteinsdóttir, I. Beijersten, D. Westerlund, Capillary electroseparations of enkephalin-related peptides and protein kinase A peptide substrates, *Electrophoresis*, 16 (1995) 564-573.
- [309] A. Kowalczyk, T.J. Martin, O.R. Price, J.R. Snape, R.A. van Egmond, C.J. Finnegan, H. Schäfer, R.J. Davenport, G.D. Bending, Refinement of biodegradation tests methodologies and the proposed utility of new microbial ecology techniques, *Ecotoxicology and Environmental Safety*, 111 (2015) 9-22.

- [310] K. Czechowska, V. Sentchilo, S. Beggah, S. Rey, M. Seyfried, J.R. Van Der Meer, Examining chemical compound biodegradation at low concentrations through bacterial cell proliferation, *Environmental Science and Technology*, 47 (2013) 1913-1921.
- [311] D. Dean-Raymond, M. Alexander, Bacterial metabolism of quaternary ammonium compounds, *Applied and Environmental Microbiology*, 33 (1977) 1037-1041.
- [312] C. Ramprasad, L. Philip, Sorption of surfactants and personal care products in Indian soils, *International Journal of Environmental Science and Technology*, 14 (2017) 853-866.
- [313] J.I. Martinez-Costa, R. Leyva-Ramos, Effect of surfactant loading and type upon the sorption capacity of organobentonite towards pyrogallol, *Colloids and Surfaces A: Physicochemical and Engineering Aspects*, 520 (2017) 676-685.
- [314] M.E. Essington, *Soil and Water Chemistry: An Integrative Approach*, Second Edition, CRC Press 2015.
- [315] R. van Egmond, C. Sparham, C. Hastie, D. Gore, N. Chowdhury, Monitoring and modelling of siloxanes in a sewage treatment plant in the UK, *Chemosphere*, 93 (2013) 757-765.
- [316] M.P. Gomez, M.F. Gazulla, E. Zumaquero, M. Orduna, Use of coupled TG-DSC-QMS-FTIR thermal analysis techniques in characterizing clays and ceramic compositions used in ceramic tile manufacture. Quantification of carbon compounds, *Bol Soc Esp Ceram V*, 46 (2007) 259-266.
- [317] A.K. Goodhead, I.M. Head, J.R. Snape, R.J. Davenport, Standard inocula preparations reduce the bacterial diversity and reliability of regulatory biodegradation tests, *Environmental Science and Pollution Research*, 21 (2014) 9511-9521.
- [318] F. Brillet, M. Cregut, M.J. Durand, C. Sweetlove, J.C. Chenèble, J. L'Haridon, G. Thouand, Biodegradability assessment of complex chemical mixtures using a carbon balance approach, *Green Chemistry*, 20 (2018) 1031-1041.
- [319] S. Urstadt, J. Augusta, R.J. Müller, W.D. Deckwer, Calculation of carbon balances for evaluation of the biodegradability of polymers, *Journal of Environmental Polymer Degradation*, 3 (1995) 121-131.
- [320] R. Boethling, K. Fenner, P. Howard, G. Klečka, T. Madsen, J.R. Snape, M.J. Whelan, Environmental persistence of organic pollutants: Guidance for development and review of POP risk profiles, *Integrated environmental assessment and management*, 5 (2009) 539-556.
- [321] N. Prado, C. Montéléon, J. Ochoa, A. Amrane, Evaluation of the toxicity of veterinary antibiotics on activated sludge using modified Sturm tests - Application to tetracycline and tylosine antibiotics, *Journal of Chemical Technology and Biotechnology*, 85 (2010) 471-477.
- [322] P.C. Wszolek, M. Alexander, Effect of desorption rate on the biodegradation of n-alkylamines bound to clay, *Journal of agricultural and food chemistry*, 27 (1979) 410-414.
- [323] M. Alexander, Aging, bioavailability, and overestimation of risk from environmental pollutants, *Environmental Science and Technology*, 34 (2000) 4259-4265.
- [324] M.T. García, E. Campos, J. Sánchez-Leal, I. Ribosa, Effect of the alkyl chain length on the anaerobic biodegradability and toxicity of quaternary ammonium based surfactants, *Chemosphere*, 38 (1999) 3473-3483.
- [325] M.T. García, E. Campos, J. Sánchez-Leal, F. Comelles, Structure-activity relationships for sorption of alkyl trimethyl ammonium compounds on activated sludge, *Tenside Surfactants Detergents*, 41 (2004) 235.

- [326] M.T. Garcia, O. Kaczerewska, I. Ribosa, B. Brycki, P. Materna, M. Drgas, Biodegradability and aquatic toxicity of quaternary ammonium-based gemini surfactants: Effect of the spacer on their ecological properties, *Chemosphere*, 154 (2016) 155-160.
- [327] O. Kaczerewska, B. Brycki, I. Ribosa, F. Comelles, M.T. Garcia, Cationic gemini surfactants containing an O-substituted spacer and hydroxyethyl moiety in the polar heads: Self-assembly, biodegradability and aquatic toxicity, *Journal of Industrial and Engineering Chemistry*, 59 (2018) 141-148.
- [328] C.G. van Ginkel, J.B. van Dijk, A.G. Kroon, Metabolism of hexadecyltrimethylammonium chloride in *Pseudomonas* strain B1, *Appl Environ Microbiol*, 58 (1992) 3083-3087.
- [329] N. Timmer, D. Gore, D. Sanders, T. Gouin, S.T.J. Droge, Toxicity mitigation and bioaccessibility of the cationic surfactant cetyltrimethylammonium bromide in a sorbent-modified biodegradation study, *Chemosphere*, 222 (2019) 461-468.
- [330] G. Cornelissen, H. Rigterink, M.M.A. Ferdinandy, P.C.M. Van Noort, Rapidly desorbing fractions of PAHs in contaminated sediments as a predictor of the extent of bioremediation, *Environmental Science and Technology*, 32 (1998) 966-970.
- [331] R. Zhu, J. Zhu, F. Ge, P. Yuan, Regeneration of spent organoclays after the sorption of organic pollutants: A review, *J Environ Manage*, 90 (2009) 3212-3216.
- [332] S.M. Lee, D. Tiwari, Organo and inorgano-organo-modified clays in the remediation of aqueous solutions: An overview, *Applied Clay Science*, 59-60 (2012) 84-102.
- [333] L.B. de Paiva, A.R. Morales, F.R. Valenzuela Díaz, Organoclays: Properties, preparation and applications, *Applied Clay Science*, 42 (2008) 8-24.
- [334] S. Ganguly, K. Dana, T.K. Mukhopadhyay, T.K. Parya, S. Ghatak, Organophilic Nano Clay: A Comprehensive Review, *Transactions of the Indian Ceramic Society*, 70 (2011) 189-206.
- [335] J.N. Pendleton, B.F. Gilmore, The antimicrobial potential of ionic liquids: A source of chemical diversity for infection and biofilm control, *Int J Antimicrob Agents*, 46 (2015) 131-139.
- [336] G. Tang, Y. Liu, G. Ding, W. Zhang, Y. Liang, C. Fan, H. Dong, J. Yang, D. Kong, Y. Cao, Ionic liquids based on bromoxynil for reducing adverse impacts on the environment and human health, *New Journal of Chemistry*, 41 (2017) 8650-8655.
- [337] K. Shrivastava, H.F. Wu, A rapid, sensitive and effective quantitative method for simultaneous determination of cationic surfactant mixtures from river and municipal wastewater by direct combination of single-drop microextraction with AP-MALDI mass spectrometry, *Journal of Mass Spectrometry*, 42 (2007) 1637-1644.
- [338] L.N. Nguyen, S. Oh, Impacts of antiseptic cetylpyridinium chloride on microbiome and its removal efficiency in aerobic activated sludge, *International Biodeterioration and Biodegradation*, 137 (2019) 23-29.
- [339] E. Ertekin, J.K. Hatt, K.T. Konstantinidis, U. Tezel, Similar Microbial Consortia and Genes Are Involved in the Biodegradation of Benzalkonium Chlorides in Different Environments, *Environmental Science and Technology*, 50 (2016) 4304-4313.
- [340] T. Egli, How to live at very low substrate concentration, *Water research*, 44 (2010) 4826-4837.
- [341] K. Fenner, S. Canonica, L.P. Wackett, M. Elsner, Evaluating pesticide degradation in the environment: Blind spots and emerging opportunities, *Science*, 341 (2013) 752-758.

- [342] S.T.J. Droge, L. Yarza-Irusta, J.L.M. Hermens, Modeling nonlinear sorption of alcohol ethoxylates to sediment: the influence of molecular structure and sediment properties, *Environmental science & technology*, 43 (2009) 5712–5718.
- [343] K.M. Kerr, R.J. Larson, D.C. McAvoy, Evaluation of an inactivation procedure for determining the sorption of organic compounds to activated sludge, *Ecotoxicology and Environmental Safety*, 47 (2000) 314-322.
- [344] W.C. Jolin, R. Goyetche, K. Carter, J. Medina, D. Vasudevan, A.A. Mackay, Predicting Organic Cation Sorption Coefficients: Accounting for Competition from Sorbed Inorganic Cations Using a Simple Probe Molecule, *Environmental Science and Technology*, 51 (2017) 6193-6201.
- [345] J.L. Pleysier, A.S. Juo, A single-extraction method using silver-thiourea for measuring exchangeable cations and effective cec in soils with variable charges, *Soil Science*, 129 (1980) 205-211.
- [346] K.M. Scow, M. Alexander, Effect of diffusion on the kinetics of biodegradation: experimental results with synthetic aggregates, *Soil Science Society of America Journal*, 56 (1992) 128-134.
- [347] K.M. Scow, J. Hutson, Effect of diffusion and sorption on the kinetics of biodegradation. Theoretical considerations, *Soil Science Society of America Journal*, 56 (1992) 119-127.
- [348] G.Y. Chung, B.J. McCoy, K.M. Scow, Criteria to assess when biodegradation is kinetically limited by intraparticle diffusion and sorption, *Biotechnology and Bioengineering*, 41 (1993) 625-632.
- [349] U.C. Ugochukwu, D.A.C. Manning, C.I. Fialips, Microbial degradation of crude oil hydrocarbons on organoclay minerals, *Journal of Environmental Management*, 144 (2014) 197-202.
- [350] U.C. Ugochukwu, C.I. Fialips, Crude oil polycyclic aromatic hydrocarbons removal via clay-microbe-oil interactions: Effect of acid activated clay minerals, *Chemosphere*, 178 (2017) 65-72.
- [351] S.C. Smith, C.C. Ainsworth, S.J. Traina, R.J. Hicks, Effect of sorption on the biodegradation of quinoline, *Soil Science Society of America Journal*, 56 (1992) 737-746.
- [352] J.C. Lo, G.N. Allard, S.V. Otton, D.A. Campbell, F.A.P.C. Gobas, Concentration dependence of biotransformation in fish liver S9: Optimizing substrate concentrations to estimate hepatic clearance for bioaccumulation assessment, *Environ Toxicol Chem*, 34 (2015) 2782-2790.
- [353] M. Lahlou, H. Harms, D. Springael, J.J. Ortega-Calvo, Influence of soil components on the transport of polycyclic aromatic hydrocarbon-degrading bacteria through saturated porous media, *Environmental Science and Technology*, 34 (2000) 3649-3656.
- [354] A.R. Johnsen, L.Y. Wick, H. Harms, Principles of microbial PAH-degradation in soil, *Environmental Pollution*, 133 (2005) 71-84.
- [355] M.B. Heringa, R.H. Schreurs, F. Busser, P.T. van der Saag, B. van der Burg, J.L. Hermens, Toward more useful in vitro toxicity data with measured free concentrations, *Environmental science & technology*, 38 (2004) 6263-6270.
- [356] J.L. Hermens, M.B. Heringa, T.L. ter Laak, Bioavailability in dose and exposure assessment of organic contaminants in (eco)toxicology, *J Toxicol Environ Health A*, 70 (2007) 727-730.
- [357] M.C. Bubalo, K. Radosevic, I.R. Redovnikovic, J. Halambek, V.G. Srcek, A brief overview of the potential environmental hazards of ionic liquids, *Ecotoxicol Environ Saf*, 99 (2014) 1-12.
- [358] C. Pretti, M. Renzi, S.E. Focardi, A. Giovani, G. Monni, B. Melai, S. Rajamani, C. Chiappe, Acute toxicity and biodegradability of N-alkyl-N-methylmorpholinium and N-alkyl-DABCO based ionic liquids, *Ecotoxicol Environ Saf*, 74 (2011) 748-753.

- [359] M.C. Wiles, H.J. Huebner, T.J. McDonald, K.C. Donnelly, T.D. Phillips, Matrix-immobilized organoclay for the sorption of polycyclic aromatic hydrocarbons and pentachlorophenol from groundwater, *Chemosphere*, 59 (2005) 1455-1464.
- [360] M.T. García, E. Campos, J. Sánchez-Leal, F. Comelles, Sorption of alkyl benzyl dimethyl ammonium compounds by activated sludge, *Journal of Dispersion Science and Technology*, 27 (2006) 739-744.
- [361] M.F. Bergero, G.I. Lucchesi, Degradation of cationic surfactants using immobilized bacteria: Its effect on adsorption to activated sludge, *Journal of Biotechnology*, 272-273 (2018) 1-6.
- [362] M.J. Scott, M.N. Jones, The biodegradation of surfactants in the environment, *Biochimica et Biophysica Acta (BBA) - Biomembranes*, 1508 (2000) 235-251.
- [363] K. Richterich, J. Steber, The time-window - An inadequate criterion for the ready biodegradability assessment of technical surfactants, *Chemosphere*, 44 (2001) 1649-1654.
- [364] European Commission, Opinion on Proposed "Ready Biodegradability" Approach to Update Detergents Legislation. Scientific Committee on Toxicity, Ecotoxicity and the Environment. *Adopted at the 12th CSTEE plenary meeting 25-11-1999*, 1999.
- [365] N. Timmer, D. Gore, D. Sanders, T. Gouin, S.T.J. Droge, Sorbent-modified biodegradation studies of the biocidal cationic surfactant cetylpyridinium chloride, *Ecotoxicology and Environmental Safety*, 182 (2019).
- [366] D.B. Knaebel, T.W. Federle, D.C. McAvoy, J.R. Vestal, Microbial mineralization of organic compounds in an acidic agricultural soil: Effects of preadsorption to various soil constituents, *Environ Toxicol Chem*, 15 (1996) 1865-1875.
- [367] F.A. Groothuis, N. Timmer, E. Opsahl, B. Nicol, S.T.J. Droge, B.J. Blaauboer, N.I. Kramer, Influence of in Vitro Assay Setup on the Apparent Cytotoxic Potency of Benzalkonium Chlorides, *Chemical research in toxicology*, 32 (2019) 1103-1114.
- [368] L.E. McAllister, K.T. Temple, Chapter 17: Role of Clay and Organic Matter in the Biodegradation of Organics in Soil, in: L.L. Barton, M. Mandl, A. Loy (Eds.) *Geomicrobiology: Molecular and Environmental Perspective*, Springer Netherlands 2010, pp. 367-384.
- [369] K.T. Semple, K.J. Doick, L.Y. Wick, H. Harms, Microbial interactions with organic contaminants in soil: Definitions, processes and measurement, *Environmental Pollution*, 150 (2007) 166-176.
- [370] N. Nyholm, Biodegradability testing of poorly soluble compounds by means of manometric respirometry, *Chemosphere*, 21 (1990) 1477-1487.
- [371] D.B. Knaebel, T.W. Federle, D.C. McAvoy, J.R. Vestal, Effect of mineral and organic soil constituents on microbial mineralization of organic compounds in a natural soil, *Applied Environmental Microbiology*, 60 (1994) 4500-4508.
- [372] D.C. McAvoy, C.E. White, B.L. Moore, R.A. Rapaport, Chemical fate and transport in a domestic septic system: Sorption and transport of anionic and cationic surfactants, *Environ Toxicol Chem*, 13 (1994) 213-221.
- [373] ECHA, *Cetrimonium bromide* - Registration Dossier.
- [374] ECHA, *Cetylpyridinium chloride* - Registration Dossier.
- [375] G.J. Churchman, W.P. Gates, B.K.G. Theng, G. Yuan, Clays and Clay Minerals for Pollution Control, in: F. Bergaya, B.K.G. Theng, G. Lagaly (Eds.) *Developments in Clay Science*, Elsevier 2006, pp. 625-675.
- [376] J.G. Churchman, Soil phases: the inorganic solid phase, in: G. Certini, R. Scalenghe (Eds.) *Soils: Basic Concepts and Future Challenges*, Cambridge University Press, Cambridge, 2006, pp. 23-44.



- [377] B. Sarkar, Y. Xi, M. Megharaj, G.S.R. Krishnamurti, M. Bowman, H. Rose, R. Naidu, *Bioreactive Organoclay: A New Technology for Environmental Remediation*, *Critical Reviews in Environmental Science and Technology*, 42 (2012) 435-488.
- [378] M.L.R. Jackson, P. Barak, *Soil Chemical Analysis: Advanced Course*, Parallel Press, University of Wisconsin-Madison Libraries 2005.
- [379] G.K. Batchelor, Mass transfer from small particles suspended in turbulent fluid, *Journal of Fluid Mechanics*, 98 (2006) 609-623.
- [380] Y. Chen, *Sorption behavior and acute toxicity of cationic surfactants in the aquatic environment*, Utrecht University, 2014.
- [381] J. Hower, T.C. Mowatt, The mineralogy of illites and mixed-layer illite/montmorillonites, *American Mineralogist*, 51 (1966) 825-854.
- [382] S. Carroll, M. Smith, N. Marks, Z. Dai, Characterization of starting minerals to be used in kinetic experiments, ; Lawrence Livermore National Lab. (LLNL), Livermore, CA (United States), 2014, pp. Medium: ED; Size: PDF-file: 7 pages; size: 1.6 Mbytes.
- [383] T. Polubesova, S. Nir, Modeling of organic and inorganic cation sorption by illite, *Clays And Clay Minerals*, 47 (1999) 366-374.
- [384] B.A. Manning, S. Goldberg, Adsorption and stability of arsenic(III) at the clay mineral-water interface, *Environmental Science and Technology*, 31 (1997) 2005-2011.
- [385] L. Meier, Determination of the Cation Exchange Capacity (CEC) of Clay Minerals Using the Complexes of Copper(II) Ion with Triethylenetetramine and Tetraethylenepentamine, 1999.
- [386] D.A. Laird, Layer charge influences on the hydration of expandable 2:1 phyllosilicates, *Clays and Clay Minerals*, 47 (1999) 630-636.
- [387] D. Borden, R.F. Giese, Baseline studies of the clay minerals society source clays: Cation exchange capacity measurements by the ammonia-electrode method, *Clays and Clay Minerals*, 49 (2001) 444-445.
- [388] H. Van Olphen, J.J. Fripiat, *Data Handbook for Clay Minerals and Other Non-metallic Minerals*, Pergamon Press, New York, 1979.
- [389] A. Maes, M.S. Stul, A. Cremers, Layer Charge - Cation-Exchange Capacity Relationships In Montmorillonite, *Clays and Clay Minerals*, 27 (1979) 387-392.
- [390] A. Maes, A. Cremers, Charge density effects in ion exchange. Part 1.-Heterovalent exchange equilibria, *Journal of the Chemical Society, Faraday Transactions 1: Physical Chemistry in Condensed Phases*, 73 (1977) 1807-1814.
- [391] B.K. Schroth, G. Sposito, Surface charge properties of kaolinite, *Clays and Clay Minerals*, 45 (1997) 85-91.
- [392] H. Zhao, S. Bhattacharjee, R. Chow, D. Wallace, J.H. Masliyah, Z. Xu, Probing surface charge potentials of clay basal planes and edges by direct force measurements, *Langmuir*, 24 (2008) 12899-12910.
- [393] I. Bérend, J.M. Cases, M. François, J.P. Uriot, L. Michot, A. Masion, F. Thomas, Mechanism of Adsorption and Desorption of Water Vapor by Homoionic Montmorillonites: 2. The Li<sup>+</sup>, Na<sup>+</sup>, K<sup>+</sup>, Rb<sup>+</sup>, and Cs<sup>+</sup>-exchanged Forms, *Clays and Clay Minerals*, 43 (1995) 324-336.
- [394] J.M. Cases, I. Bérend, M. François, J.P. Uriot, L.J. Michot, F. Thomas, Mechanism of adsorption and desorption of water vapor by homoionic montmorillonite: 3. The Mg<sup>2+</sup>, Ca<sup>2+</sup>, Sr<sup>2+</sup> and Ba<sup>2+</sup>-exchanged forms, *Clays and Clay Minerals*, 45 (1997) 8-22.

- [395] J.M. Cases, I. Bérend, G. Besson, M. Francois, J.P. Uriot, F. Thomas, J.E. Poirier, Mechanism of Adsorption and Desorption of Water Vapor by Homoionic Montmorillonite. 1. The Sodium-Exchanged Form, *Langmuir*, 8 (1992) 2730-2739.
- [396] Y. Zheng, A. Zaoui, How water and counterions diffuse into the hydrated montmorillonite, *Solid State Ionics*, 203 (2011) 80-85.
- [397] W.D. Burgos, N. Pisutpaisal, M.C. Mazzarese, J. Chorover, Adsorption of quinoline to kaolinite and montmorillonite, *Environmental Engineering Science*, 19 (2002) 59-68.
- [398] T.J. Martin, J.R. Snape, A. Bartram, A. Robson, K. Acharya, R.J. Davenport, Environmentally Relevant Inoculum Concentrations Improve the Reliability of Persistent Assessments in Biodegradation Screening Tests, *Environmental Science and Technology*, 51 (2017) 3065-3073.
- [399] E.J. O'Loughlin, S.J. Traina, G.K. Sims, Effects of sorption on the biodegradation of 2-methylpyridine in aqueous suspensions of reference clay minerals, *Environ Toxicol Chem*, 19 (2000) 2168-2174.
- [400] H. Chen, X. He, X. Rong, W. Chen, P. Cai, W. Liang, S. Li, Q. Huang, Adsorption and biodegradation of carbaryl on montmorillonite, kaolinite and goethite, *Applied Clay Science*, 46 (2009) 102-108.
- [401] J.B. Weber, H.D. Coble, Microbial Decomposition of Diquat Adsorbed on Montmorillonite and Kaolinite Clays, *Journal of agricultural and food chemistry*, 16 (1968) 475-478.
- [402] P. Besse-Hoggan, T. Alekseeva, M. Sancelme, A.M. Delort, C. Forano, Atrazine biodegradation modulated by clays and clay/humic acid complexes, *Environmental Pollution*, 157 (2009) 2837-2844.
- [403] S. Masaphy, T. Fahima, D. Levanon, Y. Henis, U. Mingelgrin, Parathion Degradation by *Xanthomonas* sp. and Its Crude Enzyme Extract in Clay Suspensions, *Journal of Environmental Quality*, 25 (1996) 1248-1255.
- [404] P. Ye, A.T. Lemley, Adsorption effect on the degradation of carbaryl, mecoprop, and paraquat by anodic Fenton treatment in an SWy-2 montmorillonite clay slurry, *Journal of agricultural and food chemistry*, 56 (2008) 10200-10207.
- [405] J.N. Meegoda, L. Martin, In-Situ Determination of Specific Surface Area of Clays, *Geotechnical and Geological Engineering*, 37 (2019) 465-474.
- [406] F. Macht, K. Eusterhues, G.J. Pronk, K.U. Totsche, Specific surface area of clay minerals: Comparison between atomic force microscopy measurements and bulk-gas (N<sub>2</sub>) and -liquid (EGME) adsorption methods, *Applied Clay Science*, 53 (2011) 20-26.
- [407] X. Feng, A.J. Simpson, M.J. Simpson, Chemical and mineralogical controls on humic acid sorption to clay mineral surfaces, *Organic Geochemistry*, 36 (2005) 1553-1566.
- [408] M.D. Luh, R.A. Baker, Vapor phase sorption of phenol on selected clays, *Journal of colloid and interface science*, 33 (1970) 539-547.
- [409] D. Vasudevan, T.A. Arey, D.R. Dickstein, M.H. Newman, T.Y. Zhang, H.M. Kinnear, M.M. Bader, Nonlinearity of cationic aromatic amine sorption to aluminosilicates and soils: Role of intermolecular cation- $\pi$  interactions, *Environmental Science and Technology*, 47 (2013) 14119-14127.
- [410] A.H. Gemeay, A.S. El-Sherbiny, A.B. Zaki, Adsorption and kinetic studies of the intercalation of some organic compounds onto Na<sup>+</sup>-montmorillonite, *Journal of colloid and interface science*, 245 (2002) 116-125.
- [411] C. Quintelas, Z. Rocha, B. Silva, B. Fonseca, H. Figueiredo, T. Tavares, Removal of Cd(II), Cr(VI), Fe(III) and Ni(II) from aqueous solutions by an *E. coli* biofilm supported on kaolin, *Chemical Engineering Journal*, 149 (2009) 319-324.

- [412] A. Fathima, J.R. Rao, B. Unni Nair, Trivalent chromium removal from tannery effluent using kaolin-supported bacterial biofilm of *Bacillus* sp isolated from chromium polluted soil, *Journal of Chemical Technology and Biotechnology*, 87 (2012) 271-279.
- [413] C. Quintelas, Z. Rocha, B. Silva, B. Fonseca, H. Figueiredo, T. Tavares, Biosorptive performance of an *Escherichia coli* biofilm supported on zeolite NaY for the removal of Cr(VI), Cd(II), Fe(III) and Ni(II), *Chemical Engineering Journal*, 152 (2009) 110-115.
- [414] A. Alimova, M. Roberts, A. Katz, E. Rudolph, J.C. Steiner, R.R. Alfano, P. Gottlieb, Effects of smectite clay on biofilm formation by microorganisms, *Biofilms*, 3 (2006) 47-54.
- [415] S.K. Chaerun, K. Tazaki, M. Okuno, Montmorillonite mitigates the toxic effect of heavy oil on hydrocarbon-degrading bacterial growth: implications for marine oil spill bioremediation, *Clay Minerals*, 48 (2013) 639-654.
- [416] L.E. McAllister, K.T. Semple, Role of Clay and Organic Matter in the Biodegradation of Organics in Soil, in: L.L. Barton, M. Mandl, A. Loy (Eds.) *Geomicrobiology: Molecular and Environmental Perspective*, Springer Netherlands, Dordrecht, 2010, pp. 367-384.
- [417] A.S. Gordon, F.J. Millero, Adsorption mediated decrease in the biodegradation rate of organic compounds, *Microbial Ecology*, 11 (1985) 289-298.
- [418] R. Pedrazzani, E. Ceretti, I. Zerbini, R. Casale, E. Gozio, G. Bertanza, U. Gelatti, F. Donato, D. Feretti, Biodegradability, toxicity and mutagenicity of detergents: Integrated experimental evaluations, *Ecotoxicol Environ Saf*, 84 (2012) 274-281.
- [419] W. Tian, J. Yao, R. Liu, M. Zhu, F. Wang, X. Wu, H. Liu, Effect of natural and synthetic surfactants on crude oil biodegradation by indigenous strains, *Ecotoxicol Environ Saf*, 129 (2016) 171-179.
- [420] K.E. Kapo, M. Paschka, R. Vamshi, M. Sebasky, K. McDonough, Estimation of U.S. sewer residence time distributions for national-scale risk assessment of down-the-drain chemicals, *Sci Total Environ*, 603-604 (2017) 445-452.
- [421] S.E. Belanger, P.B. Dorn, G.M. Boeije, S.J. Marshall, T. Wind, R. van Compernelle, D. Zeller, Aquatic risk assessment of alcohol ethoxylates in North America and Europe, *Ecotoxicology and Environmental Safety*, 64 (2006) 85-99.
- [422] S.E. Belanger, J.L. Brill, J.M. Rawlings, K.M. McDonough, A.C. Zoller, K.R. Wehmeyer, Aquatic toxicity structure-activity relationships for the zwitterionic surfactant alkyl dimethyl amine oxide to several aquatic species and a resulting species sensitivity distribution, *Ecotoxicology and Environmental Safety*, 134 (2016) 95-105.
- [423] K. McDonough, N. Itrich, J. Menzies, K. Casteel, S. Belanger, K. Wehmeyer, Environmental fate of amine oxide: Using measured and predicted values to determine aquatic exposure, *Sci Total Environ*, 616-617 (2018) 164-171.
- [424] S.E. Belanger, J.L. Brill, J.M. Rawlings, B.B. Price, Development of acute toxicity quantitative structure activity relationships (QSAR) and their use in linear alkylbenzene sulfonate species sensitivity distributions, *Chemosphere*, 155 (2016) 18-27.
- [425] K. McDonough, K. Casteel, N. Itrich, J. Menzies, S. Belanger, K. Wehmeyer, T. Federle, Evaluation of anionic surfactant concentrations in US effluents and probabilistic determination of their combined ecological risk in mixing zones, *Sci Total Environ*, 572 (2016) 434-441.
- [426] S.E. Quinn, S.D. Dyer, M. Fan, V.D.J. Keller, A.C. Johnson, R.J. Williams, Predicting risks from down-the-drain chemicals in a developing country: Mexico and linear alkylbenzene sulfonate as a case study, *Environ Toxicol Chem*, 37 (2018) 2475-2486.

- [427] C.V. Eadsforth, A.J. Sherren, M.A. Selby, R. Toy, W.S. Eckhoff, D.C. McAvoy, E. Matthijs, Monitoring of environmental fingerprints of alcohol ethoxylates in Europe and Canada, *Ecotoxicology and Environmental Safety*, 64 (2006) 14-29.
- [428] C. Cowan-Ellsberry, S. Belanger, P. Dorn, S. Dyer, D. McAvoy, H. Sanderson, D. Versteeg, D. Ferrer, K. Stanton, Environmental safety of the use of major surfactant classes in North America, *Critical Reviews in Environmental Science and Technology*, 44 (2014) 1893-1993.
- [429] J.Z. Menzies, K. McDonough, D. McAvoy, T.W. Federle, Biodegradation of nonionic and anionic surfactants in domestic wastewater under simulated sewer conditions, *Biodegradation*, 28 (2017).
- [430] A. Vazquez, M. López, G. Kortaberria, L. Martín, I. Mondragon, Modification of montmorillonite with cationic surfactants. Thermal and chemical analysis including CEC determination, *Applied Clay Science*, 41 (2008) 24-36.
- [431] X.-T. Peng, Z.-G. Shi, Y.-Q. Feng, Rapid and high-throughput determination of cationic surfactants in environmental water samples by automated on-line polymer monolith microextraction coupled to high performance liquid chromatography-mass spectrometry, *J Chromatogr A*, 1218 (2011) 3588-3594.
- [432] K. Shrivastava, H.F. Wu, Oxidized multiwalled carbon nanotubes for quantitative determination of cationic surfactants in water samples using atmospheric pressure matrix-assisted laser desorption/ionization mass spectrometry, *Anal Chim Acta*, 628 (2008) 198-203.
- [433] E. Martinez-Carballo, A. Sitka, C. Gonzalez-Barreiro, N. Kreuzinger, M. Furhacker, S. Scharf, O. Gans, Determination of selected quaternary ammonium compounds by liquid chromatography with mass spectrometry. Part I. Application to surface, waste and indirect discharge water samples in Austria, *Environmental Pollution*, 145 (2007) 489-496.
- [434] D. Cierniak, M. Woźniak-Karczewska, A. Parus, B. Wyrwas, A.P. Loibner, H.J. Heipieper, Ł. Ławniczak, Ł. Chrzanowski, How to accurately assess surfactant biodegradation-impact of sorption on the validity of results, *Applied microbiology and biotechnology*, (2019).



## Nederlandse Samenvatting

Mijn onderzoeksproject had als doel om de milieurisicobeoordeling van positief geladen stoffen te verbeteren, met name positief geladen oppervlakte-actieve stoffen ("*kationische surfactanten*"). Deze kationische surfactanten worden bijvoorbeeld gebruikt in wasverzachter, crèmespoeling, en mondwater, en komen in veel gevallen via de riolering in het milieu. Om de milieurisicobeoordeling voor deze stoffen te verbeteren heb ik geprobeerd om het gedrag van kationische surfactanten en de mechanismen die zorgen voor binding aan deeltjes of oppervlakken in het milieu ("*sorptie*") beter te begrijpen. Sommige kationische surfactanten kunnen al bij relatief lage concentraties giftig zijn voor planten en dieren die in oppervlaktewater leven. De giftigheid (en tegelijk de biologische afbreekbaarheid) neemt echter af als deze stoffen gebonden zijn aan in het water zwevende deeltjes, of aan bodemsediment, want de gebonden fractie wordt niet direct opgenomen in organismen. Hetzelfde geldt wanneer de stoffen in standaard toxiciteitstesten sterk plakken aan de wanden van de test-container waar de dieren in blootgesteld worden. Een belangrijk deel van mijn project was gericht op het ophelderen van de impact van het sorptiegedrag van deze stoffen op diverse standaardmetingen die nodig zijn voor milieurisicobeoordeling. Dat begint bij de correcte analyse van opgeloste concentraties en het bepalen van stoffeigenschappen die het chemische gedrag kunnen voorspellen. Daarna wordt dit in detail uitgewerkt bij het bepalen van giftigheid in testen met cellen gekweekt uit viskieuwen, en bij het uitvoeren van biologische afbreekbaarheid studies (biodegradatiestudies) met bacteriën uit een rioolwaterzuiveringsinstallatie.

In **hoofdstuk 1** worden de uitdagingen en analytische beperkingen beschreven bij het identificeren en kwantificeren van kationische surfactanten met standaard laboratoriumtechnieken. Om deze uitdagingen en beperkingen in de praktijk te evalueren was het nodig om eerst analytische methodes op te zetten voor een groep van 30 kationische surfactanten. Monsters met een concentratie tussen 0.001 en 4 mg/L konden nauwkeuring gemeten worden met behulp van LC-MS/MS (**hoofdstuk 2**). Met behulp van een Oasis weak-cation exchange (WCX) solid-phase extraction (SPE) kolom konden anorganische zouten en andere verontreinigingen uit de monsters gespoeld worden. De recovery na toepassing van WCX-SPE was  $\geq 80\%$  voor alle 30 kationische surfactanten die getest werden, en zelfs  $\geq 90\%$  voor 16 van de 30 (**hoofdstuk 2**). De resultaten wijzen ook uit dat WCX-SPE gebruikt kan worden voor technische mengsels van kationische surfactanten en complexe monsters uit het milieu, mits de bindingscapaciteit van het WCX materiaal niet wordt overschreden.

Kationische verbindingen binden ook sterk aan glas en dit maakt experimenteren met deze stoffen niet eenvoudig. Glasbinding van simpele ioniseerbare en permanent geladen surfactanten bleek recht evenredig te zijn met de alkylketenlengte. Dit effect was het grootst in autosampler vials van 1.5 mL, waarschijnlijk door de ongunstige oppervlakte-volume verhouding. Bij een alkylketenlengte van 12 koolstofatomen vond ik bij een concentratie van 300 nM een glasbinding van 40% voor quaternaire amines en 60% voor primaire amines. Doordat een groot deel van de moleculen gebonden zit aan het glaswerk levert dit dus aanzienlijk lagere opgeloste concentraties op dan gebaseerd op de nominaal toegevoegde hoeveelheid, vooral bij surfactanten met nog langere alkylketens. Bij alkylketenlengtes van 16 koolstofatomen of langer kan de glasbinding in glaswerk met een grotere inhoud echter nog steeds significant zijn (20-60%) (**hoofdstuk 2**). Ik heb ook ontdekt dat er significante binding van kationische surfactanten kan optreden aan de binnen- en buitenkant van pipetpuntjes. Als pipetpuntjes vervolgens deels worden ondergedompeld in vloeistoffen met een component organisch oplosmiddel kan deze gebonden fractie weer loslaten. Dit effect was het grootst voor langere alkylketenlengtes. Vanaf een alkylketenlengtes van 18 koolstofatomen verwacht ik aanzienlijke problemen met de nauwkeurigheid van watermonsters die met een pipet zijn genomen (**hoofdstuk 2**). De impact kan verkleind worden door de buitenkant van pipetpuntjes niet onder te dompelen in oplosmiddel, en de binnenkant van de pipetpuntjes meerdere malen te spoelen met oplosmiddel. Gezien de eerder beschreven glasbinding is het sowieso aan te raden om monsters met kationische surfactanten altijd aan te lengen met organisch oplosmiddel voorafgaand aan de analyse, zodat glasbinding wordt tegengegaan. Uiteraard moeten al deze effecten meegewogen worden om betrouwbare uitspraken te doen over de representativiteit van gemeten concentraties in monsters voor de daadwerkelijke concentratie.

Uit eerder onderzoek is gebleken dat vrij opgeloste kationische surfactanten zich snel en gelijkmatig verdelen over fibers van polyacrylaat, zogenaamde *solid-phase microextraction* (SPME) fibers. Dit maakt het in theorie mogelijk om op een makkelijke en efficiënte manier opgeloste concentraties te bepalen, mits de verhouding tussen de concentratie in de fiber en de concentratie in oplossing bekend is en constant blijft. Deze SPME methodiek is in het verleden veelvuldig toegepast om vrij opgeloste concentraties van allerlei stoffen te meten en is een bruikbare methode om biologische beschikbaarheid te bestuderen. Mijn doel was om partiticoëfficiënten te bepalen voor een serie van verschillende types kationische surfactanten, iets dat in de praktijk helaas niet haalbaar bleek te zijn omdat er veel variabiliteit was in de extracten van de SPME fibers (**hoofdstuk 2**). Gebaseerd

hierop heb ik moeten concluderen dat de gebruikte batch van polyacrylaat SPME-fibers niet geschikt was voor kationische surfactanten met een alkylketenlengte van meer dan 12 koolstofatomen. Tevens adviseer ik om bij elk afzonderlijk experiment dat met SPME wordt uitgevoerd een set van kalibratiemonsters mee te nemen, om te kunnen corrigeren voor variabiliteit.

De opname in de SPME fibers van een primaire en quaternaire amine, beide met een alkylketenlengte van 12 koolstofatomen, was snel genoeg om de fibers na 24 uur blootstellen te meten. De opname van de ongeladen vorm van de primaire amine, dus met name bij hoge pH, was echter langzamer. Dit effect was meer significant met dikkere polyacrylaat coatings. Mijn hypothese is dat dit komt omdat de neutrale vorm wordt geabsorbeerd in het polyacrylaat polymeer en niet geadsorbeerd aan het oppervlak. Overigens vond ik ook een bescheiden pH-effect met de quaternaire amine, die eigenlijk alleen aan het oppervlak zou moeten binden. Dit is waarschijnlijk te verklaren doordat het aantal negatief geladen groepen aan de oppervlakte van de fiber afhankelijk is van de pH, omdat er zuurgroepen aanwezig zijn met een  $pK_a$  tussen 6 en 10. Dit soort eigenschappen van de gebruikte polyacrylaat fibers zijn niet nauwkeurig beschreven, daarom is mijn suggestie om ook naar de geschiktheid van andere fibers en samplers te kijken.

In de zoektocht naar een geschikte SPME coating voor kationische surfactanten heb ik vervolgens een SPME fiber getest die gebaseerd was op C18 en strong cation exchange (SCX) materiaal. Hierbij heb ik een gevarieerde set amines getest met een alkylketenlengte tot 12 koolstofatomen (**hoofdstuk 3**). Uit deze experimenten kan geconcludeerd worden dat de C18/SCX fibers lineaire sorptie laten zien tot aan een fiberconcentratie van 1 mmol/L coating; boven deze concentratie treedt competitie op vanwege verzadiging van de anionische SCX-groepen. De gegenereerde data was voldoende om opname in de C18/SCX fiber provisorisch te modelleren. Mede gebaseerd op dit model schat ik dat dit type fiber geschikt is voor kationische surfactanten met een alkylketenlengte tot 14 of misschien zelfs 16 koolstofatomen. Bij langere alkylketenlengtes neemt de fiber vrijwel alle analyt op uit een oplossing van <100 mL. Voor zulke analyten zou een coating met een lagere dichtheid SCX-groepen of gebruik van WCX-materiaal (zoals in de SPE-kolommetjes) geschikt kunnen zijn. Het gebruik van poreuze coatings is hierbij een manier om de sorptie-efficiëntie te verhogen bij kortere alkylketenlengtes, maar kan juist contraproductief uitpakken bij de langere alkylketenlengtes.



In samenwerking met een aantal collega's is ook een set van 14 werkzame farmaceutische stoffen getest met de C18/SCX fiber (**hoofdstuk 3**). De meeste van deze stoffen waren voor meer dan 98% geladen bij de pH in de matrix. De gevonden partiticoëfficiënten waren, mede gezien de relatief hoge wateroplosbaarheid van geladen stoffen, hoger dan verwacht. Interessant is dat ook een aantal neutrale benzodiazepines relatief sterk aan de coating bonden, een effect dat niet verklaard kon worden met de octanol-water distributicoëfficiënt ( $D_{ow}$ ).  $D_{ow}$  is een maat voor de oplosbaarheid van een stof in octanol ten opzichte van de oplosbaarheid in water en geeft aan hoe lipofiel een stof is.  $D_{ow}$  wordt vaak gebruikt in modellen die het gedrag van moleculen proberen te simuleren of voorspellen. Het niet kunnen verklaren van de binding met behulp van  $D_{ow}$  onderschrijft het belang van relevante alternatieven, zoals beschreven in **hoofdstuk 5**. Terwijl de verwachting was dat de negatief geladen SCX-groepen de negatief geladen vorm van diclofenac (een pijnstillert) zouden afstoten, bleek ook diclofenac bij fysiologische pH met een sterke affiniteit aan de C18/SCX fiber te binden.

De binding van kationische surfactanten aan laboratoriumapparatuur en andere oppervlakken kan ook het interpreteren van *in vitro* toxiciteitsstudies beïnvloeden. Hierbij valt te denken aan binding aan multititerplaten (ook wel "wells plate" genoemd) en pipetpuntjes (**hoofdstuk 2**), maar ook aan eiwitten (zoals albumine) in het medium dat bij *in vitro* toxiciteitstesten wordt gebruikt (**hoofdstuk 4**). Dit kan de vrij opgeloste concentratie verlagen, terwijl resultaten van *in vitro* toxiciteitstesten vaak gebaseerd worden op de toegevoegde (nominale) concentratie. Om de impact van deze processen te onderzoeken heb ik daarom een serie van benzalkonium surfactanten met verschillende alkylketenlengtes getest (**hoofdstuk 4**). Hiervoor is een cellijn gebruikt van gekweekte kieuwcellen van regenboogforel. Bij dit type cellen is de toevoeging van serum en eiwitten niet noodzakelijk, waardoor de vrije concentratie bepaald kon worden zonder toepassing van SPME of andere extractietechnieken. Uit de resultaten bleek dat zowel toxiciteit als de mate van binding aan wells platen (plastic) toenam bij langere alkylketens. Tot een alkylketenlengte van 10 koolstofatomen zijn nominale concentraties afdoende om toxiciteit te beschrijven. Met langere alkylketens kan de vrije concentratie echter tot een factor 30 lager zijn dan de nominale concentratie. Tevens kwam naar voren dat zaken als celdichtheid, duur van blootstelling, en herhaaldelijk doseren een impact kunnen hebben op de gemeten *in vitro* toxiciteit.

Gebaseerd op deze resultaten is het mijn aanbeveling om de vrije concentratie te gebruiken om de toxiciteit te evalueren van benzalkonium surfactanten, en mogelijk alle kationische

surfactanten, met een alkylketenlengte van meer dan 10 koolstofatomen. Het gebruik van betrouwbare data is van zeer groot belang voor een gedegen risicobeoordeling. Het gebruik van membraan- of intracellulaire concentraties zou theoretisch nog beter zijn, en maken het mogelijk ook makkelijker om *in vitro* data te extrapoleren naar *in vivo* effecten. Hier zijn modellen voor beschikbaar, maar deze zijn gebaseerd op  $D_{ow}$  en zijn daarom niet algemeen toepasbaar voor surfactanten (**hoofdstuk 1**).

Partitie tussen fosfolipiden en water is een goede kandidaat om het gedrag en de accumulatie in organismen (bioaccumulatie) van ioniseerbare moleculen te kunnen modelleren, met name modellen gebaseerd op celmembranen. Om deze membraan-water partiticoëfficiënt ( $D_{mw}$ ) van kationische surfactanten te bepalen heb ik gebruik gemaakt van een commercieel beschikbare testkit. Deze testkit bevat parels van silica die gecoat zijn met een dubbele laag fosfolipiden (SSLM; solid supported lipid membrane), vergelijkbaar met natuurlijke celmembranen. Door de hoge dichtheid van de silica parels kunnen deze door kort centrifugeren makkelijk gescheiden worden van het vloeibare medium, waarin vervolgens de vrij opgeloste concentratie bemonsterd en gemeten kan worden. Voordat deze methode toegepast kon worden op kationische surfactanten moest het bestaande protocol aangepast worden. Hierbij heb ik ervoor gekozen om de parels over te brengen in autosampler vials, zodat deze na centrifugeren meteen in de autosampler geplaatst konden worden. Dit zorgde er tevens voor dat het eventuele binden van analyt aan pipetpuntjes (**hoofdstuk 2**) niet langer een potentieel probleem was.

Gebaseerd op mijn eerste SSLM-experimenten moest ik helaas concluderen dat ongeveer 1% van de totale hoeveelheid fosfolipiden losliet van de silica parels en na centrifugeren nog in de vrij opgeloste vorm aanwezig was in het medium (**hoofdstuk 5**). Dit had met name een significante impact op kationische surfactanten met een  $D_{mw}$  groter dan 10.000 L/kg. Door het originele medium van de testkit af te pipetteren en te vervangen met vers medium was het mogelijk om de losgelaten fosfolipiden te verwijderen. Het probleem van de "lekkende" fosfolipiden en de voorgestelde oplossing is erg belangrijk voor het accuraat testen van moleculen met een (verwachte) membraan-water distributicoëfficiënt ( $D_{mw}$ ) groter dan 10.000 L/kg, bijvoorbeeld kationische surfactanten met een alkylketenlengte van meer dan 10 koolstofatomen. In de praktijk komt het erop neer dat alkylamines en benzalkonium surfactanten tot een alkylketenlengte van 12 koolstofatomen getest kunnen worden, en quaternaire alkylamines tot een alkylketenlengte van 14 koolstofatomen. SSLM is overigens ook geschikt voor  $D_{mw}$ -bepaling van anionische surfactanten en perfluoralkyl-anionen (PFAS).

Uiteindelijk kon ik de data van 19 moleculen gebruiken om een simpele QSAR (quantitative structure-activity relationship) op te zetten, gebaseerd op type kopgroep en alkylketenlengte (**hoofdstuk 5**). Een QSAR beschrijft een verband tussen activiteit of “chemisch gedrag” en chemische structuur, en maakt het mogelijk activiteit en/of gedrag te voorspellen voor niet geteste stoffen. De met behulp van deze QSAR berekende  $D_{MW}$  lag voor alle 19 moleculen binnen een factor 3 van de experimentele waarde. In tegenstelling tot wat normaal wordt geacht bij voorspelling gebaseerd op  $D_{OW}$  bleek uit mijn QSAR dat het toevoegen van methylgroepen aan de kopgroep leidt tot een lagere  $D_{MW}$ . De benzalkonium kopgroep had juist een sterk verhogende invloed op de  $D_{MW}$ . Het effect van kopgroep-methylatie wordt waarschijnlijk onderschat bij “IAM-HPLC”-metingen van  $D_{MW}$ . IAM staat voor “immobilized artificial membrane”, en betekent dat er gebruik wordt gemaakt van fosfolipiden die permanent gebonden zijn aan de HPLC-kolom. Fragmentwaarden bepaald voor additionele  $CH_2$ -subunits zijn daarnaast niet zonder meer toepasbaar op moleculen met meer dan één alkylketen. Dit maakt kationische surfactanten met meerdere alkylketens uitzonderlijk goed geschikt voor kruisvalidatie van verschillende modellen omdat alleen modellen, die op de juiste manier kunnen differentiëren tussen één of meer alkylketens, deze moleculen correct zullen modelleren.

Met de huidige stand van de computertechniek is het steeds eenvoudiger om simulaties uit te voeren met molecuulstructuren. De  $D_{MW}$  van kationische surfactanten blijkt ook te berekenen met dit soort computermodellen, bijvoorbeeld met behulp van de COSMOmic software. COSMOmic is een programma dat gebruik maakt van kwantumchemische berekeningen om de oriëntatie en het gedrag van moleculen in bijvoorbeeld water of een celmembraan te simuleren. Het voordeel van COSMOmic is dat deze software zowel de elektrostatische eigenschappen als de geoptimaliseerde driedimensionale structuur van het molecuul binnen het anisotrope fosfolipidenmembraan meeweegt. Ondanks dat er kleine verschillen waren tussen simulaties met COSMOmic en de experimentele SSLM-data, kan ik concluderen dat COSMOmic het effect van kopgroep-methylatie correct kan modelleren. Daarnaast is het zeer interessant dat COSMOmic ook in staat is om het gedrag van kationische surfactanten met twee alkylketens correct te simuleren.

Een tweede belangrijk aspect in mijn onderzoek was het bestuderen van de afbreekbaarheid van kationische surfactanten door bacteriën (biodegradatie) en met name het belang van biologische beschikbaarheid bij deze afbraak. Meestal wordt bij de uitvoering van biodegradatietesten geen analytiek gebruikt, maar wordt de mate van biodegradatie bepaald door het meten van  $CO_2$ -productie of  $O_2$ -consumptie. Voor dit type

metingen zijn relatief hoge concentraties teststof nodig, waardoor de gebruikte bacteriën last kunnen hebben van toxische of remmende effecten. Mijn hypothese was dat er een stapsgewijze aanpak moet zijn om dit probleem te omzeilen. Eerst moet een veilige concentratie vastgesteld worden, gevolgd door het vinden van een geschikt sorbent. Dan moet bepaald worden wat de benodigde sorbent-concentratie is om potentieel negatieve effecten tegen te gaan. Tot slot kan een biodegradatietest uitgevoerd worden met de juiste hoeveelheid sorbent. Ik besloot om deze hypothese als eerste te testen met de kationische surfactant CTAB (cetyltrimethylammonium bromide; **hoofdstuk 6**), omdat deze stof ook bij een groot vergelijkend onderzoek over meerdere Europese laboratoria is gebruikt.

CTAB remt de degradatie van de referentiestof aniline bij een concentratie van 0.3 mg/L, wat bijna 100 keer lager is dan de voorgeschreven concentratie in een standaard biodegradatietest. Dit betekent dat voor het gericht bepalen van de biodegradatie de concentratie onder de 0.3 mg/L moet zijn, omdat verwacht wordt dat bij concentraties boven de 0.3 mg/L de remming toeneemt waardoor mogelijk geen biodegradatie meer optreedt. Gebaseerd op de sorptiecoëfficiënt van CTAB voor SiO<sub>2</sub> (silicium dioxide) en illiet (klei) was ik in staat om te berekenen hoeveel sorbent nodig was om de vrije concentratie CTAB onder de grens van 0.3 mg/L te brengen. Bij de toepassing van deze aanpak bleek echter dat er significante biodegradatie van CTAB optrad bij een vrije concentratie van 16.8 mg/L. Door de onverwachte afwezigheid van remmende effecten was het niet mogelijk om de potentie om remmende effecten te verminderen te evalueren, en is de focus verschoven naar beoordelen van de biologische beschikbaarheid en lag-fase. De lag-fase is een veelvoorkomende periode van enkele dagen tot weken aan het begin van een biodegradatiestudie, waarbij het lijkt alsof er geen afbraak optreedt omdat de bacteriën zich nog moeten aanpassen. Deze lag-fase was korter in alle groepen met sorbent, maar er was ook een verminderde beschikbaarheid bij de hoge concentraties sorbent. De mate van sorptie was in overeenstemming met berekeningen gebaseerd op de sorptiecoëfficiënten. Binding aan glaswerk was echter minder sterk dan verwacht op basis van het werk in **hoofdstuk 2**. De gecombineerde resultaten laten zien dat het mogelijk is om met toevoeging van een nauwkeurig berekende hoeveelheid sorbent potentieel remmende effecten tegen te gaan. In het specifieke geval van CTAB heeft dat ertoe geleid dat de criteria voor snelle afbraak makkelijker worden behaald.

Bij eenzelfde soort experiment met CPC (cetylpyridinium chloride; een kationische surfactant) vond ik snelle afbraak bij een vrije concentratie onder de 100 µg/L, met

licht remmende effecten vanaf 300 µg/L en sterke remming bij hogere concentraties (**hoofdstuk 7**). Zoals hierboven beschreven voor CTAB heb ik ook voor CPC met behulp van SiO<sub>2</sub> en illiet de vrije concentratie tot onder de 100 µg/L gebracht, bij nominale concentraties van 1 en 10 mg/L. Bij 1 mg/L was er sprake van een lag-fase van 3 weken, die significant korter werd door toevoeging van SiO<sub>2</sub>, al waren er wel problemen met verminderde biologische beschikbaarheid bij 20 g/L SiO<sub>2</sub>. Met illiet trad dit effect ook op bij 4 g/L, maar bij 0.8 g/L was er wel duidelijk sprake van vermindering van de remmende effecten van CPC. Een concentratie CPC van 10 mg/L was niet voldoende biologisch beschikbaar na toevoeging van 20 g/L illite, maar met toevoeging van 20 g/L SiO<sub>2</sub> was er een zeer geleidelijke biodegradatie. Het lijkt er dus op dat er een balans is tussen vermindering van remmende effecten en vermindering van de biologische beschikbaarheid, waardoor de hoeveelheid sorbent goed moet worden afgestemd op de te testen stof om gunstige effecten te maximaliseren.

De in hoofdstuk 7 en 8 toegepaste biodegradatietest maakt gebruik van grote hoeveelheden replica's per tijdstip. Om de efficiëntie van de test en het detail van de metingen te verhogen, heb ik ook een systeem met automatische manometrische respirometers gebruikt, die het biodegradatieproces in het testsysteem vrijwel continu kunnen volgen gedurende de hele testperiode. Manometrische respirometers zijn in staat om het zuurstofverbruik (respiratie) te meten door gebruik van een drukmeter (manometer). Deze manometrische systemen heb ik gebruikt om de hoge concentraties van CPC (13.6 mg/L) en CTAB (20 mg/L) opnieuw te testen, in combinatie met zeven verschillende soorten klei. Sommige soorten klei waren zogenaamde zwelklei, die water kunnen opnemen en daardoor opzwellen, en mede als gevolg van het opzwellen zeer effectief kationische surfactanten kunnen binden. Alle soorten klei waren in staat om remmende effecten van CPC te verminderen, met versnelde afbraak en een hoger percentage afbraak tot gevolg (**hoofdstuk 8**). De verschillen met **hoofdstuk 7** zijn waarschijnlijk deels te verklaren door het feit dat de respirometer-systemen actief geroerd worden, waardoor desorptie en diffusie versneld kunnen worden. De optimale balans tussen vermindering van ongewenste remmende effecten en behoud van biologische beschikbaarheid werd behaald met twee verschillende soorten illiet (IMt-1 en IMt-2) en kaolien (KGa-2). IMt-1 en KGa-2 waren zelfs zo effectief dat CPC als snel afbreekbaar kon worden geclassificeerd bij deze hoge concentratie. Met bentoniet (C-ben) en montmorilloniet (SCa-3), twee soorten zwelklei, was er langzame en geleidelijke afbraak na een korte lag-fase, wat zou kunnen wijzen op beperkte biologische beschikbaarheid. Voor een andere soort montmorilloniet

(SAz-2) was dit effect niet aanwezig, wellicht doordat  $K^+$  en  $Na^+$  in SAz-2 vervangen waren met  $Ca^{2+}$ , waardoor het sorptiegedrag anders kan zijn geweest.

In het experiment met CTAB en de zeven kleisoorten vond ik omvangrijke afbraak in de flessen zonder sorbent. Hierdoor was ik genoodzaakt om vooral naar effecten op de lag-fase en plateauhoogte te kijken. IMt-1, IMt-2, en commercieel beschikbare illiet (C-ill) leiden alle drie tot een snellere afbraak. Het plateau was 6 tot 19% hoger; een sterke aanwijzing dat biologische beschikbaarheid ruim voldoende was. KGa-2 had nauwelijks invloed, terwijl deze kleisoort bij CPC juist wel een significant effect had. De resultaten met SAz-2 en SCa-3 wijzen ook op een voldoende biologische beschikbaarheid. Vanwege het 19% hogere plateau leveren deze twee soorten zwelklei daarmee nog meer bewijs voor de juistheid van mijn hypothese, dat correct toepassen van het juiste sorbent remmende effecten kan verminderen en zo de mate van biodegradatie kan verhogen. Toevoeging van C-ben leidt tot een 13% hoger plateau, met kinetiek die het meest lijkt op die van de drie soorten illiet. Mijn uiteindelijke conclusie is dat toepassing van sorbent ervoor zorgt dat de biodegradatie van CTAB sneller verloopt, en dat de lag-fase significant korter wordt (**hoofdstuk 8**).

De resultaten van mijn promotieonderzoek kunnen relevant zijn bij het verbeteren van de milieurisicobeoordeling van kationische surfactanten. Inzichten uit **hoofdstuk 2 en 3** zijn essentieel om het gedrag van kationische moleculen te begrijpen, al zal niet elk aspect van toepassing zijn op elk kationisch molecuul. Alle kationische surfactanten met een alkylketenlengte van 16 koolstofatomen of langer zijn zeer uitdagend om mee te werken. Indien mogelijk moeten experimentele concentraties door analytische ondersteuning geverifieerd worden. Het feit dat veel moleculen positief geladen zijn, waaronder veel farmaceutische stoffen en stoffen met industriële of huishoudelijke toepassingen die in grote volumes in het milieu kunnen belanden (**hoofdstuk 1 en 3**), is in mijn ogen een belangrijk argument om de milieurisicobeoordeling voor deze groep chemicaliën verder te verbeteren. Er bestaan hulpmiddelen om organische kationen te isoleren of bemonsteren, maar het is altijd zaak om deze hulpmiddelen nauwkeurig te kalibreren. Hoewel de toxiciteit en het gedrag in het milieu van kationische surfactanten nog beter bestudeerd moeten worden draagt het werk in **hoofdstuk 4 en 5** bij aan meer begrip met betrekking tot het gedrag in *in vitro* toxiciteitsscreening, en bij het bepalen van geschikte parameters voor model-simulaties. De partiticoëfficiënt naar fosfolipidemembranen kan naar mijn mening een sleutelrol vervullen bij de vervanging van  $D_{ow}$  in risicomodellen, zeker bij het schatten van toxiciteit en bioaccumulatie. De stapsgewijze aanpak voor de toevoeging van sorbent aan biodegradatietesten (**hoofdstuk 6, 7 en 8**) kan de

relevantie van onderzoeksresultaten voor het milieu vergroten, omdat overal in het milieu negatief geladen oppervlakken voorkomen (actief slib, sediment, biomassa, humuszuren). Sommige kationische surfactanten worden zelfs wereldwijd teruggevonden in sedimenten van rivieren en oceanen. Automatische manometrische respirometers lijken vanwege hun hoge meetfrequentie en flexibiliteit bij uitstek geschikt voor standaardisering van biodegradatie testen met stoffen zoals kationische surfactanten in combinatie met sorbents, en detailonderzoek naar onderliggende processen.

Mijn onderzoek heeft enkele belangrijke inzichten opgeleverd die helpen bij het correct omgaan, bemonsteren, en beoordelen van kationische surfactanten. Aangezien de meeste methodes uiteindelijk afhankelijk zijn van betrouwbare analytische kwantificatie is mijn evaluatie van de uitdagingen die ontstaan bij de chemische analyse een belangrijke bijdrage aan de bestaande literatuur. Het correct toepassen van mijn bevindingen kan voorkomen dat er meetfouten van een factor 10 tot 1.000 gemaakt worden bij het bepalen van concentraties in toxiciteitsscreenings of van monsters uit het milieu. Van vergelijkbaar belang is de voorgestelde stapsgewijze toepassing van sorbent in biodegradatietesten, waarmee meetfouten met een factor 10 tot 100 bij de bepaling van de afbreekbaarheid van kationische surfactanten voorkomen kunnen worden. De beoordeling van stoffen die belangrijk zijn omdat ze dagelijks in onze samenleving worden gebruikt, kan dankzij mijn onderzoek voor kationische surfactanten worden aangevuld met sterk verbeterde experimentele parameters. Daarmee draagt mijn werk eraan bij dat de milieurisicobeoordeling sterk verbeterd kan worden.

## Dankwoord

Ten eerste wil ik mijn promotoren en copromotoren bedanken. Voor alle mails die jullie hebben beantwoord, alle manuscripten die jullie van commentaar hebben voorzien, en alle kritiek die altijd opbouwend werd gebracht. Joop, wat een eer dat ik met jouw begeleiding ben gestart aan mijn onderzoek. Wat ontzettend fijn om met zo'n bevlogen professor, met fans van over de hele wereld, te mogen werken. Juliette jij hebt het einde van mijn PhD begeleid, dank voor je inzet en begeleiding. Het was altijd fijn om je adviezen en input te krijgen om zo mijn boekje succesvol af te ronden. Steven, dank voor je begeleiding gedurende alle jaren. Het was erg fijn om een copromotor te hebben die meedenkt, soms tegengas geeft, maar vooral ook mij vertrouwen gaf in mijn kunnen.

Collega's van de UU, jullie bedankt voor de samenwerking. We hebben veel gesproken, gediscussieerd, en gebrainstormd. De medewerkers van het laboratorium, dank voor jullie hulp bij het uitvoeren van alle ingewikkelde tests die we weer verzonnen. Special thank you to the colleagues of Unilever. It was great to spend a few months in Sharnbrook!

Heeren van Tsaar, wat is het een plezier om onderdeel te mogen zijn van een dispuut als het onze. Van rally rijden tot wijnproeven, altijd een moment van ontspanning in tijden van promotiestress. Speciaal woord van dank voor Nas de Rofje.

Collega's van Charles River Laboratories, Beppy en Marcel in het bijzonder, jullie hebben het vertrouwen in mij gehad dat ik mijn PhD zou afronden. Nu krijg ik bij jullie de kans om nieuwe onderzoeksopzetten uit te testen en ga ik verder met biodegradatie werk. Dagelijks geven jullie mij de vrijheid en het vertrouwen om mezelf en het onderzoek verder te ontwikkelen. Heel erg dank hiervoor!

Thomas en Mark, de beste paranimfen die er zijn. Thomas, jij bent altijd vol interesse over mijn onderzoek en stimuleert mij om door te zetten als ik het liefste even aan andere dingen denk. De filmavonden, het borrelen en het lekkere eten gaven de ontspanning die nodig was tijdens de afronding. Mark, wat ben jij een goede vriend. Wanneer het even minder goed ging, zorgde jij voor een opbeurend gevoel. Samen over muziek ouwehoeren, feestjes en chillen. En dat altijd precies op het goede moment. Dank!



Ik wil ook graag mijn ouders, Kees en Toos, mijn broertje, zusje en hun partners bedanken. Jullie hebben mijn chagrijnige momenten moeten verdragen als het even tegenzat, mijn gezeur over al het gedoe, mijn afwezigheid op sommige momenten. Ik ben blij dat ik in een gezin als het onze ben opgegroeid, en dat wij altijd welkom zijn thuis.

Natuurlijk wil ik ook al mijn andere vrienden en overige familie en schoonfamilie bedanken.

Elisa, mijn lieve vriendin, wat heb jij een geduld gehad met mij. Avonden achter de computer, terwijl ik overdag bij CRL aan het werk was geweest. Jij bracht mij dan kopjes thee, nootjes, zelfgebakken taart, lekker eten en een knuffel als het even tegen zat. Dankjewel lieverd.







UU - IRAS